Biology and biotechnology of dissimilatory metal reduction in *Shewanella oneidensis*

Zur Erlangung des akademischen Grades eines

DOKTORS DER NATURWISSENSCHAFTEN

(Dr. rer. nat.)

Fakultät für Chemie und Biowissenschaften

Karlsruher Institut für Technologie (KIT) - Universitätsbereich

genehmigte

DISSERTATION

von

Clemens Bücking

aus

Berlin

Dekan: Prof. Dr. Bastmeyer

Referent: Prof. Dr. Gescher

Korreferent: Prof. Dr. Fischer

Tag der mündlichen Prüfung: 10.02.2012

I. Table of contents

II. Tables

III. Zusammenfassung

Bei vielen globalen Nährstoffkreisläufen spielen anaerobe Atmungen von Mikroorganismen eine wichtige Rolle. Ein Beispiel für eine wichtige anaerobe Atmung ist die dissimilatorische Metallatmung, die Metalloxide, auch in mineralischer Form, als terminale Elektronenakzeptoren nutzt. Das fakultativ anaerobe Proteobakterium der γ-Gruppe, *Shewanella oneidensis*, ist ein wichtiger Modellorganismus für diese Form der Atmung. In den letzten Jahren ist das Interesse an der Physiologie von *Shewanella* stark gestiegen, vor allem wegen der möglichen Nutzung der Bakterien in mikrobiellen Brennstoffzellen und bei der Sanierung von schwermetallverseuchten Böden.

Die aktuelle Modellvorstellung, wie der Elektronentransfer von den Bakterien zu den Metalloxid-Partikeln funktioniert, geht von einer erweiterten Elektronentransferkette aus. Elektronen, die bei oxidativen Prozessen an der Cytoplasmamembran entstehen, werden mit Hilfe von *c*-Typ Cytochromen übertragen und überbrücken so den periplasmatischen Raum und die äußere Membran, um zum terminalen Elektronenakzeptor zu gelangen, der außerhalb der Zelle verbleibt. Auch der finale Reduktionsschritt wird von Cytochromen in der äußeren Membran katalysiert.

Im ersten Teil dieser Doktorarbeit wird die Herstellung einer Deletionsmutante beschrieben, der alle fünf äußeren Membrancytochrome fehlen. In diese Mutante, ΔOMC, wurden die einzelnen Membrancytochrome exprimiert und ihre Aktivitäten gemessen. Das wichtigste neue Ergebnis dieser Arbeit war, dass das Gen *mtrF* („**m**e**t**al **r**educing“) für ein funktionales Membrancytochrom kodiert und dass OmcA („**o**uter **m**embrane **c**ytochrome“) nicht funktional zu sein scheint, wenn es alleine exprimiert wird (Bücking *et al.*, 2010)[1].

Im zweiten Teil dieser Arbeit wurde versucht, die Reduktionsrate von *S. oneidensis* zu erhöhen, was vorteilhaft für einen möglichen Einsatz in der Biotechnologie wäre. Dazu wurde ein synthetisches Operon konstruiert, das eine kontrollierte extrazelluläre Reduktion ermöglichte. Die Fe(III)-citrat Reduktionsrate war 1,8fach höher als beim Wildtyp[2].

[1] Diese Publikation ist im Appendix zu dieser Doktorarbeit abgedruckt.

[2] Der Großteil dieser Daten wurde als Manuskript bei Biosensors and Bioelectronics eingereicht. Das gesamte Manuskript ist im Appendix zu dieser Doktorarbeit abgedruckt.

Im dritten Teil dieser Doktorarbeit wurde eine Spontanmutante aus einer Kultur von ΔOMC Zellen isoliert und charakterisiert. Der neue Stamm, genannt ΔOMC^S, hatte die Fähigkeit Fe(III)-citrat zu reduzieren, obwohl er keine äußeren Membrancytochrome bilden kann. Zielgerichtete Mutagenese und Sequenzierung des Genoms von ΔOMC^S zeigten, dass einzelne Punktmutationen in den Schlüsselgenen für extrazelluläre Atmung, *mtrA* und *mtrB*, für diesen neuen Reduktionsmechanismus verantwortlich waren. Es wurde daher postuliert, dass dieser Mechanismus eine evolutionär ältere Form der dissimilatorischen Eisenreduktion darstellen könnte (Bücking *et al.*, 2012)[3].

[3] Diese Publikation ist im Appendix zu dieser Doktorarbeit abgedruckt.

IV. Abstract

Anaerobic bacterial respiration is an important process for the global cycling of many nutrients. Dissimilatory metal reduction is a form of anaerobic respiration that uses solid metal oxide minerals as terminal electron acceptors. One important model organism for dissimilatory metal reduction is the facultative anaerobic γ-proteobacterium *Shewanella oneidensis*. The interest in understanding the physiology of *Shewanella* has greatly increased since putative applications of the bacteria in microbial fuel cells and in bioremediation of heavy metal polluted soils were discovered.

The current model for electron transfer to solid metal oxides by *S. oneidensis* describes an extended respiratory chain. Electrons that are derived from oxidative processes at the cytoplasmic membrane are transferred mainly via *c*-type cytochromes through the periplasm and through the outer membrane to reach the terminal electron acceptor which remains outside of the cell. The final reduction of the electron acceptor is believed to be catalyzed by outer membrane cytochromes.

In the first part of the thesis, a deletion mutant lacking all five genes coding for outer membrane cytochromes called ΔOMC was constructed and the activities of reintroduced single outer membrane cytochromes were measured. The main finding of this study was that the gene *mtrF* (**m**e**t**al **r**educing) codes for a functional outer membrane cytochrome and that OmcA (**o**uter **m**embrane **c**ytochrome) seems to be non-functional when it is expressed on its own (Bücking *et al.*, 2010)[4].

In the second part of the thesis we tried to increase the reduction rate of *S. oneidensis* for putative applications in biotechnology. We used a rational design approach constructing a synthetic operon which allowed for controlled extracellular reduction. An 1.8-fold higher Fe(III)-citrate reduction rate was achieved[5].

In the third part a spontaneous mutant that was isolated from a ΔOMC culture was characterized. This new strain called ΔOMC^S had the ability to reduce Fe(III)-citrate although it did not contain any outer membrane cytochromes. Directed mutagenesis studies and genome sequencing revealed that single point mutations in key genes for extracellular respiration, *mtrA* and *mtrB* allowed for a new reduction mechanism. It was postulated that this mechanism might represent a more ancient form of dissimilatory

[4] This publication is printed in the Appendix of this thesis.

[5] Manuscript submitted to Biosensors and Bioelectronics, for complete manuscript, see Appendix of this thesis.

metal reduction and that the invention of outer membrane cytochrome might be an example for upstream evolution that enhanced reduction rates (Bücking *et al.*, 2012)[6].

[6] This publication is printed in the Appendix of this thesis.

V. Introduction

1. Anaerobic respiration

Respiratory processes are commonly associated to the use of molecular oxygen. For most organisms (including ourselves) this is true, as aerobic respiration means oxidation of substrates with oxygen to gain energy for living. Anaerobic respiration follows the same principle only that the terminal electron acceptor is not oxygen but another compound (e.g. nitrate, fumarate or sulfate). The energy gain from anaerobic respiration is smaller than from aerobic respiration but usually higher than from fermentations (Schlegel *et al.*, 2007).

Although today nearly all eukaryotic organisms and a large number of prokaryotes rely fundamentally on aerobic respiration, this was not always the case in earth history. After the emergence of life (~3.5 billion years ago), there was a long period of prokaryotic life without oxygen (Nisbet and Sleep, 2001).

It was not until 2.45 billion years ago that the amount of oxygen increased dramatically (Bekker *et al.*, 2004) and restricted the occurrence of anaerobic lifestyles from global to specific niches in the environment. Still, the importance of anaerobic respiratory processes should not be underestimated as they thrive important processes in the global cycling of elements. Furthermore, they enable prokaryotes to occupy virtually every place on planet Earth.

2. Alternative electron acceptors – electrochemical potentials

The theoretical energy gain for a form of respiration can be calculated from the standard reduction potential (E_0') of the electron donor and of the electron acceptor. As already mentioned above, the highest energy gain can be derived from electron transfer to oxygen. Substantially less energy can be conserved by the reduction of nitrate, followed by fumarate, and sulfate. If an organism can use several electron acceptors, it usually uses them in the hierarchical order of possible energy gain (Unden and Bongaerts, 1997).

2.1 Dissimilatory metal reduction

Another possible terminal electron acceptor for respiratory processes can be a metal oxide like Fe(III) or Mn(IV). Although this form of respiration has only be recognized about ~30 years ago, a large number of organisms from different domains can respire metals. The most intensely studied organisms to date couple the oxidation of reduced carbon

sources to the reduction of a metal oxide to sustain growth. First isolates were described by Myers and Nealson (Myers and Nealson, 1988) and Lovley (Lovley and Phillips, 1988).

It was speculated that one of the first respiratory processes relied on Fe(III)-oxide as electron acceptor (Vargas *et al.*, 1998). The origin of Fe(III)-oxides in a reductive environment like the early earth is still under debate. The most common hypotheses are Fe(II) photooxidation by UV-radiation, oxidation of Fe(II) with oxygen originating from cyanobacteria and anoxygenic photosynthesis with Fe(II) as electron donor (Posth *et al.*, 2008).

2.2 Insoluble electron acceptors – influence on redox potential

The standard reduction potential of the Fe(III)/Fe(II) couple (at pH 0) is 770 mV and therefore almost as high as the oxygen/water couple with 820 mV. However, this high redox potential is relevant only for iron reduction at pH values below 3 and therefore only relevant for acidophilic organisms (Bird *et al.*, 2011). At neutral pH values, the solubility of iron oxides is very low: The solubility constant for $Fe(OH)_3$ is $K=10^{38}$ l mol^{-1} which corresponds to a Fe(III) concentration of ~10^{-18} mol l^{-1} (Schlegel *et al.*, 2007). The low solubility influences strongly the redox potential of Fe(III)-oxides and oxyhydroxides which varies between -177 and +24 mV. Iron oxide reduction is therefore in some cases thermodynamically almost as unfavorable as sulfate reduction (E_0'= -220 mV; (Majzlan, 2011; Thamdrup, 2000). Due to this low redox potential ubiquinone (E_0'= +66 mV) is not suitable as electron carrier in the cytoplasmic membrane and instead menaquinone (E_0'= -74 mV) is necessary (Saffarini *et al.*, 2002).

2.2.1 Excursus: Assimilatory iron reduction

An important distinction needs to be made between dissimilatory and assimilatory iron reduction. The latter process is ubiquitously distributed among organisms of all domains of life because iron is a very important micronutrient. Its availability in most contexts with neutral pH values is limited due to the very low solubility described above. Hence, successful iron-uptake is a very important mechanism for most organisms and a pathogenicity factor in a number of pathogens as well.

To catalyze iron uptake, the microorganisms secrete low molecular weight (0.5-2 kDa) iron chelators called siderophores with a very high binding affinity for Fe(III). The affinity for Fe(III) is for some compounds even higher than the affinity of iron chelators

commonly used in biochemistry (stability constant of enterobactin from *Enterobacteria* is 10^{52} l mol^{-1} (Harris *et al.*, 1979) whereas the stability constant of EDTA is only 10^{25} l mol^{-1} (Schlegel *et al.*, 2007)). These siderophores bind Fe(III) and the iron charged siderophores are then taken up by the cell in a energy-dependent manner by specialized transporters. Depending on the stability of the iron-siderophore-complex, the siderphore is either hydrolyzed or the Fe(III) is reduced by ferric chelate reductases (Miethke and Marahiel, 2007).

3. Gram-negative bacteria

The problem that all organisms face at neutral pH values with insoluble electron acceptors is especially valid for the group of Gram-negative bacteria. These organisms have an additional membrane, the so called outer membrane. Although it is also a bilayered membrane, the two layers are not similar as it is the case with the cytoplasmic membrane. It is composed of a phospholipid layer at the inner side and a lipopolysaccharide layer at the outside. The periplasmic space between the cytoplasmic membrane and the outer membrane is an important catalytic area filled with a large number of proteins and has therefore a gelatinous consistence (Hobot *et al.*, 1984). The outer membrane and the periplasmic space constitute an additional diffusion barrier which hinders direct contact of the respiratory chain in the cytoplasmic membrane to insoluble electron acceptors.

4. *Shewanella oneidensis* MR-1

One of the most important model organisms for metal reduction is the Gram-negative γ-proteobacterium *S. oneidensis* MR-1. It was originally isolated from Lake Oneida in Upstate New York, USA, due to its capability of reducing manganese (IV) oxides (Myers and Nealson, 1988; Venkateswaran *et al.*, 1999). In some older publications it is referred to as *Shewanella putrefaciens* (all changes in names are reviewed in (Hau and Gralnick, 2007)). *S. oneidensis* can use a variety of compounds as electron acceptors for anaerobic respiration such as ferric iron, manganese dioxide, and uranium as well as nitrate, nitrite, sulfur, thiosulfate, fumarate, sulfite, dimethylsulfoxide, and trimethylamine-N-oxide (Burns and DiChristina, 2009; Cruz-Garcia *et al.*, 2007; Hau and Gralnick, 2007; Myers and Nealson, 1988; Schwalb *et al.*, 2002, , 2003; Shirodkar *et al.*, 2011). *S. oneidensis* can further grow aerobically with oxygen as terminal electron acceptor but it cannot thrive fermentativly. The organism is believed to live in stratified environments at the oxic/anoxic interface where a multitude of electron acceptors could be available

(Venkateswaran *et al.*, 1999). *S. oneidensis* uses fermentation end products (lactate, formate, H_2) and N-acetylglucosamine (main component of chitin) as carbon and electron sources (Scott and Nealson, 1994; Yang *et al.*, 2006). Surprisingly, substrate-level phosphorylation seems to be the primary source for ATP generation under anaerobic conditions (Hunt *et al.*, 2010; Pinchuk *et al.*, 2011).

The interest in metal reducing bacteria has greatly increased during the last two decades. This is to a large extent caused by potential applications in biotechnology that will be discussed in section 5 of the introduction. The advantages of using *Shewanella* species to study these processes – mainly their good genetic tractability – led to genome sequencing projects for 23 *Shewanella* species so far, mostly funded by the department of energy (DOE) of the USA. Besides genome information, a detailed knowledge about the physiology of the organisms is crucial for biotechnology applications. In the following, the current knowledge about the biochemistry of *Shewanella* will be described.

4.1 Biochemistry of an extended respiratory chain

S. oneidensis evolved an extended respiratory chain to the cell surface mainly composed of *c*-type cytochromes. It enables the organisms to bring respiratory electrons into contact with sparsely soluble electron acceptors like ferric or manganese oxides (Figure 1). *c*-type cytochromes are very important electron carrier proteins in all domains of life. They are evolutionary very old proteins (1.5-2 billions years (Berg *et al.*, 2007)) that fulfill typically functions in respiratory processes and photosynthesis. Their central component is the cofactor heme with a catalytic iron in the center (biosynthesis of heme reviewed by (O'Brian and Thony-Meyer, 2002)). Heme is covalently attached to the protein via a conserved binding motif "CXXCH" (X can be any amino acid). Several proteins are necessary for *c*-type cytochrome maturation (reviewed by (Kranz *et al.*, 2009)).

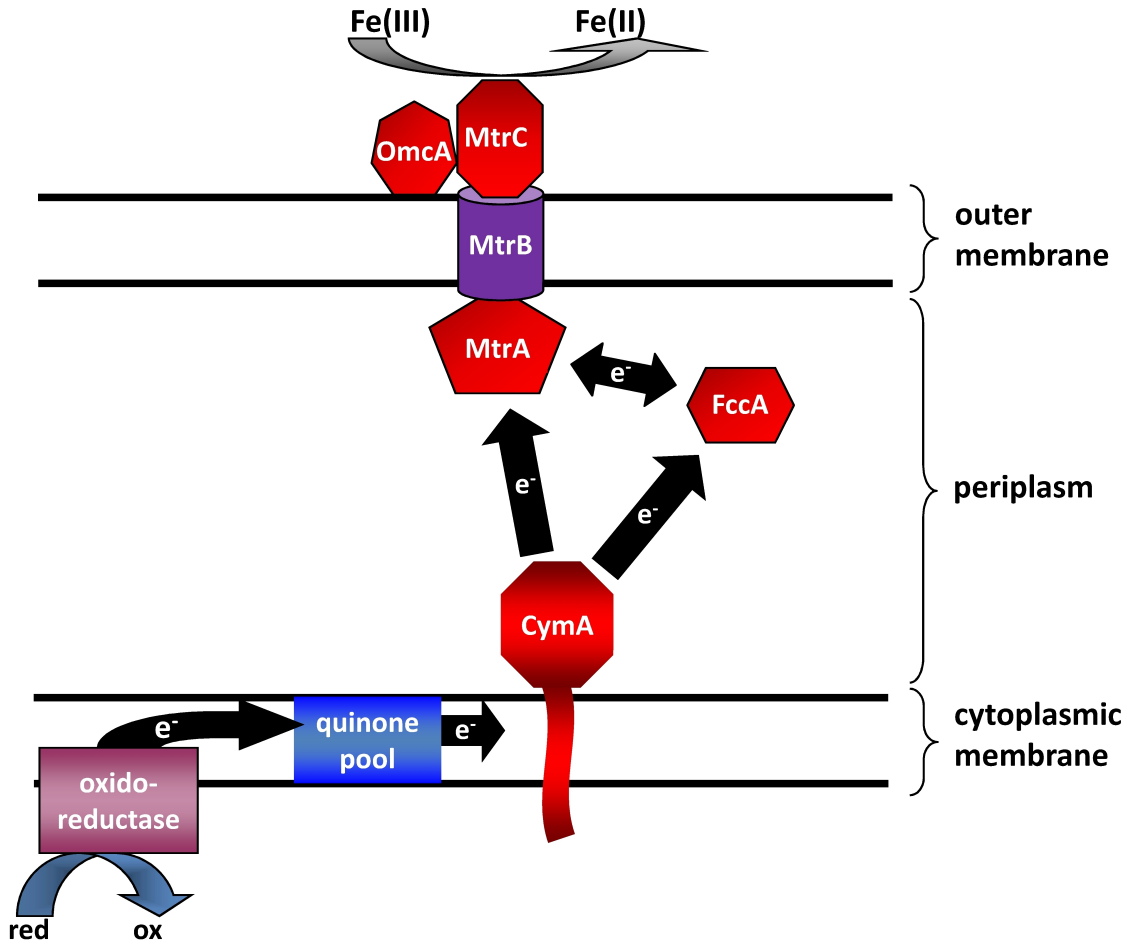

Figure 1: Current model of the extended respiratory chain for insoluble metal oxides in S. oneidensis. *Multiheme c-type cytochromes are depicted in red.*

While *c*-type cytochromes in eukaryotes have only one heme group, bacterial *c*-type cytochromes contain often multiple hemes (Kranz *et al.*, 2009). Generally, multiheme *c*-type cytochromes seem to play an important role in the respiratory electron transport chains to the cell surface in mesophilic prokaryotes (Thomas *et al.*, 2008). Importantly, the redox potential of the well known soluble electron carrier in mitochondria, cytochrome *c*, (E_0'= +220 mV, (Schlegel *et al.*, 2007)) differs much from the potential of multiheme *c*-type cytochromes in *S. oneidensis* (i.e. MtrA: E_0'= -100 mV, CymA: E_0'= -200 mV).

The genome of *S. oneidensis* contains the genetic information for 41 *c*-type cytochromes, mostly multiheme proteins. Nine proteins are putatively located in the cytoplasmic membrane, five in the outer membrane, and 27 in the periplasm (Meyer *et al.*, 2004; Romine *et al.*, 2008). *E. coli,* which belongs to the same class of bacteria, has only seven genes encoding *c*-type cytochromes (Blattner *et al.*, 1997). The expression of cytochrome proteins by *Shewanella* is very easy to recognize because cells appear dark red in color when cultivated under anaerobic conditions. The phenomenon of the expression of a high number of *c*-type cytochromes is also valid for other metal reducing organisms like *Geobacter sulfurreducens*, belonging to the δ-proteobacteria and encoding 111 genes for *c*-type cytochromes in its genome (Methe *et al.*, 2003).

The number of *c*-type cytochromes seems to be a selective advantage for the organisms but leads to a number of complications when researchers try to outline a path of electron transfer. In *Shewanella*, multiple *c*-type cytochromes are coexpressed under anaerobic conditions. Transcriptome studies showed that in several cases the availability of oxygen rather than the available anaerobic terminal electron acceptor seems to be the trigger for *c*-type cytochrome expression (Beliaev *et al.*, 2005).

It is therefore very well conceivable that some electron transfer pathways in *Shewanella* are much more intertwined than in *E. coli*. Schuetz *et al.* proposed recently such a kind of interconnection between different respiratory pathways regarding the function of the soluble fumarate reductase FccA in iron reduction (Schuetz *et al.*, 2009).

A difficulty for the researcher arises from the fact that the main class of redox-active proteins in the extended respiratory chain, the *c*-type cytochromes, do not seem to catalyze specific electron transfer reactions (Bretschger *et al.*, 2007; Gao *et al.*, 2010; Myers and Myers, 2003b). *in vitro*, several purified cytochromes were shown to be able to

exchange electrons (Firer-Sherwood *et al.*, 2011b; Schuetz *et al.*, 2009). The differences in redox potentials of these proteins are very small.

An exception to this low specificity is the *c*-type cytochrome peroxidase CcpA which is apparently dependent on the small monoheme protein ScyA (Schütz *et al.*, 2011). For all other *c*-type cytochrome proteins, a connection of electron transfer pathways seems to be conceivable.

Due to the coexpression of multiple cytochromes and the low overall specificity, single mutants in *S. oneidensis* cytochromes frequently do not show a clear phenotype (Bretschger *et al.*, 2007; Myers and Myers, 2003b).

4.2 The route for electrons

The description of the electron transport chain to Fe(III) or Mn(IV) in *S. oneidensis* will be separated in four parts following the electron flow to the insoluble acceptor.

First, the electron transfer reactions at the cytoplasmic membrane (4.2.1) and in the periplasm (4.2.2) will be summarized briefly. Then, in a second part and more detailed, the current knowledge about electron transfer over the outer membrane (4.2.3) and the final reduction of the insoluble acceptor will be discussed.

4.2.1 Electron transfer between the menaquinone pool and the periplasm

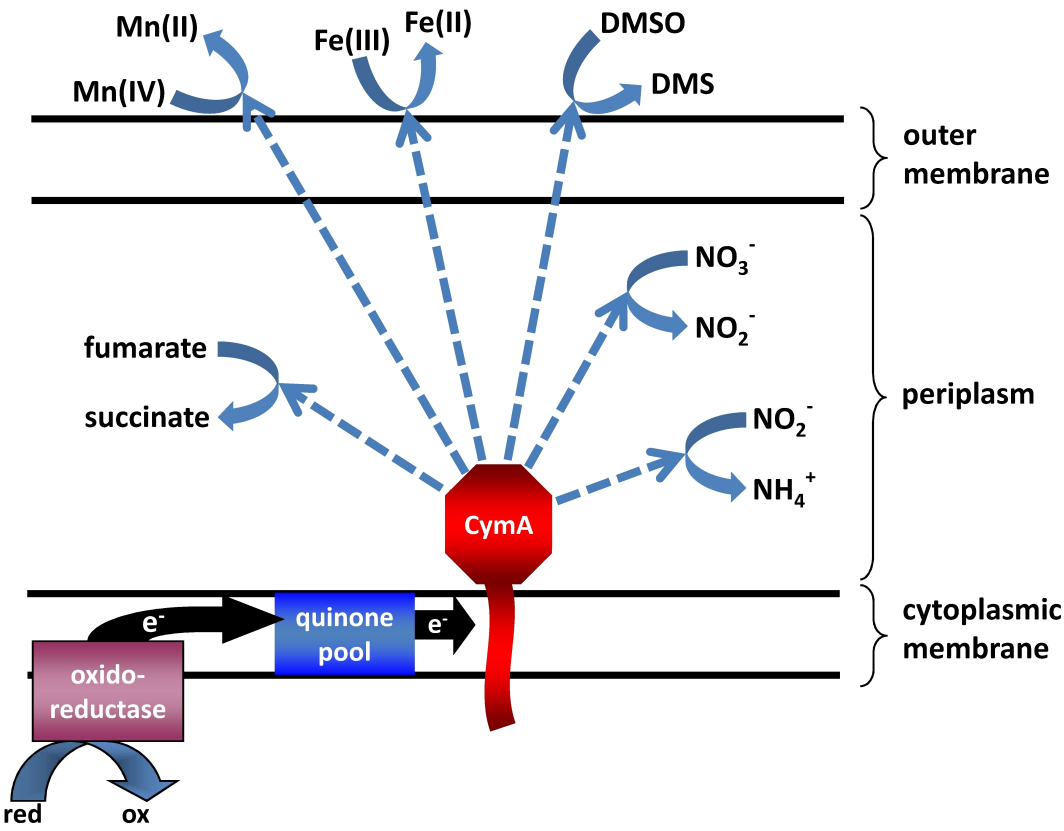

Figure 2: Connection between CymA and periplasmic as well as extracellular respiratory chains.

In *Shewanella*, electrons are transported from the menaquinole pool to the periplasm by the catalytic activity of a tetraheme *c*-type cytochrome protein called CymA (**cy**toplasmic **m**embrane protein **A**). CymA seems to be the central branching point for several electron transfer pathways transferring electrons from the menaquinone pool to several oxidoreductases located in the periplasm (Figure 2). Therefore, deletion of the *cymA* gene from the chromosome leads to a mutant that is unable to use not only ferric iron or manganese oxides as terminal electron acceptor, but also nitrate, nitrite, fumarate and DMSO (Myers and Myers, 1997) (Schwalb *et al.*, 2003). The reduction of thiosulfate, sulfides, and TMAO is independent from CymA.

Of note, in terms of bioenergetics, the energy conservation associated with respiration of electron acceptors that are dependent on CymA is most likely only associated with electron input into the menaquinone pool. All further electron transfer steps in the extended respiratory chain do not seem to conserve energy. This is different from well known electron transfer chains of anaerobic respiration: In *E. coli*, most reductases are located in the cytoplasmic membrane (e.g. fumarate reductase, nitrate reductase, DMSO

reductase (Unden and Bongaerts, 1997; Weiner *et al.*, 1992)). The active center of most enzymes is oriented to the cytoplasm. They either add to the proton motive force by proton pumping or by a net consumption of protons in the cytoplasm like the fumarate reductase during the formation of succinate. In *S. oneidensis,* these effects are precluded by the localization of many final reductases: the fumarate and the nitrate reductase are localized to the periplasm and the DMSO reductase is localized to the outer membrane (Gao *et al.*, 2009; Gralnick *et al.*, 2006; Myers and Myers, 1992b). The amount of energy gain is therefore not dependent on the potential difference $\Delta E_0'$ between NADH and the terminal acceptor but on the $\Delta E_0'$ between NADH and CymA and thus the same for all three pathways (Bird *et al.*, 2011). This might explain why there seems to be no differential regulation of these pathways depending on the terminal electron acceptor (Beliaev *et al.*, 2005).

Minor differences in the redox potentials of the cytochromes involved in electron transport to ferric iron seem to be sufficient for electron transfer since they exclusively serve as a "wire" that connects the menaquinol pool to ferric iron. The potential windows of several important *c*-type cytochromes are very similar as revealed using protein film voltammetry (Firer-Sherwood *et al.*, 2008). Interestingly, the apparent midpoint potential of CymA (revealed using protein film voltammetry) is with -200 mV below the potential of the menaquinole/menaquinone couple. It was hypothesized that a predominantly reduced menaquinole pool is necessary to enable electron transfer (Firer-Sherwood *et al.*, 2008; Hartshorne *et al.*, 2007).

4.2.2 Periplasmic electron transfer reactions

Isolated periplasmic fractions from *S. oneidensis* cells grown under ferric iron reducing conditions have a bright to dark red color, which is due to the high amount of *c*-type cytochromes that are located in the periplasm. The current knowledge about the most abundant periplasmatic cytochromes is presented in the following.

4.2.2.1 MtrA

The most important periplasmic *c*-type cytochrome for electron transfer in metal reduction is the 32 kDa monomeric decaheme *c*-type cytochrome MtrA (**m**e**t**al **r**educing protein A). It was one of the first proteins that were identified as being necessary for iron reduction (Beliaev and Saffarini, 1998). This central function for metal reduction was confirmed by numerous groups (Bretschger *et al.*, 2007; Hartshorne *et al.*, 2009;

Schicklberger *et al.*, 2010). MtrA is partly localized in a soluble form in the periplasm but also strongly associated to the outer membrane (Pitts *et al.*, 2003; Ross *et al.*, 2007; Schuetz *et al.*, 2009). The association to the outer membrane is probably mediated by binding to a protein complex that will be described later on. *in vitro*, MtrA can be directly reduced by CymA (Firer-Sherwood *et al.*, 2011b; Schuetz *et al.*, 2009). It is so far unknown whether this periplasmic MtrA is the electron donor for MtrA that is located in the outer membrane within the MtrABC complex (see below).

4.2.2.2 FccA

One of the most abundant periplasmic *c*-type cytochromes is FccA (**f**lavo**c**ytochrome **c** protein A), which is the respiratory fumarate reductase of *S. oneidensis*. Surprisingly, FccA is the most prominent cytochrome even in cells that were grown under ferric iron reducing conditions. Usually, FccA receives electrons from CymA to reduce fumarate (Myers and Myers, 1997; Schwalb *et al.*, 2003) but *in vitro* data indicated that it can also receive electrons from reduced MtrA. Therefore, as MtrA and FccA can exchange electrons, the electron transport chains to fumarate and to insoluble metal oxides might be interconnected. The high abundance of FccA would allow for a second function of this enzyme. It was proposed that FccA could act – besides its function as fumarate reductase – as a transient electron storage protein or capacitor that is filled with electrons via reaction kinetics that are faster than electron transfer to an extracellular electron acceptor. This strategy would also allow *Shewanella* cells to use a carbon and electron source even if no terminal electron acceptor is present, since the transient electron storage would act as an intermediate electron acceptor (Schuetz *et al.*, 2009). The transiently stored electrons could then be discharged on several terminal acceptors depending on availability.

Recently, Uria *et al.* measured such an electron storage effect within biofilms in a microbial fuel cell (Uria *et al.*, 2011). Similar hypotheses for other organisms with a multitude of *c*-type cytochromes were raised by other groups (Esteve-Nunez *et al.*, 2008; Rodrigues *et al.*, 2006).

The existence of a periplasmic electron transfer network could also explain the partial or general lack of phenotypes observed in mutants defective in a number of periplasmic *c*-type cytochromes (Bretschger *et al.*, 2007; Gao *et al.*, 2010).

4.2.3 Electron transfer reactions at the outer membrane

The hydrophobic thickness of outer membranes of Gram-negative bacteria (i.e. the distance between the glycerol molecules of the two layers without the lipopolysaccharide layer) is approximately 25 Å (Lomize *et al.*, 2006). It represents a very good electric insulator precluding a direct electron transfer through the membrane. The most convincing current model how electron transfer over the membrane is possible is based on a transmembrane protein complex. The integral membrane protein MtrB is associated with two cytochromes, MtrA on the inside and an outer membrane cytochrome on the outside of the outer membrane. Hartshorne *et al.* demonstrated *in vitro* that this complex has the capacity to transport electrons over a liposomal membrane (Hartshorne *et al.*, 2009). It was therefore suggested that the two cytochromes are partly inserted into the β-barrel structure of MtrB, which would probably enable interprotein electron transfer.

Genes for outer membrane cytochromes are characterized by the presence of a signal sequence for transport accross the cytoplasmic membrane by the general secretory pathway (Sec translocon) of Gram-negative bacteria. Furthermore, they contain a lipid anchor that enables attachment to membranes. Bioinformatical analysis of the genome of *S. oneidensis* revealed genetic information for five putative outer membrane *c*-type cytochromes (Heidelberg *et al.*, 2002; Meyer *et al.*, 2004). The deduced amino acid sequences of OmcA, MtrC, MtrF and SO_1659 indicate 10 putative heme attachment sites. The genes coding for these proteins are believed to originate from gene duplications of a pentaheme motif (Meyer *et al.*, 2004). SO_2931 is expected to be a diheme *c*-type cytochrome. It does not display any sequence homologies to known *c*-type cytochromes and is therefore classified as hypothetical protein (Meyer *et al.*, 2004). Many studies on the role of outer membrane cytochromes have been published to date. Similar to the multitude of cytochrome proteins in the periplasm, it is still a matter of ongoing research to assign specific functions to the individual outer membrane cytochromes.

Probably the most important outer membrane cytochrome protein for metal reduction, MtrC (**met**al **r**educing), was identified by two groups (Beliaev *et al.*, 2001; Myers and Myers, 2001). Mutants were shown to be impaired in iron- and manganese-oxide reduction and to mislocalize OmcA to the cytoplasmic membrane and to the soluble fraction (Myers and Myers, 2001). The second outer membrane cytochrome protein that was shown to have a role in metal reduction was the just mentioned OmcA (**o**uter **m**embrane **c**ytochrome). An *omcA* single deletion mutant was shown to possess lower

MnO_2 reduction rates, whereas activity of this mutant towards insoluble iron oxides is controversial: Myers *et al.* reported that it had no effect on iron reduction whereas Coursolle *et al.* saw a mild effect on growth with a similar mutant (Coursolle and Gralnick, 2010; Myers and Myers, 2001). MtrC and OmcA were shown to be lipoproteins that are exposed to the outer surface of the cell (Myers and Myers, 2003a, , 2004).

Several further studies report on mutant and complementation studies with *mtrC* and *omcA*. Results of these studies on outer membrane cytochromes are often conflicting and contradictory. As an example, Myers *et al.* showed that within 24 hours an *mtrC* deletion mutant had only 10-15% of the reducing activity towards manganese oxide and amorphous ferric oxide compared to the wild type (Myers and Myers, 2002a). Examining the reduction of the same compounds within the same time frame by a *mtrC*/*omcA*-double mutant by Bretschger *et al.*, published in the same journal, yielded reduction activities of ~80% of the wild type level (Bretschger *et al.*, 2007). In part, these conflicting results might be due to differences in metal oxide composition. Another possibility would be the appearance of suppressor mutations that compensate for the loss of an important protein. The genome of *Shewanella* contains a high number of IS-elements and has therefore quite a high plasticity (Romine *et al.*, 2008). The existence of four genes coding for very similar outer membrane cytochromes (MtrC, OmcA, MtrF, and SO_1659) suggests the possibility of an unnoticed upregulation of genes in the studies with *mtrC* and *omcA* mutants.

4.2.3.1 Importance of the type II secretion system for metal reduction

Early work by DiChristina *et al.* showed that electron transfer to insoluble acceptors in *Shewanella* is dependent on a functional type II secretion system (DiChristina *et al.*, 2002). Type II secretion is one export pathway for the secretion of proteins to the outside of the cell. It can be necessary for the cells to release proteins to the environment (e.g. AB_5 cholera toxin in *Vibrio cholerae*) or to secrete cell proteins that are supposed to interact with the cell surface. The protein machinery for type II secretion consists of 12 subunits. The current model is that the mature protein is recognized (probably due to structural properties of the protein) by the type II secretion system in the periplasm. It is thought that a pilus with similarity to type IV pili is assembled and pushes the protein towards the outer membrane. Here, a special secretion pore is formed through which the protein can be secreted (Sandkvist, 2001).

It was recognized that the dependence of metal reduction on the type II secretion system is due to the translocation of outer membrane cytochromes to their final localization on the surface of the outer membrane. Hence, the secretion system is non-functional and metal reduction not possible, if main components of the secretion system like building blocks for the pilus (encoded mainly by *gspG*) or the secretion pore (*gspD*) are missing (Shi *et al.*, 2008).

4.2.4 Reduction mechanisms at the microbe-mineral interface

Different models were proposed of how the terminal metallic electron acceptor is finally reduced. MtrC and OmcA were shown to directly reduce iron minerals *in vitro* (Reardon *et al.*, 2010; Xiong *et al.*, 2006). The transfer rates to ferric iron were rather low and could not explain entirely the fast rates of iron reduction by whole cells. It was therefore proposed that endogenous flavin redox shuttles are involved in this electron transfer process (Marsili *et al.*, 2008; Ross *et al.*, 2009; von Canstein *et al.*, 2008). Still, reduction of the flavin shuttle molecules depends on the whole electron transfer chain since they apparently cannot pass the outer membrane and therefore have to be reduced by outer membrane cytochromes as well (Coursolle *et al.*, 2010; Richter *et al.*, 2010). In natural habitats of *Shewanella*, humic acids are frequently present. They represent exogenous electron shuttles. Consequently, it was shown that Fe(III) reduction by *S. oneidensis* was stimulated by humic substances in concentrations as low as 5-10 mg carbon per liter. Humic substances can occur in dissolved or solid-phase form. Both have been studied extensively with respect to their effect on microbial Fe(III) reduction due to electron shuttling (Jiang and Kappler, 2008; Lovley *et al.*, 1996; Roden *et al.*, 2010). Furthermore, it was hypothesized that redox active membrane vesicles containing outer membrane cytochromes as redox active molecules might act as complex electron shuttles. (Gorby *et al.*, 2008)

Another possible mode of electron transfer are so called nanowires that were first described by Reguera *et al.* for *Geobacter sulfurreducens* and shortly later by Gorby *et al.* for *S. oneidensis* (Gorby *et al.*, 2006; Reguera *et al.*, 2005). It was hypothesized that these cell appendages can transfer electrons to an electron acceptor that is not in direct contact to the cell but rather distantly localized. In *S. oneidensis*, electron transfer along the pilus is dependent on the presence of MtrC and OmcA (El-Naggar *et al.*, 2010). Probably, several modes of electron transfer (i.e. direct contact, electron shuttling and nanowires)

operate simultaneously, but all of them fundamentally rely on the catalytic activity of outer membrane *c*-type cytochromes.

5. Shewanella biotechnology

Many researchers are currently investigating the physiology of *S. oneidensis.* This is for a large part due to the putative utilization of the organism in several biotechnology processes that will be presented briefly.

5.1 Bioremediation

Besides iron and manganese oxides, *S. oneidensis* can also reduce uranium species. Hexavalent uranium, or U(VI), is an environmental contaminant prevalent e.g. at several former nuclear weapon test sites in the USA. *Shewanella* and other metal reducing organisms can reduce the highly mobile U(VI) complex to poorly soluble uraninite ($U(IV)O_2$), thus limiting its migration in soils and aquifers. The mechanism for uranium reduction is also based on the metal reduction pathway described in section V. 4.1 (Marshall *et al.*, 2006). A cost effective bioremediation of the sites with microorganism is already in the pilot test phase (Wu *et al.*, 2007).

5.2 Production of nano-materials with Shewanella

The production of nano structured particles is a great issue for microbiology as these particles have a great potential for various applications. It was shown that *Shewanella* can produce arsenic-sulfide nanotubes (Lee *et al.*, 2007) and can produce graphene by graphene-oxide reduction (Jiao *et al.*, 2011). The latter process involves normally the use of toxic chemicals (Park and Ruoff, 2009) which could be avoided by microbial production. The reduction of graphene-oxide by *S. oneidensis* was shown to be dependent on the *mtr*-gene cluster (Jiao *et al.*, 2011).

5.3 Microbial fuel cells

The ability to transfer electrons to insoluble terminal electron acceptors enables the organisms to reduce electrodes. This transfer of electrons can be used to produce electricity in a microbial fuel cell (Logan, 2009). The microorganisms are used as biocatalysts processing organic matter to electricity. Microbial fuel cells are very promising tools for remote electricity generation as they avoid costly noble metal catalysts or limited life time of enzymatic fuel cells. Additionally, some attempts have been made to use the cells as a platform for a biosensor based on a microbial fuel cell (Davila *et al.*, 2011; Tront *et al.*, 2008).

6. Research questions

The initial research question at the beginning of this work was:

- What is the role and specificity of outer membrane cytochromes in *Shewanella oneidensis* MR-1?

The first part of this thesis is trying to answer this question with the help of a mutant strain that was generated in the course of this work, called ΔOMC. This mutant was used as a background for examining single outer membrane cytochromes.

In the second part, the biotechnological potential of *S. oneidensis* for bioremediation (e.g. chromium reduction, uranium reduction) or electricity production in microbial fuel cells was explored. This aspect was motivated by the following research question:

- Can we genetically optimize the extended respiratory chain to construct a new strain with a higher reduction rate?

The third part was based on the phenotype of a spontaneous variant of ΔOMC mutant that was able to reduce Fe(III)-citrate without outer membrane cytochromes. Hence the following question was raised:

- What is the genetic origin of a spontaneous mutation that makes outer membrane cytochromes redundant?

VI. Materials and methods

1. Growth conditions and media

The growth in liquid cultures was followed by measuring the **o**ptical **d**ensity (OD) at 600 nm. In a few cases, the number of viable cells was determined by plating serial dilutions on LB agar plates and counting colony forming units (CFU). The number is given as CFU ml^{-1}.

All *E. coli* cultures were incubated at 37°C, while *S. oneidensis* and yeast cells were grown at 30°C. Aerobic growth was routinely performed in test tubes (3-5 ml) or Erlenmeyer flasks (50-500 ml) under vigorous shaking.

1.1 Media for aerobic cultures

For aerobic growth *E. coli* and *S. oneidensis* strains were grown as batch cultures in Luria-Bertani (LB) medium consisting of 1% (w/v) bactotryptone, 0.5% (w/v) yeast extract and 0.5% (w/v) NaCl. The medium for *E. coli* strain WM3064 was additionally supplemented with 0.3 mM **di**amino**p**imelic acid (DAP) because this strain has an auxotrophie and needs to be supplied with building blocks for cell wall synthesis. If necessary, kanamycin (25 µg ml^{-1} or 50 µg ml^{-1}) was added to the medium.

Yeast cells were grown in YPD medium (1% (w/v) Bacto yeast extract, 2% (w/v) Bacto peptone, 2% (w/v) D-glucose; pH 6.9). The yeast strain used in this work was an uracil auxotroph being unable to synthesize uracil *de novo*. To select for cells that had taken up plasmid DNA conferring the ability to grow on uracil-free medium, special Ura-agar plates were made containing 46.7 g l^{-1} Minimal SD agar base, and 0.77 g l^{-1} Ura-drop out supplement (Clontech).

For growth on agar plates 2% agar was added to both LB and YPD medium prior to autoclaving. For preparation of agar plates containing 10% (w/v) sucrose, one volume of filter-sterilised, 3-fold concentrated sucrose solution was heated to 60°C and mixed with two volumes of autoclaved, 1.5-fold concentrated LB medium.

1.2 Media for anoxic cultures

Under anoxic conditions, *S. oneidensis* strains were usually cultivated in *4M* minimal medium that was prepared from *4M*-buffer stock (Table 1) that already contained the necessary trace elements (Table 2). Lactate (50 mM) was used as electron donor and

carbon source during all experiments, while fumarate (100 mM) was routinely chosen as electron acceptor.

Table 1: 4M-buffer (stock solution 20-fold concentrated).

Substance	***Final concentration in medium***	***Amounts needed per litre of medium***
KH_2PO_4	0.73 mM	1.98 g
K_2HPO_4	1.27 mM	4.42 g
Sodium 4-(2-hydroxyethyl)-1-piperazineethanesulphonic acid (HEPES)	5 mM	23.8 g
$(NH_4)_2SO_4$	8.32 mM	22 g
NaCl	50 mM	58.4 g
Trace elements stock solution	-	200 ml

Table 2: Trace elements (100-fold stock solution).

Substance	***Final concentration in medium***
$CoCl_2$	5 µM
$CuSO_4 \cdot 5H_2O$	0.2 µM
$FeCl_2 \cdot 2 H_2O$	5.4 µM
H_3BO_3	56.6 µM
$MnSO_4$	1.3 µM
Na_2EDTA	67.2 µM
Na_2MoO_4 2 H_2O	3.9 µM
Na_2SeO_4	1.5 µM
$NiCl_2 \cdot 6 H_20$	5 µM
$ZnSO_4$	1 µM

All components of *4M*-buffer stock solution were dissolved in Aqua dest, 200 ml trace element solution was added and the pH was adjusted to match 7.4. Finally, Aqua dest was added to obtain a final volume of 1 litre.

Table 3: Anoxic lactate/fumarate medium.

Component	***Concentration***	***Amounts needed per liter of medium***
4M-buffer stock solution	see above	50 ml
Sodium lactate 50% (w/w)	50 mM	11.2 g
Disodium fumarate	100 mM	16 g
Casamino acids	0.1% (w/v)	1 g
$MgSO_4$ 7 H_2O	1 mM	1 ml from 1000-fold stock
$CaCl_2$ 2 H_2O	0.1 mM	1 ml from 1000-fold stock

All components of the anoxic lacate/fumarate medium (Table 3) were dissolved in Aqua dest and the pH was controlled to be 7.4. $MgSO_4$ and $CaCl_2$ were added from a 1000-fold concentrated stock solution.

For metallic electron acceptors, fumarate was replaced by either Fe(III)-citrate or birnessite. Medium was filled in glass bottles sealed with butyl rubber stoppers. Before autoclaving oxygen was removed from the medium. This was achieved by flushing the headspace with nitrogen (99.9% purity) for 2 min and by degassing it afterwards for the same amount of time using a vacuum pump under vigorous shaking. The whole procedure was repeated for 10 to 20 cycles.

After autoclaving the medium, kanamycin and arabinose was added if necessary. Ferrihydrite was also added after autoclaving the medium. Anaerobic cultures were inoculated with aerobic overnight cultures. No more than 1% of the final culture volume was injected with a sterile syringe.

1.2.1 Preparation of chelated metals and metal oxides for anoxic media

1.2.1.1 Fe(III)-citrate

Fe(III)-citrate powder was dissolved in Aqua dest and boiled in the microvave oven for 25 min. Afterwards, pH was slowly adjusted to pH 7.4 with 1 M NaOH. Usually, the final concentration in the medium was 50 mM Fe(III)-citrate.

1.2.1.2 Ferrihydrite

2-line ferrihydrite was prepared by adding slowly 290 ml 1 M KOH to 500 ml 200 mM $FeCl_6$ 6 H_2O under continuous stirring. The pH was then further adjusted to 7.5 but should never be above 8. The particles formed were washed three times with Aqua dest by centrifugation to remove ions from the solution and dried overnight on Whatmann paper. The protocol for 2-line ferrihydrite production is based on personal communication from Dr. Sonia Ackermann and is a slightly modified version of a protocol from Schwertmann *et al.* (Schwertmann and Cornell, 2000).

The dry ferrihydrite particles were ground in a mortar. Ferrihydrite cannot be autoclaved because secondary minerals like goethite would form under the elevated temperatures in the autoclave. The particles were therefore sterilized with UV radiation for 15 min and added to the medium immediately before inoculation. A suspension of ferrihydrite particles was added to the sterile medium through a syringe to exclude larger particles that would cause clogging when taking samples.

1.2.1.3 Birnessite (manganese dioxide)

Birnessite (manganese dioxide) was prepared as described previously (Burdige and Nealson, 1985). A 30 mM $MnCl_2$ solution was added dropwise to a 20 mM $KMnO_4$ solution under continuous stirring. The birnessite precipitate formed was washed three times with Aqua dest., dried and stored as a powder until used. A suspension of birnessite particles was added to the medium through a syringe to exclude larger particles that would cause clogging when taking samples. The birnessite content of the medium was determined to be 2.5 mM.

1.3 Conservation of strains

Strain collections of all relevant strains of this thesis were maintained in freezer stocks. An overnight culture was supplemented with 5% (v/v) DMSO and immediately shock-frozen in liquid nitrogen and stored at -70°C. Strains that were used throughout the thesis were periodically reactivated from the freezer stocks. To do this, some of the frozen bacteria were scraped off the surface and streaked on an agar plate. Liquid cultures were inoculated with freshly formed colonies from that plate.

2. Molecular biology methods

2.1 DNA isolation and purification

Bacterial genomic DNA was isolated using the Illustra bacteria genomic Prep kit (GE Healthcare). Bacterial plasmid DNA was isolated using Wizard® Plus SV Miniprep DNA Purification System (Promega). DNA fragments within agarose gel pieces were purified using Promega's Wizard® SV Gel and PCR Clean-Up System (Promega) which was also used to purify polymerase chain reaction (PCR) products directly or from excised agarose gel pieces. The experimental procedure for all three kits was carried out according to the manufacturer's instructions.

DNA from yeast cells was obtained by performing the so-called 'Smash & Grab' procedure (Shanks *et al.*, 2006). A 3 ml overnight culture was pelleted and resuspended in 200 µl Smash&Grab-buffer (Table 4). Approximately 0.3 g of sterile glass beads (diameter 0.5 mm) and 200 µl phenol:chloroform:isoamyl alcohol (25:24:1) solution was added. The eppendorf tubes were vortexed at maximum speed for 2 min to disrupt the cells mechanically and to denature proteins. After centrifugation (5 min at 5000 rpm) which led to the sedimentation of glass beads, cell remnants and proteins, the upper aqueous phase containing the DNA was transferred into a fresh tube and mixed with 0.7 volumes of isopropanol. The tubes were incubated for 5 min to allow for the precipitation of DNA. After another centrifugation step the pelleted DNA was washed twice in 70% (v/v) ethanol, dried in a vacuum concentrator and resuspended in 15 µl Aqua dest. Usually 2 µl from this DNA solution were used to transform *E. coli* cells.

Table 4: Smash&Grab buffer for DNA preparation from yeast cells.

Substance	***Concentration***
SDS	1% (w/v)
Triton X-100	2% (w/v)
NaCl	100 mM
Tris-HCl (pH 8)	100 mM
EDTA	1 mM

2.1.1 Amplification of DNA

DNA was amplified using the polymerase chain reaction. The oligonucleotides that were used as primers are listed in Table 7, page 32.

For control PCRs a Taq-polymerase mixture (MangoMix, Biozym) containing furthermore buffer, dNTPs, loading dye and glycerol was used. If further cloning steps were performed with the PCR fragments, a synthetic Pfu-polymerase with a proof-reading function (iProof polymerase, Biorad) was chosen in order to achieve higher accuracy. Primer solutions were diluted to obtain a working concentration of 2 pmol μl^{-1}. Either purified DNA or single bacterial colonies ('colony PCR') were used as DNA templates. The DNA from the bacterial colonies is accessible for the Taq- or Pfu-polymerase due to cell lysis that occurs during the first 95°C/98°C heating steps of the PCR reaction. The components contained in standard PCR reactions are given in Table 5, standard cycler programs in Table 6.

Table 5: Components of standard PCR reactions.

Control PCR (Mango Mix)	***iProof-PCR***
5 µl forward primer	12.5 µl forward primer
5 µl reverse primer	12.5 µl reverse primer
10 µl ready-to-use Taq-polymerase mixture	10 µl iProof buffer 5x
	1 µl dNTP mix [10 mM]
	1.5 µl DMSO
	12 µl Aqua dest.
	0.5 µl iProof DNA polymerase (2 U μl^{-1})
Template: A single colony or 0.5 µl of plasmid DNA solution (~50 ng ml^{-1})	

Table 6: Standard PCR-cycler programs.

			Taq polymerase		***iProof polymerase***
No	*Phase*	*Temperatur e*	*Duration*	*Temperature*	*Duration*
1	Initial denaturation	95°C	2:30 min	98°C	2:30 min

2	Denaturation	95°C	0:30 min	98°C	0:30 min
3	Annealing	55°C	0:30 min	55°C	0:30 min
4	Elongation	72°C	0:30 min per 1000 base pairs	72°C	0:30 min per 1000 base pairs
5	Final Elongation	72°C	5 min	72°C	10 min
6	Cooling	12°C	forever	12°C	forever

Thirty cycles consisting of phases 2 to 4 were routinely performed.

2.1.1.1 Fusion-PCR reaction

To combine two DNA fragments by PCR, both fragments were first amplified separately but with primers that added a 20 base pair region homologous between both fragments. Both purified fragments were then used as templates in a second PCR reaction with two primers from the first reaction that amplify the entire fragment (compare Figure 3, page 42).

2.1.1.2 Primer list

Table 7: Primers used in this thesis (5'-3').

	Name	***Sequence***	***Function of the primer***
1	S1659upstrfor	ATGATTACGAATTCGAGCTCGGTACCCGGGTCGGCGCTACAATCAAACCC	Amplifies a 500 base pair region upstream of *SO_1659*
2	S1659upstr_rev	CAAAGGTACTAGTACCATCGCGTCCCTTTTCTTTC	Amplifies a 500 base pair region upstream of *SO_1659*
3	S1659downstr_for	AAAAGGGACGCGATGGTACTAGTACCTTTGGGTTG	Amplifies a 500 base pair region downstream of *SO_1659*
4	S1659downstrrev	CGGCCAGTGCCAAGCTTGCATGCCTGCAGGGCGGGTTGACATTCCAAGG	Amplifies a 500 base pair region downstream of *SO_1659*
5	Delta1659for2	CTCGTACCGCTATCAGTATC	Testprimer to control SO_1659 deletion.
6	Delta1659rev2	GGTTTACGAGCCTGACAC	Testprimer to control SO_1659 deletion.

	Name	***Sequence***	***Function of the primer***
7	S2931upstrfor	ATGATTACGAATTCG AGCTCGGTACCCGGG GGATGAAACGACAG TCGCG	Amplifies a 500 base pair region upstream of *SO_2931*
8	S2931upstrrev	GTTGAGGTTATGTAC ATGAGTTATCCGCTC GTGAG	Amplifies a 500 base pair region upstream of *SO_2931*
9	S2931downstrfor	GAGCGGATAACTCAT GTACATAACCTCAAC TCGGC	Amplifies a 500 base pair region upstream of *SO_2931*
10	S2931downstrrev	CGGCCAGTGCCAAGC TTGCATGCCTGCAGG GAGCGATCGCAGTTT TCGAC	Amplifies a 500 base pair region upstream of *SO_2931*
11	Del_2931for	ACCTTAGCCAAGTGT CAC	Testprimer to control SO_2931 deletion.
12	Del_2931rev	TTGAAACTGTGCTGA AGG	Testprimer to control SO_2931 deletion.
13	OmcA_AflIII_for	GAAATATCATGATGA AACGGTTC	Amplifies *omcA* for cloning in pBad202
14	omcA_TOPO_rev	AGCTTTGTTTAAACT TATTTTTCGAACTGC GGGTGGCTCCAGTTA CCGTGTGCTTCCAT	Amplifies *omcA* for cloning in pBad202, contains sequence for strep-tag
15	OmcA_AflIII_rev	GCGTTTAAACTTAGT TACCGTGTGCTTC	Amplifies *omcA* for cloning in pBad202, contains no strep-tag
16	SO_1659_TOPO_f or	CACCATGGGCAAAA ACTACAATAAATCTC TACTG	Amplifies *SO_1659* for cloning in pBad202
17	SO1659TOPPmeIr ev	AGCTTTGTTTAAACT TATTTTTCGAACTGC GGGTGGCTCCAGTGT GCTACCTCTGCGTG	Amplifies *SO_1659* for cloning in pBad202, contains sequence for strep-tag
18	pBAD_test_for	GATTAGCGGATCCTA CCTG	Testprimer to amplify pBAD202 insert
19	pBAD_test_rev	GGACCACCGCGCTAC TGC	Testprimer to amplify pBAD202 insert
20	pMQ150for	CTGGCGAAAGGGGG ATGTG	Testprimer to amplify pMQ150 insert
21	pMQ150rev	CATTAGGCACCCCAG GCTTTAC	Testprimer to amplify pMQ150 insert
22	mtrFAB UP_for	ATGATTACGAATTCG AGCTCGGTACCCGGG CTGACCGCGAATGGT GAG	Amplifies $mtrF_{strep}$ and a 500 base pair region homologous to *araC* in ΔOMC

	Name	***Sequence***	***Function of the primer***
23	mtrFAB Strep_rev	TCTTCATAATAGGCT TCCCAATTTGTCCCA TTATTTTTCGAACTG CGGGTG	Amplifies $mtrF_{strep}$ and a 500 base pair region homologous to *araC* in ΔOMC
24	mtrFAB DOWN_for	TGGGACAAATTGGG AAGCC	Amplifies a 500 base pair region homologous to *mtrA* in ΔOMC
25	mtrFAB DOWN_rev	CGGCCAGTGCCAAGC TTGCATGCCTGCAGG GCAACATCGGCATTG TCATG	Amplifies a 500 base pair region homologous to *mtrA* in ΔOMC
26	mtrFAB Sequenzierung 1_for	GCAGACATTGCCATT GTGATGG	Sequencing of new DNA fragments in MTR-FAB strain
27	mtrFAB Seq 2	GCGTCGGCGAGCATA TTCG	Sequencing of new DNA fragments in MTR-FAB strain
28	mtrFAB Seq 3	GACCGTGATTGTGCC ATTGG	Sequencing of new DNA fragments in MTR-FAB strain
29	mtrFAB Seq 4	CATAATGTTGGTTGG TTATAGGGAG	Sequencing of new DNA fragments in MTR-FAB strain
30	mtrFAB Seq 5	TTGCAAACTTATTCA TGAATTCGCTAG	Sequencing of new DNA fragments in MTR-FAB strain
31	NapUp_for	ATGATTACGAATTCG AGCTCGGTACCCGGG _GGTATCGTGATTGG TGTTGTG	Amplifies a 500 base pair region upstream of insertion site behind *cymA*
32	NapUp_rev	TTATCCTTTTGGATA GGGGTGAG	Amplifies a 500 base pair region upstream of insertion site behind *cymA*
33	EcoliNapC_for	GGTGTCGCTCACCCC TATCCAAAAGGATAA _AGAGGTTATTATGG GAAATTCTGACC	Amplifies *napC* from *E. coli* for integration behind *cymA* of *S. oneidensis*
34	EcoliNapC_rev	TTATTTTTCGAACTG CGGGTGGCTCCA_AA AACCTGGCTCGACTT C	Amplifies *napC* from *E. coli* for integration behind *cymA* of *S. oneidensis*, contains sequence for strep-tag
35	NapDown_for	TTTTTGGAGCCACCC GCAGTTCGAAAAATA A_GGTTTAACGCTGC AATAGTG	Amplifies a 500 base pair region downstream of insertion site behind *cymA*
36	NapDown_rev	CGGCCAGTGCCAAGC TTGCATGCCTGCAGG _CAATGAGATGTTAG AACGCAC	Amplifies a 500 base pair region downstream of insertion site behind *cymA*

	Name	***Sequence***	***Function of the primer***
37	NapCym_test-for	TAGAGTAATGAACTG GCGTGC	Sequencing of new DNA fragments in MTR-FAB-NapC strain
38	NapCym_test-rev	TGACGACTCACAATC ACATGAC	Sequencing of new DNA fragments in MTR-FAB-NapC strain
39	Invit_mtrA-for	TTTGGGCTAGAAATA ATTTTGTTTAACTTTA AGAAGGAGATATAC ATACC_ GAAGCCTATTATGAA GAACTGCC	Amplifies *mtrA* for cloning in pBad202
40	Invit_mtrA-rev	GGCTGAAAATCTTCT CTCATCCGCCAAAAC AGCCAAGCTGGAGA CCGTTT_TTAGCGCT GTAATAGCTTGC	Amplifies *mtrA* for cloning in pBad202
41	Invit_mtrB-for	TTTGGGCTAGAAATA ATTTTGTTTAACTTTA AGAAGGAGATATAC ATACC_GGAGACGAG AAAATGAAATTTAAA CTC	Amplifies *mtrB* for cloning in pBad202
42	Invit_mtrBstrep-rev	GGCTGAAAATCTTCT CTCATCCGCCAAAAC AGCCAAGCTGGAGA CCGTTT_TTATTTTTC GAACTGCGGGTGGCT CCA_GAGTTTGTAAC TCATGCTCAGC	Amplifies *mtrB* for cloning in pBad202, contains sequence for strep-tag
43	mtrB_in_rev	CACCCACAGTGCCTG ATG	Amplifies *mtrA* for cloning in pBad202
44	mtrB_in_for	GCTGTAAAGGCTGCG TCG	Amplifies *mtrB* for cloning in pBad202

2.2 Transformation of bacterial cells

E. coli and *S. oneidensis* cells that are not naturally competent to incorporate foreign DNA can acquire competence by artificial means. The cells are subjected to a brief strong voltage pulse that enables DNA uptake. This technique called electroporation requires the preparation of "electro-competent" cells. For this purpose, cells were grown in SOB medium (2% bacto-tryptone, 0.5% yeast extract, 0.58 g^{-1} NaCl and 0.19 g^{-1} KCl). SOB is characterised by a reduced concentration of electrolytes. When the culture's OD_{600nm} reached 0.5-0.7, the cultivation was stopped by cooling the flask on ice for 30 min. Cell suspensions were pelleted in a cooled centrifuge and washed twice with ice-cold 10%

(v/v) glycerol solution. Aliquots of competent cells were either frozen in liquid nitrogen and stored at -70°C or used for electroporation immediately.

For the electroporation, usually 50 µl competent cells and 2 µl DNA solution were pipetted into an ice cold electroporation cuvette (Peqlab) with 1 mm distance between the electrodes. Subsequent to the voltage pulse (1.75 kV for 5 ms) from the Micropulser (Bio-Rad) 450 µl of prewarmed SOC medium devoid of antibiotics was added to the cells, mixed gently and transferred into a fresh culture tube. SOC medium consists of 9.44 ml SOB, 0.2 ml 1 M $MgCl_2$ and 0.36 ml 10% (w/v) glucose. If working with *E. coli* WM3064, the SOC medium was supplemented with 0.3 mM DAP. The cell suspension was incubated at optimal growth temperature for one hour under continuous shaking in order to promote the expression of antibiotic resistance genes. For the transformation of *Shewanella*, cells were incubated in the SOC medium for 15 h at room temperature. Afterwards, the cells were spread onto agar plates supplemented with kanamycin.

2.3 Transformation of yeast cells

Yeast cells were transformed with the LiAc/PEG/ssDNA method (Shanks *et al.*, 2006). High concentrations of alkali cations such as lithium acetate (LiAc) increase the permeability of the yeast cell wall. Single-stranded carrier DNA (ssDNA) preferentially binds to the cell wall and thereby increases the amount of plasmid DNA that is available for DNA uptake. Polyethylene glycol (PEG) was reported to deposit DNA onto the cell surface and increases thereby the DNA uptake (Gietz *et al.*, 1995).

A pellet from an overnight yeast culture was washed once and resuspended in 500 µl sterile Tris-EDTA buffer (Table 8). Single-stranded carrier DNA was obtained by boiling an aliquot of salmon sperm solution at 95°C in a water bath for 15 min and immediate transfer onto ice afterwards to maintain the single strand state. 500 µl 'Lazy bones solution' (Table 8) and 20 µl of ssDNA were added to the cell suspension, as well as the linearised plasmid and the PCR products that were supposed to be transformed into yeast cells. After vortexing thoroughly for 1 min, the whole reaction was incubated at room temperature for 36 hours. The cells were then heat-shocked at 42°C in a water bath for 10-12 min to further facilitate DNA uptake. Before plating them on Ura-plates cells were washed in Tris-EDTA buffer once and resuspended in 300 µl buffer to remove PEG which inhibits growth of the cells.

Table 8: Solutions used for transformation of yeast cells.

Solutions	***Composition***
Tris-EDTA buffer	10 mM Tris-HCl (pH 8.5) 1 mM EDTA
Lazy bones solution	40% (w/v) polyethylene glycol (PEG) 100 mM lithium acetate 10 mM Tris-HCl (pH 7.5) 1 mM EDTA
Carrier DNA solution	2 mg ml^{-1} salmon sperm dissolved in Tris-EDTA buffer

2.4 Genome sequencing

Genomic DNA was sequenced on an Illumina HiSeq 2000 with a read length of 46 base pairs by GATC Biotech. The reads were assembled using the software BWA (Li and Durbin, 2009), identification of single nucleotide polymorphisms as well as insertions and deletions was done with SAMtools (Li and Durbin, 2009) and the assembly viewer Tablet (Milne *et al.*, 2010).

2.5 General methods for plasmid cloning

General methods for plasmid cloning and mutant generation are described below. Detailed descriptions for each plasmid and each strain with all primers and enzymes used can be found in section VI. 2.6, page 39ff.

2.5.1 “Classical” cloning

The DNA fragment to be inserted in a plasmid was amplified by PCR with primers that included a recognition site for restriction endonucleases. Subsequently, vector DNA and PCR fragment were treated with restriction endonucleases to produce ends that match. After purification, vector and insert were ligated with T4 DNA Ligase and transformed into *E. coli.* All reactions were performed according to the manufacturer’s instructions.

2.5.2 TOPO-cloning

This cloning procedure takes advantage of a topoisomerase, originally from vaccinia virus. This topoisomerase is covalently bound to an opened vector and enables integration of a DNA fragment from a PCR reaction without further enzymes. The PCR fragment needs to contain a recognition sequence (CACC) and must be performed with a Pfu-

polymerase, which is producing blunt ends. The topoisomerase-reaction was performed according to manufacturer's instructions (Invitrogen).

2.5.3 Cloning based on yeast cell homologous recombination

Yeast cells recognize homologous DNA regions and can recombine them. The homology does not need to be longer than 30 base pairs. Vector and inserts can thus be assembled without the need for restriction enzyme sites (Shanks *et al.*, 2006). The vector contains an origin of replication for yeast cells (CEN/ARSH) and a selection marker for yeast cells (e.g. *Ura3* gene, conferring the ability to synthesize uracil). Additionally, it has an origin of replication for bacteria and an appropriate selection marker conferring antibiotic resistance. Cloning and transformation procedure in yeast cells is a one step method described in section VI. 2.3, page 36.

2.5.4 Isothermal DNA assembly

This cloning method used the conjoint enzymatic reactions of a T5-Endonucelase (Epicentre), of a Pfu-polymerase (Biorad), and of a T4 ligase (New England Biolabs) to combine a PCR fragment with short homologous regions to a linearized vector (Gibson *et al.*, 2009). The reaction buffer for isothermal DNA assembly (Table 9) was stored in 15 µl aliquots at -20°C. For the reaction, 2.5 µl of linearized vector (containing ca. 30 ng DNA) and 2.5 µl PCR fragment (containing ca. 60 ng DNA) were mixed with a 15 µl aliquot of reaction buffer and incubated for 1 h at 50°C in a Thermocycler. After a 30 min dialysis step, the DNA can be directly transformed into *E. coli.*

Table 9: Reaction buffer for isothermal DNA assembly.

Substance	***Components***	***Volume used***
iProof polymerase (2 U μl^{-1})	-	5 µl
Taq DNA ligase (40 U μl^{-1})	-	40 µl
T5 Exonuclease (0.1 U μl^{-1})	-	16 µl
5x reaction buffer	25% PEG-8000, 500 mM Tris-HCl pH 7.5, 50 mM $MgCl_2$, 50 mM DTT, 1 mM each of the four dNTPs and 5 mM NAD	80 µl
Aqua dest.	-	239 µl

The sequence of the insert regions of all plasmids obtained was analyzed by sequencing carried out by GATC Biotech.

2.6 Detailed cloning procedures of plasmids used in this thesis

2.6.1 Cloning of outer membrane cytochrome proteins

The genes *mtrC*, *mtrF* and SO_1659 coding for outer membrane cytochromes were already cloned during my "Staatsexamensarbeit" (Bücking, 2007).

2.6.1.1 pBAD202*SO_2931*$_{strep}$ and pBAD202*SO_1659*$_{strep}$

Gene *SO_1659*$_{strep}$ was cloned into pBAD202 via TOPO cloning (Invitrogen). The gene was amplified using primers 16 and 17 and was thereby modified to contain an NcoI restriction site and the sequence for a C-terminal strep-tag. Genomic DNA from *S. oneidensis* was used as template. His-patch thioredoxin was excised from the vector by cleavage with NcoI and subsequent religation.

2.6.1.2 pBAD202*omcA*$_{strep}$ and pBAD202*omcA*

pBAD202*SO_2931*$_{strep}$ vector was used as backbone for cloning *omcA* and *omcA*$_{strep}$ by "classical cloning" technique. *SO_2931*$_{strep}$ was excised from the vector by cleavage with NcoI/PmeI enzymes. *omcA* was amplified by PCR using primers 13 and 15 adding the sequence for BspHI and PmeI cleavage sites. *omcA*$_{strep}$ was amplified using primers 13 and 14 adding the sequence for BspHI and PmeI cleavage sites and a C-terminal strep-tag. Genomic DNA from *S. oneidensis* was used as template for both fragments. The resulting PCR fragments were digested with BspHI and PmeI and subsequently ligated into the pBAD202 vector backbone.

The length of the insert sequences introduced into pBAD202 vector was controlled by PCR with primers 18 and 19. Sequencing of the insert sequences was either done with purified DNA from this PCR reaction or with isolated plasmid DNA.

2.6.2 Cloning of *mtrA*, *mtrB* and their mutated versions *mtrA*^{S}, *mtrB*^{S}

Genomic DNA of *S. oneidensis* wild type was used as a template to amplify *mtrA* and *mtrB*. Genomic DNA of *S. oneidensis* ΔOMC^S was used as a template to amplify *mtrA*^{S} and *mtrB*^{S}. pBAD202*SO_2931*, cleaved with NcoI and PmeI was used as vector backbone. Assembly of vector backbone and inserts was conducted using the isothermal DNA assembly method. The overlap between PCR fragment and linearized plasmid or between two PCR fragments was 50 base pairs long. All inserts of the resulting plasmids were amplified with primers 18 and 19 and the sequence was verified (GATC Biotech).

2.6.2.1 pmtrA^S

mtrA^S was amplified with primers 39 and 40 using genomic DNA of *S. oneidensis* ΔOMC^S as a template. The resulting fragment was integrated into pBAD202 vector by isothermal DNA assembly method.

2.6.2.2 pmtrB^S

mtrB^S was amplified with primers 41 and 42 adding a sequence coding for a C-terminal strep-tag. Genomic DNA of *S. oneidensis* ΔOMC^S as a template. The resulting fragment was integrated into pBAD202 vector using the isothermal DNA assembly method.

2.6.2.3 pmtrAmtrB

mtrA and *mtrB* were amplified with primers 39 and 42 adding a sequence coding for a C-terminal strep-tag to *mtrB*. Genomic DNA of *S. oneidensis* wild type was used as a template. The resulting fragment was integrated into pBAD202 vector using the isothermal DNA assembly method.

2.6.2.4 pmtrA^{S}mtrB^S

mtrA^S and *mtrB*^{S} were amplified with primers 39 and 42 adding a sequence coding for a C-terminal strep-tag to *mtrB*^{S}. Genomic DNA of *S. oneidensis* ΔOMC^S was used as a template. The resulting fragment was integrated into pBAD202 vector using the isothermal DNA assembly method.

2.6.2.5 pmtrAmtrB^S

mtrA was amplified with primers 39 and 43 using genomic DNA of *S. oneidensis* wild type as a template. *mtrB*^{S} was amplified with primers 44 and 42, adding a sequence coding for a C-terminal strep-tag to *mtrB*^{S} and using genomic DNA of *S. oneidensis* ΔOMC^S as a template. Both fragments containing overlapping regions were integrated into pBAD202 vector in one step using the isothermal DNA assembly method.

2.6.3 Cloning of suicide vectors for gene deletions

2.6.3.1 pMQ150ΔSO1659 and pMQ150ΔSO2931

pMQ150ΔSO1659 was designed to delete SO_1659 from the chromosome of the existing strain JG53 (Δ*mtrD-mtrE*, *araC*, P_{BAD}). Primers 1 and 2 were used to amplify a 500 base pair region upstream of SO_1659, primers 3 and 4 amplified a 500 base pair region downstream of the gene. The fragments were combined with the yeast cloning method.

pMQ150ΔSO2931 was designed to subsequently delete SO_2931 from the chromosome. Primers 7 and 8 were used to amplify a 500 base pair region upstream of SO_1659, primers 9 and 10 amplified a 500 base pair region downstream of the gene. The fragments were also combined with the yeast cloning method.
The inserts of both plasmids were amplified with primers 20 and 21 and the sequence was verified (GATC Biotech).

2.6.3.2 pMQ150mtrFAB

pMQ150mtrFAB was designed to introduce *mtrF* into the existing strain ΔOMC behind the genes *mtrA* and *mtrB*. Figure 3 illustrates the procedure described below. Primers 22 and 23 were used to amplify *mtrF* containing a C-terminal strep-tag and a 500 base pair region homologous to the DNA upstream of the insertion site in ΔOMC corresponding to a part of *araC* gene. As a template for this PCR reaction, plasmid DNA from pBAD$mtrF_{strep}$ was used. Primers 24 and 25 were used to amplify a 500 base pair region homologous to the DNA downstream of the insertion site in ΔOMC corresponding to a part of *mtrA* gene. Both fragments were combined by fusion-PCR technique and then cloned into a linearized pMQ150 plasmid using the isothermal DNA assembly method. For verification, the insert region was amplified with primers 20 and 21 and sequenced at GATC Biotech.

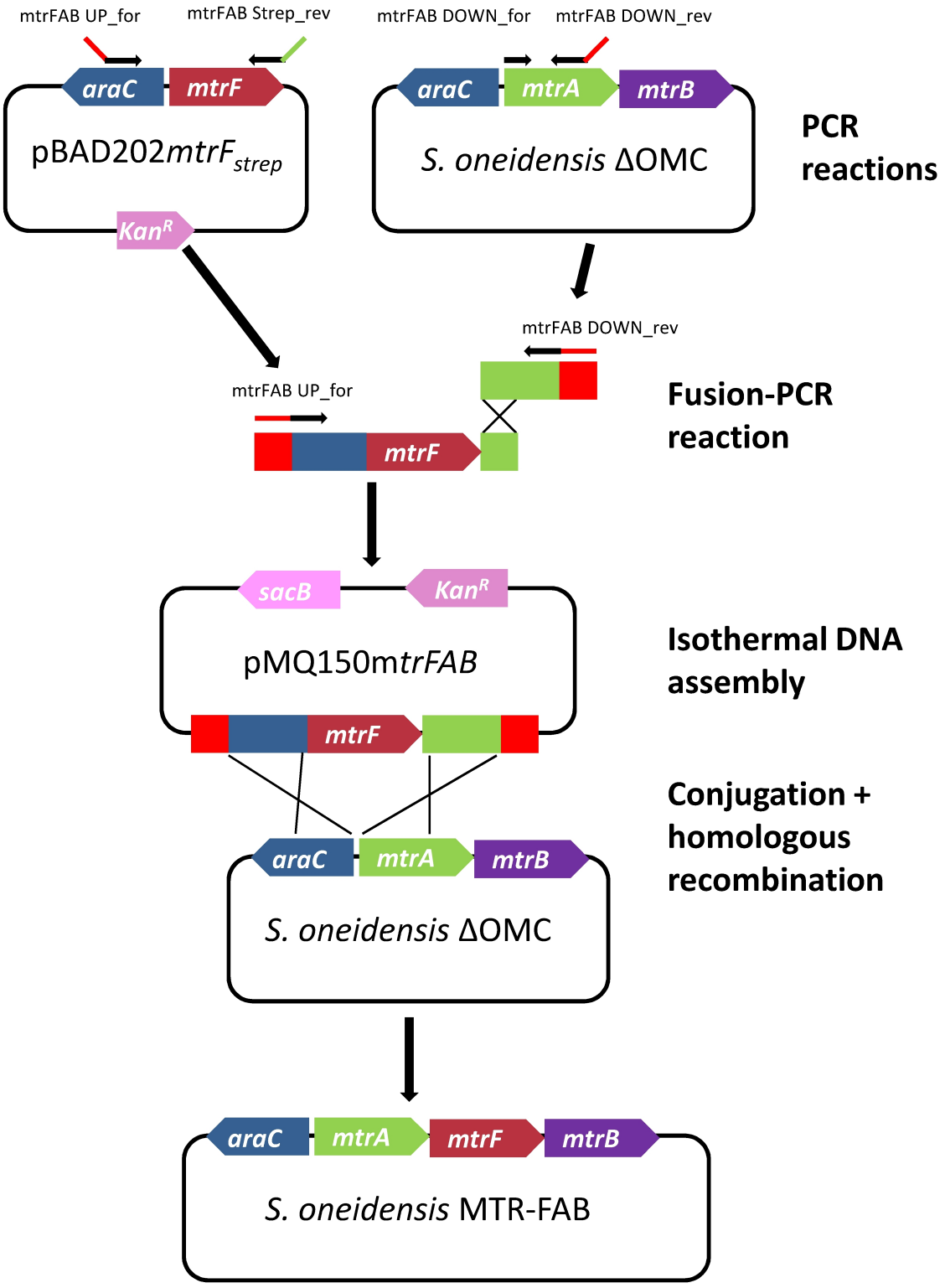

Figure 3: Cloning scheme for the construction of strain MTR-FAB.

2.6.3.3 pMQ150NapC

pMQ150NapC was designed to introduce *napC* from *E. coli* into the existing strain ΔOMC behind the *cymA* gene. Primers 31 and 32 were used to amplify a 500 base pair region upstream of the insertion site, corresponding to a part of *cymA*, primers 35 and 36 were used to amplify a 500 base pair region downstream of the insertion site. For both reactions, genomic DNA of *S. oneidensis* wild type was used as a template. The third fragment was amplified with primers 33 and 34 using a single colony from *E. coli* DH5α as a template. All three fragments were assembled with the yeast cloning method in one step. For verification, the insert region was amplified with primers 20 and 21 and sequenced at GATC Biotech.

2.6.4 Plasmid list

All plasmids used in this thesis are listed in Table 10.

Table 10: Plasmids used in this thesis.

Plasmid	***Relevant genotype***	***Source or Reference***
pMQ150	Deletion vector, cen/arsh, *ura3*, Km^r, *sacB,* R6K-ori	(Shanks *et al.*, 2006), accession no.: EU546823
pMQ150ΔSO1659	pMQ150 for deletion of SO_1659	(Bücking *et al.*, 2010)
pMQ150ΔSO2931	pMQ150 for deletion of SO_2931	(Bücking *et al.*, 2010)
pMQ150ΔgspD	pMQ150 for deletion of *gspD*	this thesis
pMQ150ΔdmsA-1 dmsB-1	pMQ150 for deletion of *dmsA-1* and *dmsB-1*	this thesis
pMQ150ΔdmsA-2 dmsB-2	pMQ150 for deletion of *dmsA-2* and *dmsB-2*	this thesis
pMQ150mtrFAB	pMQ150 for integration of *mtrF* into ΔOMC	this thesis
pMQ150NapC	pMQ150 for integration of *napC* into MTR-FAB strain	this thesis
pBAD202	Expression vector, Km^r, arabinose inducible promoter	Invitrogen
pBAD202-$omcA_{strep}$	pBAD202 with $omcA_{strep}$	(Bücking *et al.*, 2010)

Plasmid	***Relevant genotype***	***Source or Reference***
pBAD202-*mtrC*$_{strep}$	pBAD202 with *mtrC*$_{strep}$	(Bücking *et al.*, 2010)
pBAD202-*mtrF*$_{strep}$	pBAD202 with *mtrF*$_{strep}$	(Bücking *et al.*, 2010)
pBAD202-*SO_1659*$_{strep}$	pBAD202 with *SO_1659*$_{strep}$	(Bücking *et al.*, 2010)
pBAD202-*SO_2931*$_{strep}$	pBAD202 with *SO_2931*$_{strep}$	(Bücking *et al.*, 2010)
pBAD202-*omcA*	pBAD202 with *omcA*	(Bücking *et al.*, 2010)
pBAD202mtrA$_{strep}$	pBAD202 with *mtrA*$_{strep}$	(Schuetz *et al.*, 2009)
pmtrA^{S}	pBAD202 with *mtrA*^{S}	this thesis
pmtrB^{S}	pBAD202 with *mtrB*^{S}	this thesis
pmtrAmtrB	pBAD202 with *mtrA* and *mtrB*	this thesis
pmtrA^{S}mtrB^{S}	pBAD202 with *mtrA*^{S} and *mtrB*^{S}	this thesis
pmtrAmtrB^{S}	pBAD202 with *mtrA* and *mtrB*^{S}	this thesis

2.7 Construction of deletion mutants

In-frame deletions were introduced into *Shewanella* strains by using a two-step homologous recombination protocol (Saltikov and Newman, 2003). pMQ150 suicide plasmids with regions homologous to the genome were integrated into the genome and transiently rendered cells resistant to kanamycin. After a second recombination event, suicide plasmids were lost thereby either restoring the original state or removing the gene of interest.

pMQ150 plasmid DNA with inserts was either isolated from yeast cells by 'Smash and Grab' method or directly produced *in vitro* by isothermal DNA assembly. In both cases, the plasmid DNA was transformed into *E. coli* DH5α λ(*pir)* strain (JG152). This strain was necessary because pMQ150 has a R6K-type origin of replication and is only replicated in cells that are expressing the π protein, encoded by the *pir* gene. π protein is essential for the stabilisation of the R6K ori. Afterwards, the plasmid was subcloned into the mobilizing strains *E. coli* WM3064 (JG98) or S17 (JG144) which both have *pir* genes for plasmid maintenance and *tra* genes that enable conjugation. Additionally, strain

WM3064 is auxotrophic and can only grow if a building block for cell wall synthesis (diaminopimelic acid, DAP) is present in the medium.

Conjugation of *E. coli* with *Shewanella* was done by incubation on LB-agar plates for 8 hours. For this purpose, 1 ml of a *Shewanella* overnight culture and 2 ml of a WM3064 culture grown overnight on LB+DAP were harvested and washed twice in LB+DAP. The pellets were combined in 0.5 ml LB+DAP and 100 µl of the resulting cell suspension was plated on a 'mating plate' (LB+DAP). After 8 hours of incubation at 30°C, cells were resuspended by the addition of 1 ml LB. Several dilutions from the resulting suspension were spread on LB plates containing 25 µg ml^{-1} kanamycin (LB+Kan). *E. coli* WM3064 cells were not able to grow on LB plates because DAP was absent. Since the genome of *S. oneidensis* does not contain the *pir* gene, pMQ150 cannot be replicated. Thus only transconjugants which had integrated the plasmid into the genome through a cross-over event were able to grow on kanamycin. The procedure with *E. coli* S17 was principally the same but is based on a growth advantage of *S. oneidensis* at 30°C and visual differentiation between white *E. coli* colonies and reddish *S. oneidensis* colonies. Additional steps to streak-purify the transconjugants were necessary. The integration of pMQ150 into the genome of *S. oneidensis* was further checked by testing the growth behaviour of the cells on LB supplemented with 10% sucrose (Suc). This was done by 'Pick & Patch' technique that consists of re-streaking single colonies with a sterile pipette tip on three different fresh LB plates: First on LB+Kan, followed by LB+Kan+Suc and an LB plate in the end. Growth on the last LB plate made sure that a sufficient number of cells had adhered to the tip. In contrast, growth deficiency on sucrose confirmed the successful integration of pMQ150 into the genome. pMQ150 contains the *sacB* gene conferring a sensitivity to sucrose due to the activity of the enzyme levansucrase. This enzyme catalyses the synthesis of sugar polymers in the periplasm which hinders diffusion and eventually causes cell death.

The second cross-over was performed by culturing positive clones from the first cross-over event for 8 hours in liquid LB in the absence of antibiotic. Several dilutions were prepared in fresh LB (1:10, 1:100, 1:1000) and plated on LB+Suc plates to screen for cells having lost the deletion plasmid from their chromosome. Single colonies appearing on LB+Suc plates were streak-purified once and finally tested by 'Pick & Patch' in the order LB+Suc, by LB+Kan, and LB. Cells not growing on LB+Kan plates were screened by colony PCR to differentiate between cells that had restored the original state and cells

that had a truncated or modified DNA fragment. One positive clone was chosen and the mutation obtained was analysed by a PCR reaction with primers binding outside of the 500 base pair homologous regions. The PCR product was sequenced (GATC Biotech).
All gene deletions introduced during this thesis were done with this technique. Strain JG53 (*S. oneidensis* MR-1 Δ(*mtrD-mtrC*), generated during my "Staatsexamensarbeit" was used as basis for the deletion of SO_1659 and SO_2931 that resulted in strain JG132 (ΔOMC) (Bücking, 2007).

3. Electrophoretic techniques

3.1 Agarose gel electrophoresis

Agarose gel electrophoresis was used to separate and visualize DNA samples (Sambrook *et al.*, 1989). Small format gels were made by boiling 1% (w/v) dry agarose suspended in 50 ml TAE buffer (Table 11) until it became clear. The solution was cooled to 60°C and then 5 µl of a Redsafe (Chempur) stock solution (diluted 1:5) was added before pouring. Redsafe intercalates into the DNA helix and shows then fluorescence of orange color upon excitation with UV-light (312 nm). The Redsafe concentration was 2.5 times less than recommended by the manufacturer but yielded strong fluorescence. DNA samples were mixed with 6-fold loading buffer (Table 12) unless they already contained it, e.g. MangoMix PCR reactions. The gel chamber was filled with TAE buffer and a constant voltage of 120 V was applied. A DNA size marker was always included in the gel (Gene ladder, Fermentas) to determine relative sizes of DNA fragments.

Table 11: TAE-buffer (50-fold stock solution).

Component	***Amount used***
Tris-HCl pH 8	242 g
Glacial acetic acid	57.1 ml
0.5 M EDTA	100 ml
Aqua dest.	ad 1000 ml

Table 12: Agarose gel loading buffer (6-fold).

Component	***Amount used***

Glycerol	6 ml
50x TAE buffer stock	1.2 ml
Aqua dest.	2.8 ml
Bromophenol blue 0.25% (w/v)	1 ml

3.2 Polyacrylamide gel electrophoresis

Discontinuous sodium dodecyl sulphate polyacrylamide gel electrophoresis (SDS-PAGE) was used to separate mixtures of proteins (Laemmli, 1970). Components for separating gel and stacking gel are listed in Table 13 and 14. Glass plates were cleaned using 70% (v/v) ethanol to remove traces of fat from the surface and stacked in multicasting chamber (Biorad) that allows to prepare 10 mini gels at once. All components of the separating gel were mixed with the exception of TEMED and APS. These two substances that promote polymerisation of the gel were added immediately before pouring the separating gel with a 60 ml syringe. The gels were covered with isopropanol to create a flat surface. After polymerisation (ca. 30 min), the isopropanol was washed away with Aqua dest. and the stacking gel solution was added from the top. A clean comb was inserted to create pouches for sample loading. SDS-gels were used immediately or stored at 4°C wrapped in wet paper towels to avoid drying of the gels.

Samples were first boiled in sample buffer (Table 15) containing SDS and β-mercaptoethanol for 2 min to unfold proteins and mask their native charge. PageRuler™ Prestained Protein Ladder (Fermentas) was included as a length marker on every gel.

Gels were run at room temperature in electrophoresis buffer (Table 16). A constant voltage of 120 V was applied until the electrophoresis front reached the bottom of the gel.

Table 13: Separating gel 10% (w/v), mixtures for 11 mini gels.

Component	***Volume***	***Composition***
Acrylamide solution	28.9 ml	30% (w/v) acrylamide, 0.8% (w/v) bisacrylamide
Separating gel buffer	21.6 ml	2 M Tris-Hcl pH 8.8
SDS stock solution	866 µl	10% (w/v) SDS in Aqua dest.

Aqua dest.	35.2 ml	
TEMED	116 µl	
Ammonium persulfate solution (APS)	578 µl	10% (w/v) APS in Aqua dest.

Table 14: Stacking gel 4% (w/v), Mixture for 11 mini-gels.

Component	***Volume***	***Composition***
Acrylamide solution	6.8 ml	30% (w/v)acrylamide, 0.8% (w/v) bisacrylamide
Stacking gel buffer	6.2 ml	1 M Tris-Hcl pH 6.8
SDS stock solution	495 µl	10% (w/v) SDS in Aqua dest.
Aqua dest.	35.9 ml	
TEMED	83 µl	
Ammonium persulfate solution (APS)	330 µl	10% (w/v) APS in Aqua dest.

Table 15: SDS-gel sample buffer (2-fold).

Component	***Volume***
Aqua dest.	380 µl
Stacking gel buffer	120 µl
SDS stock solution	200 µl
Glycerol	150 µl
Bromophenol blue solution 0.25% (w/v)	100 µl
β-mercaptoethanol	50 µl

Table 16: SDS-gel electrophoresis buffer.

Component	***Concentration***
Tris	3 g

Glycine	14.4 g
SDS	1 g
Aqua dest.	ad 1000 ml

3.2.1 Staining of heme proteins in SDS-gels

The heme staining is based on the peroxidase activity of proteins containing heme groups. Heme containing bands on polyacrylamide gels stain blue when tetramethylbenzidine (TMB) is added in the presence of hydrogen peroxide (Thomas *et al.*, 1976). After completion of an SDS-PAGE run, gels were immediately placed in a 12.5% (w/v) trichloroacetic acid (TCA) bath for 30 min to fixate proteins in the gel matrix. After washing for 30 min with Aqua dest, the gels were covered with TMB solution supplemented with citrate buffer (Table 17). The staining reaction was initiated by the addition of H_2O_2 and gels were usually scanned after 30 min.

Interestingly, it was observed that the intensity of the heme containing bands was markedly decreased when the samples were boiled for more than 2 min.

Table 17: Solutions for heme staining of SDS-gels.

Component	***Volume***	***Composition***
Citrate buffer	1 ml	0.5 M citric acid/sodium citrate buffer pH 6.4
TMB solution	9 ml	10 mg 3,3,5,5-tetramethylbenzidine dissolved in 9 ml Aqua dest.
H_2O_2 solution	20 µl	30% (w/v) H_2O_2 in Aqua dest.

Alternatively or additionally, all proteins in the gel were stained unspecifically with Coomassie blue R250. The SDS gel was incubated in Coomassie staining and fixating solution for at least 1 hour either immediately after running the gel or after heme staining procedure. To visualize protein bands, the gel was subjected to a destaining procedure consisting of incubation in Destaining solution I until protein bands are visible and subsequent incubation in Destaining solution II to reduce background staining. All solutions needed are listed in Table 18.

Table 18: Solutions for Coomassie blue staining of SDS-gels.

Solution	***Composition***
Coomassie staining and fixating solution	0.25% (w/v) Coomassie Blue R250 30% (v/v) methanol 20% (v/v) acetic acid
Destaining solution I	30% (v/v) methanol 20% (v/v) acetic acid
Destaining solution II	10% (v/v) acetic acid

3.3 Western blotting

Proteins that had been separated by SDS-PAGE were transferred onto sheets of nitrocellulose paper by Western blotting using the semi-dry protocol to visualize proteins detected with immunostaining procedures.

For that purpose six Whatman filter papers and one sheet of nitrocellulose paper (Schleicher und Schüll) were cut to the size of the separating gel that was to be blotted. The filter papers and the nitrocellulose membrane were soaked in transfer buffer (Table 19). A stack of three filter papers followed by the polyacrylamide gel, nitrocellulose membrane, and three more filter papers were placed onto the cathode. The anode was placed on top of the sandwich and the whole assembly was connected to a power supply and a current of 1.5 mA cm^{-2} was applied for one hour.

Table 19: Solutions for western blot transfer buffer.

Component	***Concentration***
Glycine	39 mM
Tris	48 mM
Methanol	20% (v/v)
SDS	0.037%

3.3.1 Immunodetection on western blots

Strep-tag labelled protein that had been immobilised on a nitrocellulose membrane was detected with antibodies. The first antibody, raised in mice, binds to the strep-tag epitope (primary sequence: WSHPQFEK). As secondary antibody, either an anti-mouse antibody

coupled to an alkaline phosphatase (AP) enzyme (Quiagen) or an anti-mouse antibody coupled to a horseradish peroxidase enzyme (Sigma-Aldrich) were used.

The detection procedure consisted of several washing and incubation steps performed on a shaking platform at room temperature. All solutions for the different washing step are listed in Table 20. First, the membranes were washed twice in TBS for 10 min, followed by 1 h incubation in blocking buffer to mask unspecific binding sites. Then the solution was exchanged and the primary antibody, also dissolved in blocking buffer, was applied for 1 h. To wash away unbound molecules of the first antibody from the membrane, TBS-Tween-Triton was applied twice and TBS once for 10 min each. Then the secondary antibody, also dissolved in blocking buffer was applied for 1 h followed by four washing steps with TBST for 5 min each and five washing steps with Aqua dest for 2 min each. After the last washing step either the chromogenic reaction based on alkaline phosphatase reaction was performed using the AP conjugate substrate Kit (Biorad) according to the manufacturer's indications. When protein bands became visible the reaction was stopped by rinsing the membrane in Aqua dest. Alternatively, the chemiluminescence reaction catalyzed by horseradish peroxidase was performed using the AceGlow kit (Peqlab) according to the manufacturer's indications. The luminescence was recorded with a ChemiDoc system (Biorad).

Table 20: Solutions for immunodetection on western blots.

Solution	***Composition***
TBS	10 mM Tris 150 mM NaCl pH 7.5
TBS-Tween-Triton	20 mM Tris 500 mM NaCl 0.05% Tween 20 0.2% Triton X100 pH 7.5

TBST	20 mM Tris 500 mM NaCl 0.05% Tween 20 pH 7.5
Blocking buffer	3% (w/w) milk powder in TBS

4. Preparation of membrane and soluble fractions

For the preparation of cellular fractions, bacterial cells were disrupted by a single passage through a *French press* cell (American Instruments Company). Fresh or frozen cells were resuspended in one volume 20% (w/v) glycerol. 0.1 mg/ml DNase I was added to bacterial cell suspensions prior to French pressing in order to degrade any DNA aggregates that might form. A pressure of 1260 psi which is equivalent to ca. 87 bar was applied. The cells were disrupted by shearing forces and decompression. Intact cells were removed by centrifuging at 1500 g for 10 min. The supernatant was centrifuged in a Ti70 rotor at 4°C and 208,000 g for 1 h in a L60-Ultracentrifuge (Beckman-Coulter) to sediment membranes. Membrane pellets were carefully resuspended in HEPES buffer supplemented with 10% glycerol. Soluble and membrane fractions were stored at -20°C until needed.

5. Analytical methods

5.1 Protein determination

Protein concentration was determined according to the method described by (Bradford, 1976). Bovine serum albumin (BSA) served as protein standard. Protein content of cell suspensions was determined after lysing the cells in alkaline solution (0.2 M NaOH final concentration) at 95°C for 5 min.

5.2 Quantification of metal reduction

Fe(II) concentrations can be measured by a photometric assay with ferrozine reagent that is forming a blue complex (Stookey, 1970). Fe(II) in the sample is easily reoxidized by molecular oxygen from the air. This can be avoided if the sample is acidified immediately after withdrawing from the culture flask. At pH values below 3.5 the oxidation of Fe(II) proceeds very slowly (Singer and Stumm, 1970). Unfortunately, the formation of the blue

ferrozine complex shows only a linear dependence to Fe(II) concentration for pH values between 4 and 10 (Stookey, 1970). To resolve this problem, 0.1% (w/v) ferrozine reagent was combined with 50% (w/v) ammonium acetate to form a strongly alkaline solution which could neutralize the acidified sample. Usually, 180 µl ferrozine solution was added to 20 µl sample in a microtiter plate and the absorption at 562 nm was measured after 5 min. Dilutions of all samples were made with 1 M HCl. Ammonium iron(II) sulfate solution, dissolved in 1 M HCl was used as a Fe(II) standard.

Manganese reduction was determined in three independent cultures using leucoberbellin blue (Boogerd and de Vrind, 1987). Leucoberbellin forms a blue complex with Mn(IV). The rate of abiotic Mn(IV) decrease in culture flasks, probably due to absorption to the walls of the vessel, was subtracted from the measured values.

The maximal metal reduction rates were determined by a non-linear curve fit done with GraphPad Prism software.

5.3 Quantification of flavin content in the culture supernatant

Different flavins were detected in culture supernatants from anaerobically growing *S. oneidensis* cultures (von Canstein *et al.*, 2008). Flavins show characteristic fluorescence features upon excitation at 440 nm with emmision at 525 nm. The fluorescence properties of different flavin molecules like flavin mononucleotide or riboflavin are very similar, therefore only relative fluorescence units of the different strains were compared with the uninoculated medium. The values are given in relative fluorescence units (RFU).

5.4 Proteinase K assay

Cells were incubated with proteinase K to determine the orientation and exposure of proteins. Proteinase K degrades proteins that are solvent exposed, e.g. outer membrane cytochromes which are exposed to the cell surface. Proteinase K assays were performed as described before by Myers *et al.* with minor modifications (Myers and Myers, 2003a). Cells were incubated with proteinase K or buffer as negative control at 37°C for one hour. Protein degradation was stopped by addition of protease inhibitor (Roche) and cells were washed four times in 2 volumes of buffer with respect to the original volume. Protein content of samples was determined before lysing cells in a SDS solubilisation mix (Table 21) (Myers and Myers, 2003a; Myers and Myers, 1998). 15 µg protein of each sample

were loaded on an SDS gel and degradation of outer membrane cytochrome was examined by Western blotting.

Table 21: SDS solubilisation mix.

Component	***Concentration***
Tris-HCl (pH 6.8)	125 mM
SDS	4%
Glycerol	21%
Dithiothreitol	100 mM
Bromophenol blue	0.0005%
Urea	4 M

6. Outer membrane integrity testing

An ethidium bromide influx assay was performed to measure outer membrane permeability. The assay was performed according to Murata *et al.* with minor modifications (Murata *et al.*, 2007). Cells were grown under anoxic conditions with fumarate as electron acceptor and in the presence of 1 mM arabinose to induce *mtrA* and *mtrB* expression. Thereafter, the cells were washed in an anoxic glove box using 100 mM HEPES, pH 7.4. The assay was performed in a microtiter plate and was initiated by the addition of ethidium bromide (final concentration 6 µM). Fluorescence was measured continuously over 5 min (excitation and emission wavelengths of 545 and 600 nm, respectively) using a microtiter plate reader (Varioscan, ThermoFisher). Ethidium bromide influx rates are displayed as relative fluorescence units (RFU) per min and milligram protein. As a positive control, 1 mg ml^{-1} polymyxin B was added to the cells. Polymyxin B destabilizes the membrane and increases permeability (Vaara, 1992).

As a second test, antibiotic susceptibility was tested in a disc diffusion test. 100 µl cell suspension (OD_{600nm} 0.132, corresponding to McFarland standard 0.5) was spread on LB plates supplemented with 1 mM arabinose and subsequently paper discs containing either 25 µg colistin, 30 µg kanamycin or 30 µg chloramphenicol (Oxoid, Thermo Fisher) were applied to the surface. After overnight incubation at 30°C, plates were photographed and zones of inhibition were measured with ImageJ (http://imagej.nih.gov/ij/).

7. Cell suspension assays

7.1 Fe(III)-citrate reduction assay

Cells were grown under anoxic conditions over night in minimal media with fumarate or Fe(III)-citrate as electron acceptor and with 1 mM arabinose to induce *mtrA* and *mtrB* expression. Alternatively, the cells were grown without inductor until they reached an OD_{600nm} of ~0.2 and were then induced with arabinose for additional four hours. Cells were harvested and washed twice using minimal media without fumarate and lactate under anoxic conditions and resuspended to a final OD_{600nm} between 3 and 5. Specific reduction rates of independent triplicate cultures were obtained by normalization to the protein content of the cell suspension. 50 µl of cell suspension were pipetted in a well of a microtiter plate. The assay was started through the addition of 150 µl of a solution containing 10 mM lactate and 10 mM Fe(III)-citrate. At different time points (0-30 min) the reaction was stopped by the addition of 100 µl of 3 M HCl. The Fe^{2+} concentration of the samples was determined using the ferrozine reagent (Stookey, 1970).

7.2 AQDS reduction assay

Anthraquinone-2,6-disulfonate (AQDS) reduction can be measured photometrically due to a clearly visible colour change when AQDS is transformed into the anthraquinol form (ε_{436nm}= 3.5 mM^{-1} cm^{-1}) (Bayer *et al.*, 1996). The reaction was carried out in glass cuvettes with butyl rubber stoppers at 30°C. The assay contained 1 mM AQDS, 100 mM HEPES, pH 7.4, 10 mM lactate and 50 µl of cell suspension. The headspace of the cuvette was flushed with nitrogen gas to maintain anoxic conditions. The assay was initiated by the addition of AQDS with a Hamilton syringe and continuous measuring of absorption at 436 nm. Cells for this assay were grown under anoxic conditions with fumarate or Fe(III)-citrate as electron acceptor and, if necessary, in the presence of arabinose as inductor for gene expression. Cells were harvested and washed twice with HEPES buffer, pH 7.4 under aerobic conditions. Reduction rates were calculated as a function of protein content. The assay was typically finished within 20 min.

7.3 Riboflavin reduction assay

Riboflavin reduction was also measured in cuvettes with butyl rubber stoppers at 30°C and 450 nm (ε_{450nm}= 12.2 mM^{-1} cm^{-1}). The assay contained 60 µM riboflavin, 100 mM HEPES, pH 7.4, 10 mM lactate and was initiated by the addition of riboflavin. Cells were

grown and prepared as described for the AQDS reduction assay. The assay was typically finished within 20 min.

8. Modelling of the tertiary structure of mutated MtrB protein

The tertiary structure of the MtrB protein was modelled based on the amino acid sequence. Therefore, the leader peptide for sec-dependent protein export was determined using the program signalP (Nielsen *et al.*, 1997). The amino acid sequence without the leader peptide was used to calculate the three-dimensional structure based on known β-barrel proteins with TMBpro (Randall *et al.*, 2008). The 3D structure was displayed using PyMOL (Schrodinger, 2010)

9. Reduction of a graphite felt anode

The setup used in this thesis to measure the reduction of an anode by the bacteria features an anode and cathode chamber with a working volume of 8 ml each, separated by a Nafion-117 membrane (Quintech). A saturated calomel reference electrode (SCE) was separated from the anode compartment by another Nafion membrane. Electrodes were made of graphite felt cubes (Alpha Aesar) connected with platinum wires of 0.1 mm diameter (Chempur). The anode compartment was filled with 5.5 ml mineral media containing 50 mM lactate and 0.1 mM arabinose. 500 µl of a cell suspension with an optical density (OD_{600nm}) of 4 were added to start the experiment. All anode reduction experiments were performed in duplicates and conducted at a constant temperature of 30°C. The whole setup was connected to a potentiostat (Pine Instruments). The standard measurement protocol consisted of two phases: after a conditioning period with a constant current flux over 5 hours (0.3 µA cm^{-3}) a continuous increase in current density with a rate of 1.1 µA cm^{-3} h^{-1} over 45 h (*current sweep* phase) was applied to the anode. The anode compartment was continuously flushed with nitrogen gas to maintain anoxic conditions. Additional terminal electron acceptors were not added.

The setups used in this thesis were designed by Arne Kloke and were kindly provided by the Department of Microsystems Engineering (IMTEK, University of Freiburg, Kloke *et al.*, 2010).

10. Yeast and bacterial strains

All yeast and bacterial strains used in this thesis are listed in Table 22.

Table 22: Yeast and bacterial strains used in this thesis.

Strain No.	***Strain***	***Relevant genotype***	***Source or Reference***
JG26	*Saccharomyces cerevisiae* InvSc1	*MATa/MATα leu2/leu2 trp1-289/trp1-289 ura3-52/ura3-52 his3-Δ1/his3-Δ1*	Invitrogen

Escherichia coli strains used in this thesis.

Strain No.	***Strain***	***Relevant genotype***	***Source or Reference***
JG22	*E. coli* DH5α Z1	*aci^{q}, PN25-tetR, Sp^{R}, deoR, supE44, Δ(lacZYA-argFV169), Φ80 lacZ ΔM15*	(Lutz and Bujard, 1997)
JG98	*E. coli* WM3064	*thrB1004 pro thi rpsL hsdS lacZΔM15 RP4–1360 Δ(araBAD)567 ΔdapA1341::[erm pir(wt)]*	(Saltikov and Newman, 2003)
JG144	*E. coli* S17-1	*thi pro recA hsdR* [RP4-2Tc::Mu-Km::Tn7] *λpir Tpr Smr*	(Simon *et al.*, 1983)
JG152	*E. coli* DH5α λ(*pir*)	*F-Δ(argF-lac)169 Φ80dlacZ58(ΔM15) glnV44(AS) rfbD1 gyrA96(NalR) recA1 endA1 spoT1 thi-1 hsdR17 deoR λpir+*	(Stalker *et al.*, 1982)
JG202	*E. coli* WM3064 pMQ150ΔgspD	JG98 / pMQ150ΔdgspD	this thesis
JG305	*E. coli* WM3064 pMQ150 ΔdmsA-2 dmsB-2	JG98 / pMQ150ΔdmsA-2 dmsB-2	this thesis
JG370	*E. coli* S17-1 pMQ150mtrFAB	JG144 / pMQ150mtrFAB	this thesis
JG411	*E. coli* WM3064 pMQ150ΔdmsA-1 dmsB-1	JG98 / pMQ150ΔdmsA-1 dmsB-1	this thesis
JG494	*E. coli* WM 3064 pMQ150-NapC	JG98 / pMQ150-NapC	this thesis

Shewanella oneidensis strains used in this thesis.

Strain No.	***Strain***	***Relevant genotype***	***Source or Reference***
JG7	*S. oneidensis* MR-1	Wild type	(Venkateswaran *et al.*, 1999)
JG12	*S. oneidensis* MR-1 ΔOMC^{S} (suppressor of outer membrane cytochrome deletion mutant)	JG132 / *mtrA*: position 869 C to A, *mtrB*: position 656 C to A	this thesis
JG50	*S. oneidensis* MR-1 Δmtra pBAD*mtrA*$_{strep}$	JG52 / pBAD202mtrA$_{strep}$	(Schuetz *et al.*, 2009)
JG52	*S. oneidensis* MR-1 ΔmtrA	ΔmtrA	(Schuetz *et al.*, 2009)
JG53	*S. oneidensis* MR-1 Δ(*mtrD-mtrC)*	*Δ(mtrD-mtrC), 3100633:: (araC, P_{BAD})*	(Bücking *et al.*, 2010)
JG55	*S. oneidensis* MR-1 ΔmtrB	ΔmtrB	(Schuetz *et al.*, 2009)
JG132	*S. oneidensis* MR-1 ΔOMC *(outer membrane cytochrome deletion mutant)*	*Δ(mtrD-mtrC) ΔSO_2931 ΔSO_1659, 3100633:: (araC, P_{BAD})*	(Bücking *et al.*, 2010)
JG137	*S. oneidensis* MR-1 ΔOMC pBAD*omcA*$_{strep}$	JG132 / pBAD202-*omcA*$_{strep}$	(Bücking *et al.*, 2010)
JG138	*S. oneidensis* MR-1 ΔOMC pBAD*mtrC*$_{strep}$	JG132 / pBAD202-*mtrC*$_{strep}$	(Bücking *et al.*, 2010)
JG139	*S. oneidensis* MR-1 ΔOMC pBAD*mtrF*$_{strep}$	JG132 / pBAD202-*mtrF*$_{strep}$	(Bücking *et al.*, 2010)
JG140	*S. oneidensis* MR-1 ΔOMC pBAD*SO_1659*$_{strep}$	JG132 / pBAD202-*SO_1659*$_{strep}$	(Bücking *et al.*, 2010)

Strain No.	***Strain***	***Relevant genotype***	***Source or Reference***
JG141	*S. oneidensis* MR-1 ΔOMC pBAD*SO_2931*$_{strep}$	JG132 / pBAD202-*SO_2931*$_{strep}$	(Bücking *et al.*, 2010)
JG162	*S. oneidensis* MR-1 ΔOMC pBAD*omcA*	JG132 / pBAD202-*omcA*	(Bücking *et al.*, 2010)
JG311	*S. oneidensis* MR-1 pBAD*mtrF*$_{strep}$	pBAD*mtrF*$_{strep}$	this thesis
JG410	*S. oneidensis* MR-1 MTR-FAB	Δ(*mtrD-mtrC*) ΔSO_2931 ΔSO_1659, 3100633 :: (araC, P_{BAD}, *mtrF*$_{strep}$)	this thesis
JG434	*S. oneidensis* MR-1 ΔOMC^{S} ΔdmsA-1 ΔdmsB-1 ΔdmsA-2 ΔdmsB-2	JG12 / ΔdmsA-1 ΔdmsB-1 ΔdmsA-2 ΔdmsB-2	this thesis
JG443	*S. oneidensis* MR-1 ΔgspD	ΔgspD	this thesis
JG444	*S. oneidensis* MR-1 ΔOMC^{S}ΔgspD	JG12 / ΔgspD	this thesis
JG449	*S. oneidensis* MR-1 ΔOMC pmtrA^{S}mtrB^{S}	JG132 / pmtrA^{S}mtrB^{S}	this thesis
JG450	*S. oneidensis* MR-1 ΔOMCpmtrA mtrB	JG132 / pmtrAmtrB	this thesis
JG462	*S. oneidensis* MR-1 ΔOMC pmtrA^{S}	JG132 / pmtrA^{S}	this thesis
JG463	*S. oneidensis* MR-1 ΔOMC pmtrB^{S}	JG132 / pmtrB^{S}	this thesis
JG468	*S. oneidensis* MR-1 ΔmtrA pmtrA^{S}	JG52 pmtrA^{S}	this thesis

Strain No.	***Strain***	***Relevant genotype***	***Source or Reference***
JG469	*S. oneidensis* MR-1 ΔmtrB pmtrB^{S}	JG55 pmtrB^{S}	this thesis
JG474	*S. oneidensis* MR-1 ΔOMC pmtrAmtrB^{S}	JG132 / pmtrAmtrB^{S}	this thesis
JG495	*S. oneidensis* MR-1 MTR-FAB-NapC	JG410, 184441 :: (*napC$_{strep}$)*	this thesis

VII. Results

1. Role and specificity of outer membrane cytochromes

1.1 Preparation of the outer membrane cytochrome deficient mutant

Bioinformatical analysis of the genome of *S. oneidensis* MR-1 revealed the presence of five genes coding for putative outer membrane cytochromes. They were identified based on the presence of heme binding motifs and export signals (Meyer *et al.*, 2004). Four of these genes are coding for decaheme outer membrane cytochromes (MtrC, OmcA, MtrF, and SO_1659) that share strong sequence homologies. It was speculated that they might originate from a gene duplication of a pentaheme motif (Meyer *et al.*, 2004). MtrF, OmcA, and MtrC are clustered together while SO_1659 has a different location on the genome. The fifth outer membrane cytochrome is a putative diheme protein with no similarities to known proteins (Meyer *et al.*, 2004).

The aim of this section was to analyze the role and specificity of each of the five outer membrane cytochromes. For this purpose, a markerless multi-deletion mutant in all annotated outer membrane cytochromes of *S. oneidensis* was constructed called ΔOMC. This strain platform allows for analysis of outer membrane cytochrome activity without the potential detection of redundant activities from similar proteins. In this background, single outer membrane cytochrome proteins were expressed and their activities were compared.

To generate the ΔOMC mutant, genes coding for MtrF, MtrC, and OmcA were deleted in one step[7]. This deletion led to further excision of *mtrD* and *mtrE* from the chromosome. The function of these genes is unknown so far as gene deletion did not show a phenotype under the conditions tested (Bretschger *et al.*, 2007). The genes for the decaheme *c*-type cytochrome SO_1659 and the diheme cytochrome SO_2931 were deleted subsequently. The presence of MtrA and MtrB was shown to be a requirement for metal reduction by *S. oneidensis* (Beliaev and Saffarini, 1998; Bretschger *et al.*, 2007). Hence, possible effects of the removal of promoter regions and genes ranging from *mtrF* to *mtrC* on expression of *mtrA* and *mtrB* were circumvented by the concomitant introduction of an

[7] The generation of strain JG53 *S. oneidensis* MR-1 Δ(*mtrD-mtrC);3100633:: (araC, P_{BAD})*, was done during my „Staatsexamensarbeit“ (Bücking, 2007). The quintuple mutant ΔOMC (JG132) was generated during this thesis.

arabinose inducible P_{BAD}-promoter and the *araC* repressor. A scheme of the gene cluster before and after the deletions is shown in Figure 4.

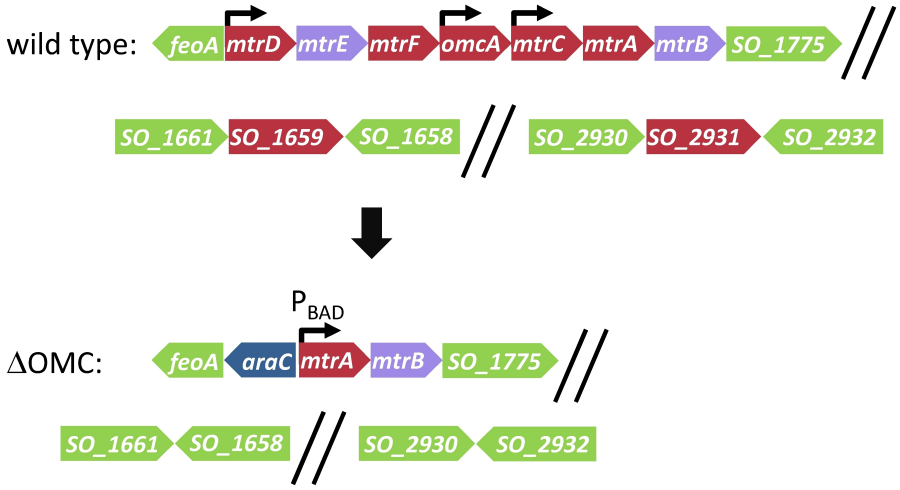

Figure 4: Gene structure in S. oneidensis wild type and ΔOMC strain. *Genes coding for c-type cytochromes are depicted in red. Black arrows above the gene symbols indicate promoter regions – the natural promoters that were excised from the genome of the wild type were replaced by an arabinose inducible P_{BAD}-promoter in ΔOMC.*

The expression of membrane proteins from *S. oneidensis* wild type and ΔOMC can be seen in Figure 5. It is clearly visible that no heme proteins of the size of OmcA (predicted size 78.6 kDa) and MtrC (predicted size 71.2 kDa) are present in the ΔOMC mutant. It can furthermore be seen that the expression of MtrA (predicted size 36.1 kDa) is dependent on the arabinose induction level. At an induction of 0.1 mM arabinose, MtrA is present but at a slightly lower amount than the wild type, while at 1 mM arabinose, the amount of MtrA seems to be almost equal between wild type and mutant.

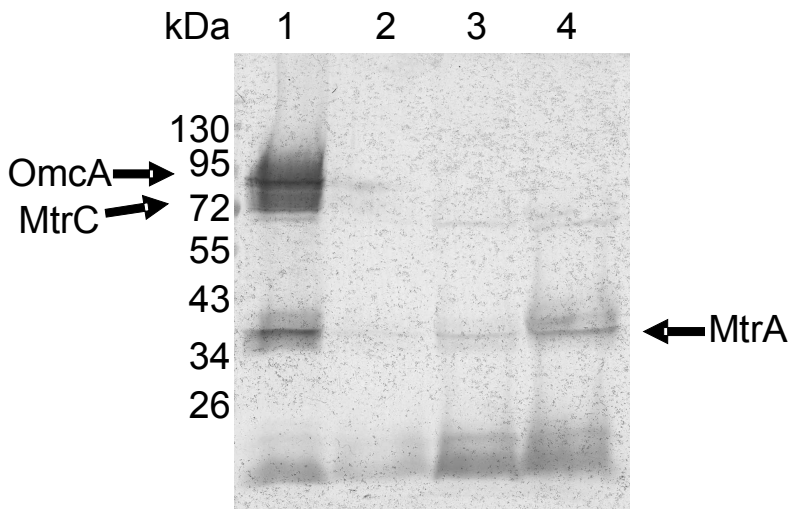

Figure 5: SDS-PAGE of membrane fractions from fumarate grown S. oneidensis wild type and ΔOMC mutant cells. *Lane 1: wild type, lanes 2-4 ΔOMC induced with 0, 0.1 and 1 mM arabinose. 140 µg protein was loaded on each lane.*

1.2 Cloning and production of outer membrane cytochromes in the ΔOMC mutant

Genes coding for outer membrane cytochromes from *S. oneidensis* were cloned separately into plasmid pBAD202 to assign in further experiments specific functions to these proteins[8]. The sequence information for a C-terminal strep-tag was added to allow for specific detection of expressed proteins. The induction level was set to 0.1 mM arabinose throughout all following experiments of this section to allow for a comparison of the activities of the single outer membrane cytochrome proteins. Previous experiments had shown that higher induction levels hampered cell growth at least for strain JG138 (ΔOMC pBAD*mtrC*$_{strep}$). The relative amounts of the expressed outer membrane cytochromes were quantified via immunodetection of the added strep-tag epitope (Figure 6a). For a series of control experiments, the native form of OmcA without strep-tag was produced. OmcA was detected using heme activity staining and compared to OmcA$_{strep}$ (Figure 6b). OmcA$_{strep}$ production resulted in the strongest strep-tag derived signal compared to all other expressed outer membrane cytochromes (Figure 6c). Signals resulting from MtrC$_{strep}$ and MtrF$_{strep}$ production were detected in similar quantities which indicate similar production levels. In contrast, production of SO_1659$_{strep}$ and SO_2931$_{strep}$ seems to be strongly reduced compared to the other three outer membrane cytochromes.

[8] The cloning of MtrC$_{strep}$, SO_2931$_{strep}$,and MtrF$_{strep}$ was done during my "Staatsexamensarbeit" (Bücking, 2007).

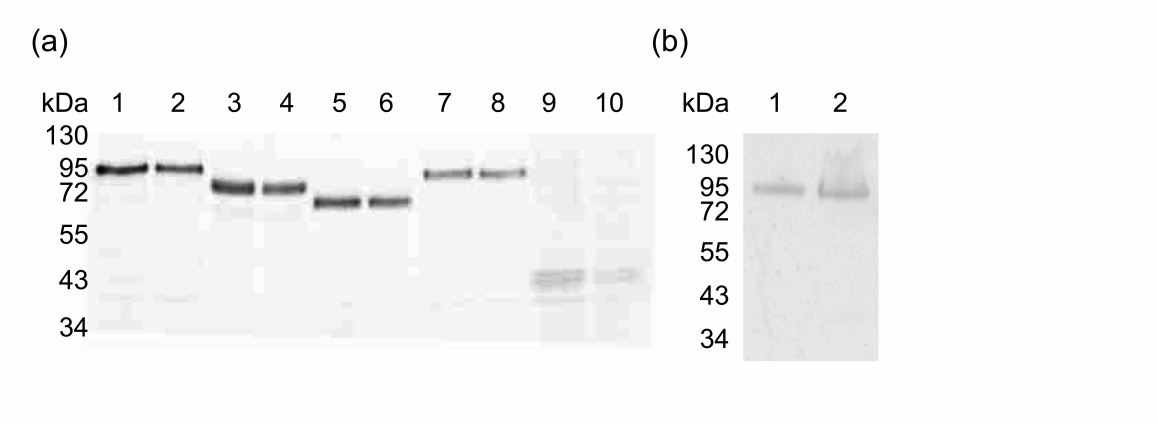

(c)

	$OmcA_{strep}$	$MtrC_{strep}$	$MtrF_{strep}$	SO_1659_{strep}	SO_2931_{strep}
$OmcA_{strep}$	1.000	0.969	0.787	0.468	0.109

Figure 6: Relative quantification of produced outer membrane cytochromes. *SDS-PAGE gels were loaded with membrane fractions prepared from S. oneidensis ΔOMC strains grown anaerobically on fumarate and induced with 0.1 mM arabinose to produce single outer membrane cytochromes. A) Western blot of cells producing OmcAstrep (lane 1 and 2), MtrCstrep (lane 3 and 4), MtrFstrep (lane 5 and 6), SO_1659strep (lane 7 and 8) and SO_2931strep (lane 9 and 10). 3 mg membrane fraction was loaded in lanes 1, 3, 5, and 7. 2 mg were loaded in lanes 2, 4, 6, and 8. Lanes 9 and 10 contain 8 and 6 mg membrane fraction, respectively. B) Heme stain with 25 mg of the membrane fractions from cells producing either the native form OmcA (lane 1) or OmcAstrep (lane 2) were loaded. C) Relative quantification of the detected hrp derived signals. Mean values from two independent quantifications are shown. The single values varied within a range of not more than 5%. The OmcAstrep signal intensity was set to 100%.*

1.3 Surface exposure of outer membrane cytochromes

To investigate whether the proteins are oriented towards the periplasm or the surrounding media, proteinase K assays according to Myers *et al.* (Myers and Myers, 2003a) were performed (Figure 7). Only proteins that are exposed to the outer surface of the cell are prone to proteinase K degradation. Proteinase K is a serine protease with a broad specificity that was originally isolated from the fungus *Engyodontium album*. Interestingly, the protease is not inhibited by SDS or urea and must thus be inactivated by heat or by protease inhibitors.

Detection of the outer membrane cytochromes was based on the added strep-tag epitope. A control reaction using strain JG50 which expresses a strep-tagged MtrA protein was performed, to ensure that the assay conditions did not interfere with cell integrity. The cellular localization of MtrA is the periplasm and the inner leaflet of the outer membrane. Localization of OmcA and MtrC to the cell surface was already shown by other research

groups (Myers and Myers, 2003a; Shi *et al.*, 2008). Hence $MtrC_{strep}$ and $OmcA_{strep}$ were used as proteinase K degradable control proteins. As Figure 7 shows, $OmcA_{strep}$, $MtrC_{strep}$, $MtrF_{strep}$, and the decaheme cytochrome SO_1659_{strep} are clearly hydrolyzed by the proteinase. The positive control $MtrA_{strep}$ and the diheme SO_2931_{strep} were not degraded in the assay. The reason could be that SO_2931_{strep} is not surface exposed or that it is not degradable by proteinase K.

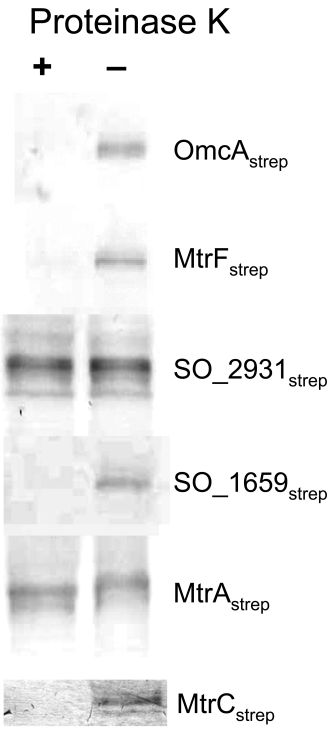

Figure 7: Cell surface exposure of OM cytochromes tested by proteinase K assays. *Outer membrane cytochromes were detected with immunostaining based on the strep-tag epitope. Assays conducted with addition of proteinase K are indicated by a +. The periplasmic decaheme cytochrome MtrA was chosen as a control for cell integrity under the assay conditions.*

1.4 Reduction activities towards different terminal electron acceptors

1.4.1 Reduction of Fe(III)-citrate

To measure the *in vivo* activities of single outer membrane cytochromes, cell suspensions of the different mutant strains were prepared from anaerobic cultures grown with fumarate as terminal electron acceptor. These washed cell suspensions were used to measure specific Fe(III)-citrate reduction rates within 30 min eliminating the putative influence of endogenous shuttling substances produced during growth.

Cell suspension assays showed that only the production of $MtrC_{strep}$ and $MtrF_{strep}$ could partly rescue the mutant phenotype for Fe(III)-citrate reduction (Figure 8a and 8b). $MtrF_{strep}$ production resulted in a 1.2-fold accelerated Fe(III)-citrate reduction rate compared to the $MtrC_{strep}$ expressing strain.

Surprisingly, the presence of $OmcA_{strep}$ did not lead to increased ferric iron reduction rates compared to the ΔOMC mutant. To exclude possible effects of the strep-tag epitope on protein activity, control experiments with the native form of *omcA* in the same vector backbone were performed. Production of the native form of OmcA was shown via heme activity staining (Figure 6b). Still, even the presence of the native form of OmcA did not lead to an altered phenotype compared to the ΔOMC mutant.

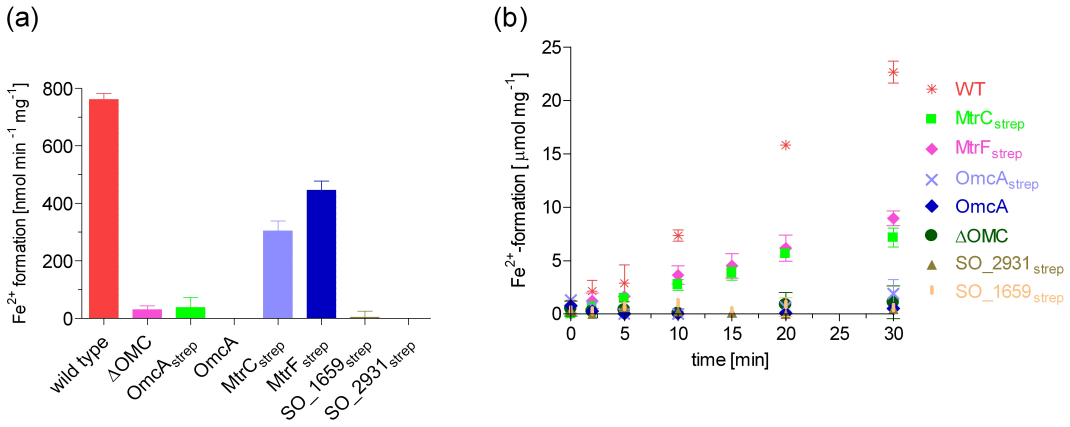

Figure 8: Fe(III)-citrate reduction by S. oneidensis wild type and mutant strains *(a) Fe(III)-citrate reduction rates were measured in cell suspension experiments using cells that were grown anaerobically with fumarate as electron acceptor. Outer membrane cytochromes and MtrAB production was induced with 0.1 mM arabinose. (b) Time course of the Fe(III)-citrate reduction experiments. Reduction rates remained almost constant over a total time period of 30 min.*

1.4.2 Reduction of Fe(III) nitrilotriacetic acid (NTA)

Fe(III) nitrilotriacetic acid or Fe(III)-NTA is an iron chelate that was shown to be membrane permeable (Gescher *et al.*, 2008). To measure the Fe(III)-NTA reduction activities of the different strain, the same method as described for Fe(III)-citrate was employed. The overall pattern of the strains was strikingly similar to the results from Fe(III)-citrate although the rates being generally roughly 1.66-fold higher for Fe(III)-NTA (Figure 9). Again, the expression of $MtrC_{strep}$ and $MtrF_{strep}$ could partly rescue the mutant phenotype. Although Fe(III)-NTA could theoretically be reduced by periplasmic or cytoplasmic localized *c*-type cytochromes in all mutant strains, it seems as if the outer membrane represents an important diffusion barrier under the experimental conditions of

the cell suspension assay. The interprotein electron transfer of the extended respiratory chain seems to be much faster than the diffusion into the cell. The main part of Fe(III)-NTA is therefore probably reduced at the outer surface of the cell.

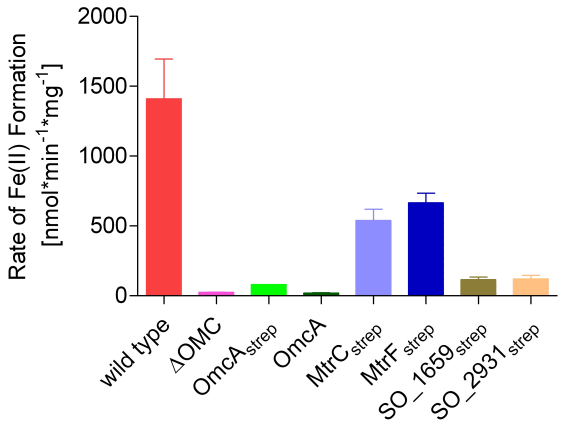

Figure 9: Fe(III)-NTA reduction by S. oneidensis wild type and mutant strains. *(a) Fe(III)-NTA reduction rates were measured in cell suspension experiments using cells that were grown anaerobically with fumarate as electron acceptor. Outer membrane cytochromes and MtrAB production was induced with 0.1 mM arabinose.*

1.4.3 Reduction of anthraquinone-2,6-disulfonate (AQDS)

AQDS is a model compound for quinone moieties in humic acids, which are ubiquitously present in soils and can act as electron shuttles (Jiang and Kappler, 2008; Roden *et al.*, 2010). AQDS reduction was measured in cell suspension assays based on its extinction coefficient at 436 nm (Bayer *et al.*, 1996). Cells expressing $OmcB_{strep}$ or $MtrF_{strep}$ displayed the highest reduction rates of all complemented mutant strains (Figure 10). These rates were with 90 versus 85 nmol min^{-1} mg^{-1} protein almost identical. On the contrary, the ΔOMC mutant and all other complemented strains exhibited only a low level reduction activity.

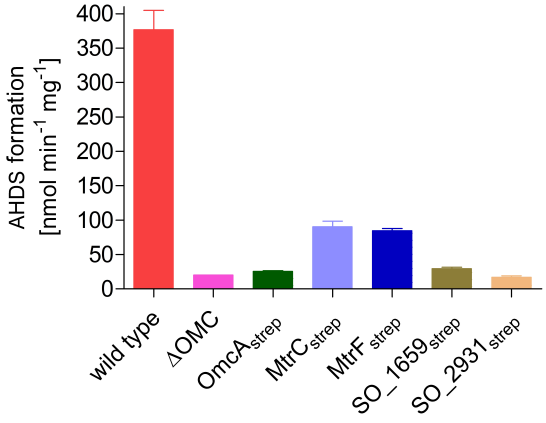

Figure 10: AQDS reduction by cell suspensions. *Washed cell suspensions were prepared from anaerobic cultures with fumarate as terminal electron acceptor and induction for 4 hours with 0.1 mM arabinose. All experiments were carried out under anoxic conditions. Maximal reduction rates (means of duplicate measurements) were normalized to the protein content. The reduction AQDS was measured in a continuous spectrophotometric assay using an absorption maximum at 436 nm.*

1.4.4 Ferrihydrite reduction

Bretschger *et al.* showed that a Δ*omcA*Δ*mtrC* double mutant reduced roughly 75% of the hydrous ferric oxide that was reduced by the wild type within the same time frame (Bretschger *et al.*, 2007). The cell suspension experiments in this thesis with Fe(III)-citrate displayed a significantly stronger effect of the deletion of all outer membrane cytochromes. Hence, the question was whether growth experiments with ferrihydrite as sole electron acceptor would lead to different results compared to the cell suspension experiments with Fe(III)-citrate.

After 24 h the reduction pattern of the different strains were very similar to the results obtained in cell suspension experiments. (Figure 11A). Only the background activity of the ΔOMC mutant was markedly higher than in the cell suspension assays (15% compared to the wild type). Surprisingly, after 72 h all mutant strains had reduced roughly 70% of the amount of ferrihydrite reduced by the wild type (Figure 11B). This effect could be due to partial cell lysis and the concomitant release or to the specific production of electron shuttling components. An alternative explanation would be the appearance of suppressor mutations masking the mutant phenotype.

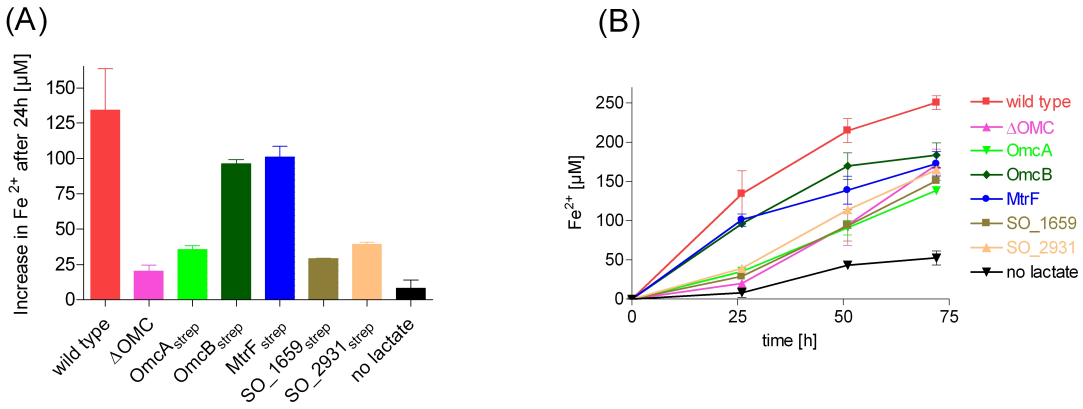

Figure 11: Reduction of ferrihydrite under growth conditions. *2-line ferrihydrite (10 mM) was added to the growth medium as sole electron acceptor. (a) Concentrations of Fe^{2+} after 24 h. (b) Evolution of Fe^{2+} concentrations over the whole time course of the experiment.*

1.4.5 Birnessite reduction

Birnessite was used to study the effect of outer membrane cytochrome production on reduction of manganese oxides under growth conditions (Figure 12). Interestingly, the complementation pattern was different from the reduction experiments with ferric iron compounds and AQDS (compare Figure 8-11). Although $MtrF_{strep}$ and $MtrC_{strep}$ production markedly increased the ability of the ΔOMC mutant to reduce Mn(IV) (53 ± 1,8% Mn(IV) reduction after 50 h compared to wild type), an effect of OmcA and $OmcA_{strep}$ production (30% Mn(IV) reduction after 50 h compared to wild type) was also detectable (Figure 12). Production of the diheme cytochrome SO_2931_{strep} and the decaheme cytochrome SO_1659_{strep} did not lead to birnessite reduction rates that differed from the ΔOMC mutant. Still, even these three strains exhibited a low-level reduction capability, a similar effect as observed with ferrihydrite.

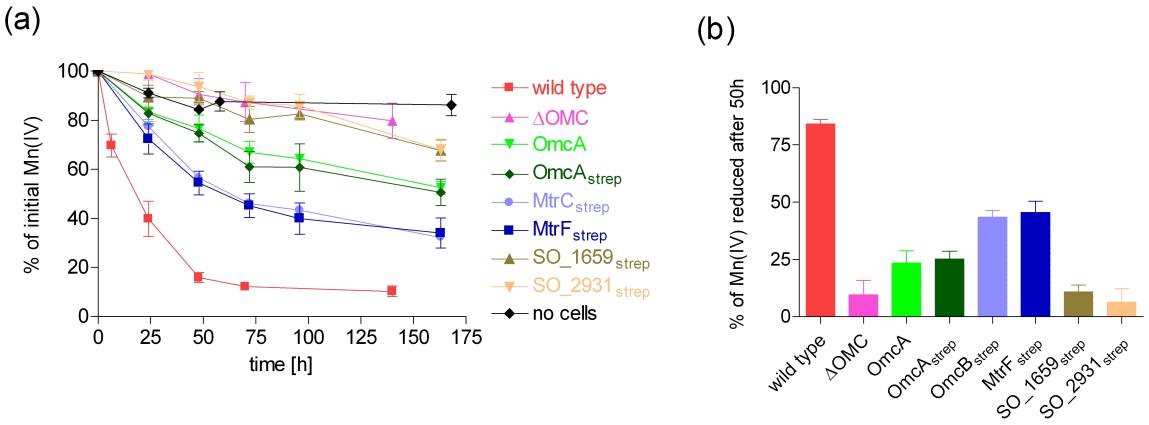

Figure 12:Manganese reduction in growth experiments. *2.5 mM birnessite (manganese dioxide) were added to mineral medium with lactate as electron donor and 0.1 mM arabinose to induce outer membrane cytochromes and MtrA/B. 500 µl of washed cells (OD_{600nm}= 4) from an anaerobically grown culture were used as inoculum. Percentage Mn(IV) is relative to the starting concentration. Initial values for Mn(IV) varied slightly (± 0.266 mM) and were therefore set to 100%. (a) Percentage of Mn(IV) over the whole time course of the experiment, (b) percentage of Mn(IV) after 50 h.*

1.4.6 Anode reduction

Metal reducing organisms are usually able to transfer electrons to a solid surface like a graphite felt anode if a certain potential is applied. The electron transfer onto the electrode proceeds either directly or via mediators. The anode is connected to a cathode by external wiring. The electrons derived from bacterial respiratory processes flow to the cathode where typically oxygen is reduced. The electrical circuit is closed by a proton flux between the anode compartment and the cathode through a proton permeable membrane.

To characterize the ability of the different mutant strains to transfer electrons to an anode, a *current-sweep* (continuous linear increase in current density) was performed. Each bacterial strain displayed a characteristic *current density-potential* plot (Figure 13A). Common to all cultures was a steep rise in potential at the beginning of the current sweep, followed by a region where potentials increased more linearly in response to higher currents. In this region bacterial cells behaved analogous to Ohmic resistances. At higher current fluxes another rapid increase in potential was observed, and above these currents all *current density-potential* plots merged into one common line that presumably results from hydrolysis of the base electrolyte. The current density at which bacteria failed to convey sufficient quantities of electrons to sustain a given current flux represents a characteristic feature of each mutant strain. To simplify comparison between performances of different bacterial strains in current sweep experiments the **l**imiting **c**urrent **d**ensity (LCD) was defined as current flux beyond which the measured anode

potential first exceeded 512 mV vs. SCE (Figure 13A), which roughly corresponds to the potential range where the *current density-potential* plots of all strains exhibit the second striking rise in potential. The ΔOMC mutant showed a 75% reduced LCD value compared to the wild type and could be rescued to a small degree by production of $MtrF_{strep}$ (Figure 13B). Presence of $MtrC_{strep}$, by contrast, caused a more significant effect. LCD values of the other strains were similar to the ΔOMC mutant and are therefore not shown.

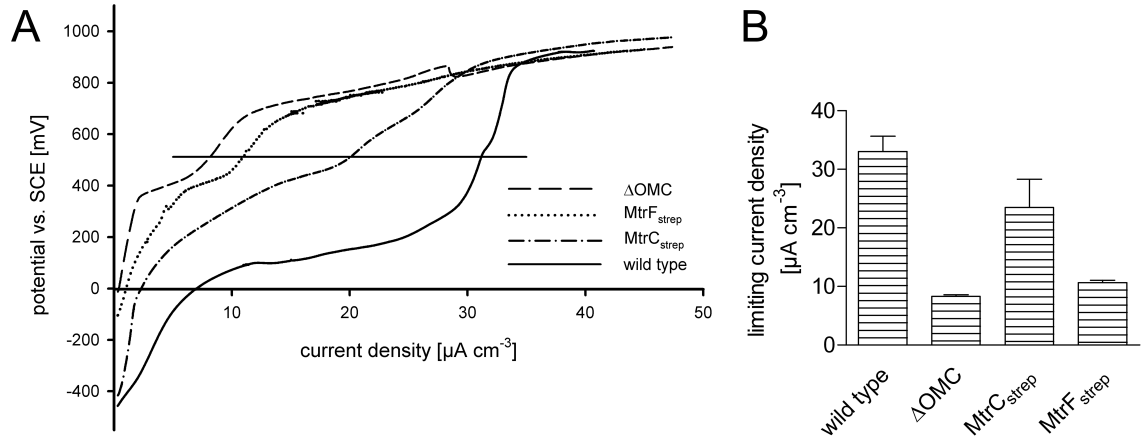

Figure 13: Anode potentials measured against a saturated calomel electrode (SCE) at varying current densities. *(A) Representative current density-potential plots from selected mutant strains. The horizontal line represents the potential of 512 mV vs. SCE where the system starts to consume electricity. Curves for cells producing SO_1659 or SO_2931 were not distinguishable from the ΔOMC data and therefore excluded. (B) Mean limiting current densities (LCD) from two independent experiments. The LCD was defined as the current density where the recorded anode potential exceeds 512 mV vs. SCE.*

2. Increasing the rate of electron transfer to insoluble electron acceptors

A number of putative biotechnological applications using *S. oneidensis* depend fundamentally on the rate of electron transfer to insoluble acceptors. Bacterial strains with increased transfer rates could be beneficial, e.g. for faster bioremediation processes or for enhanced current production in microbial fuel cells.

It was hypothesized that the electron transfer to the terminal acceptor is the rate limiting step in the electron transfer reaction of the extended respiratory chain of *S. oneidensis*. The idea was therefore to modulate the number of enzymes catalyzing this step in order to accelerate the overall reduction reaction.

2.1 Modulating the amount of final reductases on the cell surface

It was tested first whether and to what extent the outer membrane cytochromes MtrC and MtrF can be overexpressed in an *S. oneidensis* strain that is devoid of any other genes encoding outer membrane cytochromes. To this end, strains ΔOMC with pBad$mtrC_{strep}$ vector (JG138) and ΔOMC with pBad$mtrF_{strep}$ vector (JG139) were used.

Fe(III)-citrate reduction in batch cultures was recorded at varying levels of arabinose in the medium ranging from 0-1 mM (Figure 14). Fastest reduction was observed with 0.1 mM and 0.2 mM arabinose for strain JG138 and JG139, respectively. Surprisingly, a higher induction lowered the ferric iron reduction rate and full induction nearly prohibited reduction at all (Figure 14). Toxic effects of the expression might account for this phenomenon. The concentration range of inductor amount that were proportional to the reduction rate were rather narrow for both strains (for JG138 from 0-100 µM and for JG139 from 0-200 µM). Still, it was twofold bigger if MtrF instead of MtrC was used.

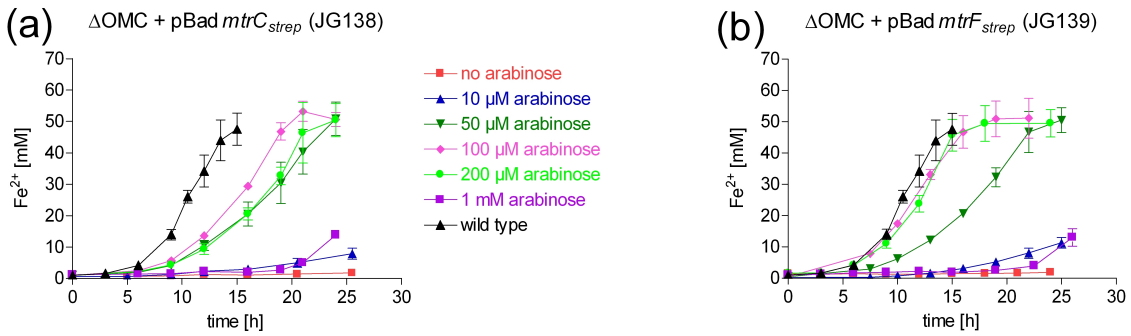

Figure 14: Iron reduction with ΔOMC cells complemented with pBadmtrC$_{strep}$ and pBadmtrF$_{strep}$ plasmids. *Fe(II) production was monitored over time using the ferrozine assay. Mutant strains were induced with arabinose as indicated. Symbols refer to means of triplicate experiments, error bars indicate standard deviation.*

Summarizing the results from the two strains, it can be said that the reduction rate depends on the amount of outer membrane cytochrome produced by the cell. Nevertheless, the rate did not reach the level of the wild type which expresses two different outer membrane cytochromes MtrC and OmcA in parallel under ferric iron reducing conditions (Myers and Myers, 2001). Strains JG138 and JG139 can only express one outer membrane cytochrome at once. *in vitro* studies by Shi *et al.* showed a cooperative effect between outer membrane cytochrome resulting in higher reduction rates when two of these proteins are present in parallel (Shi *et al.*, 2006).

This raised the question whether this cooperative effect could even be expanded and hence expression of MtrF in wild type *S. oneidensis* could be beneficial for iron reduction rates. In other words, is it possible to expand the number of cooperating terminal reductases on the cell surface to a level that is advancing the wild type.

Therefore, the vector construct pBad*mtrF*$_{strep}$ was transformed into the wild type strain and the Fe(III)-citrate reduction in batch cultures was recorded at varying levels of arabinose in the medium ranging from 0-1 mM. This strain, *S. oneidensis* MR-1 pBAD*mtrF*$_{strep}$ (JG311) expresses the outer membrane cytochromes MtrF$_{strep}$, MtrC, and OmcA (Figure 15). At increasing induction levels, one can see that the amount of MtrC and OmcA decreases while the amount of MtrF is rising (Figure 15).

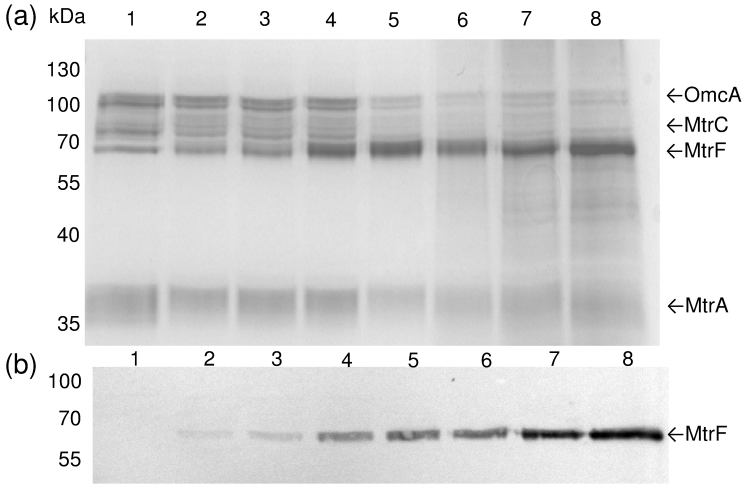

Figure 15: SDS-PAGE of membrane fractions from strain S. oneidensis MR-1 pBADmtrF$_{strep}$ (JG311) and wild type. *(a) Heme acitivity staining (b) Western Blot with anti-strep antibody to detect MtrF$_{strep}$. Lanes 1: S. oneidensis wild type; lanes 2-8: S. oneidensis MR-1 pBADmtrF$_{strep}$ with 0 µM, 10 µM, 50 µM, 100 µM, 200 µM, 500 µM, and 1 mM, arabinose, respectively.*

However, the reduction rate of JG311 at induction levels between 0 µM and 200 µM were indistinguishable from the wild type (Figure 16). The contribution of MtrF to the reduction rate cannot be determined exactly but it seems as if it replaces the roles of the other two outer membrane cytochromes. But importantly, the rate of strain JG311 never exceeded the rate of the wild type. The highest induction level (1 mM) had a markedly negative effect on reduction probably being harmful for the cells by the high amount of outer membrane cytochrome present. In conclusion, the parallel expression of three outer membrane cytochromes did not seem to increase the reduction rate.

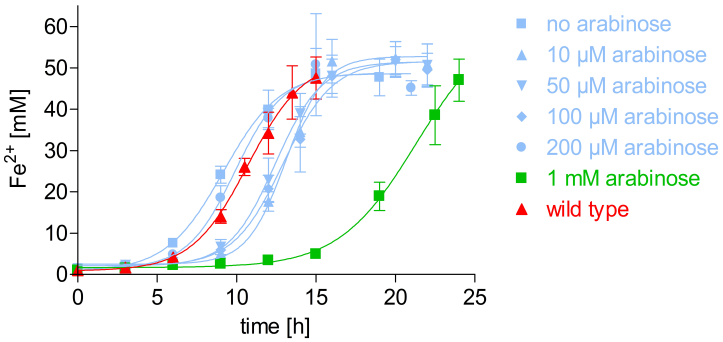

Figure 16: ***Iron reduction with S. oneidensis cells complemented with pBadmtrF$_{strep}$ plasmid.*** *Fe(II) production was monitored over time using the ferrozine assay. Mutant strains were induced with arabinose as indicated. Symbols refer to means of triplicate experiments, error bars indicate standard deviation.*

A disadvantage of the strains described so far, is that the components of the outer membrane spanning complex are not produced in equal amounts. *mtrA* and *mtrB* are encoded in one copy per cell in the genome, while *mtrC* and *mtrF* were expressed from a low copy plasmid and probably still have a 10-30-fold higher copy number. The expression of the outer membrane cytochromes as well as the expression of MtrA and MtrB is triggered by the same P_{BAD} promoter which results consequently in a higher concentration of the outer membrane cytochromes compared to MtrA and MtrB. It seems as if outer membrane cytochromes that are produced in excess were unable to connect to the underlying electron transfer chain. Another disadvantage of these strains is that their function in a biotechnological application would rely on plasmids which need to be maintained in the cell through a continuous addition of an antibiotic.

2.2 Increasing the amount of reductase-complexes in the outer membrane

A new *S. oneidensis* strain was constructed to overcome the limitations mentioned above and to integrate the information gained from the expression experiments. Therefore, a ΔOMC strain backbone was used and the genes encoding *mtrF*, *mtrA* and *mtrB* were placed in a row behind a P_{BAD}-promoter in the genome resulting in strain MTR-FAB (JG410, Figure 17).

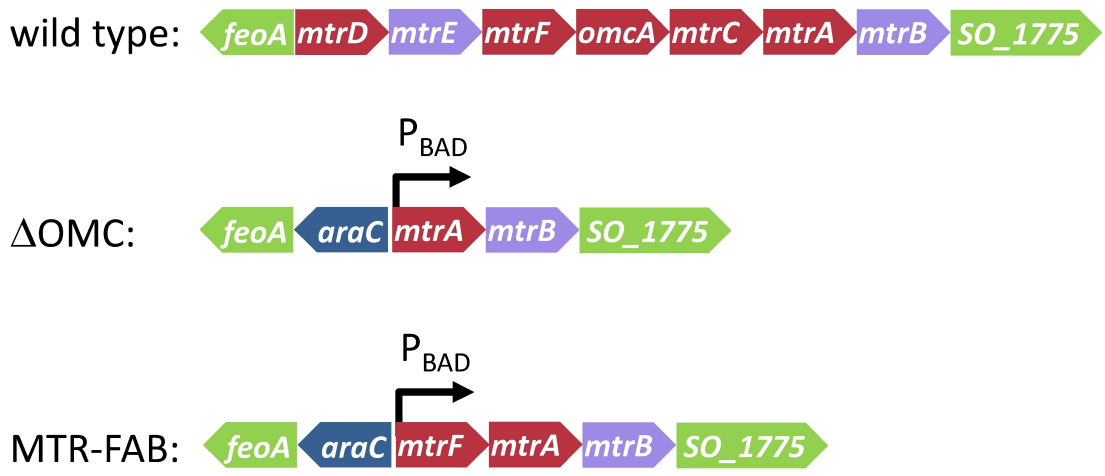

Figure 17: Schematic view of the mtr-gene structure of S. oneidensis MR-1 and mutant strains. *Genes coding for c-type cytochrome proteins are depicted in grey. The gene araC codes for the repressor/activator protein AraC that is interacting with the P_{BAD} promoter which is symbolized by a black arrow.*

The newly inserted operon should allow for the expression of similar amounts of each component of the outer membrane spanning MtrFAB-complex. To verify this hypothesis MTR-FAB cells were grown under ferric iron reducing conditions in the presence of varying levels of arabinose. As Figure 18 indicates, the concentration of MtrF and MtrA increases proportionally with the induction level (Figure 18). Although the expression of MtrB could not be shown directly due to the absence of an antibody, the protein is very likely to be present in similar amounts since it is part of the same operon.

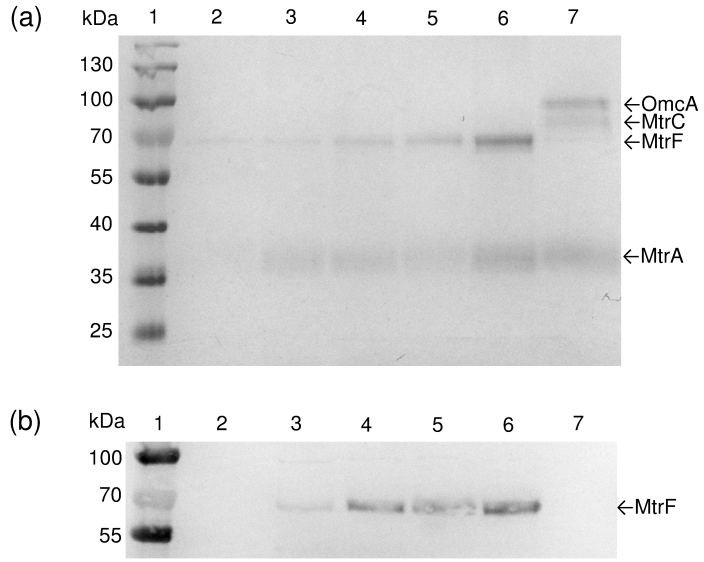

Figure 18: SDS-PAGE of membrane fractions from strain S. oneidensis MTR-FAB and wild type. *(a) Heme activity staining (b) Western Blot with anti-strep antibody to detect $MtrF_{strep}$. Lanes 1: protein marker; lanes 2-6: S. oneidensis MTR-FAB with 100 µM, 200 µM, 500 µM, 1 mM, and 2 mM arabinose, respectively; lanes 7: S. oneidensis wild type.*

The Fe(III)-citrate reduction rate of MTR-FAB responded to a much greater range of inductor concentrations as compared to the above described experiments with plasmid encoded copies of *mtrF*. Fastest ferric iron reduction rates were reached using 1 mM arabinose (Figure 19). Interestingly, the maximal reduction rate of MTR-FAB with an induction of 1 mM arabinose was 1.8-fold higher than that of the wild type (Figure 19). Further increase in arabinose concentration did not increase the maximal reduction rate and the onset of reduction was even delayed, probably due to a negative effect from protein overproduction. As the final electron transfer to the terminal acceptor seems to be the rate limiting step of the extended respiratory chain, a higher number of complexes than in the wild type might be responsible for the higher rate.

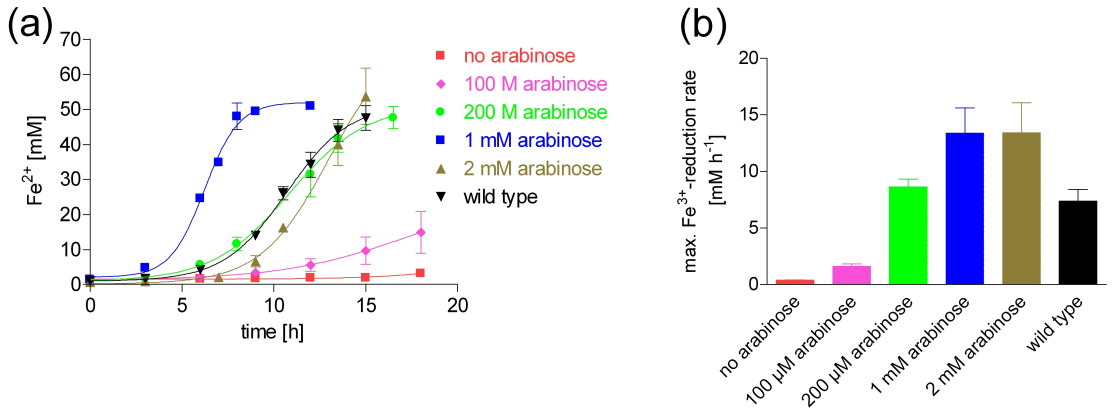

Figure 19: Fe(III)-citrate reduction and maximal reduction rates by strain MTR-FAB (JG410). *(a) Fe(II) production was monitored over time using the ferrozine assay. MTR-FAB strain was induced with arabinose as indicated. Symbols refer to means of triplicate experiments, error bars indicate standard deviation. (b) Maximal reduction rates during the course of the experiment calculated for each biological replicate with GraphPad Prism 4. Error bars represent standard deviation.*

2.3 Increasing the amount of menaquinone reductases in the cytoplasmic membrane

Besides the amount of complexes in the outer membrane in strain MTR-FAB, other proteins of the extended respiratory chain could be rate limiting in iron reduction. An important candidate is the menaquinone reductase CymA which is localized on the periplasmic side of the cytoplasmic membrane. The protein is the only known menaquinone reductase in *S. oneidensis* and is thus the only electron donor for periplasmic *c*-type cytochrome of the respiratory chain to ferric iron. An overexpression of CymA easily leads to toxic effects (Dr. J. Gescher, personal communication). A orthologous protein in *E. coli*, NapC, was shown to carry out ferric reductase activity although at a lower rate (Gescher *et al.*, 2008). The idea was therefore to express CymA and NapC in parallel from the natural promoter of CymA to increase the amount of menaquinone reductases in the cytoplasmic membrane. *napC* gene was integrated in the genome behind *cymA* resulting in strain *S. oneidensis* MTR-FAB-NapC (JG495). The expression of NapC in JG495 could be seen by the presence of a band of the predicted size of 23.1 kDa on SDS-PAGE with heme activity staining (Figure 20b). Nevertheless, the reduction of Fe(III)-citrate by strains MTR-FAB and MTR-FAB-NapC proceeded nearly with identical reduction rates (Figure 20a). It was therefore concluded that the reactions catalyzed by the menaquinone reductases are probably not rate limiting in ferric iron reduction.

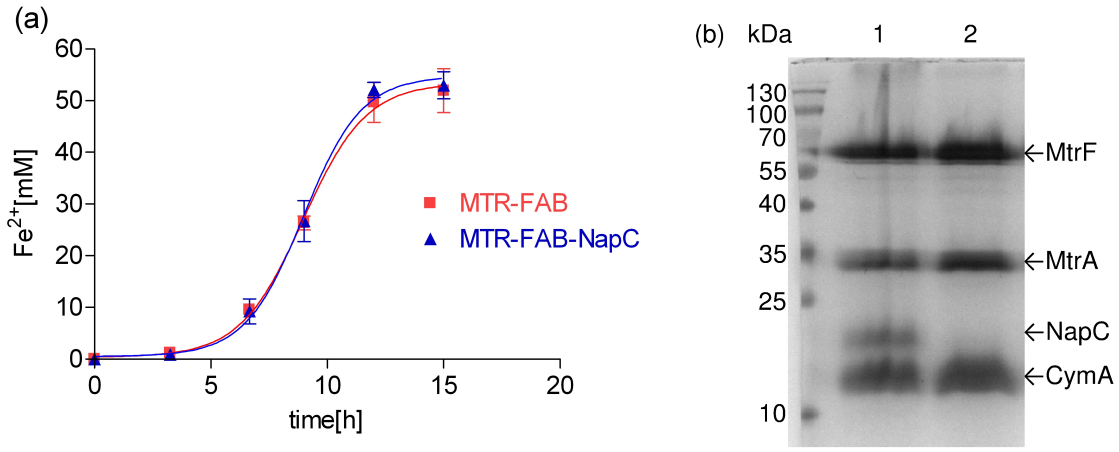

Figure 20: Fe(III)-citrate reduction by strain MTR-FAB-NapC (JG495) compared to strain MTR-FAB (JG410). *(a) Fe(II) production was monitored over time using the ferrozine assay. Both strains were induced with 1 mM arabinose. Symbols refer to means of triplicate experiments, error bars indicate standard deviation. (b) SDS-PAGE of membrane fractions from strain S. oneidensis MTR-FAB-NapC (JG495) and MTR-FAB with heme activity staining. Lane 1: MTR-FAB-NapC, lane 2: MTR-FAB. NapC has a predicted size of 23.1 kDa.*

3. Evolution of a ΔOMC suppressor mutant

In the first section of results, the generation and the properties of a ΔOMC mutant were described. The deletion of the outer membrane cytochromes resulted in an almost complete loss of the ability to reduce poorly soluble electron acceptors (Bücking *et al.*, 2010). However, two interesting observations were made that could not be explained readily. First, in growth experiments with ferrihydrite, after 3 days the ΔOMC mutant had reduced roughly 70% of the amount of ferrihydrite reduced by the wild type (Figure 11, page 69). Second, it was observed that ΔOMC cells in culture flasks with anoxic Fe(III)-citrate medium had a minimal Fe(III)-citrate reducing activity. The growth medium showed complete discoloration after 60 days indicating a complete Fe(III)-citrate reduction (data not shown).

To further explore these phenotypes, the ΔOMC strain was cultivated for several generations in serum vials containing anoxic medium with Fe(III)-citrate until a substantial acceleration of Fe(III)-citrate reduction was visible which can be easily seen by discoloration of the medium. The accelerated iron reduction after several generations suggested the development of a suppressor mutation. In order to characterize a potential suppressor mutant ΔOMC^S, single cells were isolated using dilution series and subsequent plating on LB-agar plates.

3.1 Fe(III)-citrate and birnessite reduction by the suppressor mutant ΔOMC^S

Fe(III)-citrate reduction curves were recorded in batch cultures with *S. oneidensis* wild type, ΔOMC, and ΔOMC^S. For the last one, reduction was measured in the presence and absence of 1 mM arabinose as inducer for *mtrA* and *mtrB* expression (Figure 21). Of note, *S. oneidensis* cannot grow with arabinose as a substrate (Gralnick *et al.*, 2006). As indicated in Figure 21, ferric iron reduction of the suppressor mutant ΔOMC^S was strictly dependent on arabinose induction upon which the reduction rate reached 76% of the wild type rate (Figure 21). The original mutant ΔOMC, induced with 1 mM arabinose showed almost no ferric iron reduction activity within 35 h.

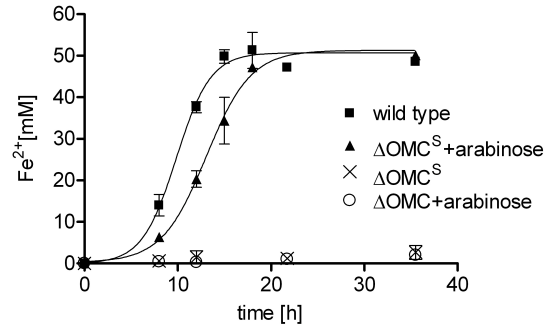

strain	specific iron reduction rate μ in [h^{-1}]
wild type	0.534±0.045
ΔOMC^S+arabinose	0.451±0.104
ΔOMC^S	not determinable
ΔOMC+arabinose	not determinable

Figure 21: Fe(III)-citrate reduction by ΔOMC^S and wild type strains. *Iron reduction by S. oneidensis strains growing on minimal medium with 50 mM lactate and 50 mM Fe(III)-citrate and addition of 1 mM arabinose if indicated. Symbols refer to means of triplicate measurements, error bars indicate standard deviation. Solid line represents a curve-fit done with GraphPad Prism 4. Specific iron reduction rate was calculated for each biological replicate; means and standard deviation are indicated.*

Birnessite, as a mineral phase electron acceptor was used to assess the ability of ΔOMC^S to reduce oxidized manganese species (Figure 22). While ΔOMC has only background reducing activity, ΔOMC^S is able to reduce birnessite 10-fold faster compared the original mutant and with 20% of the wild type rate. Albeit, the phenotype of birnessite reduction of ΔOMC^S is not as pronounced as with Fe(III)-citrate as electron acceptor.

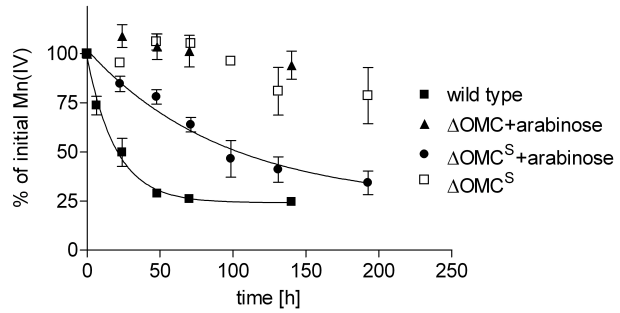

strain	specific birnessite reduction rate μ in [h^{-1}]
wild type	0.051±0.008
ΔOMC+arabinose	not determinable
ΔOMC^S+arabinose	0.008±0.002
ΔOMC^S	not determinable

Figure 22: Birnessite reduction by ΔOMC^S and wild type strains. *Manganese reduction was quantified in growth experiments. Birnessite (2.5 mM) was added to 50 ml mineral medium with lactate as an electron donor and 1 mM arabinose if indicated. Percentage Mn(IV) is relative to the starting concentration. Initial values for Mn(IV) varied slightly (±0.266 mM) and were therefore set to 100%. Abiotic decrease in the measurable Mn(IV) (probably due to adhesion to the culture flask) was subtracted. Symbols refer to means of triplicate measurements, error bars indicate standard deviation. Solid line represents a curve-fit done with GraphPad Prism 4. The specific Mn(IV) reduction rate was calculated for each biological replicate; means and standard deviation are indicated.*

3.2 Reduction of electron shuttles by ΔOMC^S

Electron shuttles have been proposed to be involved in *S. oneidensis* catalyzed metal and mineral reduction. They can either be produced and secreted by the cell endogenously, mainly in the form of riboflavin (Marsili *et al.*, 2008; von Canstein *et al.*, 2008) or can be

present in soils typically in the form of dissolved or solid-phase humic substances (Jiang and Kappler, 2008; Roden *et al.*, 2010). As humic substances are a structurally diverse group of substances, AQDS can be used as a surrogate for small fulvic acid molecules and for quinone moieties in humic acids (Jiang and Kappler, 2008). Reduction of large humic acid molecules was measured with Pahokee peat humic acids (PPHA). These measurements were done by our cooperation partners of the group of Prof. Dr. Kappler, University of Tübingen.

For riboflavin and AQDS, the reduction activity was recorded over 20 min using washed cell suspensions of anoxically grown cells that should be free of any additional electron shuttle. As Figure 23a indicates, reduction of riboflavin was rather slow for ΔOMC and ΔOMC^S (12% and 21% of wild type activity, respectively). In contrast to this, AQDS was reduced by the suppressor mutant with 81% of the wild type rate while the original ΔOMC strain reduced AQDS with only 32% of the wild type rate (Figure 23b). This effect was even more pronounced when the cells were pregrown on Fe(III)-citrate leading to a ΔOMC^S AQDS reducing activity of 99% compared to the wild type (Figure 23b). The higher rate of AQDS reduction by the ΔOMC strain compared to previous results (Figure 10, page 68) can be explained by the induction with 1 mM arabinose instead of 0.1 mM arabinose used before.

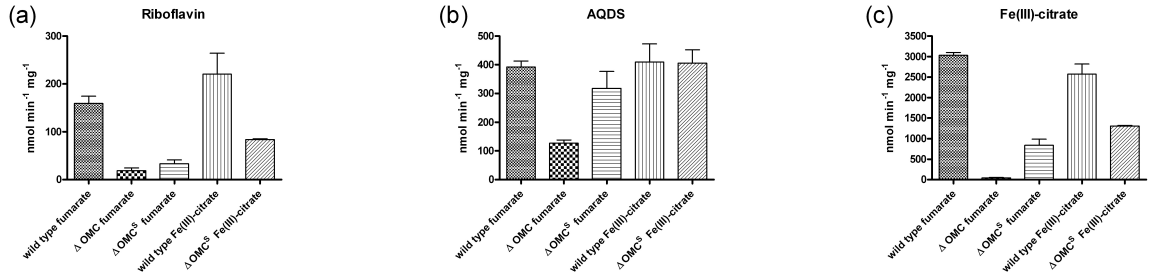

Figure 23: Cell suspension experiments with S. oneidensis wild type, ΔOMC mutant, and ΔOMC^S mutant strains with riboflavin, AQDS, and Fe(III)-citrate. *Washed cell suspensions were prepared from cultures grown under anoxic conditions with fumarate or Fe(III)-citrate as terminal electron acceptor. All experiments were carried out under anoxic conditions. Maximal reduction rates (means of triplicate measurements) were normalized to the protein content. The reduction of riboflavin (a) and AQDS (b) was measured in a continous spectrophotometric assay using absorption maxima at 450 nm and 436 nm, respectively. Fe(III)-citrate reduction rates (c) were measured by determining Fe(II) content discontinuously using the ferrozine reagent.*

The reduction of PPHA was measured over a time frame of 18 days in a growth experiment (Figure 24). For the reduction of PPHA, the situation resembled the results of the riboflavin reduction experiments. The maximal PPHA reduction rate reached in ΔOMC 18% and in ΔOMC^S 35% of wild type activity (Figure 24).

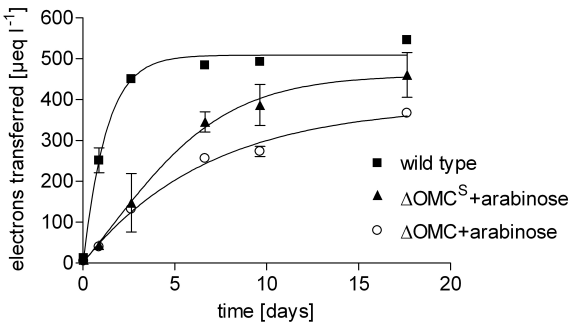

strain	specific PPHA reduction rate µ in [d^{-1}]
wild type	0.972±0.180
ΔOMC^{S}+arabinose	0.261±0.053
ΔOMC+arabinose	0.151±0.014

Figure 24: Humic acid reduction. *Electrons transferred to Pahokee peat humic acids (PPHA) by different S. oneidensis strains. Values are given in electron equivalents measured with Fe(III)-citrate in an electron shuttling assay. Symbols refer to means of duplicate measurements, error bars indicate deviation from the mean. Solid line represents a curve-fit done with GraphPad Prism 4. Specific PPHA reduction rate was calculated for each biological replicate; means and deviations from the mean value are indicated.*

3.3 Reduction of Fe(III)-citrate by washed cell suspensions

Cell suspension experiments were conducted to assess the ability of ΔOMC^{S} cells to reduce Fe(III)-citrate without the putative involvement of endogenous electron shuttles. The different *S. oneidensis* strains were pregrown on minimal medium with fumarate or Fe(III)-citrate as electron acceptors and were induced with 1 mM arabinose. Cells were then washed twice in buffer without electron acceptor under anoxic conditions and thereafter used for Fe(III)-citrate reduction assays. Fumarate grown ΔOMC^{S} cells reduced Fe(III)-citrate with 28% of the wild type rate, while ΔOMC showed no detectable activity. When the cells were pregrown on Fe(III)-citrate, the activity of ΔOMC^{S} increased to 51% of the wild type ferric iron reduction rate (Figure 23c, page 81).

3.4 Putative involvement of other outer membrane protein complexes

Several experimental results point towards the role of the outer membrane *c*-type cytochromes MtrC and OmcA as the final metal and flavin reductases of *S. oneidensis* (Bücking *et al.*, 2010; Coursolle *et al.*, 2010). The mechanism of metal reduction in ΔOMC^{S} must be independent of outer membrane cytochromes because all five corresponding genes are completely deleted (Bücking *et al.*, 2010). To find out if additional heme proteins were expressed in ΔOMC^{S} under ferric iron reducing conditions, membrane and soluble fraction were analyzed by SDS-PAGE. Figure 25 shows that no additional heme proteins are visible.

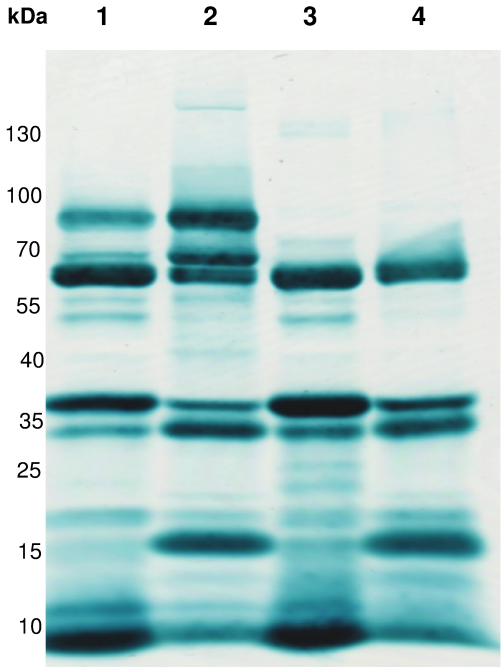

Figure 25: SDS-PAGE with staining of heme proteins. *SDS-PAGE of soluble and membrane fractions from wild type and ΔOMC^S cells grown on Fe(III)-citrate. Lane 1: soluble fraction from wild type; lane 2: membrane fraction from wild type; lane 3: soluble fraction from ΔOMC^S; lane 4: membrane fraction from ΔOMC^S. 50 µg protein were loaded in each lane of the gel.*

A recent study described the modularity of different outer membrane spanning complexes in *S. oneidensis* (Coursolle and Gralnick, 2010). Hence, it was asked whether another surface localized terminal reductase could functionally replace outer membrane cytochromes. The only other enzyme fulfilling this prerequisite is the DMSO reductase DmsAB (Gralnick *et al.*, 2006). The genome of *S. oneidensis* holds besides the genes encoding the functional protein, *dmsA-1* and *dmsB-1*, (SO_1429 and SO_1430) also a duplication of the locus, *dmsA-2* and *dmsB-2*, (SO_4357 and SO_4358). Both loci are still present in ΔOMC, the parental strain of suppressor mutant ΔOMC^S. Hence, *dmsAB-1* and *dmsAB-2* were deleted in ΔOMC^S and it was sought for an effect of these deletions on the Fe(III)-citrate reduction rate of this strain. The deletions did not lead to a change of the ΔOMC^S phenotype regarding Fe(III)-citrate reduction (data not shown). Hence, an involvement of these proteins in the described iron reduction phenotype was excluded.

If other proteins functionally replaced the outer membrane cytochromes in ΔOMC^S during Fe(III)-citrate reduction, one would expect that they occupied the same location on the outside of the outer membrane. Protein secretion and export to the outer membrane is catalyzed in *S. oneidensis* by the type II secretion system. Consequently, this export machinery is essential for metal reduction because it translocates the outer membrane

cytochrome to their final destination (DiChristina *et al.*, 2002; Shi *et al.*, 2008). The genes for the type II secretion systems are clustered in the *gsp*-locus. Deletion of *gspD*, a key gene within the cluster, is sufficient to disable the function of the secretion system (Shi *et al.*, 2008). As expected, *gspD* deletion from the wild type chromosome (resulting in strain JG443) led to a complete loss of ferric reductase activity (Figure 26). In contrast to this, deleting *gspD* from the chromosome of ΔOMC^S (resulting in strain JG444, ΔOMC^{S}Δ*gspD*) did not affect the Fe(III)-citrate reduction significantly. The maximal reduction rates of ΔOMC^S and ΔOMC^S Δ*gspD* were almost identical with a slightly longer lag-phase of the ΔOMC^{S}Δ*gspD* strain which might be due to a minimally lower initial cell number (Figure 26).

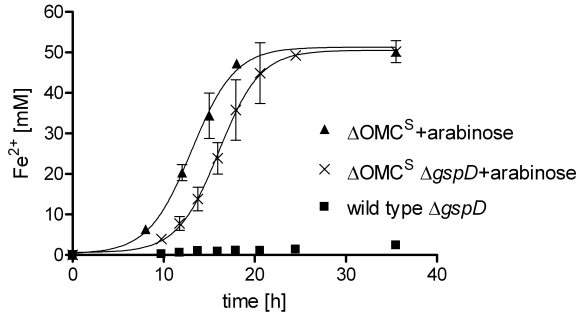

strain	specific iron reduction rate μ in [h^{-1}]
wild type Δ*gspD*	not determinable
ΔOMC^{S}Δ*gspD*+arabinose	0.445±0.082
ΔOMC^S+arabinose	0.451±0.104

Figure 26: Fe(III)-citrate reduction with gspD-mutants. *Fe(III)-citrate reduction by S. oneidensis ΔgspD mutant, ΔOMC^S and ΔOMC^{S}ΔgspD mutant strains growing on minimal medium with 50 mM lactate and 50 mM Fe(III)-citrate. Arabinose was added to all experiments in a concentration of 1 mM. Symbols refer to means of triplicate measurements, error bars indicate standard deviation. Solid line represents a curve-fit done with GraphPad Prism 4. Specific iron reduction rate was calculated for each biological replicate; means and standard deviation are indicated.*

3.5 Confirmation of outer membrane integrity in ΔOMC^S

A higher permeability of the outer membrane could cause the observed phenotype of ΔOMC^S since it is known that periplasmic cytochromes can catalyze ferric iron reduction as well. Still, outer membrane cytochromes are usually necessary since electron acceptors like Fe(III)-citrate or birnessite cannot pass the outer membrane. Therefore, two tests were performed to exclude the possibility that the general stability or permeability of the outer membrane might be the reason for the observed phenotype of the ΔOMC^S-mutant. First ethidium bromide uptake rates were determined by measuring the increase in fluorescence over time. Ethidium bromide is a large, hydrophobic dye (about 0.12 nm wide) with a delocalized positive charge that makes it unlikely to diffuse through narrow

porin channels (0.7 by 1.1 nm in *E. coli* OmpF; (Cowan *et al.*, 1992). It can therefore be used to measure permeability of the outer membrane (Murata *et al.*, 2007). The detected ethidium bromide uptake kinetics of wild type, ΔOMC, and ΔOMC^S were almost identical (Figure 25). As a positive control, cells were treated with polymyxin B which destabilizes the outer membrane (Vaara, 1992). The ethidium bromide uptake rate increased approximately twofold (Figure 25) but was again identical in the three tested strains.

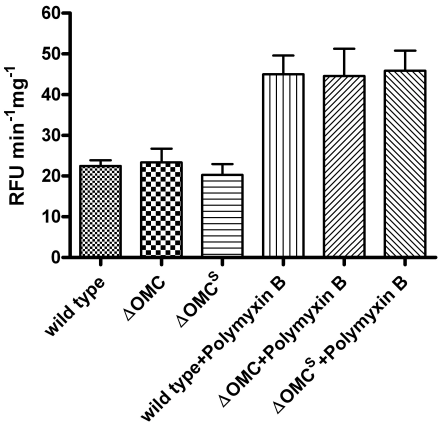

Figure 27: Ethidium bromide influx rates. *Ethidium bromide influx measured with S. oneidensis wild type, ΔOMC and ΔOMC^S strains. Influx rates were calculated from the continuously measured increase in fluorescence (excitation 545 nm, emission 600 nm), normalized to the protein content. As a positive control, 1 mg ml^{-1} polymyxin B, which destabilizes the outer membrane, was added to the cells.*

As a second test, antibiotic susceptibility of the different strains was compared using kanamycin A as an aminoglycoside, colistin as a polymixine, and chloramphenicol forming its own group of rather small reagents with an aromatic ring. As Figure 28 indicates, the inhibitory zones around the test plates containing the antibiotic drugs are either highly similar for wild type, ΔOMC, and ΔOMC^S or even smaller for ΔOMC^S compared to the other two strains. Therefore, the results of the ethidium bromide uptake test were verified and it seems rather unlikely that altered outer membrane permeability caused the observed phenotype of ΔOMC^S.

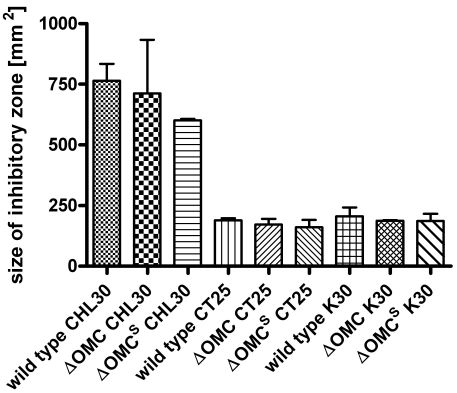

Figure 28: Minimal inhibitory concentration towards antibiotics. *Antibiotic susceptibility was tested in a disc diffusion test. Paper discs containing either 25 µg colistin (CT25), 30 µg kanamycin (K30) or 30 µg chloramphenicol (CHL30) were applied to the surface. After overnight incubation at 30°C, plates were photographed and zones of inhibition were measured with ImageJ.*

3.6 Identification of point mutations as genetic basis of ΔOMC-suppression

The genetic source of the ΔOMC^S-mutant phenotype was addressed using Solexa sequencing of the genome and mapping to the published sequence of *S. oneidensis* MR-1 (accession number NC_004347). Analysis of the assembled Solexa reads revealed 85 point mutations but no larger insertions or rearrangements of genes (Table 23, page 88). Two of the point mutations raised our interest, since they were localized in *mtrA* and *mtrB*, respectively. In both cases, a nucleotide base exchange from cytosine to adenosine occurred. These exchanges resulted in the replacement of an asparagine by a lysine in MtrA and MtrB, respectively (MtrA: Asn 290* Lys; MtrB: Asn 219* Lys; *Numbers refer to the amino acid sequence of MtrA and MtrB, the corresponding chromosomal positions are 1858407 and 1857606, respectively).

Both proteins are crucial for dissimilatory metal reduction as well as reduction of extracellular electron shuttles. Furthermore, arabinose induction was necessary for extracellular respiration in ΔOMC^S. Therefore, it was our aim to assess whether these point mutations in *mtrA* and *mtrB* caused the observed ΔOMC^S phenotype. Hence, both genes were cloned in their wild type and suppressor mutant form (designated *mtrA^S* and *mtrB^S*) in a pBAD202 expression vector resulting in plasmids pmtrAmtrB and pmtrA^{S}mtrB^S (Table 2). These plasmids were transferred into the parental strain ΔOMC and the resulting strains were tested for their ability to reduce Fe(III)-citrate (Figure 29). Expression of the wild type allele (strain JG450) did not lead to an alteration of the ΔOMC phenotype, but expression of the allele carrying the point mutations (strain

JG449) resulted in a phenotype highly similar to ΔOMC^S (Figure 29). Since these data demonstrated that the point mutations in *mtrA*^{S} and *mtrB*^{S} were essential for suppression of the ΔOMC^S mutation, it was concluded that the other observed point mutations might be interesting but of minor importance for this study.

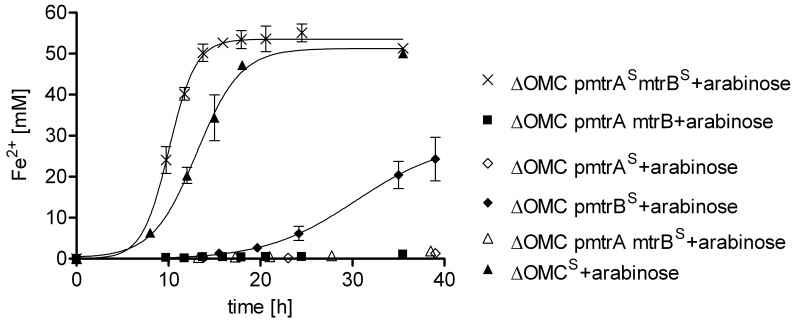

strain (all induced with 1 mM arabinose)	**specific iron reduction rate μ in [h^{-1}]**
ΔOMC pmtrA^{S}mtrB^S	0.602±0.169
ΔOMC pmtrAmtrB	not determinable
ΔOMC pmtrA^S	not determinable
ΔOMC pmtrB^S	0.218±0.062
ΔOMC pmtrAmtrB^S	not determinable
ΔOMC^S	0.451±0.104

Figure 29: ΔOMC complementation with pmtr-plasmids. *Fe(III)-citrate reduction by S. oneidensis ΔOMC mutant strains, complemented with different plasmids and growing on minimal medium with 50 mM lactate and 50 mM Fe(III)-citrate. Arabinose was added to all experiments in a concentration of 1 mM. Symbols refer to means of triplicate measurements, error bars indicate standard deviation. Solid line represents a curve-fit done with GraphPad Prism 4. Specific iron reduction rate was calculated for each biological replicate; means and standard deviation are indicated.*

Table 23: Single nucleotide polymorphisms (SNP) in ΔOMC^S

(SNP positions are given relative to the genome of *S. oneidensis* MR-1 wild type. If no locus tag is indicated, the position of the SNP is intergenic.

A>G means: A in ΔOMC-genome was replaced by G in ΔOMC^S-genome.

T>* means: T in ΔOMC-genome was deleted in ΔOMC^S-genome.

Y>C means: C or T in ΔOMC-genome was replaced by C in ΔOMC^S-genome)

Position SNP S.oneidensis MR-1	***Change in nucleotide***	***Locus tag***	***Gene symbol***	***Gene description***	***Remarks***
18204	G>A				
131994	T>C	SO_0122		amino acid transporter LysE	
408350	C>*				
434822	T>C				
514080	A>*				
618045	T>*	SO_0588		transporter, putative	
698256	G>C	SO_0680		hypothetical protein	
735021	G>T	SO_0719		TonB-dependent receptor, putative	
735043	G>T	SO_0719		TonB-dependent receptor, putative	
801756	A>T	SO_0787		hypothetical protein	
1006476	G>T	SO_0975		hypothetical protein	
1026745	G>A	SO_0992	*lysS*	lysyl-tRNA synthetase	
1201298	G>C	SO_1156		TonB-dependent receptor	
1201355	G>T				
1227963	G>C	SO_1184	*pth*	peptidyl-tRNA hydrolase	
1227985	G>C	SO_1184	*pth*	peptidyl-tRNA hydrolase	

Position SNP S.oneidensis MR-1	***Change in nucleotide***	***Locus tag***	***Gene symbol***	***Gene description***	***Remarks***
1367113	A>C	SO_1311		transcriptional regulator	
1413688	G>A				
1508296	A>G				
1719465	T>C	SO_1637		surface antigen	
1753711	T>G	SO_1666	*phhA*	phenylalanine 4-monooxygenase	
1850852	A>C	SO_1771		GntP family permease	
1850853	T>G	SO_1771		GntP family permease	
1857606	C>A	SO_1778	*mtrB*	outer membrane protein precursor MtrB	
1858407	C>A	SO_1777	*mtrA*	decaheme cytochrome c MtrA	
1954935	T>A	SO_1862	*pgsA*	CDP-diacylglycerol-glycerol-3-phosphate 3-phosphatidyl transferase	
2112141	G>T	SO_2013	*dnaX*	DNA polymerase III, gamma and tau subunits	
2112150	A>G	SO_2013	*dnaX*	DNA polymerase III, gamma and tau subunits	
2113380	A>C	SO_2014		hypothetical protein	
2113456	A>C	SO_2014		hypothetical protein	
2122997	A>G	SO_2024		hypothetical protein	
2407195	A>*				
2407389	G>*				

Position SNP S.oneidensis MR-1	***Change in nucleotide***	***Locus tag***	***Gene symbol***	***Gene description***	***Remarks***
2415870	G>A	SO_2304	*ald*	other	
2453867	T>G				
2632050	C>T				
2632051	C>T				
2632076	A>C				
2632079	C>T				
2632106	C>G				
2632194	C>A				
2632262	A>C				
2632279	C>A				
2632295	A>T				
2632364	C>G				
2632476	T>G				
2799389	A>G	SO_2671		hypothetical protein	
2876561	A>*	SO_2754		MotY sodium type flagellar protein	Stop-Codon>TAT
2900888	G>C	SO_2778	*fabH-1*	3-oxoacyl-(acyl carrier protein) synthase III	
3001147	G>C	SO_2880		glutaredoxin domain-containing protein	
3001210	G>C	SO_2880		glutaredoxin domain-containing protein	
3242135	T>C	SO_3113	*tgt*	queuine tRNA-ribosyltransferase	
3259672	G>C	SO_t072	*tRNA-Ala-3*	tRNA	
3260658	A>C	SO_3128.2		glutamate tRNA synthetase	
3261767	C>G	SO_t073	*tRNA-Val-5*	tRNA	

Position SNP S.oneidensis MR-1	***Change in nucleotide***	***Locus tag***	***Gene symbol***	***Gene description***	***Remarks***
3261770	T>C	SO_t073	*tRNA-Val-5*	tRNA	
3384877	C>T	SO_3245	*flgF*	flagellar basal body rod protein FlgF	
3417774	A>G				
3419919	T>A	SO_3279		AcrB/AcrD/AcrF family protein	
3427554	C>A	SO_3286	*cydA*	cytochrome d ubiquinol oxidase, subunit I	
3427582	T>A	SO_3286	*cydA*	cytochrome d ubiquinol oxidase, subunit I	
3489938	T>G				
3588500	Y>A	SO_3443		ISSod4, transposase	
3588512	Y>A	SO_3443		ISSod4, transposase	
3588719	Y>G	SO_3443		ISSod4, transposase	
3588812	Y>G	SO_3443		ISSod4, transposase	
3653128	C>G	SO_3502		hypothetical protein	
3655317	A>C	SO_3504		hypothetical protein	
3750389	C>G	SO_3583	*rsuA-1*	other	
3783035	T>C	SO_3622		hypothetical protein	
3843377	C>A	SO_3692		ABC transporter, ATP-binding protei	
4052809	T>A	SO_3904	*tolC*	outer membrane channel protein	

Position SNP S.oneidensis MR-1	***Change in nucleotide***	***Locus tag***	***Gene symbol***	***Gene description***	***Remarks***
4216207	A>G	SO_4062	*psrA*	polysulfide reductase, subunit A	
4505871	C>T	SO_4319		HlyD family secretion protein	
4512655	C>T	SO_4324		GGDEF domain-containing protein	
4521417	G>*	SO_4327		HlyD family secretion protein	
4614019	G>*	SO_4423		hypothetical protein	
4687941	A>G				
4687972	C>T				
4687973	T>C				
4687987	A>G				
4721421	T>*	SO_4525		hypothetical protein	
4841973	A>G	SO_4645		hypothetical protein	
4842089	A>C	SO_4645		hypothetical protein	
4894203	Y>C	SO_4692		AcrB/AcrD/AcrF family protein	

Still, a further question was if a single mutated gene is sufficient for ferric iron reduction without outer membrane cytochromes. Therefore, *mtrA*^{S} and *mtrB*^{S} were cloned into separate vectors resulting in pmtrA^{S} and pmtrB^{S} (strains JG462 and 463). Expression of both proteins could be shown by SDS-page (Figure 30, page 93). Only *mtrB*^{S} expression (strain JG463) resulted in iron reduction but on a lower level compared to ΔOMC^{S} or the ΔOMC strain carrying pmtrA^{S}mtrB^{S} (Figure 29, page 87). Hence, both variants, MtrA^{S} and MtrB^{S}, have to be present to enable rapid reduction of Fe(III)-citrate.

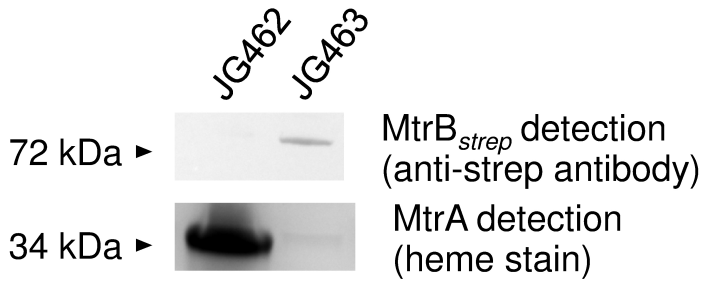

Figure 30: Expression of MtrA^S in strain JG462 and MtrB^S in strain JG463. *The upper panel shows a western blot developed with anti-strep antibody to detect MtrB (20 µg protein were loaded on the gel). The lower panel shows staining of heme proteins at the size of ~35 kDa to detect MtrA. (40 µg protein were loaded on the gel).*

3.7 Complementation of ΔmtrA and ΔmtrB mutants using *mtrA^S* and *mtrB^S*

MtrA and MtrB form a complex in the outer membrane of *S. oneidensis* cells (Hartshorne *et al.*, 2009). Furthermore, MtrA is necessary for periplasmic stability of MtrB (Schicklberger *et al.*, 2010). Since this interaction seems to be highly specific, it was asked whether the observed point mutations led to variants of the corresponding proteins that were only able to operate in the presence of the other variant. In other words, can MtrB^S only operate in an MtrA^S strain or is an interaction with wild type MtrA still possible. Consequently, *mtrA^S* and *mtrB^S* were expressed in *S. oneidensis* ΔmtrA and ΔmtrB strains, respectively. As Figure 31 indicates, both genes can complement also the corresponding deletion mutants in a wild type background. Hence, the point mutations do not seem to be localized to positions that disable interaction with the wild typic partner proteins.

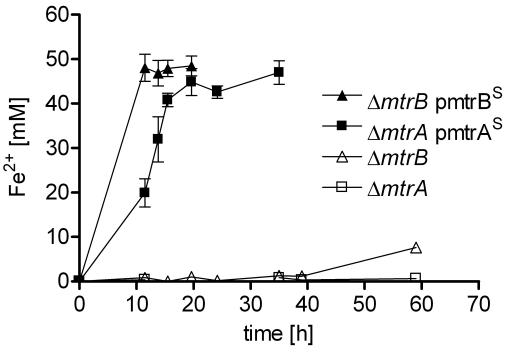

Figure 31: Complementation of ΔmtrA with pmtrA^S, and ΔmtrB with pmtrB^S. *Fe(III)-citrate reduction by S. oneidensis ΔmtrA, and ΔmtrB mutant and their complementation with pmtrA^S and pmtrB^S, respectively. All strains were grown in minimal medium with 50 mM lactate and 50 mM Fe(III)-citrate and addition of 1 mM arabinose. Symbols refer to means of triplicate measurements.*

3.8 Identification of the putative position of the point mutation within the protein structure

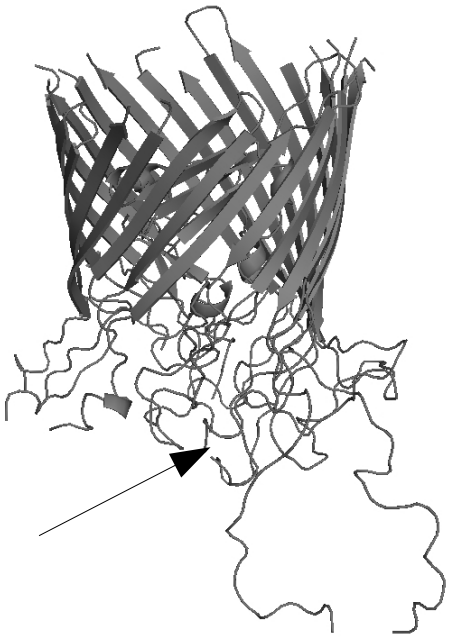

Figure 32: ***Model of three-dimensional structure of MtrB^S.*** *3D model of the mutated version of MtrB, calculated with TMBpro and displayed with PyMOL. The location of the point mutation is indicated by an arrow.*

TMBpro was used to predict the 3D structure of MtrB based on the typical structure of other outer membrane β-barrel proteins (Randall *et al.*, 2008). As Figure 32 indicates, Asn 219 of MtrB^S, is probably localized to a protein loop outside of the barrel structure. The 3D structure of MtrB^S was not markedly different from the predicted structure of the MtrB wild type allele (data not shown). Modeling of the 3D structure of MtrA is so far not possible since not enough data is available on which a model could be based on. A recent publication proposed an elongated molecular "wire" structure using data from small-angle X-ray scattering experiments (Firer-Sherwood *et al.*, 2011a). The point mutation in MtrA^S is close to the ninth heme binding motif, which might be a part of the protein that is embedded into the barrel structure of MtrB.

VIII. Discussion

Organisms belonging to the genus *Shewanella* have been found mostly in marine and freshwater environments around the world (Hau and Gralnick, 2007). One main feature of the organisms seems to be their ability to live in environments with a great variability of terminal electron acceptors. The organisms transfer electrons derived from the oxidation of fermentation end products like lactate or pyruvate[9] to at least 20 different electron acceptors like fumarate, nitrate, dimethylsulfoxide, thiosulfate, sulfides and several metal (oxyhydr)oxides but also oxygen if it is available (Hau and Gralnick, 2007).

This great variability of possible terminal electron acceptors of the *Shewanellaceae* is probably one reason for the amount and number of *c*-type cytochromes expressed under anaerobic conditions (Gralnick and Newman, 2007). The genome of the best studied organisms of the genus, *S. oneidensis* MR-1, contains the genetic information for 41 *c*-type cytochromes (9 proteins putatively localized in the cytoplasmic membrane, 5 in the outer membrane, 27 in the periplasm) (Meyer *et al.*, 2004; Romine *et al.*, 2008). It was shown that many *c*-type cytochromes are coexpressed under several anaerobic conditions independent of the electron acceptor used (Beliaev *et al.*, 2005).

For experimental research, this high number of genes coding for *c*-type cytochrome with putatively many similarities is challenging because classical approaches like transposon mutagenesis or single gene knock-out mutations often fail to show conclusive results (Bretschger *et al.*, 2007). For some genes, even a functional overlap was clearly shown (Myers and Myers, 2003b).

From the three subgroups of *c*-type cytochrome genes mentioned above, the proteins that are putatively localized to the outer membrane are of outstanding interest because of their central role for metal oxide reduction. What I aim at with this thesis is to contribute to the better understanding of the function of these proteins in the metabolism of *S. oneidensis*.

1. Conflicting results of outer membrane cytochrome mutant strains in the literature

The importance of outer membrane proteins and especially of *c*-type cytochromes for the reduction of insoluble metallic electron acceptors by *S. oneidensis* has been recognized for almost 20 years (Myers and Myers, 1992a; Myers and Myers, 1993). Since then

[9] Main known electron donors of *S. oneidensis* are lactate, pyruvate, H_2, and N-actetylglucosamine (Hau and Gralnick, 2007; Yang *et al.*, 2006).

numerous studies on the function of outer membrane proteins were published. Nearly all important genes for metal reduction are in close proximity on the chromosome in the *mtr*-gene cluster (**met**al **r**educing) depicted in Figure 4, page 62. The genes *mtrC*, *mtrA*, and *mtrB* form an operon and are regulated by a promoter in front of *mtrC*. It was shown by several groups that the *c*-type cytochrome MtrA and the β-barrel protein MtrB, localized in the outer membrane are essential for metal reduction (Bretschger *et al.*, 2007; Hartshorne *et al.*, 2009; Schicklberger *et al.*, 2010).

When we are talking about genes coding for outer membrane cytochromes in *S. oneidensis*, the genes *omcA*, *mtrC* (which is sometimes called *omcB* in older publications), *mtrF*, SO_1659, and SO_2931 are meant. The genes were identified based on the presence of heme binding motifs (CXXCH) and because they contain a cysteine residue after the signal peptidase cleavage site (Meyer *et al.*, 2004). After signal peptide cleavage, this cysteine is probably providing a site of covalent modification through addition of diacylglycerol and subsequent binding to the outer membrane (Okuda and Tokuda, 2011). Therefore, they are called outer membrane cytochromes.

The role of the outer membrane cytochromes in metal reduction is much less resolved than the roles of MtrA and MtrB. Numerous studies have been published on this subject and the results are often difficult to compare and the conclusions drawn are sometimes conflicting. The following section summarizes the results of the most important studies published about this subject.

Beliaev *et al.* reported on a *mtrC* mutant and showed that it is impaired in Fe(III)[10] reduction and manganese oxide reduction (showing only qualitative results for manganese). They further referred to unpublished data on a *omcA* mutant that showed no phenotype during growth on Fe(III) and manganese oxide (Beliaev *et al.*, 2001).

The validity of these results was questioned by Myers *et al.* who point out that a polar effect of the *mtrC* mutation lowering the expression of *mtrA* and *mtrB* in the study by Beliaev *et al.* is probable. The mutant studies by Myers *et al.* indicate a role for *mtrC* and *omcA* during the reduction of manganese (with greater importance for *mtrC*) while they did not see a role for these genes during the reduction of Fe(III)-citrate. Only a light effect of the *mtrC* mutation was seen when amorphous ferric oxyhydroxide was used as electron acceptor (Myers and Myers, 2001, , 2002b). Myers *et al.* further showed that the gene dosage is of great importance because the overexpression of *mtrC* could compensate for

[10] Beliaev *et al.* do not indicate the exact nature of the Fe(III) electron acceptor but it is likely that they used Fe(III)-citrate (Beliaev *et al.*, 2001).

the loss of *omcA* during manganese reduction (Myers and Myers, 2003b). A *mtrF* insertional mutation did not lead to a phenotype during Fe(III) or manganese reduction (Myers and Myers, 2002a).

Bretschger *et al.* confirm the absence of a phenotype for the Δ*mtrF* mutation during manganese reduction. Surprisingly, the same mutant showed a very high activity on hydrous ferric oxide exceeding more than twofold the activity of the wild type (Bretschger *et al.*, 2007). The authors further use *mtrC*/*omcA* double mutants and showed that they were only slightly impaired under manganese reducing conditions (~80% of wild type activity) while rather strongly impaired under Fe(III)[11] reducing conditions (~40% of wild type activity) (Bretschger *et al.*, 2007). Gorby *et al.* used the same mutants and came to very similar results using batch Fe(III) reduction experiments (~30% of wild type activity). The main topic of the study by Gorby *et al.* was the discovery of nanowires that are only poorly conductive in this mutant (Gorby *et al.*, 2006). Both groups did not test for putative polar effects of the deletions.

Borloo *et al.* analyzed again *mtrC, omcA* and *mtrC*/*omcA* double mutants during Fe(III)-citrate and Fe(III)-NTA reduction and came to the following results: *mtrC* mutation caused severe defects, *omcA* mutation only minor defects and the double mutant *mtrC*/*omcA* was devoid of Fe(III)-NTA reductase activity. The authors did kinetic calculations and came to the conclusion that MtrC and OmcA are the only Fe(III) reductases present in *S. oneidensis*. Borloo *et al.* tested polar effects of the mutations and could show that only the gene product of the respective mutated gene is missing. Still, the methods of the iron reduction measurements are somehow questionable because the authors used very low concentrations of terminal metallic electron acceptors (2 mM Fe(III)-citrate and 0.5 mM Fe(III)-NTA) and still observed a rise in cell densities as high as OD_{600nm} 0.3 for Fe(III)-NTA. The concentrations of terminal acceptors used are in strong contrast to all other published studies which use concentrations ranging from 20-50 mM Fe(III) chelates for growth experiments (Borloo *et al.*, 2007).

A very recent study by Coursolle *et al.* addressed some of the controversial results from above and postulated modularity of the different extended respiratory pathways with promiscuous *c*-type cytochromes that are thought to fulfill different functions in different mutant backgrounds (Coursolle and Gralnick, 2010). The authors tested single gene deletion mutants in *mtrC*, *omcA*, and *mtrF* and all four combinations of multiple gene

[11] Bretschger *et al.* used hydrous ferric oxide synthesized according to Schwertmann&Cornell (Bretschger *et al.*, 2007; Schwertmann and Cornell, 2000).

deletions that are possible. While Δ*omcA,* Δ*mtrF* and Δ*omcA*/Δ*mtrF* did not have a phenotype during Fe(III)-citrate reduction, the effect of the mutations increased in the order Δ*mtrC* < Δ*mtrC*/Δ*omcA* < Δ*mtrC*/Δ*mtrF* < Δ*mtrC*/Δ*mtrF*/Δ*omcA*. The effect of the mutations on iron oxide[12] reduction was similar to the results with Fe(III)-citrate except for the *omcA* deletion that showed only a little negative effect on iron oxide reduction being visible when high cell densities were used. Unfortunately, the study by Coursolle *et al.* did not address putative polar effects on the expression of MtrA and MtrB (Coursolle and Gralnick, 2010).

An interesting study by Lies *et al.* investigated the reduction iron oxide trapped in porous glass beads. The size of the pores was so small that the bacterial cells could not have direct contact to the iron oxide. Still, the reduction of the iron oxide was possible and the deletion of *mtrC* or *mtrB* lowered the reduction rate by 50% (Lies *et al.*, 2005).

Another study analyzed the role of outer membrane cytochromes in the reduction of flavin compounds. Flavins were shown to be secreted by *S. oneidensis* cells and it is believed that they catalyze metal oxide reduction by an electron shuttling mechanism (Marsili *et al.*, 2008; von Canstein *et al.*, 2008). Coursolle *et al.* could show that the majority of flavin reduction is catalyzed by MtrC and OmcA (Coursolle *et al.*, 2010).

Gao *et al.* used a different approach compared to all previous studies. The authors were testing the relative fitness of single gene deletion mutants compared to the wild type under certain growth conditions. All five deletions of a single outer membrane cytochrome had a negative effect on the fitness with Δ*mtrC* being the strongest by far when grown on Fe(III)-citrate (Gao *et al.*, 2010).

What is common for all mutant experiments described so far is the possibility of unperceived expression of another outer membrane cytochrome when one gene was deleted or mutated. Coursolle *et al.* reported an enhanced transcription of *mtrF* in a Δ*mtrC* strain (Coursolle and Gralnick, 2010). The origin of this regulatory effect was not explored but it is possible that a similar regulation could have occurred in other mutant strains of other studies. A study by Dale *et al.* showed that a mutant impaired in *c*-type cytochrome maturation that produced strongly reduced amounts of *c*-type cytochrome (nearly invisible on SDS-PAGE) was still able to reduce Fe(III)-citrate and manganese oxide with very high rates (Dale *et al.*, 2007). An upregulation of MtrF, SO_1659 and

[12] Coursolle *et al.* did not indicate the preparation of the iron oxide used (Coursolle and Gralnick, 2010).

SO_2931 could thus very possibly remain unperceived even if cellular fractions are analyzed by SDS-PAGE.

Another point that was not addressed by most studies is the possible polar effect of gene deletions on the expression of adjacent genes, especially the effect of *mtrC* deletions. The following genes are controlled by the same promoter region (compare Figure 4, page 62) and the phenotypes of *mtrC* deletion or disruption mutants could therefore very well be influenced by an altered expression of *mtrA* and *mtrB*.

2. The quintuple outer membrane cytochrome mutant ΔOMC

The emphasis of this study[13] was to analyze the activity of single outer membrane cytochromes in an *in vivo* context. Therefore, a mutant called ΔOMC devoid of all five of these proteins was generated to allow for the expression of single outer membrane cytochromes in a defined background.

To avoid any doubts about the correct expression of *mtrA* and *mtrB* in the ΔOMC mutant, we included an arabinose inducible promoter and an *araC* gene coding for a repressor/activator protein in the genome. There has been some controversy about the use of P_{BAD} promoters in *E. coli* because the arabinose triggered expression of defined amounts of protein was hampered by an influence of the repressor/activator protein AraC on arabinose uptake catalyzed by AraE leading to mixed populations at subsaturating arabinose concentrations (Khlebnikov *et al.*, 2001; Siegele and Hu, 1997). Still, this problem is presumably not virulent in *S. oneidensis* because the genome contains no homologue to AraE and thus the expression of a certain level of MtrA and MtrB should be similar in every single cell of a batch with the same induction.

The growth behaviour of the ΔOMC strain under aerobic conditions on LB and under anaerobic conditions with fumarate as terminal electron acceptor was indistinguishable from wild type (data not shown). Analysis of membrane fractions from fumarate grown cells by SDS-PAGE and staining of heme proteins showed that the most prominent bands corresponding to OmcA and MtrC are missing in ΔOMC. The production of MtrA is dependent on the arabinose induction level, being clearly visible at 0.1 mM and reaching wild type level at 1 mM arabinose.

To be able to measure reduction rates specific for single outer membrane cytochromes, the background activity of strain ΔOMC reducing different terminal electron acceptors

[13] Most data presented here concerning the ΔOMC mutant were published in FEMS Microbiology Letters (Bücking *et al.*, 2010)

was determined. Cell suspensions prepared from fumarate grown cultures did not show any measurable reduction activity on Fe(III)-citrate. This might be surprising at first sight because Fe(III)-citrate is a soluble iron chelate and several periplasmic and cytoplasmic membrane bound *c*-type cytochromes from *S. oneidensis* were shown to catalyze ferric iron reduction (Gescher *et al.*, 2008; Pitts *et al.*, 2003). Still, the nuclear speciation of Fe(III)-citrate seems to hinder a passage through the outer membrane. Large, polymeric Fe(III)-citrate complexes that were observed under certain conditions might explain this effect (Spiro *et al.*, 1967). Gescher *et al.* showed that Fe(III)-citrate was only reduced by CymA if protoplasts (i.e. cells in isotonic solution without outer membrane) were prepared from an *E. coli* strain expressing this protein (Gescher *et al.*, 2008). The results of the cell suspension experiments with ΔOMC bolstered the hypothesis that Fe(III)-citrate cannot diffuse through the outer membrane because CymA in the cytoplasmic membrane of the mutant could catalyze the reduction if it had contact to Fe(III)-citrate. The expression of CymA in ΔOMC can easily be seen by the reduction of fumarate which is dependent on CymA. Fe(III)-citrate can therefore be used as a model substance to study extracellular respiration.

A recent publication by Qian *et al.* proposed an outer membrane cytochrome independent iron chelate uptake mechanism catalyzed by SO_2907 and subsequent periplasmic ferric iron reduction (Qian *et al.*, 2011). This would certainly challenge the assumption that Fe(III)-citrate can be used as a model substance to study extracellular respiration. The authors found that a deletion mutant in a gene encoding a putative TonB-dependent receptor protein (SO_2907) was affected in Fe(III)-citrate reduction and proposed a role of the protein in iron chelate uptake into the periplasm and subsequent reduction by periplasmatic *c*-type cytochromes. However, several different laboratories published that mutants in *mtrC*, *mtrB* or *mtrA* are unable to grow with Fe(III)-citrate as electron acceptor (Beliaev and Saffarini, 1998; Beliaev *et al.*, 2001; Borloo *et al.*, 2007; Hartshorne *et al.*, 2009; Myers and Myers, 2002b). All these groups should not have seen a strong effect of their mutant strains if the TonB-dependent receptor protein SO_2907 had major influence on Fe(III)-citrate reduction. Still, Qian *et al.* observed furthermore that the corresponding protein is an efficient Fe(III)-NTA binding protein. Hence, the observed growth phenotype might also be caused by the lack of an efficient iron acquisition protein in the outer membrane of a SO_2907 deletion mutant. Unfortunately, the authors did not show a complementation of the mutant using SO_2907. It is therefore not absolutely clear

whether a polar effect of the mutation also accounts at least partly for the observed growth disadvantage.

Fe(III)-NTA is another soluble iron chelate that was shown to cross much easier the outer membrane. It was shown to be reduced by cytoplasmic membrane anchored *c*-type cytochrome CymA (Gescher *et al.*, 2008) and by periplasmatic *c*-type cytochrome MtrA (Pitts *et al.*, 2003). Surprisingly, ΔOMC cells showed only very little reductase activity on Fe(III)-NTA compared to the wild type and compared to the MtrC and MtrF expressing ΔOMC strains. The situation was very similar for the reduction of anthraquinoe-2,6-disulfonate (AQDS). AQDS is a substance that is used as an analogue for quinone moieties in humic acids. Shyu *et al.* showed that AQDS diffused partly in the periplasm of *S. oneidensis* cells but not in amounts that were sufficient to support growth (Shyu *et al.*, 2002). Our studies showed that the ΔOMC mutant catalyzed the reduction of small amounts of AQDS. An explanation for the AQDS and Fe(III)-NTA reduction phenotypes of *S. oneidensis* wild type could be that the diffusion of both substances into the cell is much slower than their reduction at the cell surface by outer membrane cytochromes. This could mean that ΔOMC cells reduced only such small amounts of AQDS or Fe(III)-NTA during the cell suspension experiment because they were diffusion limited.

The reduction of the insoluble metallic electron acceptors birnessite (a manganese dioxide) and ferrihydrite by ΔOMC cells proceeded slowly compared to the wild type. Interestingly, within this long incubation time, a very low level reduction of the insoluble electron acceptors was present leading to the production of substantial amounts of reduced substrate after several days. One explanation for this could be that during the elongated incubation time of these experiments spontaneous suppressor mutations could occur as the one described in chapter VII. 3., page 79.

Furthermore, the amount of electrons transferred to an anode was small compared to the wild type facilitating the analysis of the effects of single outer membrane cytochrome expression. The reduction of an anode is as surface limited as the reduction of an insoluble metal. However, anode reduction experiments can provide an additional set of information due to the possibility to change the rate of electron abstraction from the anode surface and thus the potential. Biotechnological applications of this process in microbial fuel cells will be discussed in chapter 3.1.

2.1 The ΔOMC mutant as a platform for single outer membrane *c*-type cytochrome testing

To analyze activity and specificity of the different outer membrane cytochromes, we compared electron transfer to metals and to an anode surface. It was not the purpose of this study to reach wild type reduction rates with complemented strains, which would most probably necessitate production of two or more outer membrane cytochromes, but rather to establish a reliable test platform for outer membrane cytochrome activities.

To measure reductase activities with cell suspensions, cells were precultured under anaerobic conditions with fumarate as electron acceptor. The transcription of genes coding for *c*-type cytochromes seems to be similar under fumarate and iron reducing conditions (Beliaev *et al.*, 2005). Still, it was reported that the activities of membrane fractions were higher when the cells were cultured under iron reducing conditions (Ruebush *et al.*, 2006). For the characterization of outer membrane cytochromes in our ΔOMC system, determination of absolute rates is not central because the results are anyway not comparable to other studies without a *mtrA-mtrB* operon controlled by arabinose induction. The aim of this work was therefore to compare the relative activities of each single outer membrane cytochrome in a defined background.

2.1.1 OmcA

OmcA production did not lead to accelerated reduction rates compared to the ΔOMC mutant in ferric iron reduction assays. This effect does not seem to be due to the reported partial mislocalization of OmcA in a Δ*mtrC* mutant (Myers and Myers, 2001) since proteinase K assays clearly demonstrated the surface exposure of OmcA in the ΔOMC mutant. OmcA is part of the core proteins that can be found in ferric iron reducing *S. oneidensis* cells (Shi *et al.*, 2007). Purified OmcA was shown to transfer electrons to hematite (Xiong *et al.*, 2006), ferrihydrite (Reardon *et al.*, 2010) and different Fe(III) chelates (Wang *et al.*, 2008).

A very recent study by Rollefson *et al.* showed that *Geobacter* contains *c*-type cytochromes embedded in a polysaccharide matrix on the surface of the cells. This matrix was shown to be important for attachment of the cells to positively charged surfaces like poised anodes or metal oxide surfaces and it was suggested that a similar matrix could be important for *Shewanella* (Rollefson *et al.*, 2011). A conductive matrix by means of cytochromes would allow for biofilm formation with several layers of cells and might explain the observed reduction of metal oxide at a distance to cell attachment (Rosso *et*

al., 2003). We hypothesize that OmcA plays a prominent role in this matrix being an *in vivo* ferric iron reductase that is dependent on electron transport by another outer membrane cytochrome. This cytochrome would be most probably MtrC which would receive electrons from periplasmatic cytochromes. In this view, the two proteins fulfil slightly different roles in the extracellular reduction. The difference in the distribution of MtrC and OmcA on the cell surface observed by two groups would be in line with this hypothesis (Lower *et al.*, 2009; Reardon *et al.*, 2010).

However, OmcA expression in the absence of MtrC had a clear influence on birnessite reduction. We cannot explain this effect but it seems as if OmcA is linked to the periplasmic electron pool under manganese reducing conditions while it is not under ferric iron reducing conditions. Still, our data indicating a function of OmcA under manganese reducing conditions are in line with results obtained previously by Myers *et al.* (Myers and Myers, 2001, , 2003b).

2.1.2 MtrC

The conducted reduction experiments showed that MtrC could partly rescue the ΔOMC phenotype. A central role of MtrC in metal reduction is in agreement with other studies (Beliaev *et al.*, 2001; Borloo *et al.*, 2007; Bretschger *et al.*, 2007; Coursolle and Gralnick, 2010) and might reflect the recently discovered capability of a complex of MtrC with the β-barrel protein MtrB and the decaheme cytochrome MtrA to transport electrons over a liposomal membrane and hence most probably also over the outer membrane of *S. oneidensis* cells (Hartshorne *et al.*, 2009). It was shown that this MtrABC complex had a very high stability towards different detergents (Ross *et al.*, 2007 and personal communication by Simon Stephan). The proteins in the complex showed furthermore a strong reciprocal dependance: when MtrB is missing, MtrC was mislocalized to the cytoplasmic membrane (Myers and Myers, 2002a); if MtrA is missing, MtrB was unstable (Hartshorne *et al.*, 2009; Schicklberger *et al.*, 2010).

Besides a MtrABC complex, Shi *et al.* described an MtrC-OmcA complex in the outer membrane (Shi *et al.*, 2006). Although this complex was not observed by Hartshorne *et al.*, it might exist in parallel putatively forming a MtrABC-OmcA supercomplex (Hartshorne *et al.*, 2009). Two studies on the distribution of outer membrane cytochromes on the cell surface speak against this idea of a supercomplex. Reardon *et al.* and Lower *et al.* showed with different techniques that the distribution of OmcA and MtrC on the cell surface is not identical (Lower *et al.*, 2009; Reardon *et al.*, 2010). Reardon *et al.* showed

that MtrC localized in close association to iron precipitates on the cell surface when *S. oneidensis* cells were grown with ferrihydrite as electron acceptor. On the contrary, OmcA was distributed more diffusely on the cell exterior and was also detected outside of the cell in the layer of extracellular polymeric substances. Lower *et al.* saw a distribution that is exactly the inverse with OmcA associated with the iron minerals and MtrC distributed more diffusely (Lower *et al.*, 2009).

Purified MtrC was shown to transfer electrons to ferrihydrite (Reardon *et al.*, 2010) and different Fe(III) chelates (Wang *et al.*, 2008).

2.1.3 MtrF

Our experiments with heterologous expression of *mtrF* in ΔOMC showed for the first time that *mtrF* codes for a functional reductase that has under several conditions an even accelerated activity compared to MtrC. It is probable that a complex of MtrF, MtrA, and MtrB complex is formed similar to the MtrCAB complex described by Hartshorne *et al.* (Hartshorne *et al.*, 2009). We could further show that MtrF is exposed to the outer surface of the cell because it was prone to proteinase K degradation. The here presented experiments underline at least that MtrF is a reductase that could have this hypothetical function. The relative reduction activities of MtrF compared to MtrC follow the same pattern for all electron acceptors except for anode reduction. Here, the limiting current density (LCD) of MtrF expressing cells is only 46% compared to the LCD achieved with MtrC expressing cells. Therefore, we hypothesize that MtrF might be not as well connected to the periplasmic electron pool which could be due to a reduced capability of forming a complex with MtrA and MtrB. This interprotein electron transfer might not be rate limiting under metal reducing conditions but could become important when a certain current is abstracted from the anode controlled by a potentiostat.

mtrF is part of a gene cluster that includes with *mtrD* and *mtrE* genes that are highly similar to *mtrA* and *mtrB*. The transcription of *mtrF* is not significantly upregulated under anaerobic conditions (Beliaev *et al.*, 2005). A clear *in vivo* function of *mtrF* was not shown so far and mutations in *mtrF* did not show strong phenotypes (Bretschger *et al.*, 2007; Myers and Myers, 2002a). McLean *et al.* speculate that the *mtrDEF* gene cluster could encode a reductase that is active under oxic or suboxic conditions and might have a function in reduction-based detoxification of radionuclides (McLean *et al.*, 2008). Gao *et al.* see a reduced fitness of a Δ*mtrF* mutant under chromate reducing conditions which is another indicator for a *in vivo* function of MtrF in metal detoxification (Gao *et al.*, 2010).

MtrF protein was recently crystallized and the structure was solved with a resolution of 3.2 Å. The arrangement of heme groups in the protein allows for several routes of the electrons to reach their final acceptors at different sites of the protein (Clarke *et al.*, 2011).

2.1.4 SO_2931 and SO_1659

Our experiments showed that the production of SO_2931 and SO_1659 was less efficient compared to OmcA production. Nevertheless, we could show that the genes SO_2931 and SO_1659 code for heme proteins that are localized in the membrane fraction. The protein SO_1659 was prone to proteinase K degradation and is thus attached to the outer membrane and exposed to the outer surface. SO_2931 was not degraded in the assay. The reason could be that SO_2931 is not surface exposed or that it is not degradable by proteinase K. In a study published recently by Richter *et al.*, the authors can show with another technique that the SO_2931 protein is localized to the outer membrane and seems to be oriented towards the outer surface (Richter *et al.*, 2010). It is therefore likely that SO_2931 cannot be degraded by proteinase K. The expression of SO_2931 and SO_1659 never resulted in a significantly differing phenotype during all reduction experiments compared to the ΔOMC mutant. So far we can only speculate that these proteins might be involved in other electron transfer pathways or do not have a function in the physiology of *S. oneidensis* in general.

Information about the function of these proteins in the literature is sparse. The transcription of both genes is not significantly upregulated under anaerobic conditions (Beliaev *et al.*, 2005). Bretscher *et al.* observed a positive effect of a ΔSO_1659 mutation on current production in a microbial fuel cell while the other conditions tested (manganese reduction or ferric iron reduction) and the other mutant (ΔSO_2931) showed only mild or no effects. Gao *et al.* observed for both gene deletions (ΔSO_1659 and ΔSO_2931) a slight negative effect on fitness compared to the wild type when grown on Fe(III)-citrate.

To conclude the results obtained with the quintuple mutant ΔOMC it can be said that the mutant allowed the measurement of *in vivo* activities of single outer membrane cytochromes. Polar effects of the mutations and influence on the regulation of gene expression of other outer membrane cytochromes could be avoided with this strain. Future work needs to be done to investigate the role of OmcA during manganese oxide reduction.

3. Metal reducing microorganisms in biotechnology

While the first part of this work dealt with basic research questions regarding the role and specificity of outer membrane cytochrome in *S. oneidensis*, the focus of this second part will be directed more to modifications applied to the bacteria with the objective of putative applications in biotechnology.

3.1 Microbial fuel cell technology

Microbial fuel cells (MFC) take advantage of the electron transferring capacities of bacteria which act as biocatalysts. Reduced organic matter is oxidized by the bacteria and the electrons derived from this process are transferred to an anode surface. Most dissimilatory iron reducers are able to catalyze electron transfer to anode surfaces without the addition of mediators. This is certainly not due to an evolutionary adaptation to MFCs but rather to an unspecificity of the terminal reductases. These enzymes bring respiratory electrons into contact with extracellular electron acceptors and it is not important whether this electron acceptor is a graphite electrode or hydrous ferric oxide or Fe(III)-citrate. Hence, the components of the electron transport chain to an anode and to iron oxides are either highly similar or even identical. Therefore, initial characterization of a strain can be determined with ferric iron as electron acceptor. Still, a detailed verification of the results in a MFC will be necessary in the future.

3.2 Bioremediation of soils and sediments

Heavy metal pollution of soils and sediments is a major problem in many regions of the world, especially if the contaminants could to be mobilized into the ground water. For some important pollutants, bioremediation strategies based on metal reducing bacteria were proposed. For instance, Cr(VI) is a highly toxic and highly soluble contaminant that can be found at many industrial sites. It can be reduced by *S. oneidensis* to Cr(III), which is less toxic and precipitates upon formation and is thus immobilized. Outer membrane cytochromes play a major role in Cr(VI) reduction by *S. oneidensis* (Belchik *et al.*, 2011). Another very toxic pollutant is U(VI) that is present mainly at former U.S. nuclear weapon test sites. Reduction of U(VI) and precipitation of UO_2 nanoparticles on the cell surface have also been associated with outer membrane cytochromes in *S. oneidensis* (Marshall *et al.*, 2006).

3.3 Modulating the amount of outer membrane cytochromes

Both biotechnological approaches, the MFC and the bioremediation strategies, rely on the metabolism and especially on the extended respiratory chain of *S. oneidensis*. Bacterial strains catalyzing higher electron transfer rates to Cr(VI), U(VI), or anode surfaces are highly desirable.

Extracellular respiration of insoluble electron acceptors is surface limited. Hence, outer membrane cytochromes most probably catalyze the rate limiting step if a sufficient amount of reduced carbon sources is available. It was therefore our first aim to investigate the effect of a modulated amount of outer membrane cytochromes on extracellular respiration. This was achieved by the expression of plasmid encoded copies of *mtrC* and *mtrF* in the ΔOMC strain. The amount of outer membrane cytochromes was controlled by induction with different concentrations of arabinose.

The results of these experiments were rather disappointing because the maximal rate achieved with both strains (JG138 and JG139) was below the wild type rate. However, it could be deduced that the rates increased with the amounts of outer membrane cytochrome molecules present in the outer membrane. The upper rate limit was reached at relatively low induction levels but it was twofold higher in the MtrF expressing strain than in MtrC expressing strain. Above this limit, the high amount of outer membrane cytochromes had probably a toxic effect on the cells slowing down the reaction and eventually prohibiting growth. The difference in the maximal reduction rate of the two strains might be due to a higher tolerance of the cell to high concentrations of MtrF than to high concentrations of MtrC. An alternative explanation could be a difference in the expression levels of the two proteins. The expression levels of the proteins were not quantified exactly but did not seem to differ much.

We suspected that the main problem of the two strains is the missing connection of the periplasmic electron carrier proteins to high amounts of outer membrane cytochromes when they are produced in excess. The outer membrane β-barrel protein MtrB establishes this connection between periplasmatic electron transfer proteins and the outer membrane cytochromes. It was shown that MtrB is the center of a complex with MtrA attached on the periplasmic side, and MtrC attached on the outside of the outer membrane (Ross *et al.*, 2007). This complex was shown to transfer electrons over a liposomal membrane, which is suspected to be the natural function in the outer membrane, too (Hartshorne *et al.*, 2009). At a given arabinose induction level, strains JG138 and JG139 produce much

more outer membrane cytochromes than they do produce MtrA and MtrB proteins because the genes for outer membrane cytochromes are encoded in multiple copies per cell on plasmids while *mtrA* and *mtrB* are encoded in single copy on the chromosome.

All further experiments were carried out with MtrF, since it was suspected that the tolerance of the cells towards high amounts of MtrF was higher than the tolerance towards MtrC.

To circumvent the problems with the low concentrations of MtrA and MtrB and still expressing high amounts of outer membrane cytochromes, MtrF was expressed from a plasmid in a wild type background (strain JG311). Under these conditions, MtrA and MtrB were expressed from natural promoters while MtrF was controlled by arabinose induction. A similar experiment performed by Bretschger *et al.* with overexpression of MtrC in a wild type background yielded 35% higher anode reduction rate in a microbial fuel cell (Bretschger *et al.*, 2007).

Another idea behind this experiment was to explore if a synergistic effect can be seen when several outer membrane cytochromes are present. Shi *et al.* described such an effect when they compared *in vitro* activities of OmcA, MtrC, and combinations of both (Shi *et al.*, 2006). With most induction levels, the reduction rate was identical to the wild type strain without plasmid. Only the highest induction led to a growth deficiency probably due to the toxic effect described above. Interestingly, the amount of other *c*-type cytochrome in the membrane fraction (i.e. MtrC, OmcA, and MtrA) seemed to decrease the higher the MtrF concentration was. Two mechanisms could account for this phenomenon: either the absolute amounts of the other *c*-type cytochromes remain stable while the absolute amount of MtrF increases leading to a relative increase of MtrF compared to the other *c*-type cytochrome when analyzed by SDS-PAGE. Or, the increase in absolute MtrF concentrations comes with a concomitant decrease in the absolute concentrations of the other *c*-type cytochromes. The latter case could be due to a limitation in the cytochrome protein maturation machinery which is a process that has a high energy demand (Kranz *et al.*, 2009). That would mean that only a limited amount of *c*-type cytochromes could be successfully maturated. The expression of *c*-type cytochromes that are probably not absolutely necessary like OmcA in strain JG311 would then limit the amount of mature cytochromes that are necessary for a maximal rate.

3.4 Increasing the rate of electron transfer to insoluble electron acceptors

Using a synthetic biology approach we constructed a new strain called MTR-FAB with insertion of a new operon. An outer membrane spanning module composed of MtrA, MtrB, and MtrF are expressed in similar amounts controlled by one inducible promoter that is tightly repressed in the absence of an inductor. With this strain, we can show that the number of outer membrane spanning reductase complexes triggers the rate of iron reduction. The maximal reduction rate increases with the arabinose concentration, but it is not a linear dependence. The maximal iron reduction rate of the MTR-FAB construct at this induction level was 1.8-fold higher than that of the wild type. This superiority of the MTR-FAB strain is very promising for putative applications in biotechnology. A stronger induction with 2 mM arabinose leads to a higher production of MtrF but the maximal reduction rate seems to reach saturation. Further studies are needed to find out whether the difference between the reduction behavior with Fe(III)-citrate and with the reduction of an anode by strain JG 139 (ΔOMC pBAD202*mtrF*) discussed in section VIII. 2.1.3 is also valid for strain MTR-FAB.

Interestingly, we observed a reproducible dependency of reduction rates to a very large range of inductor concentrations, ranging from 100 µM to 1 mM arabinose. New possibilities open up upon this dependency which allows to deduce inductor concentration from reduction rates. Recently, microbial fuel cell based biosensors were introduced but with very limited analyte specificity (Davila *et al.*, 2011; Tront *et al.*, 2008). This new strain could in the future enable a strategy for microbial biosensors that is based on the measurement of anode reduction rates in a microbial fuel cell.

4. Identification of a ΔOMC suppressor mutant

As was pointed out before, MtrC is believed to be the main terminal metal and flavin reductase. The phenotype of a Δ*mtrC* mutant can only be rescued if MtrC itself or the similar cytochrome MtrF is used for complementation (Bücking *et al.*, 2010; Myers and Myers, 2001). To our great surprise, we observed that the quintuple mutant in all outer membrane cytochrome encoding genes (ΔOMC) was able to regain its ability to grow as a dissimilatory metal reducer after a lag phase that was several weeks long. This new strain ΔOMC^S reduces Fe(III)-citrate nearly as fast as the wild type in growth experiments. Interestingly, the suppressor mutant reduces extracellular electron acceptors with varying activities when compared to the wild type in cell suspension experiments. Fe(III)-citrate and AQDS are reduced with rates ranging from more than 50 to 99% compared to the

recorded wild type reduction rates. In contrast to this riboflavin, Pahokee peat humic acids, and birnessite are reduced with only 20 to 35% activity compared to the wild type. The different redox potentials of these compounds are unlikely to be the reason for the observed differences. Fe(III)-citrate has a potential of +372 mV (Straub *et al.*, 2001) while AQDS is with -184 mV more than half a volt below this value (Fultz and Durst, 1982). Birnessite has a redox potential of +612 mV (Robie *et al.*, 1995) and is therefore an even better electron acceptor compared to Fe(III)-citrate. The redox potential of riboflavin is with -210 mV (Stare, 1935) very similar to the potential of AQDS. For naturally occurring humic acids no defined redox potentials but rather ranges of standard reduction potentials from +150 to 300 mV (at pH 7) were determined (Aeschbacher *et al.*, 2011) since they form a supermolecular association of very diverse organic molecules. Still, since redox potentials are most likely not the reason for the observed kinetic data, we hypothesize that substrate specificity causes the observed differences. This substrate specificity would be determined by the terminal reductase of ΔOMC^S.

4.1 Exploring the mechanism of ΔOMC^S mutant

To explore the mechanism of the ΔOMC^S strain, several further gene deletions were introduced into the chromosome. These experiments revealed that the DMSO reductases are not required as terminal reductase of Fe(III)-citrate. Furthermore the export of other potential reductases via the type II secretion system to the outside of the outer membrane is not mandatory.

Genome resequencing revealed single point mutations in *mtrA* and *mtrB* but no other important genome rearrangements were observed. Heterologous expression of the mutated proteins $MtrA^S$ and $MtrB^S$ from a plasmid transformed into ΔOMC showed that both mutated proteins are essential for extracellular reduction of ΔOMC^S.

MtrB is a typical outer membrane β-barrel protein that most probably has a structural but not an enzymatic function (Hartshorne *et al.*, 2009; Myers and Myers, 2002a). On the contrary, MtrA is a *c*-type cytochrome that was previously shown to have ferric iron reductase activity (Pitts *et al.*, 2003). Hence, we hypothesize that the point mutations enable $MtrA^S$ to contact electron acceptors at the cell surface, or that the pore of $MtrB^S$ is – when compared to wild type MtrB – altered in a way that allows extracellular electron acceptors to reach into the pore and hence contact $MtrA^S$. This second hypothesis would be in line with the results of the cell suspension experiments. Larger substances are reduced more slowly than smaller electron acceptors, independently of their redox

potential. Riboflavin, birnessite or Pahokee peat humic acids might just be too large to reach into the pore as good as Fe(III)-citrate or AQDS. Still, we cannot definitely negate the possibility that other surface localized proteins could interact with $MtrA^S$ and/or $MtrB^S$ and hence could also be involved in the observed phenotype. However our experiments suggest that $MtrA^S$ is the new terminal reductase in this strain.

Unfortunately, it is so far not possible to show how the point mutations exchanging asparagine residues by lysine residues would enable this hypothesized modified structure of the $MtrAB^S$ complex. The crystal structure of the two important proteins MtrA and MtrB is not known so far. Modeling of MtrB structure and comparison with $MtrB^S$ showed that the point mutation is located at a protein loop outside of the trans-membrane barrel. One could speculate that the point mutation is in the region of the interaction site between MtrA and MtrB but the orientation of the β-barrel in the outer membrane is not known. The structure of MtrA was modeled recently by Firer-Sherwood and coworkers based on small-angle X-ray scattering (Firer-Sherwood *et al.*, 2011a). They proposed an elongated form of MtrA, which fits well with a partial insertion into the barrel of MtrB to form a complex. The point mutation in $MtrA^S$ is near the C-terminal region and could be embedded into MtrB.

4.2 Putative evolutionary origin of MtrAB modules

Sequenced *Shewanella* strains contain up to 9 copies of an MtrAB like module. In *S. oneidensis*, it was shown that MtrAB like modules are involved in dissimilatory metal (Beliaev and Saffarini, 1998; Coursolle and Gralnick, 2010) and DMSO reduction (Gralnick *et al.*, 2006). It is commonly believed that the module attached to MtrAB seems to determine the nature of the terminal electron acceptor or the electron donor of the respiratory pathway.

The possibility to reduce extracellular electron acceptors without outer membrane cytochromes which we observed with ΔOMC^S cells raises the question whether this suppressor mutant resembles an evolutionary intermediate. The correct localization of outer membrane cytochromes is a complex process. Lipid anchors have to be added to periplasmic cytochromes. These modified cytochromes have to be recognized by the type II secretion machinery which is a multiprotein complex itself. The interaction of the type II secretion machinery with target proteins is highly specific and still not fully understood (Francetic and Pugsley, 2005; Sandkvist, 2001). Last but not least, these outer membrane cytochromes have to be contacted to half-moduls like MtrAB that thereafter can deliver

electrons originating from the cytoplasmic membrane. The situation is similar for the DMSO reductase which is also attached to the outer surface of the cell in *S. oneidensis*. Due to this complexity it seems likely that the addition of outer membrane module to existing outer membrane conduits might be a typical example of upstream evolution. Extracellular metal respiration might have been possible without these modules but the environment might have selected for higher reduction rates that were realized by outer membrane cytochromes. For extracellular DMSO reduction, an existing DMSO reductase has probably changed the cellular localization from cytoplasmic membrane to outer membrane realizing a connection to periplasmic electron donors using the existing MtrAB electron conduit through the outer membrane.

Interestingly, modules similar to MtrAB are present in bacteria belonging to the α, β, γ and δ group of the proteobacteria. The MtrAB like module in *Rhodopseudomonas palustris* (*pioABC*; Figure 33) is of outstanding interest: the *pio*-operon was shown to be essential for phototrophic Fe(II) oxidation which is the inverse reaction of Fe(III) reduction catalyzed by most MtrAB modules (Jiao and Newman, 2007). *pioA* and *pioB* code for proteins similar in structure to MtrA and MtrB, respectively while *pioC* codes for a ferredoxin which is thought to be the electron donor for the photosynthetic reaction center receiving electrons from PioA. The role of PioC during Fe(II) oxidation can therefore be compared to the role of periplasmatic cytochromes during Fe(III) reduction and is very different from MtrC-like modules which enhance the reduction reaction. The *pio*-operon contains thus only modules similar to MtrAB which is a situation similar to ΔOMC^S. Phototrophic Fe(II) oxidation is a very ancient form of metabolism probably responsible for the occurrence of Fe(III) in sediments that are older than the great oxygenation event 2.45 billion years ago (Bekker *et al.*, 2004). The evolutionary origin and age of MtrAB modules cannot be determined but its widespread occurrence in different groups of proteobacteria favors the hypothesis of MtrAB being an evolutionary intermediate.

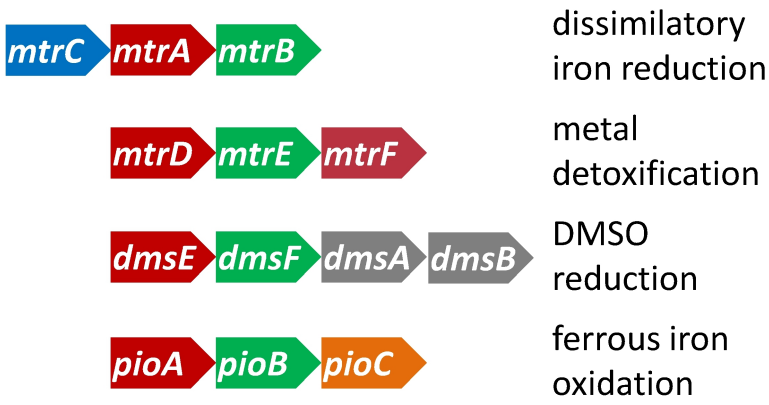

Figure 33: Alignment of gene clusters containing an MtrAB like module. *Genes similar to mtrA are drawn in green; genes similar to mtrB are drawn in red. The first three gene clusters are from S. oneidensis whereas the forth gene cluster is from Rhodopseudomonas palustris. The physiological function of the mtrDEF gene cluster is putative.*

4.3 Spontaneous mutations in *S. oneidensis* observed by other groups

Finally, it should be mentioned that the studied suppressor mutant nicely displays the plasticity of the genome of *S. oneidensis*. Other groups also reported on adaptations of the organism to gene disruptions or to new growth conditions. Dobbin *et al.* showed that new cytochromes appeared after they deleted *ifcA* from the chromosome of *Shewanella frigidimarina* (Dobbin *et al.*, 1999). Recently, Cordova *et al.* showed that in *S. oneidensis* an iron-sulfur protein replaced functionally CymA through transcriptional activation by an IS element (Cordova *et al.*, 2011). Howard *et al.* report on a spontaneous *S. oneidensis* mutant that gained the ability to utilize glucose as sole carbon source (Howard *et al.*, 2011).

It is possible that we report on a phenomenon that is more common than generally believed but can be overlooked easily. In a previous publication a similar case was observed but not followed. Myers *et al.* could show in their experiments that a Δ*mtrC*-mutant was capable of reducing Fe(III)-citrate after a three days lag phase (Myers and Myers, 2002b). The cells that were growing after 72 h might have been suppressor mutants as well. What we can learn is that the results of mutant studies have to be treated carefully at least in *S. oneidensis*. The shorter the duration of an experiment, the more one can exclude the possibility that the observed phenotype might not be due to the inserted genetic modification but to a suppressor mutation. Therefore, Fe(III)-citrate seems to be a good model substance to study extracellular electron transport pathways since it allows

fast growth and reduction rates when compared to mineral phase electron acceptors like ferrihydrite or hematite.

IX. References

Aeschbacher, M., Vergari, D., Schwarzenbach, R.P., and Sander, M. (2011) Electrochemical analysis of proton and electron transfer equilibria of the reducible moieties in humic acids. *Environ Sci Technol* **45**: 8385-8394.

Bayer, M., Walter, K., and Simon, H. (1996) Purification and partial characterisation of a reversible artificial mediator accepting NADH oxidoreductase from Clostridium thermoaceticum. *Eur J Biochem* **239**: 686-691.

Bekker, A., Holland, H.D., Wang, P.L., Rumble, D., Stein, H.J., Hannah, J.L.*, et al.* (2004) Dating the rise of atmospheric oxygen. *Nature* **427**: 117-120.

Belchik, S.M., Kennedy, D.W., Dohnalkova, A.C., Wang, Y., Sevinc, P.C., Wu, H.*, et al.* (2011) Extracellular reduction of hexavalent chromium by cytochromes MtrC and OmcA of *Shewanella oneidensis* MR-1. *Appl Environ Microbiol* **77**: 4035-4041.

Beliaev, A.S., and Saffarini, D.A. (1998) *Shewanella putrefaciens mtrB* encodes an outer membrane protein required for Fe(III) and Mn(IV) reduction. *J Bacteriol* **180**: 6292-6297.

Beliaev, A.S., Saffarini, D.A., McLaughlin, J.L., and Hunnicutt, D. (2001) MtrC, an outer membrane decahaem *c* cytochrome required for metal reduction in *Shewanella putrefaciens* MR-1. *Mol Microbiol* **39**: 722-730.

Beliaev, A.S., Klingeman, D.M., Klappenbach, J.A., Wu, L., Romine, M.F., Tiedje, J.M.*, et al.* (2005) Global transcriptome analysis of *Shewanella oneidensis* MR-1 exposed to different terminal electron acceptors. *J Bacteriol* **187**: 7138-7145.

Berg, J.M., Tymoczko, J.L., and Stryer, L. (2007) *Stryer Biochemie.* München ; Heidelberg: Elsevier, Spektrum Akademischer Verl.

Bird, L.J., Bonnefoy, V., and Newman, D.K. (2011) Bioenergetic challenges of microbial iron metabolisms. *Trends Microbiol* **19**: 330-340.

Blattner, F.R., Plunkett, G., 3rd, Bloch, C.A., Perna, N.T., Burland, V., Riley, M.*, et al.* (1997) The complete genome sequence of *Escherichia coli* K-12. *Science* **277**: 1453-1462.

Boogerd, F.C., and de Vrind, J.P. (1987) Manganese oxidation by *Leptothrix discophora*. *J Bacteriol* **169**: 489-494.

Borloo, J., Vergauwen, B., De Smet, L., Brige, A., Motte, B., Devreese, B., and Van Beeumen, J. (2007) A kinetic approach to the dependence of dissimilatory metal reduction by *Shewanella oneidensis* MR-1 on the outer membrane cytochromes *c* OmcA and OmcB. *FEBS* **274**: 3728-3738.

Bradford, M.M. (1976) A rapid and sensitive method for the quantitation of microgram quantities of protein utilizing the principle of protein-dye binding. *Anal Biochem* **72**: 248-254.

Bretschger, O., Obraztsova, A., Sturm, C.A., Chang, I.S., Gorby, Y.A., Reed, S.B.*, et al.* (2007) Current production and metal oxide reduction by *Shewanella oneidensis* MR-1 wild type and mutants. *Appl Environ Microbiol* **73**: 7003-7012.

Bücking, C. (2007) Rolle und Aktivität von äußeren Membrancytochromen während der dissimilatorischen Eisenreduktion in *Shewanella oneidensis*. Staatsexamensarbeit, Biologie II, University Freiburg.

Bücking, C., Popp, F., Kerzenmacher, S., and Gescher, J. (2010) Involvement and specificity of *Shewanella oneidensis* outer membrane cytochromes in the

reduction of soluble and solid-phase terminal electron acceptors. *FEMS Microbiol Lett* **306**: 144-151.

Bücking, C., Piepenbrock, A., Kappler, A., and Gescher, J. (2012) Outer membrane cytochrome independent reduction of extracellular electron acceptors in *Shewanella oneidensis*. *Microbiology,* doi:10.1099/mic.0.058404-0.

Burdige, D.J., and Nealson, K.H. (1985) Microbial manganese reduction by enrichment cultures from coastal marine sediments. *Appl Environ Microbiol* **50**: 491-497.

Burns, J.L., and DiChristina, T.J. (2009) Anaerobic respiration of elemental sulfur and thiosulfate by *Shewanella oneidensis* MR-1 requires *psrA*, a homolog of the *phsA* gene of *Salmonella enterica* serovar typhimurium LT2. *Appl Environ Microbiol* **75**: 5209-5217.

Clarke, T.A., Edwards, M.J., Gates, A.J., Hall, A., White, G.F., Bradley, J., *et al.* (2011) Structure of a bacterial cell surface decaheme electron conduit. *Proc Natl Acad Sci U S A* **108**: 9384-9389.

Cordova, C.D., Schicklberger, M.F., Yu, Y., and Spormann, A.M. (2011) Partial functional replacement of CymA by SirCD in *Shewanella oneidensis* MR-1. *J Bacteriol* **193**: 2312-2321.

Coursolle, D., Baron, D.B., Bond, D.R., and Gralnick, J.A. (2010) The Mtr respiratory pathway is essential for reducing flavins and electrodes in *Shewanella oneidensis*. *J Bacteriol* **192**: 467-474.

Coursolle, D., and Gralnick, J.A. (2010) Modularity of the Mtr respiratory pathway of *Shewanella oneidensis* strain MR-1. *Mol Microbiol* **77**: 995-1008.

Cowan, S.W., Schirmer, T., Rummel, G., Steiert, M., Ghosh, R., Pauptit, R.A., *et al.* (1992) Crystal structures explain functional properties of two *E. coli* porins. *Nature* **358**: 727-733.

Cruz-Garcia, C., Murray, A.E., Klappenbach, J.A., Stewart, V., and Tiedje, J.M. (2007) Respiratory nitrate ammonification by *Shewanella oneidensis* MR-1. *J Bacteriol* **189**: 656-662.

Dale, J.R., Wade, R., and DiChristina, T.J. (2007) A conserved histidine in cytochrome c maturation permease CcmB of *Shewanella putrefaciens* is required for anaerobic growth below a threshold standard redox potential. *J Bacteriol* **189**: 1036-1043.

Davila, D., Esquivel, J.P., Sabate, N., and Mas, J. (2011) Silicon-based microfabricated microbial fuel cell toxicity sensor. *Biosens Bioelectron* **26**: 2426-2430.

DiChristina, T.J., Moore, C.M., and Haller, C.A. (2002) Dissimilatory Fe(III) and Mn(IV) reduction by *Shewanella putrefaciens* requires *ferE*, a homolog of the *pulE* (*gspE*) type II protein secretion gene. *J Bacteriol* **184**: 142-151.

Dobbin, P.S., Butt, J.N., Powell, A.K., Reid, G.A., and Richardson, D.J. (1999) Characterization of a flavocytochrome that is induced during the anaerobic respiration of Fe^{3+} by *Shewanella frigidimarina* NCIMB400. *Biochem J* **342 (Pt 2)**: 439-448.

El-Naggar, M.Y., Wanger, G., Leung, K.M., Yuzvinsky, T.D., Southam, G., Yang, J., *et al.* (2010) Electrical transport along bacterial nanowires from *Shewanella oneidensis* MR-1. *Proc Natl Acad Sci U S A* **107**: 18127-18131.

Esteve-Nunez, A., Sosnik, J., Visconti, P., and Lovley, D.R. (2008) Fluorescent properties of *c*-type cytochromes reveal their potential role as an extracytoplasmic electron sink in *Geobacter sulfurreducens*. *Environ Microbiol* **10**: 497-505.

Firer-Sherwood, M., Pulcu, G.S., and Elliott, S.J. (2008) Electrochemical interrogations of the Mtr cytochromes from *Shewanella*: opening a potential window. *J Biol Inorg Chem* **13**: 849-854.

Firer-Sherwood, M.A., Ando, N., Drennan, C.L., and Elliott, S.J. (2011a) Solution-based structural analysis of the decaheme cytochrome, MtrA, by small angle X-ray sand analytical ultracentrifugation. *J Phys Chem B* **115**: 11208-11214.

Firer-Sherwood, M.A., Bewley, K.D., Mock, J.Y., and Elliott, S.J. (2011b) Tools for resolving complexity in the electron transfer networks of multiheme cytochromes *c*. *Metallomics* **3**: 344-348.

Francetic, O., and Pugsley, A.P. (2005) Towards the identification of type II secretion signals in a nonacylated variant of pullulanase from *Klebsiella oxytoca*. *J Bacteriol* **187**: 7045-7055.

Fultz, M.L., and Durst, R.A. (1982) Mediator compounds for the electrochemical study of biological redox systems - a compilation. *Analytica Chimica Acta* **140**: 1-18.

Gao, H., Yang, Z.K., Barua, S., Reed, S.B., Romine, M.F., Nealson, K.H., *et al.* (2009) Reduction of nitrate in *Shewanella oneidensis* depends on atypical NAP and NRF systems with NapB as a preferred electron transport protein from CymA to NapA. *Isme J* **3**: 966-976.

Gao, H., Barua, S., Liang, Y., Wu, L., Dong, Y., Reed, S., *et al.* (2010) Impacts of *Shewanella oneidensis c*-type cytochromes on aerobic and anaerobic respiration. *Microb Biotechnol* **3**: 455-466.

Gescher, J.S., Cordova, C.D., and Spormann, A.M. (2008) Dissimilatory iron reduction in *Escherichia coli*: identification of CymA of *Shewanella oneidensis* and NapC of *E. coli* as ferric reductases. *Mol Microbiol* **68**: 706-719.

Gibson, D.G., Young, L., Chuang, R.Y., Venter, J.C., Hutchison, C.A., and Smith, H.O. (2009) Enzymatic assembly of DNA molecules up to several hundred kilobases. *Nature Methods* **6**: 343-U341.

Gietz, R.D., Schiestl, R.H., Willems, A.R., and Woods, R.A. (1995) Studies on the transformation of intact yeast cells by the LiAc/SS-DNA/PEG procedure. *Yeast* **11**: 355-360.

Gorby, Y., McLean, J., Korenevsky, A., Rosso, K., El-Naggar, M.Y., and Beveridge, T.J. (2008) Redox-reactive membrane vesicles produced by *Shewanella*. *Geobiology* **6**: 232-241.

Gorby, Y.A., Yanina, S., McLean, J.S., Rosso, K.M., Moyles, D., Dohnalkova, A., *et al.* (2006) Electrically conductive bacterial nanowires produced by *Shewanella oneidensis* strain MR-1 and other microorganisms. *Proc Natl Acad Sci U S A* **103**: 11358-11363.

Gralnick, J.A., Vali, H., Lies, D.P., and Newman, D.K. (2006) Extracellular respiration of dimethyl sulfoxide by *Shewanella oneidensis* strain MR-1. *Proc Natl Acad Sci U S A* **103**: 4669-4674.

Gralnick, J.A., and Newman, D.K. (2007) Extracellular respiration. *Mol Microbiol* **65**: 1-11.

Harris, W.R., Carrano, C.J., and Raymond, K.N. (1979) Spectrophotometric determination of the proton-dependent stability constant of ferric enterobactin. *J Am Chem Soc* **101**: 2213-2214.

Hartshorne, R.S., Jepson, B.N., Clarke, T.A., Field, S.J., Fredrickson, J., Zachara, J., *et al.* (2007) Characterization of *Shewanella oneidensis* MtrC: a cell-surface decaheme cytochrome involved in respiratory electron transport to extracellular electron acceptors. *J Biol Inorg Chem* **12**: 1083-1094.

Hartshorne, R.S., Reardon, C.L., Ross, D., Nuester, J., Clarke, T.A., Gates, A.J., *et al.* (2009) Characterization of an electron conduit between bacteria and the extracellular environment. *Proc Natl Acad Sci U S A* **106**: 22169-22174.

Hau, H.H., and Gralnick, J.A. (2007) Ecology and biotechnology of the genus *Shewanella*. *Annu Rev Microbiol* **61**: 237-258.

Heidelberg, J.F., Paulsen, I.T., Nelson, K.E., Gaidos, E.J., Nelson, W.C., Read, T.D., *et al.* (2002) Genome sequence of the dissimilatory metal ion-reducing bacterium *Shewanella oneidensis*. *Nat Biotechnol* **20**: 1118-1123.

Hobot, J.A., Carlemalm, E., Villiger, W., and Kellenberger, E. (1984) Periplasmic gel: new concept resulting from the reinvestigation of bacterial cell envelope ultrastructure by new methods. *J Bacteriol* **160**: 143-152.

Howard, E.C., Hamdan, L.J., Lizewski, S.E., and Ringeisen, B.R. (2011) High frequency of glucose-utilizing mutants in *Shewanella oneidensis* MR-1. *FEMS Microbiol Lett (Epub ahead of print) DOI: 10.1111/j.1574-6968.2011.02450.x*.

Hunt, K.A., Flynn, J.M., Naranjo, B., Shikhare, I.D., and Gralnick, J.A. (2010) Substrate-level phosphorylation is the primary source of energy conservation during anaerobic respiration of *Shewanella oneidensis* strain MR-1. *J Bacteriol* **192**: 3345-3351.

Jiang, J., and Kappler, A. (2008) Kinetics of microbial and chemical reduction of humic substances: implications for electron shuttling. *Environ Sci Technol* **42**: 3563-3569.

Jiao, Y., and Newman, D.K. (2007) The *pio* operon is essential for phototrophic Fe(II) oxidation in *Rhodopseudomonas palustris* TIE-1. *J Bacteriol* **189**: 1765-1773.

Jiao, Y., Qian, F., Li, Y., Wang, G., Saltikov, C.W., and Gralnick, J.A. (2011) Deciphering the electron transport pathway for graphene oxide reduction by *Shewanella oneidensis* MR-1. *J Bacteriol* **193**: 3662-3665.

Khlebnikov, A., Datsenko, K.A., Skaug, T., Wanner, B.L., and Keasling, J.D. (2001) Homogeneous expression of the P_{BAD} promoter in *Escherichia coli* by constitutive expression of the low-affinity high-capacity AraE transporter. *Microbiology* **147**: 3241-3247.

Kloke, A., Rubenwolf, S., Bücking, C., Gescher, J., Kerzenmacher, S., Zengerle, R., and von Stetten, F. (2010) A versatile miniature bioreactor and its application to bioelectrochemistry studies. *Biosens Bioelectron* **25**: 2559-2565.

Kranz, R.G., Richard-Fogal, C., Taylor, J.S., and Frawley, E.R. (2009) Cytochrome *c* biogenesis: mechanisms for covalent modifications and trafficking of heme and for heme-iron redox control. *Microbiol Mol Biol Rev* **73**: 510-528, Table of Contents.

Laemmli, U.K. (1970) Cleavage of structural proteins during the assembly of the head of bacteriophage T4. *Nature* **227**: 680-685.

Lee, J.-H., Kim, M.-G., Yoo, B., Myung, N.V., Maeng, J., Lee, T., *et al.* (2007) Biogenic formation of photoactive arsenic-sulfide nanotubes by *Shewanella sp* strain HN-41. *Proc Natl Acad Sci U S A* **104**: 20410-20415.

Li, H., and Durbin, R. (2009) Fast and accurate short read alignment with Burrows-Wheeler transform. *Bioinformatics* **25**: 1754-1760.

Lies, D.P., Hernandez, M.E., Kappler, A., Mielke, R.E., Gralnick, J.A., and Newman, D.K. (2005) *Shewanella oneidensis* MR-1 uses overlapping pathways for iron reduction at a distance and by direct contact under conditions relevant for biofilms. *Appl Environ Microbiol* **71**: 4414-4426.

Logan, B.E. (2009) Exoelectrogenic bacteria that power microbial fuel cells. *Nat Rev Microbiol* **7**: 375-381.

Lomize, A.L., Pogozheva, I.D., Lomize, M.A., and Mosberg, H.I. (2006) Positioning of proteins in membranes: a computational approach. *Protein Sci* **15**: 1318-1333.

Lovley, D.R., and Phillips, E.J. (1988) Novel mode of microbial energy metabolism: organic carbon oxidation coupled to dissimilatory reduction of iron or manganese. *Appl Environ Microbiol* **54**: 1472-1480.

Lovley, D.R., Coates, J.D., BluntHarris, E.L., Phillips, E.J.P., and Woodward, J.C. (1996) Humic substances as electron acceptors for microbial respiration. *Nature* **382**: 445-448.

Lower, B.H., Yongsunthon, R., Shi, L., Wildling, L., Gruber, H.J., Wigginton, N.S., *et al.* (2009) Antibody recognition force microscopy shows that outer membrane cytochromes OmcA and MtrC are expressed on the exterior surface of *Shewanella oneidensis* MR-1. *Appl Environ Microbiol* **75**: 2931-2935.

Lutz, R., and Bujard, H. (1997) Independent and tight regulation of transcriptional units in *Escherichia coli* via the LacR/O, the TetR/O and AraC/I1-I2 regulatory elements. *Nucleic Acids Res* **25**: 1203-1210.

Majzlan, J. (2011) Pools of iron and manganese in the near-surface geomaterials and the associated redox potentials. In *Iron reduction (in preparation)*. Kappler, A. and Gescher, J. (eds).

Marshall, M.J., Beliaev, A.S., Dohnalkova, A.C., Kennedy, D.W., Shi, L., Wang, Z., *et al.* (2006) *c*-Type cytochrome-dependent formation of U(IV) nanoparticles by *Shewanella oneidensis*. *PLoS Biol* **4**: e268.

Marsili, E., Baron, D.B., Shikhare, I.D., Coursolle, D., Gralnick, J.A., and Bond, D.R. (2008) *Shewanella* secretes flavins that mediate extracellular electron transfer. *Proc Natl Acad Sci U S A* **105**: 3968-3973.

McLean, J.S., Pinchuk, G.E., Geydebrekht, O.V., Bilskis, C.L., Zakrajsek, B.A., Hill, E.A., *et al.* (2008) Oxygen-dependent autoaggregation in *Shewanella oneidensis* MR-1. *Environ Microbiol* **10**: 1861-1876.

Methe, B.A., Nelson, K.E., Eisen, J.A., Paulsen, I.T., Nelson, W., Heidelberg, J.F., *et al.* (2003) Genome of *Geobacter sulfurreducens*: Metal reduction in subsurface environments. *Science* **302**: 1967-1969.

Meyer, T.E., Tsapin, A.I., Vandenberghe, I., de Smet, L., Frishman, D., Nealson, K.H., *et al.* (2004) Identification of 42 possible cytochrome *c* genes in the *Shewanella oneidensis* genome and characterization of six soluble cytochromes. *Omics* **8**: 57-77.

Miethke, M., and Marahiel, M.A. (2007) Siderophore-based iron acquisition and pathogen control. *Microbiol Mol Biol Rev* **71**: 413-451.

Milne, I., Bayer, M., Cardle, L., Shaw, P., Stephen, G., Wright, F., and Marshall, D. (2010) Tablet-next generation sequence assembly visualization. *Bioinformatics* **26**: 401-402.

Murata, T., Tseng, W., Guina, T., Miller, S.I., and Nikaido, H. (2007) PhoPQ-mediated regulation produces a more robust permeability barrier in the outer membrane of *Salmonella enterica* serovar typhimurium. *J Bacteriol* **189**: 7213-7222.

Myers, C.R., and Nealson, K.H. (1988) Bacterial manganese reduction and growth with manganese oxide as the sole electron-acceptor. *Science* **240**: 1319-1321.

Myers, C.R., and Myers, J.M. (1992a) Localization of cytochromes to the outer membrane of anaerobically grown *Shewanella putrefaciens* MR-1. *J Bacteriol* **174**: 3429-3438.

Myers, C.R., and Myers, J.M. (1992b) Fumarate reductase is a soluble enzyme in anaerobically grown *Shewanella putrefaciens* MR-1. *FEMS Microbiol Lett* **98**: 13-19.

Myers, C.R., and Myers, J.M. (1993) Ferric reductase is associated with the membranes of anaerobically grown *Shewanella putrefaciens* MR-1. *FEMS Microbiol Lett* **108**: 15-22.

Myers, C.R., and Myers, J.M. (1997) Cloning and sequence of *cymA*, a gene encoding a tetraheme cytochrome *c* required for reduction of iron(III), fumarate, and nitrate by *Shewanella putrefaciens* MR-1. *J Bacteriol* **179**: 1143-1152.

Myers, C.R., and Myers, J.M. (2002a) MtrB is required for proper incorporation of the cytochromes OmcA and OmcB into the outer membrane of *Shewanella putrefaciens* MR-1. *Appl Environ Microbiol* **68**: 5585-5594.

Myers, C.R., and Myers, J.M. (2003a) Cell surface exposure of the outer membrane cytochromes of *Shewanella oneidensis* MR-1. *Lett Appl Microbiol* **37**: 254-258.

Myers, C.R., and Myers, J.M. (2004) The outer membrane cytochromes of *Shewanella oneidensis* MR-1 are lipoproteins. *Lett Appl Microbiol* **39**: 466-470.

Myers, J.M., and Myers, C.R. (1998) Isolation and sequence of *omcA*, a gene encoding a decaheme outer membrane cytochrome *c* of *Shewanella putrefaciens* MR-1, and detection of *omcA* homologs in other strains of *S. putrefaciens*. *Biochim Biophys Acta* **1373**: 237-251.

Myers, J.M., and Myers, C.R. (2001) Role for outer membrane cytochromes OmcA and OmcB of *Shewanella putrefaciens* MR-1 in reduction of manganese dioxide. *Appl Environ Microbiol* **67**: 260-269.

Myers, J.M., and Myers, C.R. (2002b) Genetic complementation of an outer membrane cytochrome *omcB* mutant of *Shewanella putrefaciens* MR-1 requires *omcB* plus downstream DNA. *Appl Environ Microbiol* **68**: 2781-2793.

Myers, J.M., and Myers, C.R. (2003b) Overlapping role of the outer membrane cytochromes of *Shewanella oneidensis* MR-1 in the reduction of manganese(IV) oxide. *Lett Appl Microbiol* **37**: 21-25.

Nielsen, H., Engelbrecht, J., Brunak, S., and vonHeijne, G. (1997) Identification of prokaryotic and eukaryotic signal peptides and prediction of their cleavage sites. *Protein Eng* **10**: 1-6.

Nisbet, E.G., and Sleep, N.H. (2001) The habitat and nature of early life. *Nature* **409**: 1083-1091.

O'Brian, M.R., and Thony-Meyer, L. (2002) Biochemistry, regulation and genomics of haem biosynthesis in prokaryotes. *Adv Microb Physiol* **46**: 257-318.

Okuda, S., and Tokuda, H. (2011) Lipoprotein sorting in bacteria. *Annu Rev Microbiol* **65**: 239-259.

Park, S., and Ruoff, R.S. (2009) Chemical methods for the production of graphenes. *Nat Nano* **4**: 217-224.

Pinchuk, G.E., Geydebrekht, O.V., Hill, E.A., Reed, J.L., Konopka, A.E., Beliaev, A.S., and Fredrickson, J.K. (2011) Pyruvate and lactate metabolism by *Shewanella oneidensis* MR-1 under fermentation, oxygen limitation, and fumarate respiration conditions. *Appl Environ Microbiol* **77**: 8234-8240.

Pitts, K.E., Dobbin, P.S., Reyes-Ramirez, F., Thomson, A.J., Richardson, D.J., and Seward, H.E. (2003) Characterization of the *Shewanella oneidensis* MR-1 decaheme cytochrome MtrA: expression in Escherichia coli confers the ability to reduce soluble Fe(III) chelates. *J Biol Chem* **278**: 27758-27765.

Posth, N.R., Hegler, F., Konhauser, K.O., and Kappler, A. (2008) Alternating Si and Fe deposition caused by temperature fluctuations in Precambrian oceans. *Nature Geosci* **1**: 703-708.

Qian, Y., Shi, L., and Tien, M. (2011) SO2907, A putative TonB-dependent receptor, is involved in dissimilatory iron reduction by *Shewanella oneidensis* MR-1. *J Biol Chem* **286**: 33973-33980.

Randall, A., Cheng, J.L., Sweredoski, M., and Baldi, P. (2008) TMBpro: secondary structure, beta-contact and tertiary structure prediction of transmembrane beta-barrel proteins. *Bioinformatics* **24**: 513-520.

Reardon, C.L., Dohnalkova, A.C., Nachimuthu, P., Kennedy, D.W., Saffarini, D.A., Arey, B.W., *et al.* (2010) Role of outer-membrane cytochromes MtrC and OmcA in the biomineralization of ferrihydrite by *Shewanella oneidensis* MR-1. *Geobiology* **8**: 56-68.

Reguera, G., McCarthy, K.D., Mehta, T., Nicoll, J.S., Tuominen, M.T., and Lovley, D.R. (2005) Extracellular electron transfer via microbial nanowires. *Nature* **435**: 1098-1101.

Richter, K., Bücking, C., Schicklberger, M., and Gescher, J. (2010) A simple and fast method to analyze the orientation of *c*-type cytochromes in the outer membrane of Gram-negative bacteria. *J Microbiol Methods* **82**: 184-186.

Robie, R.A., Huebner, J.S., and Hemingway, B.S. (1995) Heat-capacities and thermodynamic properties of braunite (Mn_7SiO_{12}) and rhodonite ($MnSiO_3$). *Am Mineral* **80**: 560-575.

Roden, E.E., Kappler, A., Bauer, I., Jiang, J., Paul, A., Stoesser, R., *et al.* (2010) Extracellular electron transfer through microbial reduction of solid-phase humic substances. *Nat Geosci* **3**: 417-421.

Rodrigues, M.L., Oliveira, T.F., Pereira, I.A., and Archer, M. (2006) X-ray structure of the membrane-bound cytochrome c quinol dehydrogenase NrfH reveals novel haem coordination. *Embo J* **25**: 5951-5960.

Rollefson, J.B., Stephen, C.S., Tien, M., and Bond, D.R. (2011) Identification of an extracellular polysaccharide network essential for cytochrome anchoring and biofilm formation in *Geobacter sulfurreducens*. *J Bacteriol* **193**: 1023-1033.

Romine, M.F., Carlson, T.S., Norbeck, A.D., McCue, L.A., and Lipton, M.S. (2008) Identification of mobile elements and pseudogenes in the *Shewanella oneidensis* MR-1 genome. *Appl Environ Microbiol* **74**: 3257-3265.

Ross, D.E., Ruebush, S.S., Brantley, S.L., Hartshorne, R.S., Clarke, T.A., Richardson, D.J., and Tien, M. (2007) Characterization of protein-protein interactions involved in iron reduction by *Shewanella oneidensis* MR-1. *Appl Environ Microbiol* **73**: 5797-5808.

Ross, D.E., Brantley, S.L., and Tien, M. (2009) Kinetic characterization of terminal reductases OmcA and MtrC involved in respiratory electron transfer for dissimilatory iron reduction in *Shewanella oneidensis* MR-1. *Appl Environ Microbiol* **75**: 5218-5226.

Rosso, K.M., Zachara, J.M., Fredrickson, J.K., Gorby, Y.A., and Smith, S.C. (2003) Nonlocal bacterial electron transfer to hematite surfaces. *Geochim Cosmochim Acta* **67**: 1081-1087.

Ruebush, S.S., Brantley, S.L., and Tien, M. (2006) Reduction of soluble and insoluble iron forms by membrane fractions of *Shewanella oneidensis* grown under aerobic and anaerobic conditions. *Appl Environ Microbiol* **72**: 2925-2935.

Saffarini, D.A., Blumerman, S.L., and Mansoorabadi, K.J. (2002) Role of menaquinones in Fe(III) reduction by membrane fractions of *Shewanella putrefaciens*. *J Bacteriol* **184**: 846-848.

Saltikov, C.W., and Newman, D.K. (2003) Genetic identification of a respiratory arsenate reductase. *Proc Natl Acad Sci U S A* **100**: 10983-10988.

Sambrook, J., Fritsch, E.F., Maniatis, T., and Russell, D.W. (1989) *Molecular cloning.* Cold Spring Harbor, NY: Cold Spring Harbor Laboratory Press.

Sandkvist, M. (2001) Biology of type II secretion. *Mol Microbiol* **40**: 271-283.

Schicklberger, M., Bücking, C., Schuetz, B., Heide, H., and Gescher, J. (2010) Involvement of the *Shewanella oneidensis* decaheme cytochrome MtrA in the periplasmic stability of the beta-barrel protein MtrB. *Appl Environ Microbiol* **77**: 1520-1523.

Schlegel, H.G., Fuchs, G., and Eitinger, T. (2007) *Allgemeine Mikrobiologie.* Stuttgart u.a.: Thieme.

Schrodinger, LLC (2010) The PyMOL Molecular Graphics System, Version 1.3r1.

Schuetz, B., Schicklberger, M., Kuermann, J., Spormann, A.M., and Gescher, J. (2009) Periplasmic electron transfer via the *c*-type cytochromes MtrA and FccA of *Shewanella oneidensis* MR-1. *Appl Environ Microbiol* **75**: 7789-7796.

Schütz, B., Seidel, J., Sturm, G., Einsle, O., and Gescher, J. (2011) Investigation of the electron transport chain to and the catalytic activity of the diheme cytochrome *c* peroxidase CcpA of *Shewanella oneidensis*. *Appl Environ Microbiol* **77**: 6172-6180.

Schwalb, C., Chapman, S.K., and Reid, G.A. (2002) The membrane-bound tetrahaem c-type cytochrome CymA interacts directly with the soluble fumarate reductase in *Shewanella*. *Biochem Soc Trans* **30**: 658-662.

Schwalb, C., Chapman, S.K., and Reid, G.A. (2003) The tetraheme cytochrome CymA is required for anaerobic respiration with dimethyl sulfoxide and nitrite in *Shewanella oneidensis*. *Biochemistry* **42**: 9491-9497.

Schwertmann, U., and Cornell, R.M. (2000) *Iron oxides in the laboratory.* Weinheim u.a.: Wiley-VCH.

Scott, J.H., and Nealson, K.H. (1994) A biochemical study of the intermediary carbon metabolism of *Shewanella putrefaciens*. *J Bacteriol* **176**: 3408-3411.

Shanks, R.M., Caiazza, N.C., Hinsa, S.M., Toutain, C.M., and O'Toole, G.A. (2006) *Saccharomyces cerevisiae*-based molecular tool kit for manipulation of genes from gram-negative bacteria. *Appl Environ Microbiol* **72**: 5027-5036.

Shi, L., Chen, B., Wang, Z., Elias, D.A., Mayer, M.U., Gorby, Y.A.*, et al.* (2006) Isolation of a high-affinity functional protein complex between OmcA and MtrC: Two outer membrane decaheme c-type cytochromes of *Shewanella oneidensis* MR-1. *J Bacteriol* **188**: 4705-4714.

Shi, L., Squier, T.C., Zachara, J.M., and Fredrickson, J.K. (2007) Respiration of metal (hydr)oxides by *Shewanella* and *Geobacter*: a key role for multihaem *c*-type cytochromes. *Mol Microbiol* **65**: 12-20.

Shi, L., Deng, S., Marshall, M.J., Wang, Z., Kennedy, D.W., Dohnalkova, A.C.*, et al.* (2008) Direct involvement of type II secretion system in extracellular translocation of *Shewanella oneidensis* outer membrane cytochromes MtrC and OmcA. *J Bacteriol* **190**: 5512-5516.

Shirodkar, S., Reed, S., Romine, M., and Saffarini, D. (2011) The octahaem SirA catalyses dissimilatory sulfite reduction in *Shewanella oneidensis* MR-1. *Environ Microbiol* **13**: 108-115.

Shyu, J.B., Lies, D.P., and Newman, D.K. (2002) Protective role of *tolC* in efflux of the electron shuttle anthraquinone-2,6-disulfonate. *J Bacteriol* **184**: 1806-1810.

Siegele, D.A., and Hu, J.C. (1997) Gene expression from plasmids containing the araBAD promoter at subsaturating inducer concentrations represents mixed populations. *Proc Natl Acad Sci U S A* **94**: 8168-8172.

Simon, R., Priefer, U., and Pühler, A. (1983) A broad host range mobilization system for *in vivo* genetic engineering: Transposon mutagenesis in gram negative bacteria. *Bio/Technology* **1**: 784 - 791.

Singer, P.C., and Stumm, W. (1970) Acidic mine drainage: the rate-determining step. *Science* **167**: 1121-1123.

Spiro, T.G., Pape, L., and Saltman, P. (1967) Hydrolytic polymerization of ferric citrate .I. Chemistry of polymer. *J Am Chem Soc* **89**: 5555-5559.

Stalker, D.M., Kolter, R., and Helinski, D.R. (1982) Plasmid R6K DNA replication. I. Complete nucleotide sequence of an autonomously replicating segment. *J Mol Biol* **161**: 33-43.

Stare, F.J. (1935) A potentiometric study of hepatoflavin. *J Biol Chem* **112**: 223-229.

Stookey, L.L. (1970) Ferrozine - a new spectrophotometric reagent for iron. *Anal Chem* **42**.

Straub, K.L., Benz, M., and Schink, B. (2001) Iron metabolism in anoxic environments at near neutral pH. *FEMS Microbiol Ecol* **34**: 181-186.

Thamdrup, B. (2000) Bacterial manganese and iron reduction in aquatic sediments. *Adv Microb Ecol* **16**: 41-84.

Thomas, P.E., Ryan, D., and Levin, W. (1976) An improved staining procedure for the detection of the peroxidase activity of cytochrome P-450 on sodium dodecyl sulfate polyacrylamide gels. *Anal Biochem* **75**: 168-176.

Thomas, S.H., Wagner, R.D., Arakaki, A.K., Skolnick, J., Kirby, J.R., Shimkets, L.J., *et al.* (2008) The mosaic genome of *Anaeromyxobacter dehalogenans* strain 2CP-C suggests an aerobic common ancestor to the delta-proteobacteria. *PLoS One* **3**: e2103.

Tront, J.M., Fortner, J.D., Ploetze, M., Hughes, J.B., and Puzrin, A.M. (2008) Microbial fuel cell technology for measurement of microbial respiration of lactate as an example of bioremediation amendment. *Biotechnol Lett* **30**: 1385-1390.

Unden, G., and Bongaerts, J. (1997) Alternative respiratory pathways of *Escherichia coli*: energetics and transcriptional regulation in response to electron acceptors. *Biochim Biophys Acta* **1320**: 217-234.

Uria, N., Munoz Berbel, X., Sanchez, O., Munoz, F.X., and Mas, J. (2011) Transient storage of electrical charge in biofilms of *Shewanella oneidensis* MR-1 growing in a microbial fuel cell. *Environ Sci Technol*.

Vaara, M. (1992) Agents that increase the permeability of the outer membrane. *Microbiol Rev* **56**: 395-411.

Vargas, M., Kashefi, K., Blunt-Harris, E.L., and Lovley, D.R. (1998) Microbiological evidence for Fe(III) reduction on early Earth. *Nature* **395**: 65-67.

Venkateswaran, K., Moser, D.P., Dollhopf, M.E., Lies, D.P., Saffarini, D.A., MacGregor, B.J., *et al.* (1999) Polyphasic taxonomy of the genus *Shewanella* and description of *Shewanella oneidensis* sp. nov. *Int J Syst Bacteriol* **49 Pt 2**: 705-724.

von Canstein, H., Ogawa, J., Shimizu, S., and Lloyd, J.R. (2008) Secretion of flavins by *Shewanella* species and their role in extracellular electron transfer. *Appl Environ Microbiol* **74**: 615-623.

Wang, Z., Liu, C., Wang, X., Marshall, M.J., Zachara, J.M., Rosso, K.M., *et al.* (2008) Kinetics of reduction of Fe(III) complexes by outer membrane

cytochromes MtrC and OmcA of *Shewanella oneidensis* MR-1. *Appl Environ Microbiol* **74**: 6746-6755.

Weiner, J.H., Rothery, R.A., Sambasivarao, D., and Trieber, C.A. (1992) Molecular analysis of dimethylsulfoxide reductase: a complex iron-sulfur molybdoenzyme of Escherichia coli. *Biochim Biophys Acta* **1102**: 1-18.

Wu, W.M., Carley, J., Luo, J., Ginder-Vogel, M.A., Cardenas, E., Leigh, M.B.*, et al.* (2007) In situ bioreduction of uranium (VI) to submicromolar levels and reoxidation by dissolved oxygen. *Environ Sci Technol* **41**: 5716-5723.

Xiong, Y., Shi, L., Chen, B., Mayer, M.U., Lower, B.H., Londer, Y.*, et al.* (2006) High-affinity binding and direct electron transfer to solid metals by the *Shewanella oneidensis* MR-1 outer membrane c-type cytochrome OmcA. *J Am Chem Soc* **128**: 13978-13979.

Yang, C., Rodionov, D.A., Li, X., Laikova, O.N., Gelfand, M.S., Zagnitko, O.P.*, et al.* (2006) Comparative genomics and experimental characterization of N-acetylglucosamine utilization pathway of *Shewanella oneidensis*. *J Biol Chem* **281**: 29872-29885.

X. Curriculum vitae

Clemens Bücking

born 25 september 1980 in Berlin

Formation

2008-2012	Ph.d. at the University of Freiburg and at the Karlruhe Institut für Technology. Supervisor: Prof. Dr. Johannes Gescher
2001-2008	University of Freiburg: studies of Biology, French, 1. Staatsexamen
2000	Abitur at Heinrich-von-Kleist Gymansium, Berlin

First-author publications and manuscripts

Bücking, C., Popp, F., Kerzenmacher, S., and Gescher, J. (2010) Involvement and specificity of *Shewanella oneidensis* outer membrane cytochromes in the reduction of soluble and solid-phase terminal electron acceptors. *FEMS Microbiol Lett* **306**: 144-151.

Bücking, C., Piepenbrock, A., Kappler, A., and Gescher, J. (2012) Outer membrane cytochrome independent reduction of extracellular electron acceptors in *Shewanella oneidensis*. *Microbiology,* doi:10.1099/mic.0.058404-0.

Golitsch, F., Bücking, C., and Gescher, J.: A microbial fuel cell biosensor based on *Shewanella oneidensis* outer membrane protein complexes. Submitted to: *Biosens Bioelectron*.

Bücking, C., Schicklberger, M., and Gescher, J.: The biochemistry of dissimilatory ferric iron and manganese reduction in *Shewanella oneidensis*. In *Microbial metal respiration*. Gescher, J. and Kappler, A. (Editors): Springer-Verlag, *(planned date of print: 2012).*

Further publications

Kloke, A., Rubenwolf, S., Bücking, C., Gescher, J., Kerzenmacher, S., Zengerle, R., and von Stetten, F. (2010) A versatile miniature bioreactor and its application to bioelectrochemistry studies. *Biosens Bioelectron* **25**: 2559-2565.

Richter, K., Bücking, C., Schicklberger, M., and Gescher, J. (2010) A simple and fast method to analyze the orientation of *c*-type cytochromes in the outer membrane of Gram-negative bacteria. *J Microbiol Methods* **82**: 184-186.

Schicklberger, M., Bücking, C., Schuetz, B., Heide, H., and Gescher, J. (2010) Involvement of the *Shewanella oneidensis* decaheme cytochrome MtrA in the periplasmic stability of the beta-barrel protein MtrB. *Appl Environ Microbiol* **77**: 1520-1523.

Poster and presentations, first author only

2008	Jahrestagung der Vereinigung für Allgemeine und Angewandte Mikrobiologie (VAAM), Frankfurt/Main, poster: "Reductase activity of outer membrane *c*-type cytochromes in *Shewanella oneidensis*".
2009	Jahrestagung der Vereinigung für Allgemeine und Angewandte Mikrobiologie (VAAM), Bochum, oral presentation: "Involvement and specificity of outer membrane cytochromes in extracellular electron transfer reactions".
2009	Goldschmidt conference, Davos, oral presentation: "On the role of outer membrane cytochromes in the exoelectrogenic activity of *S. oneidensis*".
2010	Jahrestagung der Vereinigung für Allgemeine und Angewandte Mikrobiologie (VAAM), Hannover, poster: "Functions of outer membrane cytochromes in *Shewanella oneidensis*".
2011	Jahrestagung der Vereinigung für Allgemeine und Angewandte Mikrobiologie (VAAM), Karlsruhe, poster: "Metal reduction without outer membrane cytochromes in *Shewanella oneidensis*".
2011	Conference of the International Society for Subsurface Microbiology, Garmisch-Partenkirchen, oral presentation: "Metal reduction without outer membrane cytochromes in *Shewanella oneidensis*".

XI. Acknowledgments

I would like to thank the following persons:

First of all, my supervisor Prof. Dr. Johannes Gescher for all the support he gave to me since the beginning of my Staatsexamensarbeit back in 2007. Being enthusiastic about his work, he showed me the fascinating world of molecular biology and microbiology. I appreciate very much that he was open to my continuous asking of questions and that he helped to find a solution to all the problems that appeared.

All actual and former members of the AG Gescher for the good teamwork and all the good moments we shared, especially Felix Popp and Frederik Golitsch for the very successful collaboration.

Dr. Sven Kerzenmacher for sharing his knowledge on fuel cells.

Caro, my family, and all my friends for everything.

XII. Appendix (Publications and Manuscripts)

Bücking, C., Popp, F., Kerzenmacher, S., and Gescher, J. (2010) Involvement and specificity of *Shewanella oneidensis* outer membrane cytochromes in the reduction of soluble and solid-phase terminal electron acceptors. *FEMS Microbiol Lett* **306**: 144-151.

Printed in the Appendix on pages 129-136.

Bücking, C., Piepenbrock, A., Kappler, A., and Gescher, J. (2012) Outer membrane cytochrome independent reduction of extracellular electron acceptors in *Shewanella oneidensis*. *Microbiology,* doi:10.1099/mic.0.058404-0.

Printed in the Appendix on pages 137-188.

Golitsch, F., Bücking, C., and Gescher, J.: A microbial fuel cell biosensor based on *Shewanella oneidensis* outer membrane protein complexes. Submitted to: *Biosens Bioelectron*.

Printed in the Appendix on pages 189-215.

RESEARCH LETTER

Involvement and specificity of *Shewanella oneidensis* outer membrane cytochromes in the reduction of soluble and solid-phase terminal electron acceptors

Clemens Bücking[1], Felix Popp[1], Sven Kerzenmacher[2] & Johannes Gescher[1]

[1]Department of Microbiology, Institute for Biology II, University of Freiburg, Freiburg, Germany; and [2]Laboratory for MEMS Applications, Department of Microsystems Engineering–IMTEK, University of Freiburg, Freiburg, Germany

Correspondence: Johannes Gescher, Institut Biologie II, Mikrobiologie, Universität Freiburg, Schänzlestr.1, D-79104 Freiburg, Germany. Tel.: +49 761 203 2685; fax: +49 761 203 2626; e-mail: johannes.gescher@biologie.uni-freiburg.de

Received 18 February 2010; revised 26 February 2010; accepted 27 February 2010.
Final version published online 30 March 2010.

DOI:10.1111/j.1574-6968.2010.01949.x

Editor: Jörg Simon

Keywords
Shewanella oneidensis; dissimilatory iron reduction; *c*-type cytochromes; MtrC; OmcA; MtrF.

Abstract

The formation of outer membrane (OM) cytochromes seems to be a key step in the evolution of dissimilatory iron-reducing bacteria. They are believed to be the endpoints of an extended respiratory chain to the surface of the cell that establishes the connection to insoluble electron acceptors such as iron or manganese oxides. The gammaproteobacterium *Shewanella oneidensis* MR-1 contains the genetic information for five putative OM cytochromes. In this study, the role and specificity of these proteins were investigated. All experiments were conducted using a markerless deletion mutant in all five OM cytochromes that was complemented via the expression of single, plasmid-encoded genes. MtrC and MtrF were shown to be potent reductases of chelated ferric iron, birnessite, and a carbon anode in a microbial fuel cell. OmcA-producing cells were unable to catalyze iron and electrode reduction, although the protein was correctly produced and oriented. However, OmcA production resulted in a higher birnessite reduction rate compared with the mutant. The presence of the decaheme cytochrome SO_2931 as well as the diheme cytochrome SO_1659 did not rescue the phenotype of the deletion mutant.

Introduction

Dissimilatory metal-reducing bacteria have been investigated intensively since the late 1980s. One important model organism for the biochemical elucidation of metal-reducing processes is *Shewanella oneidensis*. Electron transfer to insoluble metal oxides at the cell surface was shown to be mostly dependent on a *c*-type cytochrome-based conductive interprotein connection between the quinone pool within the cytoplasmic membrane and the insoluble terminal electron acceptor located at the outer membrane (OM) (Shi *et al.*, 2007).

The final reduction is catalyzed by *c*-type cytochromes that are attached to the OM by a lipid anchor. In addition to this catalysis of a direct electron transfer to metal oxides (Shi *et al.*, 2007; Wang *et al.*, 2008), other possible functions have also been ascribed to OM cytochromes, including adhesion to mineral particles (Xiong *et al.*, 2006; Lower *et al.*, 2007; Coursolle *et al.*, 2009) and interaction with shuttling compounds (Lies *et al.*, 2005; Marsili *et al.*, 2008). Many studies on the role of OM cytochromes have been published to date. Surprisingly, it is still a matter of ongoing research to assign specific functions to independent proteins. This situation might in part be attributed to the conceivable functional redundancy of these proteins and *c*-type cytochromes in general (Dobbin *et al.*, 1999; Myers & Myers, 2003b).

The aim of this study was the characterization and comparison of reductase activities of individual OM cytochromes. For this purpose, an *S. oneidensis* deletion mutant deficient in all five OM cytochromes (Meyer *et al.*, 2004) was generated to avoid data acquisition that is at least partly affected by a potential low level or upregulated production of proteins with overlapping activities. Subsequently, individually tagged proteins were produced in this background and the activity of complemented strains to reduce soluble and insoluble electron acceptors was tested.

Materials and methods

Growth conditions and media

All the microorganisms used in this study are listed in Table 1. *Escherichia coli* strains were grown in Luria–Bertani (LB)

Table 1. Yeast and bacterial strains used in this study

Strain no.	Strain	Relevant genotype	Source or reference
JG98	*E. coli* WM3064	*thrB1004 pro thi rpsL hsdS lacZΔM15 RP4–1360 Δ(araBAD)567 ΔdapA1341::[erm pir(wt)]*	Saltikov & Newman (2003)
JG22	*E. coli* DH5α Z1	*aci^{q}, PN25-tetR, Sp^{R}, deoR, supE44, Δ(lacZYA-argFV169), Φ80 lacZ ΔM15*	Lutz & Bujard (1997)
JG152	*E. coli* DH5α λ(pir)	*F-Δ(argF-lac)169 Φ80dlacZ58(ΔM15) glnV44(AS) rfbD1 gyrA96(NalR) recA1 endA1 spoT1 thi-1 hsdR17 deoRλpir+*	Stalker *et al*. (1982)
JG26	*S. cerevisiae* InvSc1	*MATa/MATα leu2/leu2 trp1-289/trp1-289 ura3-52/ura3-52 his3-Δ1/his3-Δ1*	Invitrogen
JG7	*S. oneidensis* MR-1	Wild type	Venkateswaran *et al*. (1999)
JG53	*S. oneidensis* MR-1 *Δ(mtrD-mtrC)*	*Δ(mtrD-mtrC) 3100633::(araC, P_{BAD})*	This work
JG132	*S. oneidensis* MR-1$^{\Delta OMC}$ *(OM cytochrome deletion mutant)*	*Δ(mtrD-mtrC) ΔSO_2931 ΔSO_1659, 3100633::(araC, P_{BAD})*	This work
JG137	*S. oneidensis* MR-1$^{\Delta OMC}$ pBAD*omcA$_{strep}$*	JG132/pBAD202-*omcA$_{strep}$*	This work
JG138	*S. oneidensis* MR-1$^{\Delta OMC}$ pBAD*mtrC$_{strep}$*	JG132/pBAD202-*mtrC$_{strep}$*	This work
JG139	*S. oneidensis* MR-1$^{\Delta OMC}$ pBAD*mtrF$_{strep}$*	JG132/pBAD202-*mtrF$_{strep}$*	This work
JG140	*S. oneidensis* MR-1$^{\Delta OMC}$ pBAD*SO_1659$_{strep}$*	JG132/pBAD202-*SO_1659$_{strep}$*	This work
JG141	*S. oneidensis* MR-1$^{\Delta OMC}$ pBAD*SO_2931$_{strep}$*	JG132/pBAD202-*SO_2931$_{strep}$*	This work
JG162	*S. oneidensis* MR-1$^{\Delta OMC}$ pBAD*omcA*	JG132/pBAD202-*omcA*	This work
JG50	*S. oneidensis* MR-1$^{\Delta mtra}$ pBAD*mtrA$_{strep}$*	*ΔmtrA*/pBAD202mtrA$_{strep}$	Schuetz *et al*. (2009)

medium at 37 °C. *Saccharomyces cerevisiae* InvSc1 was grown on YPD medium and was selected for transformants on uracil-free medium (Clontech, Mountain View). *Shewanella oneidensis* strains were grown aerobically at 30 °C in an LB medium or anaerobically in a mineral medium, as described elsewhere (Schuetz *et al*., 2009). If not mentioned, disodium-fumarate (100 mM) was used as an electron acceptor. If necessary, kanamycin (25 or 50 μg mL^{-1}) was added to the medium.

For growth experiments with birnessite as an electron acceptor, 2.5 mM birnessite was added to the mineral medium that was supplemented with 0.1 mM arabinose. Birnessite was prepared as described earlier (Burdige & Nealson, 1985). Manganese reduction was determined in two independent cultures using leucoberbelin blue (Boogerd & de Vrind, 1987).

Construction of a markerless *S. oneidensis* ΔOMC strain

Saccharomyces cerevisiae-based cloning according to Shanks *et al*. (2006) was used to combine three fragments into suicide plasmid pMQ150 (accession no. EU546823): two 500-bp regions flanking the upstream and downstream regions of *mtrD* and *mtrC*, respectively, and one fragment containing P_{BAD} and the *araC* gene. The fragments were amplified (primers 1–2, 3–4, 5–6; see Table 2) and contained overlapping regions to the vector and to the adjacent fragment. The three fragments and the BamHI and the SalI linearized vector were transformed into *S. cerevisiae*. The resulting suicide plasmid was used for mutagenesis of *S. oneidensis* MR-1, resulting in strain JG53 (Table 1). Subsequently, genes *SO_2931* and *SO_1659* were deleted using the same technique (fragments were amplified with primers 7–14; Table 2).

Cloning and production of OM cytochromes

Gene *SO_2931$_{strep}$* was cloned into pBAD202 via TOPO cloning (Invitrogen, Karlsruhe, Germany). The gene was amplified using primers 15 and 16 and was thereby modified to contain an NcoI restriction site and the sequence for a C-terminal strep-tag. His-patch thioredoxin was excised from the vector by cleavage with NcoI and subsequent religation. This vector was used for cloning of the other OM cytochrome genes after NcoI/PmeI restriction digest. The genes were PCR amplified using 5′ primers (primers 17, 19, 21, 23) containing a BspHI site and 3′ primers with a PmeI site and a sequence for a C-terminal strep-tag (primers 18, 20, 22, 24; Table 2). For strain JG162, *omcA* was amplified with primers 21 and 26 containing no strep-tag sequence.

Membrane preparation, SDS-PAGE, heme staining, and Western blotting

Membrane fractions were prepared as described elsewhere (Schuetz *et al*., 2009). Protein concentrations were determined using the method of Bradford (Bradford, 1976) with bovine serum albumin as a standard. For the quantification of protein concentrations in cell suspensions, 0.2 mM NaOH was added to the suspensions before a 10-min incubation at 95 °C.

Table 2. Primers used in this study (5′–3′)

No.	Sequence
1	AAGCTTGCATGCCTGCAGGTCGACTCTAGAGTTAGAACCATGAACCTGAC
2	TGGGACAAATTGGGAAGCCTATT
3	TCTTCATAATAGGCTTCCCAATTTGTCCCAGAATTCGCTAGCCCAAAAAAACG
4	GTCAAATGGACGAAGCAGGG
5	TTTGCAGAATCCCTGCTTCGTCCATTTGACAATTTGAGTTATGCTGTTGAA
6	CATGATTACGAATTCGAGCTCGGTACCCGGGGCCGTTAAATATAAGTGGCG
7	AAGCTTGCATGCCTGCAGGTCGACTCTAGAGTTAGAACCATGAACCTGAC
8	ATGATTACGAATTCGAGCTCGGTACCCGGGTCGGCGCTACAATCAAACCC
9	CAAAGGTACTAGTACCATCGCGTCCCTTTTCTTTC
10	AAAAGGGACGCGATGGTACTAGTACCTTTGGGTTG
11	CGGCCAGTGCCAAGCTTGCATGCCTGCAGGGCGGGTTGACATTCCAAGG
12	ATGATTACGAATTCGAGCTCGGTACCCGGGGGATGAAACGACAGTCGCG
13	GTTGAGGTTATGTACATGAGTTATCCGCTCGTGAG
14	GAGCGGATAACTCATGTACATAACCTCAACTCGGC
15	CGGCCAGTGCCAAGCTTGCATGCCTGCAGGGAGCGATCGCAGTTTTCGAC
16	CACCATGGGCAAAAACCGCCAAACTCTTTCG
17	TTATTTTTCGAACTGCGGGTGGCTCCAAACACAAGTTCCTAAGCTGG
18	GATAGAATCATGAATAAGTTTGC
19	AGCTTTGTTTAAACTTATTTTTCGAACTGCGGGTGGCTCCAGTTTATTGGATGGACTTTGA
20	GAAATATCATGAATAAGTTTGCAAGC
21	AGCTTTGTTTAAACTTATTTTTCGAACTGCGGGTGGCTCCACATTTTCACTTTAGTGTGATCTG
22	GAAATATCATGATGAAACGGTTC

Proteins were separated on polyacrylamide gels according to Laemmli (1970). Heme proteins were visualized by peroxidase staining (Thomas *et al.*, 1976). Proteins containing a C-terminal strep-tag were detected on a Western blot using a primary strep-tag antibody (Qiagen, Hilden, Germany) and a secondary horseradish peroxidase-labeled antibody. The blot was developed using the Ace-glow detection kit from Peqlab according to the manufacturer's instructions (Peqlab, Erlangen, Germany). Signals were visualized in a chemidoc XRS+detection system and were quantified using the IMAGE LAB software (Biorad, Munich, Germany).

Cell surface exposure of OM cytochromes

Surface exposure of OM cytochromes was detected using a proteinase K digest as described by Myers & Myers (2003a), with slight modifications. The duration of incubation was increased to 60 min. The incubation temperature was set to 37 °C. As positive controls for cell surface exposure, strains JG137 and JG138, producing $OmcA_{strep}$ and $MtrC_{strep}$, were chosen; as a control for OM integrity under the incubation conditions, the periplasmic *c*-type cytochrome MtrA containing an N-terminal strep-tag ($MtrA_{strep}$) was produced in an *S. oneidensis* Δ*mtrA* background (JG50) (Schuetz *et al.*, 2009).

Cell suspension assays

Cells were grown anaerobically overnight in minimal media with fumarate as an electron acceptor. At an $OD_{578\,nm}$ of ~0.2, 0.1 mM arabinose was added to induce OM cytochrome and MtrA/MtrB production. After 4 h of production, cells were harvested and washed twice with mineral media without fumarate and lactate and then resuspended in HEPES buffer (100 mM, pH 7.5) containing 50 μM $MgCl_2$ to obtain a final $OD_{578\,nm}$ between 3 and 5. All further measurements were performed in independent duplicates in an anaerobic glove box. Specific reduction rates were obtained by normalization to the protein content of the cell suspension. Fifty microliters of the cell suspension was pipetted in a well of a microtiter plate. The assay was started through the addition of 150 μL of a solution containing 10 mM lactate and 10 mM ferric citrate. At different time points (0–30 min), the reaction was stopped by the addition of 100 μL 3 M HCl. The Fe^{2+} concentration of the samples was determined using the ferrozine reagent (Viollier *et al.*, 2000).

Microbial fuel cell (MFC) experiments

The MFC setup used in this study features an anode and cathode chamber with a working volume of 8 mL each, separated by a Nafion-117 membrane (Quintech, Göppingen; Kloke *et al.*, 2010). A saturated calomel reference electrode (SCE) was separated from the anode compartment by another Nafion membrane. Electrodes were made of graphite felt cubes (Alpha Aesar, Karlsruhe) connected to platinum wires (0.1 mm; Chempur, Karlsruhe). The anode compartment was filled with 5.5 mL mineral media containing 50 mM lactate and 0.1 mM arabinose. Five hundred microliters of a cell suspension with an $OD_{578\,nm}$ of 4 was added to start the experiment. All MFC experiments were performed in duplicate and conducted at a constant temperature of 30 °C. The whole setup was connected to a potentiostat (Pine Instruments, Grove City). The standard measurement protocol consisted of two phases: after a conditioning period with a constant current flux over 5 h (0.3 $\mu A\,cm^{-3}$), MFC cultures were subjected to a continuous increase in current density at a rate of 1.1 $\mu A\,cm^{-3}\,h^{-1}$ over 45 h (*current sweep* phase). The anode compartment was continuously flushed with nitrogen gas to maintain anoxic conditions. Additional terminal electron acceptors were not added.

Results

Preparation of the OM cytochrome-deficient mutant

A markerless multideletion mutant in all annotated OM cytochromes of *S. oneidensis* was constructed to generate a strain platform that allows for analysis of OM cytochrome activity without the potential detection of redundant activities from similar proteins. We will refer to this mutant as ΔOMC. Genes coding for MtrF, MtrC, and OmcA were deleted in one step. This deletion led to further excision of *mtrD* and *mtrE* from the chromosome. The genes for the decaheme *c*-type cytochrome SO_1659 and the diheme cytochrome SO_2931 were deleted subsequently. The presence of MtrA and MtrB was shown to be a requirement for metal reduction by *S. oneidensis* (Bretschger *et al.*, 2007). Hence, possible effects of the removal of genes ranging from *mtrF* to *mtrC* on the expression of *mtrA* and *mtrB* were circumvented by the concomitant introduction of an arabinose-inducible promoter and the *araC* repressor.

Cloning and production of OM cytochromes in the ΔOMC mutant

Genes coding for OM cytochromes from *S. oneidensis* were cloned separately into plasmid pBAD202 to assign specific functions to these proteins in further experiments. The sequence information for a C-terminal strep-tag was added to allow for the specific detection of the proteins produced. The relative amounts of the produced OM cytochromes were quantified via immunodetection of the added strep-tag epitope (Fig. 1a). OmcA production resulted in the strongest strep-tag derived signal compared with all other OM cytochromes produced (Fig. 1c). Signals resulting from $MtrC_{strep}$ and $MtrF_{strep}$ production were detected in similar quantities, which indicates similar production levels. In contrast, the production of SO_1659_{strep} and SO_2931_{strep} seems to be strongly reduced compared with the other three OM cytochromes.

Surface exposure of OM cytochromes

Proteinase K assays according to Myers & Myers (2003a) were performed to investigate whether the proteins are oriented toward the periplasm or the surrounding media (Fig. 2). Detection was based on the added strep-tag epitope. A control reaction using production of a strep-tagged MtrA protein that is localized to the periplasm was performed, to ensure that the assay conditions did not interfere with cell integrity. Localization of OmcA and MtrC to the cell surface was already shown by other research groups (Myers & Myers, 2003a; Shi *et al.*, 2008). Hence, $MtrC_{strep}$ and $OmcA_{strep}$ were used as proteinase K-degradable control proteins. As Fig. 2 shows, $OmcA_{strep}$, $MtrC_{strep}$, $MtrF_{strep}$,

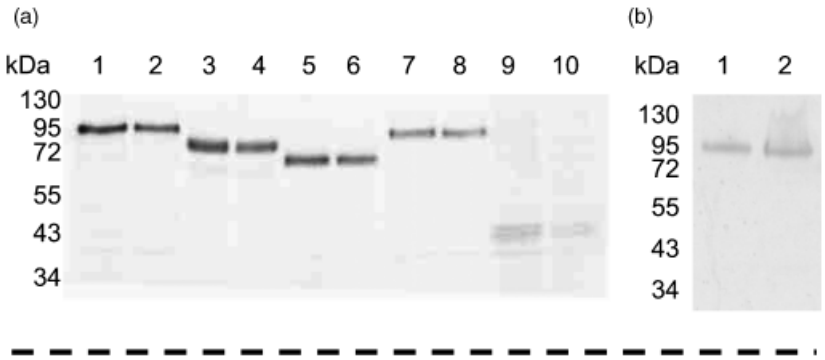

(c)

	$OmcA_{strep}$	$MtrC_{strep}$	$MtrF_{strep}$	SO_1659_{strep}	SO_2931_{strep}
$OmcA_{strep}$	1.000	0.969	0.787	0.468	0.109

Fig. 1. Relative quantification of the OM cytochromes produced. SDS-PAGE gels were loaded with membrane fractions prepared from *Shewanella oneidensis* ΔOMC strains grown anaerobically on fumarate and induced with 0.1 mM arabinose to produce single OM cytochromes. (a) Western blot of cells producing $OmcA_{strep}$ (lanes 1 and 2), $MtrC_{strep}$ (lanes 3 and 4), $MtrF_{strep}$ (lanes 5 and 6), SO_1659_{strep} (lanes 7 and 8), and SO_2931_{strep} (lanes 9 and 10). Three micrograms of the membrane fraction was loaded in lanes 1, 3, 5, and 7. Two micrograms was loaded in lanes 2, 4, 6, and 8. Lanes 9 and 10 contain 8 and 6 μg membrane fractions, respectively. (b) For a series of control experiments, the native form of OmcA was produced. The protein was detected using heme activity staining. Twenty-five micrograms of the membrane fractions from cells producing either OmcA (lane 1) or $OmcA_{strep}$ (lane 2) were loaded. (c) Relative quantification of the detected hrp-derived signals. Mean values from two independent quantifications are shown. The single values varied within a range of not $> 5\%$. The OmcA signal intensity was set to 100%.

and the decaheme cytochrome SO_1659$_{strep}$ are clearly hydrolyzed by the proteinase. Diheme SO_2931$_{strep}$ does not seem to be surface exposed or is not available for proteinase activity.

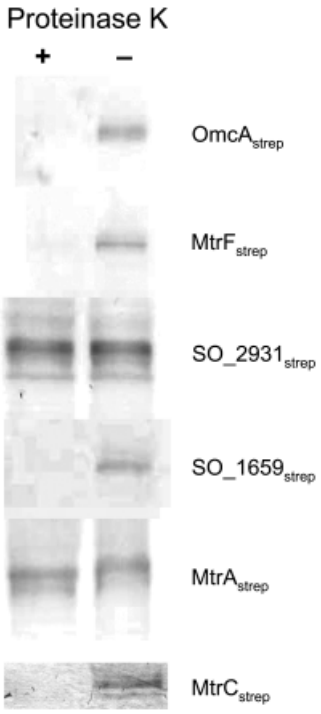

Fig. 2. Cell surface exposure of OM cytochromes tested by proteinase K assays. OM cytochromes were detected with immunostaining based on the strep-tag epitope. Assays conducted with addition of proteinase K are indicated by a +. The periplasmic decaheme cytochrome MtrA was chosen as a control for cell integrity under the assay conditions.

Reduction of ferric citrate

Cell suspension assays showed that only the production of MtrC$_{strep}$ and MtrF$_{strep}$ could partly rescue the mutant phenotype for ferric citrate reduction (Fig. 3a and b). MtrF$_{strep}$ production resulted in a 1.2-fold accelerated ferric citrate reduction rate compared with the MtrC$_{strep}$-producing strain.

Surprisingly, the presence of OmcA$_{strep}$ did not lead to increased ferric iron reduction rates compared with the ΔOMC mutant. To exclude the possible effects of the strep-tag epitope on protein activity, control experiments with the native form of *omcA* in the same vector backbone were performed. Production of the native form of OmcA was shown via heme activity staining (Fig. 1b). Still, even the presence of the native form of OmcA did not lead to an altered phenotype compared with the ΔOMC mutant.

Birnessite reduction

Birnessite was used to study the effect of OM cytochrome production on the reduction of manganese oxides. Interestingly, the complementation pattern did not resemble the results from the reduction experiments with ferric citrate (Fig. 3c). Although MtrF$_{strep}$ and MtrC$_{strep}$ production markedly increased the ability of the ΔOMC mutant to reduce Mn^{4+} ($53 \pm 1.8\%$ Mn^{4+} reduction after 50 h compared with the wild type), an effect of OmcA and OmcA$_{strep}$ production (30% Mn^{4+} reduction after 50 h compared with the wild type) was also detectable (Fig. 3c). The production of the diheme cytochrome SO_2931$_{strep}$ and the decaheme cytochrome SO_1659$_{strep}$ did not lead to birnessite reduction rates that differed from the ΔOMC mutant. Still, these three strains exhibited a low-level reduction capability (Fig. 3c).

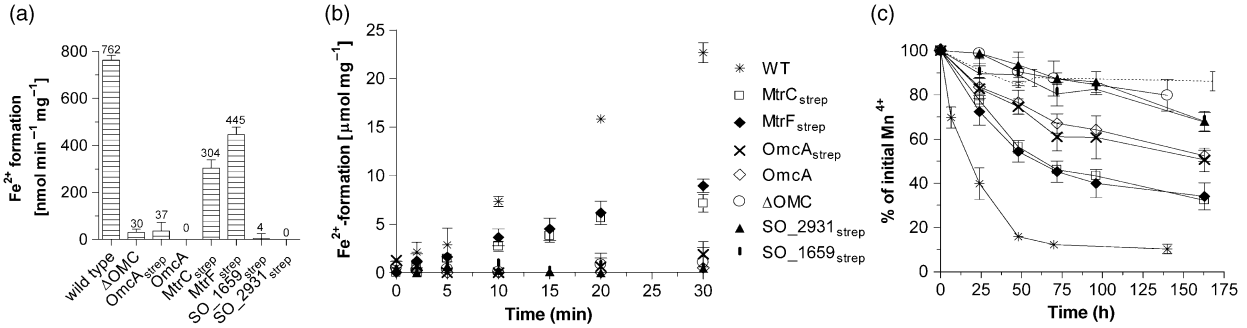

Fig. 3. Reduction rates of *Shewanella oneidensis* wild type, ΔOMC mutant, and complemented mutant strains with ferric citrate (a, b) and birnessite (c) as electron acceptors. (a) Ferric citrate reduction rates were measured in cell suspension experiments using cells that were grown anaerobically with fumarate as an electron acceptor. OM cytochrome and MtrA/B production was induced with 0.1 mM arabinose. (b) Time course of the ferric citrate reduction experiments. The reduction rates remained almost constant over a total time period of 30 min. (c) Manganese reduction was quantified in the growth experiments. Birnessite (2.5 mM) was added to mineral medium with lactate as an electron donor and 0.1 mM arabinose to induce OM cytochromes and MtrA/B. Five hundred microliters of washed cells ($OD_{578\,nm} = 4$) from an anaerobically grown culture were used as an inoculum. Percentage Mn^{4+} is relative to the starting concentration. Initial values for [Mn^{4+}] varied slightly (± 0.266 mM) and were therefore set to 100%.

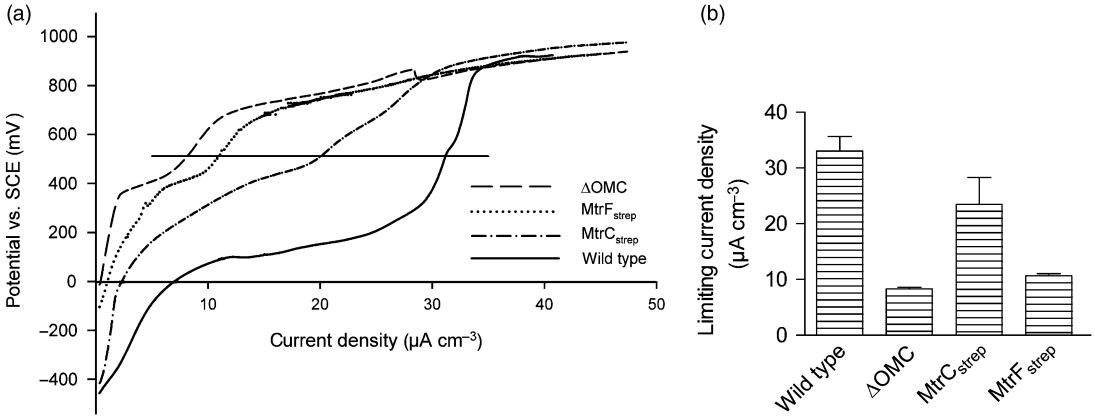

Fig. 4. Anode potentials measured against an SCE at varying current densities. (a) Representative *U–I* curves from selected mutant strains. The horizontal line represents the potential of 512 mV vs. SCE where the system starts to consume electricity. Curves for cells producing SO_1659 or SO_2931 were not distinguishable from the ΔOMC data and were therefore excluded. (b) Mean LCD from two independent experiments. The LCD was defined as the current density where the recorded anode potential exceeds 512 mV vs. SCE.

Anode reduction

MFCs represent another form of a solid terminal electron acceptor (Logan, 2009). Each bacterial strain displayed a characteristic *U–I* curve (Fig. 4a). Common to all MFC cultures was a steep increase in potential at the beginning of the current sweep, followed by a region where potentials increased more linearly in response to higher currents. In this region, bacterial cells behaved analogous to Ohmic resistances. At higher current fluxes, another rapid increase in potential was observed, and above these currents, all *U–I* curves merged into one common line that presumably results from hydrolysis of the base electrolyte. The current density at which bacteria failed to provide sufficient quantities of electrons to sustain a given current flux represents a characteristic feature of each mutant strain. To simplify comparison between performances of different bacterial strains in current sweep experiments, the limiting current density (LCD) was defined as current flux beyond which the measured anode potential first exceeded 512 mV vs. SCE (Fig. 4b), which roughly corresponds to the potential range where the *U–I* curves of all strains exhibit the second striking rise in potential. The ΔOMC mutant showed a 75% reduced LCD value compared with the wild type and could be rescued to a small degree by the production of $MtrF_{strep}$ (Fig. 4a). The presence of $MtrC_{strep}$, by contrast, exerted a more significant effect. The LCD values of the other strains were similar to the ΔOMC mutant and are therefore not shown.

Discussion

Elucidation of metal-reducing processes and the underlying cellular network in *S. oneidensis* is a puzzling subject due to the functional overlap of key components (Myers & Myers, 2003b; Bretschger *et al.*, 2007). The focus of this study was to analyze the activity of single OM cytochromes in an *in vivo* context and to examine the phenotype of a mutant deficient in all of these proteins. It was not the purpose of this study to attain wild-type reduction rates with complemented strains, which would most probably necessitate the production of two or more OM cytochromes, but rather to establish a reliable test platform for OM cytochrome activities.

To analyze the activity and specificity of the different OM cytochromes, we compared electron transfer to metals and an anode surface. The reduction of an anode is as surface limited as the reduction of an insoluble metal. However, anode reduction experiments can provide an additional set of information due to the possibility to change the rate of electron abstraction from the anode surface and thus the potential.

MtrC and MtrF

The reduction experiments conducted showed that $MtrC_{strep}$ and $MtrF_{strep}$ could partly rescue the ΔOMC phenotype, while the production of other OM cytochromes resulted only in minor effects, if at all. A central role of MtrC in metal reduction is in agreement with earlier results (Beliaev *et al.*, 2001; Myers & Myers, 2001) and might reflect the recently discovered capability of a complex of MtrC, with the β-barrel protein MtrB and the decaheme cytochrome MtrA, to transport electrons over a liposome membrane and hence most probably also over the OM of *S. oneidensis* cells (Hartshorne *et al.*, 2009).

mtrF is part of a gene cluster that includes with *mtrD* and *mtrE* genes that are highly similar to *mtrA* and *mtrB* (McLean *et al.*, 2008). We could show that $MtrF_{strep}$ is a functional reductase that has, under several conditions, an

even accelerated activity compared with $MtrC_{strep}$. McLean *et al.* (2008) speculate that the *mtrDEF* gene cluster could encode a reductase that is active under oxic or suboxic conditions and might have a function in reduction-based detoxification of radionuclides. The experiments presented here underline at least that MtrF is a reductase that could have this hypothetical function.

The relative reduction activities of $MtrF_{strep}$ compared with $MtrC_{strep}$ follow the same pattern for all electron acceptors, except for an electrode in an MFC. Here, the LCD of $MtrF_{strep}$-producing cells is only 46% compared with the LCD achieved with $MtrC_{strep}$-producing cells. Therefore, we hypothesize that $MtrF_{strep}$ might be not as well connected to the periplasmic electron pool, which could be due to a reduced capability of forming a complex with MtrA and MtrB. This interprotein electron transfer might not be rate limiting under mineral-reducing conditions, but could become important when a certain current is applied to the MFC.

OmcA

OmcA production did not lead to accelerated reduction rates compared with the ΔOMC mutant in ferric iron reduction assays. This effect does not seem to be due to the reported partial mislocalization of OmcA in a Δ*mtrC* mutant (Myers & Myers, 2001) since proteinase K assays clearly demonstrated the surface exposure of OmcA in the ΔOMC mutant. OmcA is part of the core proteins that can be found in ferric iron-reducing *S. oneidensis* cells (Shi *et al.*, 2007). We hypothesize that OmcA is an *in vivo* ferric iron reductase that is dependent on electron transport by another OM cytochrome. This cytochrome would most probably be MtrC. However, we cannot explain how OmcA might be linked to the periplasmic electron pool under manganese-reducing conditions. Still, our data, which indicate a function of OmcA under manganese-reducing conditions, are in line with the results obtained previously by Myers & Myers (2001, 2003b).

SO_2931 and SO_1659

The production of SO_2931_{strep} and SO_1659_{strep} was shown to be less efficient when compared with OmcA production. Nevertheless, the production of SO_2931 or SO_1659 was detectable, but never resulted in a significantly different phenotype compared with the ΔOMC mutant. For the diheme cytochrome SO_2931, this could be due to a periplasm-oriented localization in the OM. So far, we can only speculate that these proteins might be involved in other electron transfer pathways or do not have a function in the physiology of *S. oneidensis* in general.

ΔOMC mutant

Interestingly, a low-level reduction of birnessite and an anode surface were observed for the ΔOMC mutant. This could be due to the production of endogenous shuttling components. Still, our data indicate that if electron shuttles are the reason for this reduction, they are at least in part not dependent on the interaction with OM cytochromes and therefore seem to be OM permeable.

Acknowledgements

The authors thank Prof. Fuchs and Prof. Majzlan for fruitful discussions. J.G. is indebted to the LANDESSTIFTUNG Baden-Württemberg and the German Science Foundation (DFG) for facilitating the analysis entailed in this article.

References

Beliaev AS, Saffarini DA, McLaughlin JL & Hunnicutt D (2001) MtrC, an outer membrane decahaem *c* cytochrome required for metal reduction in *Shewanella putrefaciens* MR-1. *Mol Microbiol* **39**: 722–730.

Boogerd FC & de Vrind JP (1987) Manganese oxidation by *Leptothrix discophora*. *J Bacteriol* **169**: 489–494.

Bradford MM (1976) A rapid and sensitive method for the quantitation of microgram quantities of protein utilizing the principle of protein–dye binding. *Anal Biochem* **72**: 248–254.

Bretschger O, Obraztsova A, Sturm CA *et al.* (2007) Current production and metal oxide reduction by *Shewanella oneidensis* MR-1 wild type and mutants. *Appl Environ Microb* **73**: 7003–7012.

Burdige DJ & Nealson KH (1985) Microbial manganese reduction by enrichment cultures from coastal marine sediments. *Appl Environ Microb* **50**: 491–497.

Coursolle D, Baron DB, Bond DR & Gralnick JA (2009) The Mtr respiratory pathway is essential for reducing flavins and electrodes in *Shewanella oneidensis*. *J Bacteriol* **192**: 467–474.

Dobbin PS, Butt JN, Powell AK, Reid GA & Richardson DJ (1999) Characterization of a flavocytochrome that is induced during the anaerobic respiration of $Fe3^+$ by *Shewanella frigidimarina* NCIMB400. *Biochem J* **342**: 439–448.

Hartshorne RS, Reardon CL, Ross D *et al.* (2009) Characterization of an electron conduit between bacteria and the extracellular environment. *P Natl Acad Sci USA* **106**: 22169–22174.

Kloke A, Rubenwolf S, Bücking C, Gescher J, Kerzenmacher S, Zengerle R & von Stetten F (2010) A versatile miniature bioreactor and its application to bioelectrochemistry studies. *Biosens Bioelectron* (in press).

Laemmli UK (1970) Cleavage of structural proteins during the assembly of the head of bacteriophage T4. *Nature* **227**: 680–685.

Lies DP, Hernandez ME, Kappler A, Mielke RE, Gralnick JA & Newman DK (2005) *Shewanella oneidensis* MR-1 uses overlapping pathways for iron reduction at a distance and by

direct contact under conditions relevant for biofilms. *Appl Environ Microb* **71**: 4414–4426.

Logan BE (2009) Exoelectrogenic bacteria that power microbial fuel cells. *Nat Rev Microbiol* **7**: 375–381.

Lower BH, Shi L, Yongsunthon R, Droubay TC, McCready DE & Lower SK (2007) Specific bonds between an iron oxide surface and outer membrane cytochromes MtrC and OmcA from *Shewanella oneidensis* MR-1. *J Bacteriol* **189**: 4944–4952.

Lutz R & Bujard H (1997) Independent and tight regulation of transcriptional units in *Escherichia coli* via the LacR/O, the TetR/O and AraC/I1-I2 regulatory elements. *Nucleic Acids Res* **25**: 1203–1210.

Marsili E, Baron DB, Shikhare ID, Coursolle D, Gralnick JA & Bond DR (2008) *Shewanella* secretes flavins that mediate extracellular electron transfer. *P Natl Acad Sci USA* **105**: 3968–3973.

McLean JS, Pinchuk GE, Geydebrekht OV *et al.* (2008) Oxygen-dependent autoaggregation in *Shewanella oneidensis* MR-1. *Environ Microbiol* **10**: 1861–1876.

Meyer TE, Tsapin AI, Vandenberghe I *et al.* (2004) Identification of 42 possible cytochrome *c* genes in the *Shewanella oneidensis* genome and characterization of six soluble cytochromes. *Omics* **8**: 57–77.

Myers CR & Myers JM (2003a) Cell surface exposure of the outer membrane cytochromes of *Shewanella oneidensis* MR-1. *Lett Appl Microbiol* **37**: 254–258.

Myers JM & Myers CR (2001) Role for outer membrane cytochromes OmcA and OmcB of *Shewanella putrefaciens* MR-1 in reduction of manganese dioxide. *Appl Environ Microb* **67**: 260–269.

Myers JM & Myers CR (2003b) Overlapping role of the outer membrane cytochromes of *Shewanella oneidensis* MR-1 in the reduction of manganese(IV) oxide. *Lett Appl Microbiol* **37**: 21–25.

Saltikov CW & Newman DK (2003) Genetic identification of a respiratory arsenate reductase. *P Natl Acad Sci USA* **100**: 10983–10988.

Schuetz B, Schicklberger M, Kuermann J, Spormann AM & Gescher J (2009) Periplasmic electron transfer via the *c*-type cytochromes MtrA and FccA of *Shewanella oneidensis* MR-1. *Appl Environ Microb* **75**: 7789–7796.

Shanks RM, Caiazza NC, Hinsa SM, Toutain CM & O'Toole GA (2006) *Saccharomyces cerevisiae*-based molecular tool kit for manipulation of genes from gram-negative bacteria. *Appl Environ Microb* **72**: 5027–5036.

Shi L, Squier TC, Zachara JM & Fredrickson JK (2007) Respiration of metal (hydr)oxides by *Shewanella* and *Geobacter*: a key role for multihaem *c*-type cytochromes. *Mol Microbiol* **65**: 12–20.

Shi L, Deng S, Marshall MJ *et al.* (2008) Direct involvement of type II secretion system in extracellular translocation of *Shewanella oneidensis* outer membrane cytochromes MtrC and OmcA. *J Bacteriol* **190**: 5512–5516.

Stalker DM, Kolter R & Helinski DR (1982) Plasmid R6K DNA replication. I. Complete nucleotide sequence of an autonomously replicating segment. *J Mol Biol* **161**: 33–43.

Thomas PE, Ryan D & Levin W (1976) Improved staining procedure for detection of peroxidase-activity of cytochrome-P-450 on sodium dodecyl-sulfate polyacrylamide gels. *Anal Biochem* **75**: 168–176.

Venkateswaran K, Moser DP, Dollhopf ME *et al.* (1999) Polyphasic taxonomy of the genus *Shewanella* and description of *Shewanella oneidensis* sp. nov. *Int J Syst Bacteriol* **49**: 705–724.

Viollier E, Inglett PW, Hunter K, Roychoudhury AN & Van Cappellen P (2000) The ferrozine method revisited: Fe(II)/Fe(III) determination in natural waters. *Appl Geochem* **15**: 785–790.

Wang Z, Liu C, Wang X *et al.* (2008) Kinetics of reduction of Fe(III) complexes by outer membrane cytochromes MtrC and OmcA of *Shewanella oneidensis* MR-1. *Appl Environ Microb* **74**: 6746–6755.

Xiong Y, Shi L, Chen B *et al.* (2006) High-affinity binding and direct electron transfer to solid metals by the *Shewanella oneidensis* MR-1 outer membrane *c*-type cytochrome OmcA. *J Am Chem Soc* **128**: 13978–13979.

Outer membrane cytochrome independent reduction of extracellular electron acceptors in *Shewanella oneidensis*

Clemens Bücking[#], Annette Piepenbrock[‡], Andreas Kappler[‡], and Johannes Gescher[#]*

[#]Institut für angewandte Biowissenschaften, Angewandte Biologie, Karlsruher Institut für Technologie, Fritz-Haber-Weg 2, D-76131 Karlsruhe, Germany.

[‡]Geomicrobiology, Center for Applied Geosciences, University of Tübingen, Sigwartstrasse 10, D-72076 Tübingen, Germany

Running title: Metal reduction without outer membrane cytochromes

Content Section: Physiology and Biochemistry

* Corresponding author:

Phone:+49-721-608-41940. Fax:+49-721-608-41941.

E-mail: johannes.gescher@kit.edu

Words in summary: 227

Words in text: 6715

Number of tables: 3

Number of figures: 7

Summary

Dissimilatory metal reduction under pH-neutral conditions is dependent on an extended respiratory chain to the cell surface. The final reduction is catalyzed by outer membrane cytochromes that transfer respiratory electrons either directly to mineral surfaces and metal ions bound in larger organic complexes such as Fe(III) citrate or indirectly using endogenous or exogenous electron shuttles such as humic acids or flavins. Consequently, a *Shewanella oneidensis* deletion mutant devoid of outer membrane cytochromes is unable to reduce Fe(III) citrate or manganese oxide minerals and reduces humic acids at lower rates. Surprisingly, the phenotype of this quintuple deletion mutant can be rescued by a suppressor mutation, which enables metal or humic acid reduction without any outer membrane cytochrome. Furthermore, the type II secretion system, essential for metal reduction in *S. oneidensis* wild type, is not necessary for the suppressor strain. Using genome sequencing we identified two point mutations in key genes for metal reduction: *mtrA* and *mtrB*. These mutations are necessary and sufficient to account for the observed phenotype. This study is the first evidence for a catabolic, outer membrane cytochrome independent electron transport chain to ferric iron, manganese oxides and humic acid analogues operating in a mesophilic organism. Available bioinformatic data allows the hypothesis that outer membrane cytochrome independent electron transfer might resemble an evolutionary intermediate between ferrous iron oxidizing and ferric iron reducing microorganisms.

Introduction

Bacterial dissimilatory metal reduction has been investigated intensely in the last decades. This is due to its relevance as a respiratory process in a multitude of environments and the possible applications in biotechnology like remediation of contaminated soils or electricity production in microbial fuel cells. One of the best studied model organisms is *Shewanella oneidensis* MR-1, a γ-proteobacterium with 41 putative *c*-type cytochromes encoded in its genome (Meyer *et al.*, 2004; Romine *et al.*, 2008).

Several of these *c*-type cytochromes were shown to form a respiratory network extending the respiratory chain from the cytoplasmic membrane through the periplasm and to the outer membrane (Schuetz *et al.*, 2009; Shi *et al.*, 2007). From here, catabolic electrons are transferred directly or indirectly to a wide variety of terminal electron acceptors being either poorly soluble or soluble but unable to pass the outer membrane. Examples for poorly soluble electron acceptors are iron(III) (oxyhydr)oxides like hematite or ferrihydrite and manganese oxides like birnessite or pyrolusite. These minerals are ubiquitously distributed in soils and sediments. Examples for substances that are soluble but apparently unable to pass the outer membrane at least to an extent that supports growth are Fe(III) citrate or the humic acid analogue anthraquinone-2,6-disulfonate (Dobbin *et al.*, 1996; Gescher *et al.*, 2008; Pitts *et al.*, 2003; Shyu *et al.*, 2002).

In *S. oneidensis,* the reduction of most extracellular electron acceptors is based on a protein complex formed by MtrA, MtrB, and MtrC (mtr: **m**e**t**al **r**educing). This complex most probably is the extracellular terminal reductase (Hartshorne *et al.*, 2009; Shi *et al.*, 2006). The current model is that the decaheme *c*-type cytochromes MtrA, localized to the periplasmic side, and MtrC, localized to the outer surface of the outer membrane, are held in close proximity via the outer membrane spanning β-barrel protein MtrB. This close proximity is supposed to enable electron transfer through the outer membrane

(Hartshorne *et al.*, 2009). OmcA (**o**uter **m**embrane **c**ytochrome), a decaheme *c*-type cytochrome as well, is also localized to the cell surface and apparently involved in the reduction of manganese oxides (Bücking *et al.*, 2010; Myers & Myers, 2003). Although in vitro evidence was provided for a high affinity complex between OmcA and MtrC, it seems as if they are not colocalized in vivo (Lower *et al.*, 2009; Shi *et al.*, 2006; Zhang *et al.*, 2008). Both proteins are lipoproteins that are exported through the outer membrane by the type II secretion system (Shi *et al.*, 2008).

Different models were proposed of how the terminal metallic electron acceptor is finally reduced. MtrC and OmcA were shown to directly reduce iron minerals in vitro (Reardon *et al.*, 2010; Xiong *et al.*, 2006). The transfer rates to ferric iron were rather low and could not explain entirely the fast rates of iron reduction by whole cells. It was therefore proposed that endogenous flavin redox shuttles are involved in this electron transfer process (Marsili *et al.*, 2008; Ross *et al.*, 2009; von Canstein *et al.*, 2008). Still, reduction of the flavin shuttle molecules depends on the whole electron transfer chain since they apparently cannot pass the outer membrane and therefore have to be reduced by outer membrane cytochromes as well (Coursolle *et al.*, 2010; Richter *et al.*, 2010). In aquatic sediments from which *S. oneidensis* MR-1 was originally isolated, humic acids are frequently present (Myers & Nealson, 1988*a*; Stevenson, 1994). They represent exogenous electron shuttles. Consequently, it was shown that Fe(III) reduction by *S. oneidensis* was stimulated by humic substances in concentrations as low as 5-10 mg carbon per liter. Humic substances can occur in dissolved or solid-phase form. Both have been studied extensively with respect to their effect on microbial Fe(III) reduction due to electron shuttling (Jiang & Kappler, 2008; Lovley *et al.*, 1996; Roden *et al.*, 2010).

Another possible mode of electron transfer are so called nanowires that were first described by Reguera *et al.* for *Geobacter sulfurreducens* and shortly later by Gorby *et al.* for *S. oneidensis* (Gorby *et al.*, 2006; Reguera *et al.*, 2005). It was hypothesized that these

cell appendages can transfer electrons to an electron acceptor that is not in direct contact to the cell but rather distantly localized. In *S. oneidensis*, electron transfer along the pilus is dependent on the presence of MtrC and OmcA (El-Naggar *et al.*, 2010). Probably, all three modes of electron transfer (i.e. direct contact, electron shuttling and nanowires) operate simultaneously, but all of them fundamentally rely on the catalytic activity of outer membrane *c*-type cytochromes.

In this study we report that a quintuple deletion mutant devoid of genes for outer membrane cytochromes (Bücking *et al.*, 2010) can regain the ability to reduce extracellular electron acceptors like ferric iron, manganese dioxide, humic acids, or AQDS, a model compound for quinone moieties in humic acids. This mutant is not affected in outer membrane stability, which excludes an increased reduction of extracellular electron acceptors by periplasmic *c*-type cytochromes. Resequencing of the mutant genome and subsequent mapping to the *S. oneidensis* reference genome revealed that one point mutation in MtrA and one in MtrB are the reason for the evolution of an extended respiratory chain independent of outer membrane cytochromes.

Methods

Chemicals and biochemicals were obtained from Sigma-Aldrich, Roth and Promega. Enzymes were purchased from New England Biolabs.

Growth conditions and media

All microorganisms used in this study are listed in Table 1. *Escherichia coli* strains were grown aerobically in LB medium at 37°C. *Sacharomyces cerevisiae* InvSc1 was grown on YPD-medium and was selected for transformants on uracil-free medium purchased from Clontech. *S. oneidensis* strains were grown aerobically at 30°C in LB medium or in minimal medium under anoxic conditions, supplemented with lactate (50 mM) as electron

donor and carbon source and 50 mM Fe(III) citrate, 5 mM Fe(III) nitrilotriacetic acid (NTA) or 100 mM fumarate as electron acceptor as described previously (Schuetz *et al.*, 2009). Fe(III) citrate powder was dissolved in hot water and pH was adjusted to pH 7.4 slowly with 1 M NaOH. If necessary, kanamycin (50 μg ml^{-1}), arabinose (1 mM) or 2,6-diaminopimelic acid (100 μg ml^{-1}) was added to the medium. Fe(III) citrate and Fe(III) NTA reduction was determined by measuring ferrous iron concentrations with the ferrozine reagent (Stookey, 1970) and was used as surrogate for bacterial growth. For growth experiments with birnessite (manganese dioxide) as electron acceptor, 2.5 mM birnessite were added to minimal medium that was supplemented with 1 mM arabinose. Birnessite was prepared as described earlier (Burdige & Nealson, 1985). Manganese reduction was determined in three independent cultures using leucoberbellin blue (Boogerd & de Vrind, 1987). The rate of abiotic Mn^{IV} decrease in culture flasks was subtracted from the measured values.

Standard procedures

Membrane fractions were prepared as described earlier (Schuetz *et al.*, 2009). Protein concentrations were determined by the method of Bradford (Bradford, 1976) with bovine serum albumin as standard. Proteins were separated on polyacrylamide gels according to Laemmli (Laemmli, 1970). Heme proteins were visualized by peroxidase staining (Thomas *et al.*, 1976). Proteins containing a C-terminal strep-tag were detected on a western blot using a strep-tag antibody (Qiagen).

Construction of markerless *S. oneidensis* mutants

Strains containing a Δ*gspD*, Δ*dmsA-1 dmsB-1* and *ΔdmsA-2 dmsB-2* deletion were constructed according to (Schuetz *et al.*, 2009) with minor modifications. All primers used are listed in Table S1. Primers 1 to 4 were used to amplify 500 base pair regions up- and downstream of *gspD*. The resulting fragments were cloned into a linearized pMQ150

plasmid using a *S. cerevisiae* based recombination system (Shanks *et al.*, 2006). The resulting plasmid pMQ150-Δ*gspD* was transformed into *E. coli* WM3064, which was then used as donor strain for conjugation based mating with *S. oneidensis*. Primers 5 to 8 were used to construct pMQ150- Δ*dmsA-1 dmsB-1*, primers 9 to 12 were used to assemble pMQ150-Δ*dmsA-2 dmsB-2*.

Genome sequencing

Genomic DNA was isolated using the Illustra bacteria genomic Prep kit (GE Healthcare) according to the manufacturer's instructions. Sequencing was performed on an Illumina HiSeq 2000 with a read length of 46 base pairs by GATC Biotech. The reads were assembled using the software BWA (Li & Durbin, 2009), identification of single nucleotide polymorphisms as well as insertions and deletions was done with SAMtools (Li *et al.*, 2009) and the assembly viewer Tablet (Milne *et al.*, 2010).

Cloning of *mtrA*, *mtrB* and their mutated versions

Genomic DNA of either *S. oneidensis* WT or ΔOMC^S was used as a template to amplify *mtrA* (primer 13, 14), *mtrB* (primer 15, 16) or *mtrA* and *mtrB* (primer 13, 16). Primer 16 contains furthermore the sequence for a strep-tag, which was added to the C-terminus of MtrB. The target vector pBAD202 was digested with *Nco*I and *Pme*I. Vector and inserts were purified and then assembled via isothermal DNA assembly (Gibson *et al.*, 2009). The overlap between PCR fragment and linearized plasmid was 50 base pairs long. To construct a plasmid with a combination of wild type *mtrA* and mutated *mtrB*, we amplified an *mtrA*-fragment with primers 13 and 17 and an $mtrB^S$-fragment, containing the point mutation, with primers 18 and 16. Both fragments were combined in one step with the same method as above. All resulting plasmids were sequenced (GATC Biotech).

Ferric iron reduction cell suspension assays

Cells were grown under anoxic conditions over night in minimal media with fumarate as

electron acceptor and with 1 mM arabinose to induce *mtrA* and *mtrB* expression (mtrA and mtrB are under arabinose promoter control in ΔOMC cells) (Bücking *et al.*, 2010). Cells were harvested and washed twice using minimal media without fumarate and lactate under anoxic conditions and resuspended to a final OD_{600} between 3 and 5. Specific reduction rates of independent triplicate cultures were obtained by normalization to the protein content of the cell suspension. 50 µl of cell suspension were pipetted in a well of a microtiter plate. The assay was started through the addition of 150 µl of a solution containing 10 mM lactate and 10 mM Fe(III) citrate. At different time points (0-30 min) the reaction was stopped by the addition of 100 µl of 3 M HCl. The Fe^{2+} concentration of the samples was determined using the ferrozine reagent (Stookey, 1970).

Riboflavin and AQDS reduction rates

Cells for these assays were grown under anoxic conditions with fumarate as electron acceptor and, if necessary, in the presence of arabinose as inductor for gene expression. Cells were harvested and washed twice before start of the experiments. Riboflavin reduction was measured in cuvettes with butyl rubber stoppers at 30°C and 450 nm. The assay contained 60 µM riboflavin, 100 mM HEPES, pH 7.4, 10 mM lactate and was initiated by the addition of riboflavin. Reduction rates were calculated as a function of protein concentration in the assay. AQDS reduction was measured in a similar assay at a wavelength of 436 nm using 1 mM AQDS (extinction coefficient = 3500 M^{-1} cm^{-1}; (Bayer *et al.*, 1996). Both assays were typically finished within 20 minutes.

Humic acid reduction rates

Humic acid reduction was measured continuously over 18 days. Pahokee peat humic acids (PPHA), purchased from the International Humic Substances Society (IHSS) were added at a concentration 1 g l^{-1} with 2 mM lactate as electron donor. At selected time points, samples were withdrawn and the oxidation state of humic acids was analyzed by

an electron shuttling assay similar to that described earlier (Lovley *et al.*, 1996). Briefly, under anoxic conditions, samples were filtered (0.2 µm) and reacted with 5 mM Fe(III) citrate for 1 hour. Subsequently, the sample-Fe(III) citrate mixture was diluted 1:2 with 1 M HCl, humic acids were precipitated and removed by centrifugation and the Fe(II) concentration was determined by the ferrozine assay (Stookey, 1970). The reducing capacity in micro electron equivalents (µeq l^{-1}) was calculated as the amount of electrons transferred to Fe(III), i.e. the amount of Fe(II) formed. The amount of electrons transferred by the bacteria to humic acids was calculated by subtracting the abiotic reducing capacity of the sterile control from the reducing capacity of the humic acids at the respective time points. Experiments were performed in independent duplicates.

Outer membrane integrity testing

For outer membrane integrity testing, cells were grown under anoxic conditions with fumarate as electron acceptor and in the presence of 1 mM arabinose. After washing the cells twice with 100 mM HEPES, pH7.4, first an ethidium bromide influx assay was performed to measure outer membrane permeability. The assay was performed according to *Murata et al.* with minor modifications (Murata *et al.*, 2007). The assay was initiated by the addition of ethidium bromide (final concentration 6 µM). Fluorescence was measured continuously over 5 minutes (excitation and emission wavelengths of 545 and 600 nm, respectively) using a microtiter plate reader (Varioscan, ThermoFisher). Ethidium bromide influx rates are displayed as relative fluorescence units (RFU) per minute and milligram protein. As a positive control, 1 mg ml^{-1} polymyxin B was added to the cells. Polymyxin B destabilizes the membrane and increases permeability (Vaara, 1992).

Second, iron diffusion into the cells was measured after 30 min incubation with 10 mM Fe(III) citrate but without electron donor at room temperature. Afterwards, the cells were washed twice and acidified to a final concentration of 1 M HCl. All containing Fe(III)

was reduced with 2.5% (w/v) hydroxylamine hydrochloride and the total iron content was determined with the ferrozine assay (Stookey, 1970). As a positive control polymyxin B was added at a concentration of 50 µg ml^{-1}. A lower polymyxin B concentration was chosen because of the longer incubation time of this experiment. The iron content was calculated as a function of protein content.

As a third test, antibiotic susceptibility was tested in a disc diffusion test. 100 µl cell suspension ($OD_{600\ nm}$ 0.132, corresponding to McFarland standard 0.5) was spread on LB plates supplemented with 1 mM arabinose and subsequently paper discs containing either 25 µg colistin, 30 µg kanamycin or 30 µg chloramphenicol (Oxoid, Thermo Fisher) were applied to the surface. After overnight incubation at 30°C, plates were photographed and zones of inhibition were measured with ImageJ (http://imagej.nih.gov/ij/).

Bioinformatic analysis

The integrated microbial genomes tool of the Joint Genome Institute was used to search in available microbial genomes for homologues of *mtrAB* gene cassettes (http://img.jgi.doe.gov). The analysis was performed using the blastp algorithm and a concatamer of the protein sequences of MtrA and MtrB from *S. oneidensis*. Detected *mtrAB*-like gene clusters were analyzed for genes encoded upstream and downstream of *mtrA*. Only gene clusters that did contain *mtrAB* gene clusters without homologous genes to *mtrC* or *mtrF* were further analyzed.

Results

Evolution of a ΔOMC suppressor mutant

Previously we deleted in *S. oneidensis* all five genes coding for outer membrane cytochromes. Additionally, a P_{BAD} promoter was inserted in the genome of this strain upstream of *mtrA* and *mtrB*, two essential genes for metal reduction. The deletion of the

outer membrane cytochromes resulted in an almost complete loss of the ability to reduce poorly soluble electron acceptors (Bücking *et al.*, 2010). In Fe(III) citrate medium, the Fe(II) concentration did not climb above 2.5 mM within 35 h and a reduction rate for the ΔOMC strain could thus not be calculated (Fig. 1). However, this minimal Fe(III) citrate reducing activity apparently increased substantially during prolonged incubation and several serial transfers. The accelerated iron reduction over time suggested the development of a suppressor mutation. In order to characterize a potential suppressor mutant ΔOMC^S, single cells were isolated using dilution series and subsequent plating on LB-agar plates.

Fe(III) citrate, Fe(III) NTA and birnessite reduction without outer membrane cytochromes

It was shown that *S. oneidensis* can couple growth to the reduction of ferric iron or manganese oxides (Myers & Nealson, 1988*a*; Myers & Nealson, 1988*b*). Therefore, ferrous iron concentrations were determined as a surrogate for growth in medium containing lactate as carbon and electron source and 50 mM Fe(III) citrate or 5 mM Fe(III) NTA as electron acceptor. Iron reduction curves were recorded in the presence and absence of 1 mM arabinose as inducer for *mtrA* and *mtrB* expression (Fig. 1). Induction with 1 mM arabinose leads to the expression of wild type levels of MtrA as determined by SDS-PAGE and staining of heme containing proteins (Fig. S1). Of note, *S. oneidensis* cannot grow with arabinose as a substrate (Gralnick *et al.*, 2006). As indicated in Fig. 1, Fe(III) citrate reduction of the suppressor mutant ΔOMC^S was strictly dependent on arabinose induction upon which the reduction rate reached 84% of the wild type rate (Fig. 1) while the original mutant ΔOMC showed almost no Fe(III) citrate reduction activity. Fe(III) NTA, which is smaller and more membrane permeable iron chelate could be reduced rather slowly by ΔOMC but much faster by the suppressor mutant ΔOMC^S reaching 34% of the wild type reduction rate (Fig. 2).

Birnessite, as a mineral phase electron acceptor was used to assess the ability of ΔOMC^S to reduce oxidized manganese species (Fig. 3). While ΔOMC has only background reducing activity, ΔOMC^S is able to reduce birnessite 10-fold faster compared the original mutant and with 20% of the wild type rate. Albeit, the phenotype of birnessite reduction of ΔOMC^S is not as pronounced as with Fe(III) citrate as electron acceptor.

Reduction of electron shuttles by ΔOMC^S

Electron shuttles have been proposed to be involved in *S. oneidensis* catalyzed metal and mineral reduction. They can either be produced and secreted by the cell endogenously, mainly in the form of riboflavin (Marsili *et al.*, 2008; von Canstein *et al.*, 2008) or can be present in soils typically in the form of dissolved or solid-phase humic substances (Jiang & Kappler, 2008; Roden *et al.*, 2010). As humic substances are a structurally diverse group of substances, AQDS can be used as a surrogate for small fulvic acid molecules and for quinone moieties in humic acids (Jiang & Kappler, 2008). Reduction of large humic acid molecules was measured with Pahokee peat humic acids (PPHA).

For riboflavin and AQDS, the reduction activity was recorded over 20 min using washed cell suspensions of anoxically grown cells that should be free of any additional electron shuttle. As Fig. 4a indicates, reduction of riboflavin was rather slow for ΔOMC and ΔOMC^S (12% and 21% of wild type activity, respectively). In contrast to this, AQDS was reduced by the suppressor mutant with 81% of the wild type rate while the original ΔOMC strain reduced AQDS with only 32% of the wild type rate (Fig. 4b). This effect was even more pronounced when the cells were pregrown on Fe(III) citrate leading to a ΔOMC^S AQDS reducing activity of 99% compared to the wild type (Fig. 4b).

The reduction of PPHA was measured over a time frame of 18 days in a growth experiment (Fig. 5). For the reduction of PPHA, the situation resembled the results of the riboflavin reduction experiments. The maximal PPHA reduction rate reached in ΔOMC 18% and in ΔOMC^S 35% of wild type activity (Fig. 5).

Reduction of Fe(III) citrate by washed cell suspensions

Cell suspension experiments were conducted to assess the ability of ΔOMC^S cells to reduce Fe(III) citrate without the putative involvement of endogenous electron shuttles. The different *S. oneidensis* strains were pregrown on minimal medium with fumarate or Fe(III) citrate as electron acceptors. Cells were then washed twice in buffer without electron acceptor under anoxic conditions and thereafter used for Fe(III) citrate reduction assays. Fumarate grown ΔOMC^S cells reduced Fe(III) citrate with 28% of the wild type rate, while ΔOMC showed no detectable activity. When the cells were pregrown on Fe(III) citrate, the activity of ΔOMC^S increased to 51% of the wild type ferric iron reduction rate (Fig. 4c).

Putative involvement of other outer membrane protein complexes

Several experimental results point towards the role of the outer membrane *c*-type cytochromes MtrC and OmcA as the final metal and flavin reductases of *S. oneidensis* (Bücking *et al.*, 2010; Coursolle *et al.*, 2010). The mechanism of metal reduction in ΔOMC^S must be independent of these proteins and any other outer membrane cytochrome encoded in the genome of the strain, since all 5 corresponding genes were deleted (Bücking *et al.*, 2010). A recent study described the modularity of different outer membrane spanning complexes in *S. oneidensis* (Coursolle & Gralnick, 2010). Hence, it was asked whether another surface localized terminal reductase could functionally replace outer membrane cytochromes. The only other enzyme fulfilling this prerequisite is the DMSO reductase DmsAB (Gralnick *et al.*, 2006). The genome of *S. oneidensis* has two gene cluster encoding DMSO reductases (*dmsA-1* and *dmsB-1*, SO_1429-30) and (*dmsA-2* and *dmsB-2*, SO_4357-58). Both loci are still present in ΔOMC, the parental strain of suppressor mutant ΔOMC^S. Hence, *dmsAB-1* and *dmsAB-2* were deleted in ΔOMC^S and it was sought for an effect of these deletions on the Fe(III) citrate reduction rate of this strain. The deletions did not lead to a change of the ΔOMC^S phenotype regarding Fe(III)

citrate reduction (data not shown). Hence, an involvement of these proteins in the described iron reduction phenotype was excluded.

The type II secretion system transfers outer membrane cytochromes to the outer surface of the cell in *S. oneidensis*. Consequently, this export machinery is essential for metal reduction (DiChristina *et al.*, 2002; Shi *et al.*, 2008). If other proteins would functionally replace the outer membrane cytochromes in ΔOMC^S, one would expect a possible involvement of type II secretion in protein translocation. The genes for the type II secretion systems are clustered in the *gsp*-locus. Deletion of *gspD*, a key gene within the cluster, is sufficient to disable the function of the secretion system (Shi *et al.*, 2008). As expected, *gspD* deletion led to a complete loss of ferric reductase activity using the wild type as parental strain (Fig 6). In contrast to this, the ΔOMC^S Δ*gspD* (JG444) strain was not affected in Fe(III) citrate reduction, since the maximal reduction rates of ΔOMC^S and ΔOMC^S Δ*gspD* were almost identical. Only a slightly longer lag-phase of the ΔOMC^S Δ*gspD* strain was detectable, which might be due to a minimally lower initial cell number (Fig 6).

Confirmation of outer membrane integrity in ΔOMC^S

A higher permeability of the outer membrane could cause the observed phenotype of ΔOMC^S since it is known that periplasmic cytochromes can catalyze ferric iron reduction as well (Pitts *et al.*, 2003; Qian *et al.*, 2011*b*; Schuetz *et al.*, 2009). Still, outer membrane cytochromes are usually necessary since electron acceptors like Fe(III) citrate or birnessite cannot pass the outer membrane. Therefore, three tests were performed to exclude the possibility that the general stability or permeability of the outer membrane might be the reason for the observed phenotype of the ΔOMC^S-mutant. First ethidium bromide uptake rates were determined by measuring the increase in fluorescence over time. Ethidium bromide is a large, hydrophobic dye (about 12 Å wide) with a delocalized positive charge that makes it unlikely to diffuse through narrow porin channels (7 by

11 Å in *E. coli* OmpF; (Cowan *et al.*, 1992). It can therefore be used to measure permeability of the outer membrane (Murata *et al.*, 2007). The detected ethidium bromide uptake kinetics of wild type, ΔOMC, and ΔOMC^S were almost identical (Fig. S2). As a positive control, cells were treated with polymyxin B which destabilizes the outer membrane (Vaara, 1992). The ethidium bromide uptake rate increased approximately 2-fold (Fig. S2a) but was again identical in the three tested strains. A similar experiment was performed with Fe(III) citrate as a second test to exclude the possibility that more specific Fe(III) citrate transporter would cause the observed reduction phenotype. The amount of Fe(III) citrate diffusion into the cell was determined after 30 min incubation. The total cellular iron content after washing of the cells was nearly identical for all strains but increased when polymyxin B was added (Fig. S2b).

As a third test, antibiotic susceptibility of the different strains was compared using kanamycin A as an aminoglycoside, colistin as a polymixine, and chloramphenicol forming its own group of rather small reagents with an aromatic ring. As Fig. S3 indicates, the inhibitory zones around the test plates containing the antibiotic drugs are either highly similar for wild type, ΔOMC, and ΔOMC^S or even smaller for ΔOMC^S compared to the other two strains. Therefore, the results of the ethidium bromide and Fe(III) citrate uptake test were verified and it seems rather unlikely to suggest that an altered outer membrane permeability caused the observed phenotype of ΔOMC^S.

Identification of point mutations as genetic basis of ΔOMC-suppression

The genetic source of the ΔOMC^S-mutant phenotype was addressed using Solexa sequencing of the genome and mapping to the published sequence of *S. oneidensis* MR-1 (accession number NC_004347). The genome was nearly completely covered (>99.9% coverage). Analysis of the assembled Solexa reads revealed 85 point mutations but no larger insertions or rearrangements of genes (Table S2). Two of the point mutations raised our interest, since they were localized in *mtrA* and *mtrB*, respectively. In both cases, a

nucleotide base exchange from cytosine to adenosine occurred. These exchanges resulted in the replacement of an asparagine by a lysine in MtrA and MtrB, respectively (MtrA: Asn 290* Lys; MtrB: Asn 219* Lys; *Numbers refer to the amino acid sequence of MtrA and MtrB, the corresponding chromosomal positions are 1858407 and 1857606, respectively). The secondary structure of the mutated MtrB protein was predicted using PRED-TMBB (Bagos *et al.*, 2004). The mutation was found to be located in the middle of a hydrophilic stretch.

Both proteins are crucial for dissimilatory metal reduction as well as reduction of extracellular electron shuttles. Furthermore, arabinose induction was necessary for extracellular respiration in ΔOMC^S. Therefore, it was our aim to assess whether these point mutations in *mtrA* and *mtrB* caused the observed ΔOMC^S phenotype. Hence, both genes were cloned in their wild type and suppressor mutant form (designated $mtrA^S$ and $mtrB^S$) in a pBAD202 expression vector resulting in plasmids pmtrAmtrB and $pmtrA^SmtrB^S$ (Table 2). These plasmids were transferred into the parental strain ΔOMC and the resulting strains were tested for their ability to reduce Fe(III) citrate (Fig. 7). Expression of the wild type allele (strain JG450) did not lead to an alteration of the ΔOMC phenotype, but expression of the allele carrying the point mutations (strain JG449) resulted in a phenotype highly similar to ΔOMC^S (Fig. 7). Since these data demonstrated that the point mutations in $mtrA^S$ and $mtrB^S$ were essential for suppression of the ΔOMC^S mutation, it was concluded that the other observed point mutations might be interesting but of minor importance for this study.

A further question of this study was if a single mutated gene is sufficient for ferric iron reduction without outer membrane cytochromes. Therefore $mtrA^S$ and $mtrB^S$ were cloned into separate vectors resulting in $pmtrA^S$ and $pmtrB^S$ (strains JG462 and 463). Expression of both proteins could be shown by SDS-page (Fig. S4). Only $mtrB^S$ expression (strain JG463) resulted in iron reduction but on a lower level compared to ΔOMC^S or the ΔOMC

strain carrying pmtrA^{S}mtrB^S (Fig. 7). Hence, both variants, MtrA^S and MtrB^S, have to be present to enable rapid reduction of Fe(III) citrate.

Complementation of ΔmtrA and ΔmtrB mutants using *mtrA^S* and *mtrB^S*

MtrA and MtrB form a complex in the outer membrane of *S. oneidensis* cells (Hartshorne *et al.*, 2009). Furthermore, MtrA is necessary for periplasmic stability of MtrB (Schicklberger *et al.*, 2010). Since this interaction seems to be highly specific, it was asked whether the observed point mutations led to variants of the corresponding proteins that were only able to operate in the presence of the other variant. In other words, can MtrB^S only operate in an MtrA^S strain or is an interaction with wild type MtrA still possible. Consequently, *mtrA^S* and *mtrB^S* were expressed in *S. oneidensis* Δ*mtrA* and Δ*mtrB* strains, respectively. As Fig. S5 indicates, both genes can complement also the corresponding deletion mutants in a wild type background. Hence, the point mutations do not seem to be localized to positions that disable interaction with the wild typic partner proteins.

MtrAB clusters in microbial genomes

The possibility to respire extracellular electron acceptors without outer membrane cytochromes might be a strategy that is used by other microorganisms as well. Hence, it was asked whether clusters consisting of genes coding for a periplasmic decaheme cytochrome and β-barrel protein can be found in the database that are not accompanied by a gene coding for an outer membrane decaheme cytochrome like MtrF or MtrC directly upstream or downstream. Twenty-five gene clusters with similarities to *mtrAB* from *S. oneidensis* were detected using the integrated microbial genomes tool (Table 3). Six of these clusters belong to purple bacteria. One of these purple bacteria strains, *Rhodopseudomonas palustris* TIE-1, was shown to be dependent on this gene cluster when ferrous iron is added as electron donor for photolithotrophic growth (Jiao &

Newman, 2007). *PioAB* are the genes similar to *mtrAB* and they are accompanied by a gene encoding a periplasmic high potential iron protein that was suggested to enable periplasmic electron transfer between PioAB and tentatively the photosystem in the inner membrane of the organism (Bird *et al.*, 2011). The similarities between *pioABC* of *R. palustris* TIE-1 and all other *mtrAB*-like clusters in *Rhodopseudomonas* and *Rhodomicrobium* strains suggest a similar function in these purple bacteria as well. Interestingly, *Gallionella capsiferriformans* (also known as *Gallionella ferruginea*, subsp. *capsiferriformans*) and *Siderooxydans lithotrophicus* also contain an *mtrAB*-like gene cassettes. Both organisms are known to use the neutrophilic oxidation of ferrous iron with oxygen as energy source (Emerson *et al.*, 2010). Furthermore, similar clusters were detected in other organisms including nitrifiers, sulfate reducers and magnetotactic bacteria. Of note, a number of *Geobacter* strains contain similar clusters as well. Some of these clusters contain a β-barrel protein that has either low or almost no similarity to MtrB from *S. oneidensis*. It is so far not possible to ascribe a function to these gene clusters but it seems very well possible that they enable some kind of extracellular respiration, may it be either electron uptake like in the case of PioABC or electron disposal.

Discussion

Mesophilic dissimilatory metal reducers like *S. oneidensis* MR-1 have developed an extended respiratory chain to the cell surface. This respiratory chain is mainly composed of *c*-type cytochromes (Shi *et al.*, 2007). In previous work we have shown that expression of the cytoplasmic membrane *c*-type cytochrome CymA is sufficient to transform *E. coli* into a dissimilatory iron reducer. Still, this respiratory process is possible only when soluble, outer membrane permeable iron chelates like nitrilotriacetic acid complexed ferric iron (Fe(III)-NTA) are used (Gescher *et al.*, 2008). Environmentally relevant

electron acceptors like ferrihydrite, hematite or birnessite are poorly soluble or effectively insoluble at neutral pH (Thamdrup, 2000). Hence, their reduction depends on electron transfer through periplasm and outer membrane. As already mentioned in the introduction, even some chelated ferric iron sources like Fe(III) citrate are apparently not membrane permeable (Dobbin *et al.*, 1996; Gescher *et al.*, 2008; Pitts *et al.*, 2003). Large, polymeric Fe(III) citrate complexes that were observed under certain conditions might explain this effect (Spiro *et al.*, 1967). It is therefore not surprising that the catabolic reduction of Fe(III) citrate in *S. oneidensis* depends on the catalytic activity of outer membrane cytochromes. Interestingly, Qian *et al.* proposed an OMC independent iron chelate uptake mechanism catalyzed by SO_2907 and subsequent periplasmic ferric iron reduction (Qian *et al.*, 2011*a*). This would certainly challenge the assumption that Fe(III) citrate can be used as a model substance to study extracellular respiration. Nevertheless, the ΔOMC strain is unable to reduce Fe(III) citrate at detectable rates (Bücking *et al.*, 2010). Furthermore, several different laboratories demonstrated that mutants in *mtrC*, *mtrB* or *mtrA* are unable to grow with Fe(III) citrate as electron acceptor (Beliaev & Saffarini, 1998; Beliaev *et al.*, 2001; Borloo *et al.*, 2007; Hartshorne *et al.*, 2009; Myers & Myers, 2002*b*). MtrA, MtrB, and MtrC build the electron conduit to the cell surface and MtrC is probably the most influential terminal reductase for extracellular respiration in *S. oneidensis* (Belchik *et al.*, 2011; Beliaev *et al.*, 2001; Coursolle *et al.*, 2010; Jiao *et al.*, 2011; Marshall *et al.*, 2006; Reardon *et al.*, 2010). All this seems to be in disagreement to the experiments conducted by Qian *et al.* The authors found that a deletion mutant in a gene encoding a putative TonB-dependent receptor protein (SO_2907) was affected in ferric iron reduction. Still, the authors observed furthermore that the corresponding protein is an efficient Fe(III)-NTA binding protein. Hence, the observed growth phenotype might also be caused by the lack of an efficient iron acquisition protein in the outer membrane of a SO_2907 deletion mutant. Furthermore and unfortunately, the authors did not show a complementation of the mutant using

SO_2907. Hence, it is not absolutely clear whether a polar effect of the mutation also accounts at least partly for the observed growth disadvantage.

As was pointed out before, MtrC is believed to be the main terminal metal and flavin reductase. The phenotype of a *ΔmtrC* mutant can only be rescued if MtrC itself or the similar cytochrome MtrF is used for complementation (Bücking *et al.*, 2010; Myers & Myers, 2001). Hence, it came to our great surprise to see that a quintuple mutant in all outer membrane cytochrome encoding genes (ΔOMC) was able to regain its ability to grow as a dissimilatory metal reducer after a lag phase that was several weeks long. This new strain ΔOMC^S reduces Fe(III) citrate nearly as fast as the wild type in growth experiments. Interestingly, the suppressor mutant reduces extracellular electron acceptors with varying activities when compared to the wild type in cell suspension experiments. Fe(III) citrate and AQDS are reduced with rates ranging from more than 50 to 99% compared to the recorded wild type reduction rates. In contrast riboflavin, Pahokee peat humic acids, and birnessite are reduced with only 20 to 35% compared to the wild type. The different redox potentials of these compounds are unlikely to be the reason for the observed differences. Fe(III) citrate has a potential of +372 mV (Straub *et al.*, 2001) while AQDS is with -184 mV more than half a volt below this value (Fultz & Durst, 1982). Birnessite has a redox potential of +612 mV (Robie *et al.*, 1995) and is therefore an even better electron acceptor compared to Fe(III) citrate. The redox potential of riboflavin is with -210 mV (Stare, 1935) very similar to the potential of AQDS. For naturally occurring humic acids no defined redox potentials but rather ranges of standard reduction potentials from +150 to 300 mV (at pH 7) were determined (Aeschbacher *et al.*, 2011) since they form a supermolecular association of very diverse organic molecules. Still, since redox potentials are most likely not the reason for the observed kinetic data, we hypothesize that substrate specificity causes the observed differences. This substrate specificity would be determined by the terminal reductase of ΔOMC^S. Our experiments

suggest that $MtrA^S$ is the new terminal reductase in this strain. Evidence for this hypothesis comes from the results of the conducted mutant experiments. These experiments revealed (i) that no outer membrane cytochrome is involved in extracellular reduction of ΔOMC^S, (ii) that the DMSO reductase is not required as terminal reductase of Fe(III) citrate, (iii) that an export of other potential reductases via the type II secretion system is not required, and finally (iv) that $MtrA^S$ and $MtrB^S$ are both essential for extracellular reduction of ΔOMC^S. MtrB is a typical outer membrane β-barrel protein, that most probably has a structural but not an enzymatic function (Hartshorne *et al.*, 2009; Myers & Myers, 2002*a*). On the contrary, MtrA is a *c*-type cytochrome that was previously shown to have ferric iron reductase activity (Pitts *et al.*, 2003). Hence, we hypothesize that the point mutations enable $MtrA^S$ to contact electron acceptors at the cell surface, or that the pore of $MtrB^S$ is – when compared to wild type MtrB – altered in a way that allows extracellular electron acceptors to reach into the pore and hence contact $MtrA^S$. This second hypothesis would be in line with the results of the cell suspension experiments. Larger substances are reduced more slowly than smaller electron acceptors, independently of their redox potential. Riboflavin, birnessite or Pahokee peat humic acids might just be too large to reach into the pore as good as Fe(III) citrate or AQDS. Still, we cannot definitely negate the possibility that other surface localized proteins could interact with $MtrA^S$ and/or $MtrB^S$ and hence could also be involved in the observed phenotype.

Unfortunately, it is so far not possible to show how the point mutations exchanging asparagine residues by lysine residues would enable this hypothesized modified structure of the $MtrAB^S$ complex. The crystal structure of the two important proteins MtrA and MtrB is not known so far. The mutation in MtrB was predicted to localize to a hydrophilic stretch outside of the β-barrel and one could speculate that this stretch might be important for the interaction between MtrA and MtrB. The structure of MtrA was modeled recently by Firer-Sherwood and coworkers based on small-angle X-ray

scattering (Firer-Sherwood *et al.*, 2011). They proposed an elongated form of MtrA, which fits well with a partial insertion into the barrel of MtrB to form a complex. The point mutation in $MtrA^S$ is near the C-terminal region and could be embedded into MtrB.

The ability of the suppressor mutant to reduce extracellular electron acceptors without outer membrane cytochromes raises the question whether this suppressor mutant resembles an evolutionary intermediate. The correct localization of outer membrane cytochromes is a complex process. Lipid anchors have to be added to periplasmic cytochromes. These modified cytochromes have to be recognized by the type II secretion machinery. This machinery is a multiprotein complex itself but furthermore the interaction with target proteins is highly specific and still not fully understood (Francetic & Pugsley, 2005; Sandkvist, 2001). Last but not least, these outer membrane cytochromes have to be connected to modules like MtrAB that thereafter can deliver electrons originating from the cytoplasmic membrane. Due to this complexity it seems likely that the addition of outer membrane cytochromes to existing outer membrane conduits might be a typical example of upstream evolution. We could show that extracellular metal respiration can be possible without outer membrane cytochromes but the environment might have finally selected for organisms with higher reduction rates that were realized by outer membrane cytochromes. Interestingly, bioinformatic research revealed similarities to known ferrous iron oxidizers like the chemolithotrophs *G. capsiferriformans* and *S. lithotrophicus* or the photolithotrophic purple bacterium *R. palustris* TIE-1. For *R. palustris* TIE-1 and *S. lithotrophicus* ES-1 it is known that genes similar to MtrAB are necessary for ferrous iron oxidation (Jiao & Newman, 2007; Liu *et al.*, 2012). For the latter one it was shown that a MtoA from *S. lithotrophicus* can functionally replace MtrA in *Shewanella* (Liu *et al.*, 2012). One could envision a succession from a module necessary for ferrous iron oxidation in one species to a module that is necessary for the reverse reaction in another species. Of note, there might be

further metabolic processes that depend on MtrAB-like complexes since similar gene clusters were also detected in other organisms. Future research will reveal their role in the individual organisms.

Finally, it should be mentioned that the studied suppressor mutant nicely displays the plasticity of *S. oneidensis*. In a previous publication a similar case was observed but not followed. Myers *et al.* could show in their experiments that a *ΔmtrC*-mutant was capable of reducing Fe(III) citrate after a three days lag phase (Myers & Myers, 2002*b*). The cells that were growing after 72 h might have been suppressor mutants as well. What we can learn is that the results of mutant studies have to be treated carefully at least in *S. oneidensis*. The shorter the duration of an experiment is, the more one can exclude the possibility that the observed phenotype might not be due to the inserted genetic modification but to a suppressor mutation. Therefore, Fe(III) citrate seems to be a good model substance to study extracellular electron transport pathways since it allows fast growth and reduction rates when compared to mineral phase electron acceptors like ferrihydrite or hematite.

In conclusion, this study characterizes for the first time MtrA and MtrB as a final reductase necessary for extracellular respiration. Only two point mutations were necessary to gain this activity. It seems possible that this form of dissimilatory metal reduction resembles a premature form which might have been an intermediate state between a lithotrophic ferrous iron oxidization and heterotrophic ferric iron respiration.

References

Aeschbacher, M., Vergari, D., Schwarzenbach, R. P. & Sander, M. (2011). Electrochemical analysis of proton and electron transfer equilibria of the reducible moieties in humic acids. *Environ Sci Technol* **45**, 8385-8394.

Bagos, P. G., Liakopoulos, T. D., Spyropoulos, I. C. & Hamodrakas, S. J. (2004). A Hidden Markov Model method, capable of predicting and discriminating β-barrel outer membrane proteins. *BMC Bioinformatics* **5**, 29.

Bayer, M., Walter, K. & Simon, H. (1996). Purification and partial characterisation of a reversible artificial mediator accepting NADH oxidoreductase from Clostridium thermoaceticum. *Eur J Biochem* **239**, 686-691.

Belchik, S. M., Kennedy, D. W., Dohnalkova, A. C., Wang, Y., Sevinc, P. C., Wu, H., Lin, Y., Lu, H. P., Fredrickson, J. K. & other authors (2011). Extracellular reduction of hexavalent chromium by cytochromes MtrC and OmcA of *Shewanella oneidensis* MR-1. *Appl Environ Microbiol* **77**, 4035-4041.

Beliaev, A. S. & Saffarini, D. A. (1998). *Shewanella putrefaciens mtrB* encodes an outer membrane protein required for Fe(III) and Mn(IV) reduction. *J Bacteriol* **180**, 6292-6297.

Beliaev, A. S., Saffarini, D. A., McLaughlin, J. L. & Hunnicutt, D. (2001). MtrC, an outer membrane decahaem *c* cytochrome required for metal reduction in *Shewanella putrefaciens* MR-1. *Mol Microbiol* **39**, 722-730.

Bird, L. J., Bonnefoy, V. & Newman, D. K. (2011). Bioenergetic challenges of microbial iron metabolisms. *Trends Microbiol* **19**, 330-340.

Boogerd, F. C. & de Vrind, J. P. (1987). Manganese oxidation by *Leptothrix discophora*. *J Bacteriol* **169**, 489-494.

Borloo, J., Vergauwen, B., De Smet, L., Brige, A., Motte, B., Devreese, B. & Van Beeumen, J. (2007). A kinetic approach to the dependence of dissimilatory metal reduction by *Shewanella oneidensis* MR-1 on the outer membrane cytochromes *c* OmcA and OmcB. *FEBS* **274**, 3728-3738.

Bradford, M. M. (1976). A rapid and sensitive method for the quantitation of microgram quantities of protein utilizing the principle of protein-dye binding. *Anal Biochem* **72**, 248-254.

Bücking, C., Popp, F., Kerzenmacher, S. & Gescher, J. (2010). Involvement and specificity of *Shewanella oneidensis* outer membrane cytochromes in the reduction of soluble and solid-phase terminal electron acceptors. *FEMS Microbiol Lett* **306**, 144-151.

Burdige, D. J. & Nealson, K. H. (1985). Microbial manganese reduction by enrichment cultures from coastal marine sediments. *Appl Environ Microbiol* **50**, 491-497.

Coursolle, D. & Gralnick, J. A. (2010). Modularity of the Mtr respiratory pathway of *Shewanella oneidensis* strain MR-1. *Mol Microbiol* **77**, 995-1008.

Coursolle, D., Baron, D. B., Bond, D. R. & Gralnick, J. A. (2010). The Mtr respiratory pathway is essential for reducing flavins and electrodes in *Shewanella oneidensis*. *J Bacteriol* **192**, 467-474.

Cowan, S. W., Schirmer, T., Rummel, G., Steiert, M., Ghosh, R., Pauptit, R. A., Jansonius, J. N. & Rosenbusch, J. P. (1992). Crystal structures explain functional properties of two *E. coli* porins. *Nature* **358**, 727-733.

DiChristina, T. J., Moore, C. M. & Haller, C. A. (2002). Dissimilatory Fe(III) and Mn(IV) reduction by *Shewanella putrefaciens* requires *ferE*, a homolog of the *pulE* (*gspE*) type II protein secretion gene. *J Bacteriol* **184**, 142-151.

Dobbin, P. S., Warren, L. H., Cook, N. J., McEwan, A. G., Powell, A. K. & Richardson, D. J. (1996). Dissimilatory iron(III) reduction by *Rhodobacter capsulatus*. *Microbiology* **142**, 765-774.

El-Naggar, M. Y., Wanger, G., Leung, K. M., Yuzvinsky, T. D., Southam, G., Yang, J., Lau, W. M., Nealson, K. H. & Gorby, Y. A. (2010). Electrical transport along bacterial nanowires from *Shewanella oneidensis* MR-1. *Proc Natl Acad Sci U S A* **107**, 18127-18131.

Emerson, D., Fleming, E. J. & McBeth, J. M. (2010). Iron-oxidizing bacteria: an environmental and genomic perspective. *Annu Rev Microbiol* **64**, 561-583.

Firer-Sherwood, M. A., Ando, N., Drennan, C. L. & Elliott, S. J. (2011). Solution-based structural analysis of the decaheme cytochrome, MtrA, by small angle X-ray sand analytical ultracentrifugation. *J Phys Chem B* **115**, 11208-11214.

Francetic, O. & Pugsley, A. P. (2005). Towards the identification of type II secretion signals in a nonacylated variant of pullulanase from *Klebsiella oxytoca*. *J Bacteriol* **187**, 7045-7055.

Fultz, M. L. & Durst, R. A. (1982). Mediator compounds for the electrochemical study of biological redox systems - a compilation. *Anal Chim Acta* **140**, 1-18.

Gescher, J. S., Cordova, C. D. & Spormann, A. M. (2008). Dissimilatory iron reduction in *Escherichia coli*: identification of CymA of *Shewanella oneidensis* and NapC of *E. coli* as ferric reductases. *Mol Microbiol* **68**, 706-719.

Gibson, D. G., Young, L., Chuang, R. Y., Venter, J. C., Hutchison, C. A. & Smith, H. O. (2009). Enzymatic assembly of DNA molecules up to several hundred kilobases. *Nature Methods* **6**, 343-U341.

Gorby, Y. A., Yanina, S., McLean, J. S., Rosso, K. M., Moyles, D., Dohnalkova, A., Beveridge, T. J., Chang, I. S., Kim, B. H. & other authors (2006). Electrically conductive bacterial nanowires produced by *Shewanella oneidensis* strain MR-1 and other microorganisms. *Proc Natl Acad Sci U S A* **103**, 11358-11363.

Gralnick, J. A., Vali, H., Lies, D. P. & Newman, D. K. (2006). Extracellular respiration of dimethyl sulfoxide by *Shewanella oneidensis* strain MR-1. *Proc Natl Acad Sci U S A* **103**, 4669-4674.

Hartshorne, R. S., Reardon, C. L., Ross, D., Nuester, J., Clarke, T. A., Gates, A. J., Mills, P. C., Fredrickson, J. K., Zachara, J. M. & other authors (2009). Characterization of an electron conduit between bacteria and the extracellular environment. *Proc Natl Acad Sci U S A* **106**, 22169-22174.

Jiang, J. & Kappler, A. (2008). Kinetics of microbial and chemical reduction of humic substances: implications for electron shuttling. *Environ Sci Technol* **42**, 3563-3569.

Jiao, Y. & Newman, D. K. (2007). The *pio* operon is essential for phototrophic Fe(II) oxidation in *Rhodopseudomonas palustris* TIE-1. *J Bacteriol* **189**, 1765-1773.

Jiao, Y., Qian, F., Li, Y., Wang, G., Saltikov, C. W. & Gralnick, J. A. (2011). Deciphering the electron transport pathway for graphene oxide reduction by *Shewanella oneidensis* MR-1. *J Bacteriol* **193**, 3662-3665.

Laemmli, U. K. (1970). Cleavage of structural proteins during the assembly of the head of bacteriophage T4. *Nature* **227**, 680-685.

Li, H. & Durbin, R. (2009). Fast and accurate short read alignment with Burrows-Wheeler transform. *Bioinformatics* **25**, 1754-1760.

Li, H., Handsaker, B., Wysoker, A., Fennell, T., Ruan, J., Homer, N., Marth, G., Abecasis, G., Durbin, R. & other authors (2009). The sequence alignment/map format and SAMtools. *Bioinformatics* **25**, 2078-2079.

Liu, J., Wang, Z., Belchik, S. M., Edwards, M. J., Liu, C., Kennedy, D. W., Merkley, E. D., Lipton, M. S., Butt, J. N. & other authors (2012). Identification and

characterization of MtoA: a decaheme *c*-type cytochrome of the neutrophilic Fe(II)-oxidizing bacterium *Sideroxydans lithotrophicus* ES-1. *Front Microbio* **3**.

Lovley, D. R., Coates, J. D., BluntHarris, E. L., Phillips, E. J. P. & Woodward, J. C. (1996). Humic substances as electron acceptors for microbial respiration. *Nature* **382**, 445-448.

Lower, B. H., Yongsunthon, R., Shi, L., Wildling, L., Gruber, H. J., Wigginton, N. S., Reardon, C. L., Pinchuk, G. E., Droubay, T. C. & other authors (2009). Antibody recognition force microscopy shows that outer membrane cytochromes OmcA and MtrC are expressed on the exterior surface of *Shewanella oneidensis* MR-1. *Appl Environ Microbiol* **75**, 2931-2935.

Lutz, R. & Bujard, H. (1997). Independent and tight regulation of transcriptional units in *Escherichia coli* via the LacR/O, the TetR/O and AraC/I1-I2 regulatory elements. *Nucleic Acids Res* **25**, 1203-1210.

Marshall, M. J., Beliaev, A. S., Dohnalkova, A. C., Kennedy, D. W., Shi, L., Wang, Z., Boyanov, M. I., Lai, B., Kemner, K. M. & other authors (2006). *c*-Type cytochrome-dependent formation of U(IV) nanoparticles by *Shewanella oneidensis*. *PLoS Biol* **4**, e268.

Marsili, E., Baron, D. B., Shikhare, I. D., Coursolle, D., Gralnick, J. A. & Bond, D. R. (2008). *Shewanella* secretes flavins that mediate extracellular electron transfer. *Proc Natl Acad Sci U S A* **105**, 3968-3973.

Meyer, T. E., Tsapin, A. I., Vandenberghe, I., de Smet, L., Frishman, D., Nealson, K. H., Cusanovich, M. A. & van Beeumen, J. J. (2004). Identification of 42 possible cytochrome *c* genes in the *Shewanella oneidensis* genome and characterization of six soluble cytochromes. *Omics* **8**, 57-77.

Milne, I., Bayer, M., Cardle, L., Shaw, P., Stephen, G., Wright, F. & Marshall, D. (2010). Tablet-next generation sequence assembly visualization. *Bioinformatics* **26**, 401-402.

Murata, T., Tseng, W., Guina, T., Miller, S. I. & Nikaido, H. (2007). PhoPQ-mediated regulation produces a more robust permeability barrier in the outer membrane of *Salmonella enterica* serovar typhimurium. *J Bacteriol* **189**, 7213-7222.

Myers, C. R. & Nealson, K. H. (1988*a*). Bacterial manganese reduction and growth with manganese oxide as the sole electron-acceptor. *Science* **240**, 1319-1321.

Myers, C. R. & Nealson, K. H. (1988*b*). Microbial reduction of manganese oxides: Interactions with iron and sulfur. *Geochim Cosmochim Acta* **52**, 2727-2732.

Myers, C. R. & Myers, J. M. (2002*a*). MtrB is required for proper incorporation of the cytochromes OmcA and OmcB into the outer membrane of *Shewanella putrefaciens* MR-1. *Appl Environ Microbiol* **68**, 5585-5594.

Myers, J. M. & Myers, C. R. (2001). Role for outer membrane cytochromes OmcA and OmcB of *Shewanella putrefaciens* MR-1 in reduction of manganese dioxide. *Appl Environ Microbiol* **67**, 260-269.

Myers, J. M. & Myers, C. R. (2002*b*). Genetic complementation of an outer membrane cytochrome *omcB* mutant of *Shewanella putrefaciens* MR-1 requires *omcB* plus downstream DNA. *Appl Environ Microbiol* **68**, 2781-2793.

Myers, J. M. & Myers, C. R. (2003). Overlapping role of the outer membrane cytochromes of *Shewanella oneidensis* MR-1 in the reduction of manganese(IV) oxide. *Lett Appl Microbiol* **37**, 21-25.

Pitts, K. E., Dobbin, P. S., Reyes-Ramirez, F., Thomson, A. J., Richardson, D. J. & Seward, H. E. (2003). Characterization of the *Shewanella oneidensis* MR-1 decaheme cytochrome MtrA: expression in Escherichia coli confers the ability to reduce soluble Fe(III) chelates. *J Biol Chem* **278**, 27758-27765.

Qian, Y., Shi, L. & Tien, M. (2011*a*). SO2907, A putative TonB-dependent receptor, is

involved in dissimilatory iron reduction by *Shewanella oneidensis* MR-1. *J Biol Chem* **286**, 33973-33980.

Qian, Y., Paquete, C. M., Louro, R. O., Ross, D. E., Labelle, E., Bond, D. R. & Tien, M. (2011*b*). Mapping the iron binding site(s) on the small tetraheme cytochrome of *Shewanella oneidensis* MR-1. *Biochemistry-Us* **50**, 6217-6224.

Reardon, C. L., Dohnalkova, A. C., Nachimuthu, P., Kennedy, D. W., Saffarini, D. A., Arey, B. W., Shi, L., Wang, Z., Moore, D. & other authors (2010). Role of outer-membrane cytochromes MtrC and OmcA in the biomineralization of ferrihydrite by *Shewanella oneidensis* MR-1. *Geobiology* **8**, 56-68.

Reguera, G., McCarthy, K. D., Mehta, T., Nicoll, J. S., Tuominen, M. T. & Lovley, D. R. (2005). Extracellular electron transfer via microbial nanowires. *Nature* **435**, 1098-1101.

Richter, K., Bücking, C., Schicklberger, M. & Gescher, J. (2010). A simple and fast method to analyze the orientation of *c*-type cytochromes in the outer membrane of Gram-negative bacteria. *J Microbiol Methods* **82**, 184-186.

Robie, R. A., Huebner, J. S. & Hemingway, B. S. (1995). Heat-capacities and thermodynamic properties of braunite (Mn_7SiO_{12}) and rhodonite ($MnSiO_3$). *Am Mineral* **80**, 560-575.

Roden, E. E., Kappler, A., Bauer, I., Jiang, J., Paul, A., Stoesser, R., Konishi, H. & Xu, H. (2010). Extracellular electron transfer through microbial reduction of solid-phase humic substances. *Nat Geosci* **3**, 417-421.

Romine, M. F., Carlson, T. S., Norbeck, A. D., McCue, L. A. & Lipton, M. S. (2008). Identification of mobile elements and pseudogenes in the *Shewanella oneidensis* MR-1 genome. *Appl Environ Microbiol* **74**, 3257-3265.

Ross, D. E., Brantley, S. L. & Tien, M. (2009). Kinetic characterization of terminal reductases OmcA and MtrC involved in respiratory electron transfer for dissimilatory iron reduction in *Shewanella oneidensis* MR-1. *Appl Environ Microbiol* **75**, 5218-5226.

Saltikov, C. W. & Newman, D. K. (2003). Genetic identification of a respiratory arsenate reductase. *Proc Natl Acad Sci U S A* **100**, 10983-10988.

Sandkvist, M. (2001). Biology of type II secretion. *Mol Microbiol* **40**, 271-283.

Schicklberger, M., Bücking, C., Schuetz, B., Heide, H. & Gescher, J. (2010). Involvement of the *Shewanella oneidensis* decaheme cytochrome MtrA in the periplasmic stability of the beta-barrel protein MtrB. *Appl Environ Microbiol* **77**, 1520-1523.

Schuetz, B., Schicklberger, M., Kuermann, J., Spormann, A. M. & Gescher, J. (2009). Periplasmic electron transfer via the *c*-type cytochromes MtrA and FccA of *Shewanella oneidensis* MR-1. *Appl Environ Microbiol* **75**, 7789-7796.

Shanks, R. M., Caiazza, N. C., Hinsa, S. M., Toutain, C. M. & O'Toole, G. A. (2006). *Saccharomyces cerevisiae*-based molecular tool kit for manipulation of genes from gram-negative bacteria. *Appl Environ Microbiol* **72**, 5027-5036.

Shi, L., Squier, T. C., Zachara, J. M. & Fredrickson, J. K. (2007). Respiration of metal (hydr)oxides by *Shewanella* and *Geobacter*: a key role for multihaem *c*-type cytochromes. *Mol Microbiol* **65**, 12-20.

Shi, L., Deng, S., Marshall, M. J., Wang, Z., Kennedy, D. W., Dohnalkova, A. C., Mottaz, H. M., Hill, E. A., Gorby, Y. A. & other authors (2008). Direct involvement of type II secretion system in extracellular translocation of *Shewanella oneidensis* outer membrane cytochromes MtrC and OmcA. *J Bacteriol* **190**, 5512-5516.

Shi, L., Chen, B., Wang, Z., Elias, D. A., Mayer, M. U., Gorby, Y. A., Ni, S., Lower, B. H., Kennedy, D. W. & other authors (2006). Isolation of a high-affinity functional

protein complex between OmcA and MtrC: Two outer membrane decaheme c-type cytochromes of *Shewanella oneidensis* MR-1. *J Bacteriol* **188**, 4705-4714.

Shyu, J. B., Lies, D. P. & Newman, D. K. (2002). Protective role of *tolC* in efflux of the electron shuttle anthraquinone-2,6-disulfonate. *J Bacteriol* **184**, 1806-1810.

Spiro, T. G., Pape, L. & Saltman, P. (1967). Hydrolytic polymerization of ferric citrate .I. Chemistry of polymer. *J Am Chem Soc* **89**, 5555-5559.

Stare, F. J. (1935). A potentiometric study of hepatoflavin. *J Biol Chem* **112**, 223-229.

Stevenson, F. (1994). *Humus chemistry : genesis, composition, reactions*. New York: Wiley.

Stookey, L. L. (1970). Ferrozine - a new spectrophotometric reagent for iron. *Anal Chem* **42**.

Straub, K. L., Benz, M. & Schink, B. (2001). Iron metabolism in anoxic environments at near neutral pH. *FEMS Microbiol Ecol* **34**, 181-186.

Thamdrup, B. (2000). Bacterial manganese and iron reduction in aquatic sediments. *Adv Microb Ecol* **16**, 41-84.

Thomas, P. E., Ryan, D. & Levin, W. (1976). An improved staining procedure for the detection of the peroxidase activity of cytochrome P-450 on sodium dodecyl sulfate polyacrylamide gels. *Anal Biochem* **75**, 168-176.

Vaara, M. (1992). Agents that increase the permeability of the outer membrane. *Microbiol Rev* **56**, 395-411.

Venkateswaran, K., Moser, D. P., Dollhopf, M. E., Lies, D. P., Saffarini, D. A., MacGregor, B. J., Ringelberg, D. B., White, D. C., Nishijima, M. & other authors (1999). Polyphasic taxonomy of the genus *Shewanella* and description of *Shewanella oneidensis* sp. nov. *Int J Syst Bacteriol* **49 Pt 2**, 705-724.

von Canstein, H., Ogawa, J., Shimizu, S. & Lloyd, J. R. (2008). Secretion of flavins by *Shewanella* species and their role in extracellular electron transfer. *Appl Environ Microbiol* **74**, 615-623.

Xiong, Y., Shi, L., Chen, B., Mayer, M. U., Lower, B. H., Londer, Y., Bose, S., Hochella, M. F., Fredrickson, J. K. & other authors (2006). High-affinity binding and direct electron transfer to solid metals by the *Shewanella oneidensis* MR-1 outer membrane c-type cytochrome OmcA. *J Am Chem Soc* **128**, 13978-13979.

Zhang, H., Tang, X., Munske, G. R., Zakharova, N., Yang, L., Zheng, C., Wolff, M. A., Tolic, N., Anderson, G. A. & other authors (2008). In vivo identification of the outer membrane protein OmcA-MtrC interaction network in *Shewanella oneidensis* MR-1 cells using novel hydrophobic chemical cross-linkers. *J Proteome Res* **7**, 1712-1720.

Tables

Table 1: Yeast and bacterial strains used in this study.

Strain No.	***Strain***	***Relevant genotype***	***Source or Reference***
JG98	*E. coli* WM3064	*thrB1004 pro thirpsLhsdS lacZΔM15 RP4–1360 Δ(araBAD)567 ΔdapA1341::[ermpir(wt)]*	(Saltikov & Newman, 2003)
JG22	*E. coli* DH5α Z1	*aci^{q}, PN25-tetR, Sp^{R}, deoR, supE44, Δ(lacZYA-argFV169), Φ80 lacZ ΔM15*	(Lutz & Bujard, 1997)
JG26	*S. cerevisiae* InvSc1	*MATa/MATα leu2/leu2 trp1-289/trp1-289 ura3-52/ura3-52 his3-Δ1/his3-Δ1*	Invitrogen
JG7	*S. oneidensis* MR-1	wild type	(Venkateswaran *et al.*, 1999)
JG132	*S. oneidensis* MR-1 ΔOMC (OM cytochrome deletion mutant)	Δ(*mtrD-mtrC*) ΔSO_2931 ΔSO_1659, 3100633:: (araC, P_{BAD})	(Bücking *et al.*, 2010)
JG12	*S. oneidensis* MR-1 ΔOMC^{S} (suppressor of outer membrane cytochrome deletion mutant)	ΔOMC *mtrA*: position 869 C to A, *mtrB*: position 656 C to A	This study

JG202	*E. coli* WM3064 pMQ150ΔgspD	pMQ150ΔdgspD	This study
JG411	*E. coli* WM3064 pMQ150ΔdmsA-1 dmsB-1	pMQ150ΔdmsA-1 dmsB-1	This study
JG305	*E. coli* WM3064 pMQ150 ΔdmsA-2 dmsB-2	pMQ150ΔdmsA-2 dmsB-2	This study
JG450	*S. oneidensis* MR-1 ΔOMCpmtrA mtrB	pmtrAmtrB	This study
JG462	*S. oneidensis* MR-1 ΔOMC $pmtrA^S$	$pmtrA^S$	This study
JG463	*S. oneidensis* MR-1 ΔOMC $pmtrB^S$	$pmtrB^S$	This study
JG449	*S. oneidensis* MR-1 ΔOMC $pmtrA^S mtrB^S$	$pmtrA^S mtrB^S$	This study
JG434	*S. oneidensis* MR-1 ΔOMC^S ΔdmsA-1 ΔdmsB-1 ΔdmsA-2 ΔdmsB-2	ΔOMC^S ΔdmsA-1 ΔdmsB-1 ΔdmsA-2 ΔdmsB-2	This study
JG444	*S. oneidensis* MR-1 ΔOMC^SΔgspD	ΔOMC^SΔgspD	This study

JG443	*S. oneidensis* MR-1	ΔgspD	This study
JG52	*S. oneidensis* MR-1 ΔmtrA	ΔmtrA	(Schuetz *et al.*, 2009)
JG55	*S. oneidensis* MR-1 ΔmtrB	ΔmtrB	(Schuetz *et al.*, 2009)
JG468	*S. oneidensis* MR-1 ΔmtrA pmtrA^{S}	ΔmtrA pmtrA^{S}	This study
JG469	*S. oneidensis* MR-1 ΔmtrB pmtrB^{S}	ΔmtrB pmtrB^{S}	This study
JG474	*S. oneidensis* MR-1 ΔOMC^{S} pmtrAmtrB^{S}	ΔOMC^{S} pmtrAmtrB^{S}	This study

1

2 Table 2: Plasmids used in this study.

Plasmid	***Relevant genotype***	***Source or Reference***
pBAD202	Expression vector, Km^{r}, arabinose inducible promoter	Invitrogen
pMQ150	Deletion vector, cen/arsh, *ura3*, Km^{r}, *sacB*	(Shanks *et al.*, 2006), accession no.: EU546823
pmtrA^{S}	*mtrA* with nucleic base exchange C869A in	This study

	pBAD202	
pmtrB^{S}	*mtrB* with nucleic base exchange C656A in pBAD202	This study
pmtrAmtrB	*mtrA* and *mtrB* in pBAD202	This study
pmtrA^{S}mtrB^{S}	*mtrA* C869A and *mtrB* C656A in pBAD202	This study
pmtrAmtrB^{S}	*mtrA* and *mtrB* C656A in pBAD202	This study

1

2

3

1 Table 3: Gene clusters with similarities to *mtrAB* from *S. oneidensis.*

Genome	MtrA-homologue	Expected value	Number of amino acid residues	MtrB-homologue	Expected value	Number of amino acid residues	Gene upstream of MtrA homologue	Size of intergenic region before MtrA	function of gene upstream of MtrA
Desulfobacterium autotrophicum HRM2	HRM2_13960	4E-44	323	HRM2_13950	/[1]	583	HRM2_13970	466 bp	[3]dicarboxylate transporter protein
Desulfuromonas acetoxidans DSM 684	Dace_1556	9E-43	354	Dace_1557	/[1]	805	not sequenced	not sequenced	unknown
Gallionella capsiferriformans ES-2	Galf_2004	2E-63	343	Galf_2003	1E-23	792	Galf_2005	69 bp	[2]cytochrome c class I (very small 112aa)
Geobacter bemidjiensis Bem, DSM 16622	Gbem_3118	4E-38	334	Gbem_3117	/[1]	718	Gbem_3119	1 bp	ABC transporter related protein
Geobacter sp. FRC-32	Geob_2912	3E-39	331	Geob_2911	/[1]	701	Geob_2913	1 bp	ABC transporter related
Geobacter sp. M18 (a)	GM18_0932	2E-08	192	GM18_0933	/[1]	660	GM18_0931	60 bp	NHL repeat containing protein
Geobacter sp. M18 (b)	GM18_1019	3E-07	192	GM18_1020	/[1]	653	GM18_1018	18 bp	NHL repeat containing protein
Geobacter sp. M18 (c)	GM18_3089	1E-42	340	GM18_3088	/[1]	762	GM18_3090	1 bp	ABC transporter-like protein
Geobacter sp. M21 (a)	GM21_0397	7E-66	299	GM21_0398	3E-16	807	GM21_0396	367 bp	transcriptional regulator,
Geobacter sp. M21 (b)	GM21_1144	3E-44	334	GM21_1145	/[1]	716	GM21_1143	1 bp	ABC transporter related
Geobacter uraniireducens Rf4 (a)	Gura_2291	7E-46	335	Gura_2290	/[1]	712	Gura_2292	1 bp	ABC transporter related
Geobacter uraniireducens Rf4 (b)	Gura_3626	1E-61	299	Gura_3627	1E-17	835	Gura_3625	486 bp	transcriptional regulator
Magnetospirillum magneticum AMB-1	amb3017	6E-63	318	amb3018	2E-21	731	amb3016	3 bp	hypothetic
Nitrosococcus halophilus Nc4 (a)	Nhal_1192	7E-59	325	Nhal_1191	2E-21	827	[3]Nhal_1193	38 bp	NUDIX hydrolase

[1] These genes are predicted to code for β-barrel proteins (http://biophysics.biol.uoa.gr/PRED-TMBB/) but the E value of BLAST search against MtrB is above 1E-5.
[2] These proteins are not predicted to be lipoproteins by LipoP (http://www.cbs.dtu.dk/services/LipoP/).
[3] These genes are encoded in the opposite direction to *mtrA.*
(a)/(b)/(c) These genomes contain two or more MtrAB homologues.

Genome	MtrA-homologue	Expected value	Number of amino acid residues	MtrB-homologue	Expected value	Number of amino acid residues	Gene upstream of MtrA homologue	Size of intergenic region before MtrA	function of gene upstream of MtrA
Nitrosococcus halophilus Nc4 (b)	Nhal_1655	1E-76	312	Nhal_1654	1E-75	755	Nhal_1656	75 bp	Peptidoglycan-binding LysM
Nitrosococcus oceani AFC27	NOC27_2654	7E-45	168	NOC27_3054	1E-07	461	NOC27_2862	51 bp	hypothetic
Nitrosococcus oceani ATCC19707	Noc_2748	/[1]	315	Noc_2747	2E-27	827	Noc_2749	44 bp	[3]NUDIX hydrolase
Rhodomicrobium vannielii ATCC 17100	Rvan_3213	2E-48	476	Rvan_3214	2E-06	844	Rvan_3212	468 bp	exonuclease RecJ
Rhodopseudomonas palustris BisA53	RPE_0831	9E-49	632	RPE_0832	2E-13	793	RPE_0830	754 bp	alpha/beta hydrolase
Rhodopseudomonas palustris BisB18	RPC_2960	1E-45	577	RPC_2959	1E-14	830	[3]RPC_2961	545 bp	putative flavoprotein involved in K+ transport
Rhodopseudomonas palustris CGA009	RPA0746	5E-48	534	RPA0745	1E-08	810	cysA	775 bp	cysA, putative sulfate ABC transporter
Rhodopseudomonas palustris DX-1	Rpdx1_0796	7E-48	548	Rpdx1_0795	2E-11	810	Rpdx1_0797	548 bp	sulfate ABC transporter ATPase subunit
Rhodopseudomonas palustris TIE-1	Rpal_0817	4E-48	540	Rpal_0816	2E-08	810	Rpal_0818	742 bp	sulfate ABC transporter, ATPase subunit
Sideroxydans lithotrophicus ES-1	Slit_2497	4E-57	355	Slit_2496	2E-20	810	Slit_2498	45 bp	[1]cytochrome c class I (very small 117aa)
Sutterella wadsworthensis	HMPREF9464_01980	1E-49	293	HMPREF9464_01981	/[1]	637	HMPREF9464_01979	506 bp	[3]hypothetic
Shewanella oneidensis MR-1	**SO_1777**		**333**	**SO_1776**		**697**	**mtrC**	**69 bp**	**decaheme c-type cytochrome (671 aa)**

1

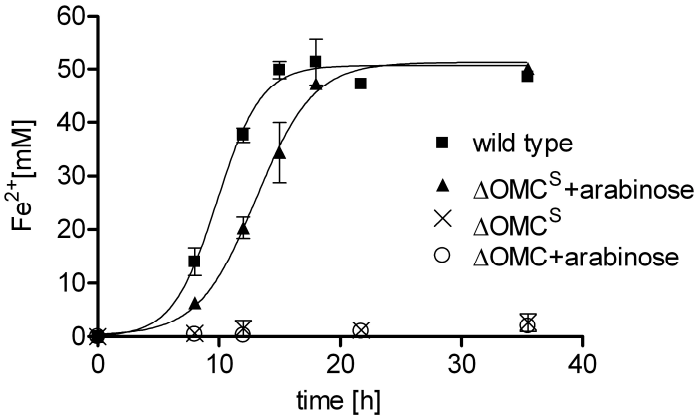

strain	**specific iron reduction rate μ in [h^{-1}]**
wild type	0.534±0.045
ΔOMC^S+arabinose	0.451±0.104
ΔOMC^S	not determinable*
ΔOMC+arabinose	not determinable*

Figure 1: Fe(III)-citrate reduction. Iron reduction by *S. oneidensis* strains growing on minimal medium with 50 mM lactate and 50 mM Fe(III)-citrate and addition of 1 mM arabinose if indicated. Symbols refer to means of triplicate measurements, error bars indicate standard deviation. Solid line represents a curve-fit done with GraphPad Prism 4. Specific iron reduction rate was calculated for each biological replicate; means and standard deviation are indicated. *Reduction rates were not determinable because curve-fit was not possible due to minimal reduction within timeframe of the experiment.

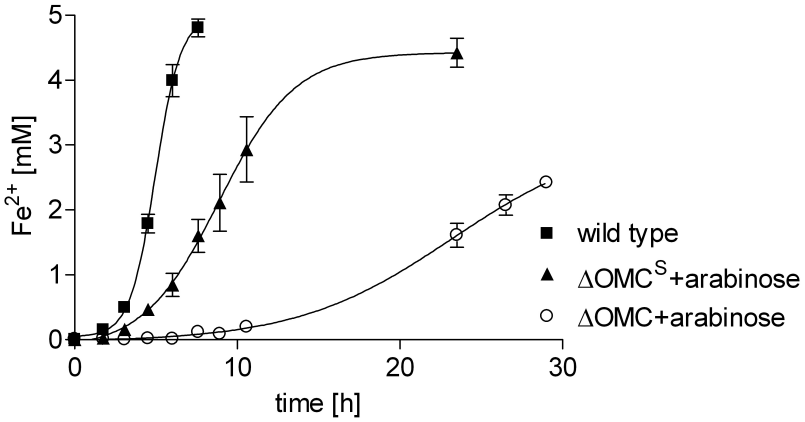

strain	**specific iron reduction rate μ in [h^{-1}]**
wild type	1.3±0.165
ΔOMC^{S}+arabinose	0.438±0.081
ΔOMC+arabinose	0.209±0.03

Figure 2: Fe(III)-NTA reduction. Iron reduction by *S. oneidensis* strains growing on minimal medium with 10 mM lactate and 5 mM Fe(III)-NTA and addition of 1 mM. Symbols refer to means of triplicate measurements, error bars indicate standard deviation. Solid line represents a curve-fit done with GraphPad Prism 4. Specific iron reduction rate was calculated for each biological replicate; means and standard deviation are indicated.

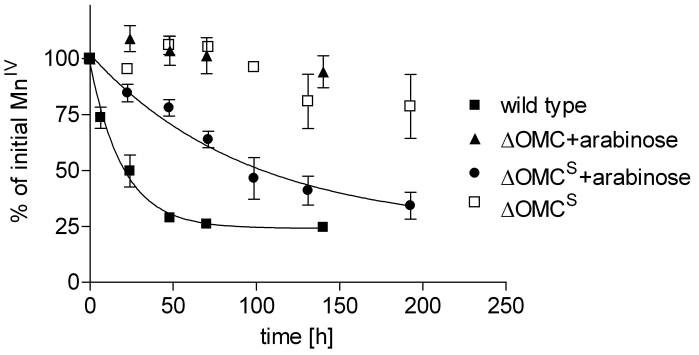

strain	**specific birnessite reduction rate μ in [h^{-1}]**
wild type	0.051±0.008
ΔOMC^S+arabinose	not determinable
ΔOMC^S	0.008±0.002
ΔOMC+arabinose	not determinable*

Figure 3: Birnessite reduction. Manganese reduction was quantified in growth experiments. Birnessite (2.5 mM) was added to 50 ml mineral medium with lactate as an electron donor and 1 mM arabinose if indicated. Percentage [Mn^{IV}] is relative to the starting concentration. Initial values for [Mn^{IV}] varied slightly (±0.266mM) and were therefore set to 100%. Abiotic decrease in the measurable [Mn^{IV}] (probably due to adhesion to the culture flask) was subtracted. Symbols refer to means of triplicate measurements, error bars indicate standard deviation. Solid line represents a curve-fit done with GraphPad Prism 4. The specific [Mn^{IV}] reduction rate was calculated for each biological replicate; means and standard deviation are indicated. *Reduction rates were not determinable because curve-fit was not possible due to minimal reduction within timeframe of the experiment.

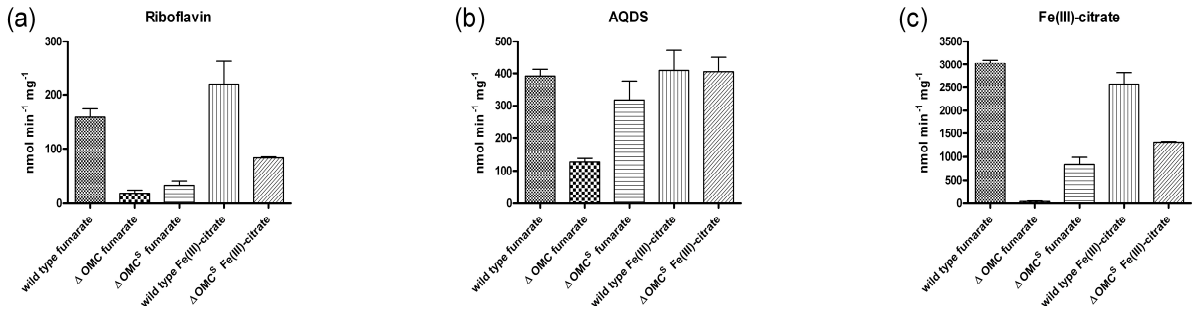

Figure 4: Cell suspension experiments. Reduction rates of *S. oneidensis* wild type, ΔOMC mutant, and ΔOMC^S mutant strains with riboflavin, AQDS, and Fe(III)-citrate. Washed cell suspensions were prepared from cultures grown under anoxic conditions with fumarate or Fe(III)-citrate as terminal electron acceptor. All experiments were carried out under anoxic conditions. Maximal reduction rates (means of triplicate measurements) were normalized to the protein content. The reduction of riboflavin (a) and AQDS (b) was measured in a continous spectrophotometric assay using absorption maxima at 450 nm and 436 nm, respectively. Fe(III)-citrate reduction rates (c) were measured by determining Fe(II) content discontinuously using the ferrozine reagent.

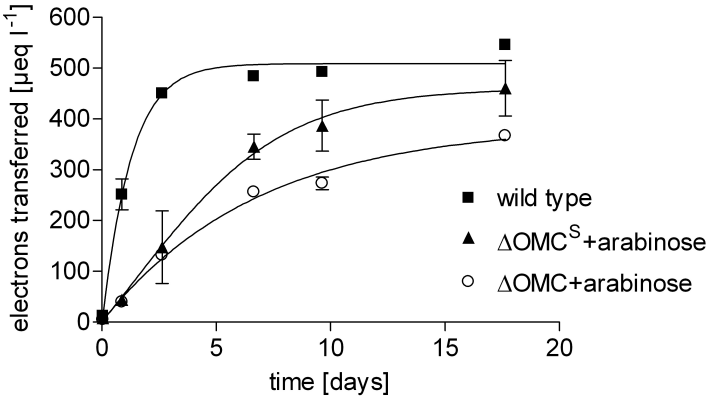

strain	**specific iron reduction rate µ in [h^{-1}]**
wild type	0.534±0.045
ΔOMC^S+arabinose	0.451±0.104
ΔOMC^S	not determinable*
ΔOMC+arabinose	not determinable*

Figure 5: Humic acid reduction. Electrons transferred to Pahokee peat humic acids (PPHA) by different *S. oneidensis* strains. Values are given in electron equivalents measured with Fe(III)-citrate in an electron shuttling assay. Symbols refer to means of duplicate measurements, error bars indicate deviation from the mean. Solid line represents a curve-fit done with GraphPad Prism 4. Specific PPHA reduction rate was calculated for each biological replicate; means and deviations from the mean value are indicated.

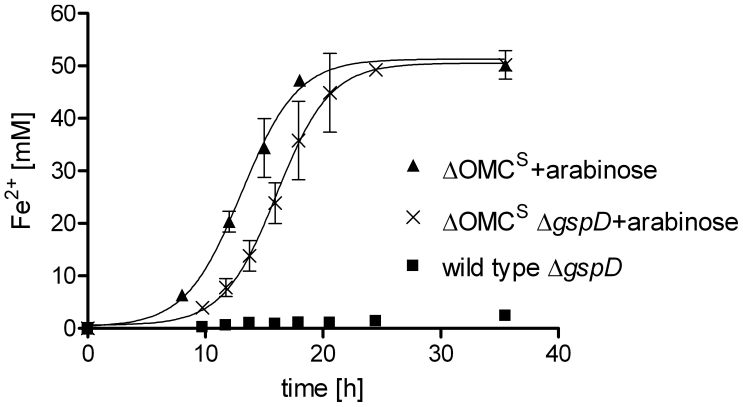

strain	**specific iron reduction rate μ in [h^{-1}]**
wild type Δ*gspD*	not determinable*
ΔOMC^{S}Δ*gspD*+arabinose	0.445±0.082
ΔOMC^S+arabinose	0.451±0.104

Figure 6: Fe(III)-citrate reduction with *gspD*-mutants. Fe(III)-citrate reduction by *S. oneidensis* Δ*gspD* mutant, ΔOMC^S and ΔOMC^{S}Δ*gspD* mutant strains growing on minimal medium with 50 mM lactate and 50 mM Fe(III)-citrate. Arabinose was added to all experiments in a concentration of 1 mM. Symbols refer to means of triplicate measurements, error bars indicate standard deviation. Solid line represents a curve-fit done with GraphPad Prism 4. Specific iron reduction rate was calculated for each biological replicate; means and standard deviation are indicated. *Reduction rates were not determinable because curve-fit was not possible due to minimal reduction within timeframe of the experiment.

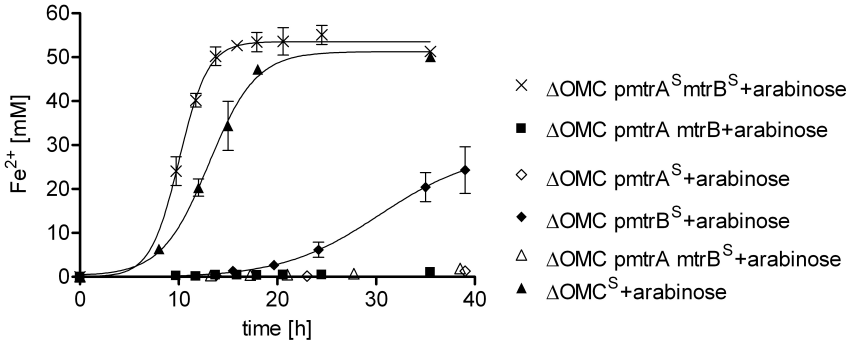

strain (all induced with 1 mM arabinose)	**specific iron reduction rate μ in [h^{-1}]**
ΔOMC pmtrA^{S}mtrB^S	0.602±0.169
ΔOMC pmtrAmtrB	not determinable*
ΔOMC pmtrA^S	not determinable*
ΔOMC pmtrB^S	0.218±0.062
ΔOMC pmtrAmtrB^S	not determinable*
ΔOMC^S	0.451±0.104

Figure 7: ΔOMC complementation with pmtr-plasmids. Fe(III)-citrate reduction by *S. oneidensis* ΔOMC mutant strains, complemented with different plasmids and growing on minimal medium with 50 mM lactate and 50 mM Fe(III)-citrate. Arabinose was added to all experiments in a concentration of 1 mM. Symbols refer to means of triplicate measurements, error bars indicate standard deviation. Solid line represents a curve-fit done with GraphPad Prism 4. Specific iron reduction rate was calculated for each biological replicate; means and standard deviation are indicated. *Reduction rates were not determinable because curve-fit was not possible due to minimal reduction within timeframe of the experiment.

Supporting information

Outer membrane cytochrome independent reduction of extracellular electron acceptors in Shewanella oneidensis

Clemens Bücking[#], Annette Piepenbrock[‡], Andreas Kappler[‡], and Johannes Gescher[#]*

[#]Institut für angewandte Biowissenschaften, Angewandte Biologie, Karlsruher Institut für Technologie, Fritz-Haber-Weg 2, D-76131 Karlsruhe, Germany.

[‡]Geomicrobiology, Center for Applied Geosciences, University of Tübingen, Sigwartstrasse 10, D-72076 Tübingen, Germany

* Corresponding author:

Phone:+49-721-608-41940. Fax:+49-721-608-41941.

E-mail: johannes.gescher@kit.edu

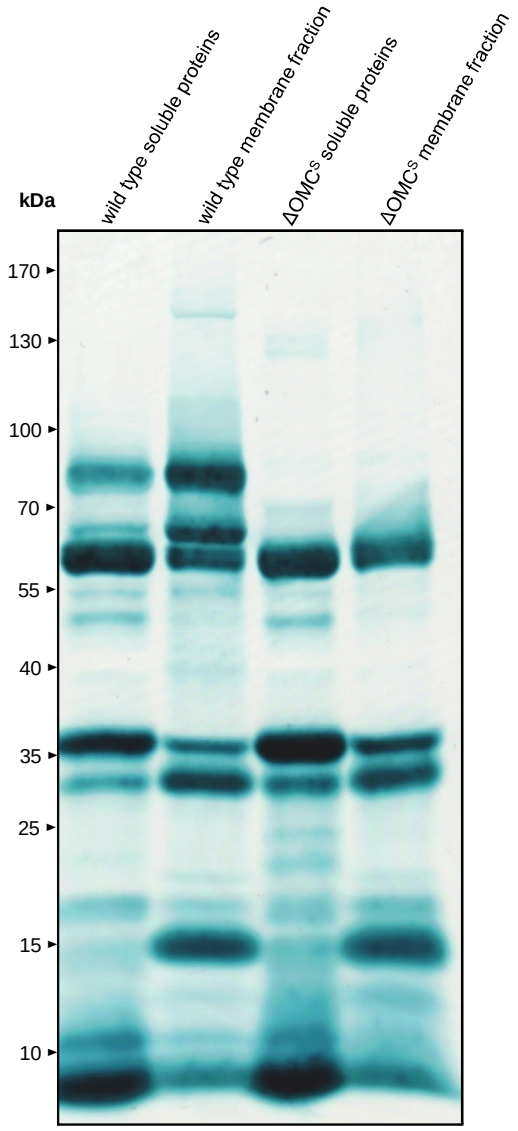

Figure S1: SDS-Page with staining of heme proteins. SDS-Page of soluble and membrane fractions from wild type and ΔOMC^S cells grown on Fe(III)-citrate. 50 µg protein were loaded in each lane of the gel.

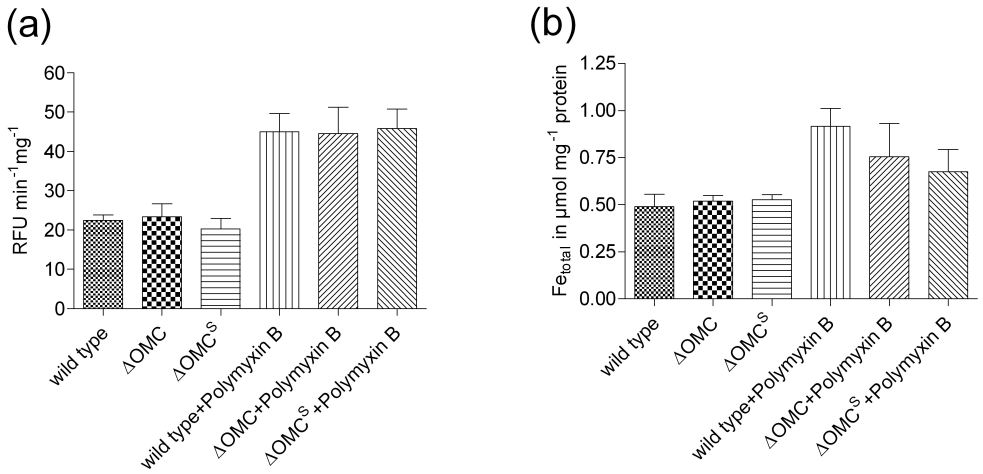

Figure S2: Ethidium bromide and Fe(III) citrate influx. (a) Ethidium bromide influx was measured in independent triplicates with *S. oneidensis* wild type, ΔOMC and ΔOMC^S strains. Influx rates were calculated from the continuously measured increase in fluorescence (excitation 545 nm, emission 600 nm), normalized to the protein content. As a positive control, 1 mg ml^{-1} polymyxin B, which destabilizes the outer membrane, was added to the cells. (b) Fe(III)-citrate influx into the cells was tested after 30 min by measuring the total iron content of washed cell suspensions. As a positive control, polymyxin B at a lower concentration of 50 µg ml^{-1} was chosen due to the longer incubation time.

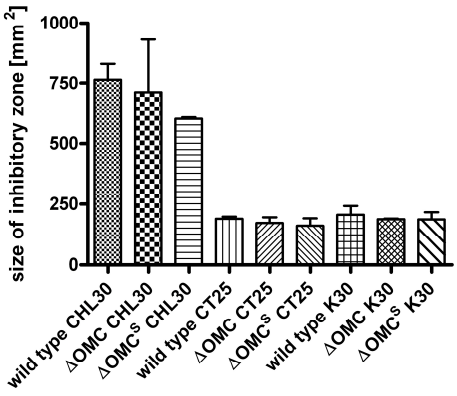

Figure S3: Minimal inhibitory concentration towards antibiotics. Antibiotic susceptibility was tested in a disc diffusion test. Paper discs containing either 25 µg colistin (CT25), 30 µg kanamycin (K30) or 30 µg chloramphenicol (CHL30) were applied to the surface. After overnight incubation at 30°C, plates were photographed and zones of inhibition were measured with ImageJ. Independent quadruplicates were performed.

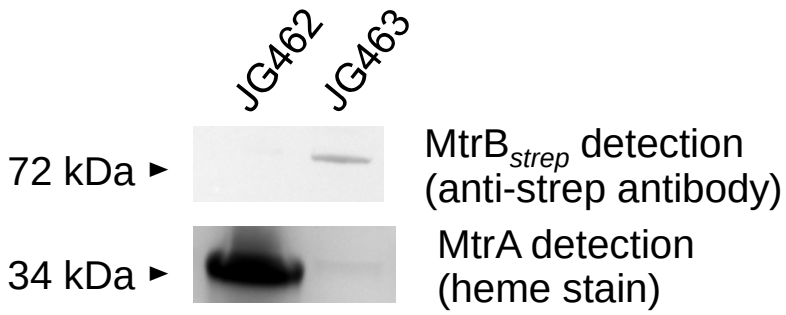

Figure S4: Expression of MtrA^S in strain JG462 and MtrB^S in strain JG463. The upper panel shows a western blot developed with anti-strep antibody to detect MtrB. The lower panel shows staining of heme proteins at the size of ~35 kDa to detect MtrA. (20 µg and 40 µg protein, respectively, were loaded on the gel).

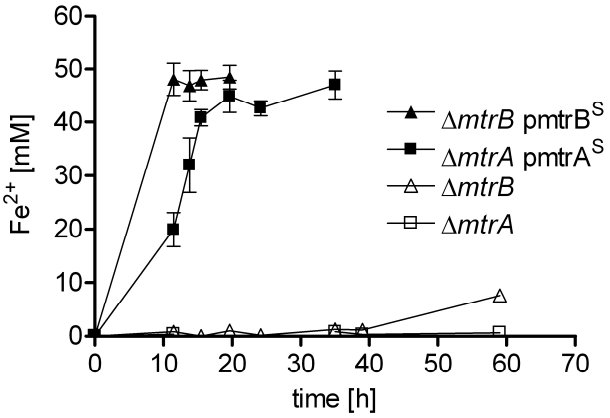

Figure S5: Complementation of Δ*mtrA* with pmtrA^S, and Δ*mtrB* with pmtrB^S. Fe(III)-citrate reduction by *S. oneidensis* Δ*mtrA*, and Δ*mtrB* mutant and their complementation with pmtrA^S and pmtrB^S, respectively. All strains were grown in minimal medium with 50 mM lactate and 50 mM Fe(III)-citrate and addition of 1 mM arabinose. Symbols refer to means of triplicate measurements.

Table S1: Primer used in this study.

Number	***Name***	***Sequence***
1	gspD_up_for	ATGATTACGAATTCGAGCTCGGTACCCGGG_GCTGACCGCATTATCATTAC
2	gspD_up_rev	TATTTTTCTTTCCCCTAACG
3	gspD_down_for	CGTTAGGGGAAAGAAAAATA_GTGAAATACAAGTATCCCAAG
4	gspD_down_rev	CGGCCAGTGCCAAGCTTGCATGCCTGCAGG_CAGTTGTTTCTCATAGGTTTC
5	dmsA1B1_up_for	ATGATTACGAATTCGAGCTCGGTACCCGGG_TGCAACTGGGGATGCAACTC
6	dmsA1B1_up_rev	TGTCTTTACCTCTTATCAATCAAGGC
7	dmsA1B1_down_for	GCCTTGATTGATAAGAGGTAAAGACA_CCAGTTGGTGGTAGTGGGC
8	dmsA1B1_down_rev	CGGCCAGTGCCAAGCTTGCATGCCTGCAGG_GGGTTCATTTCGTGTCAGAGAC
9	dmsAB_up_for	ATGATTACGAATTCGAGCTCGGTACCCGGG_GGCCTTTGTAGGGTGCAAATTC
10	dmsAB_up_rev	TAGTTGTAATAAATATGGATAGCGC
11	dmsAB_down_for	GCGCTATCCATATTTATTACAACTA_TAGAATCATCCCCTAAATTTAAAAGC
12	dmsAB_down_rev	CGGCCAGTGCCAAGCTTGCATGCCTGCAGG_ATCGGGGTGGATGTATATTC
13	Invit_mtrA-for	TTTGGGCTAGAAATAATTTTGTTTAACTTTAAGAAGGAGATATACATACC_GAAGCCTATTATGAAGAACTGCC
14	Invit_mtrA-rev	GGCTGAAAATCTTCTCTCATCCGCCAAAACAGCCAAGCTGGAGACCGTTT_TTAGCGCTGTAATAGCTTGC
15	Invit_mtrB-for	TTTGGGCTAGAAATAATTTTGTTTAACTTTAAGAAGGAGATATACATACC_GGAGACGAGAAAATGAAATTTAAACTC
16	Invit_mtrBstrep-rev	GGCTGAAAATCTTCTCTCATCCGCCAAAACAGCCAAGCTGGAGACCGTTT_TTATTTTTCGAACTGCGGGTGGCTCCA_GAGTTTGTAACTCATGCTCAGC
17	mtrB_in_rev	CACCCACAGTGCCTGATG
18	mtrB_in_for	GCTGTAAAGGCTGCGTCG

Table S2: Single nucleotide polymorphisms (SNP)

SNP positions are given relative to the genome of *S. oneidensis* MR-1 wild type. If no locus tag is indicated, the position of the SNP is intergenic.

A>G means: A in ΔOMC-genome was replaced by G in ΔOMC^S-genome.

T>* means: T in ΔOMC-genome was deleted in ΔOMC^S-genome.

Y>C means: C or T in ΔOMC-genome was replaced by C in ΔOMC^S-genome

Position SNP S.oneidensis MR-1	**Change in nucleotide**	**Locus tag**	**Gene symbol**	**Gene description**	**Remarks**
18204	G>A				
131994	T>C	SO_0122		amino acid transporter LysE	
408350	C>*				
434822	T>C				
514080	A>*				
618045	T>*	SO_0588		transporter, putative	
698256	G>C	SO_0680		hypothetical protein	
735021	G>T	SO_0719		TonB-dependent receptor, putative	
735043	G>T	SO_0719		TonB-dependent receptor, putative	
801756	A>T	SO_0787		hypothetical protein	
1006476	G>T	SO_0975		hypothetical protein	silent mutation
1026745	G>A	SO_0992	lysS	lysyl-tRNA synthetase	
1201298	G>C	SO_1156		TonB-dependent receptor	
1201355	G>T				
1227963	G>C	SO_1184	pth	peptidyl-tRNA hydrolase	silent mutation
1227985	G>C	SO_1184	pth	peptidyl-tRNA hydrolase	
1367113	A>C	SO_1311		transcriptional regulator	silent mutation
1413688	G>A				
1508296	A>G				
1719465	T>C	SO_1637		surface antigen	
1753711	T>G	SO_1666	phhA	phenylalanine 4-	

Position SNP S.oneidensis MR-1	Change in nucleotide	Locus tag	Gene symbol	Gene description	Remarks
				monooxygenase	
1850852	A>C	SO_1771		GntP family permease	
1850853	T>G	SO_1771		GntP family permease	
1857606	C>A	SO_1778	mtrB	outer membrane protein precursor MtrB	
1858407	C>A	SO_1777	mtrA	decaheme cytochrome c MtrA	
1954935	T>A	SO_1862	pgsA	CDP-diacylglycerol--glycerol-3-phosphate 3-phosphatidyltransferase	
2112141	G>T	SO_2013	dnaX	DNA polymerase III, gamma and tau subunits	
2112150	A>G	SO_2013	dnaX	DNA polymerase III, gamma and tau subunits	
2113380	A>C	SO_2014		hypothetical protein	
2113456	A>C	SO_2014		hypothetical protein	
2122997	A>G	SO_2024		hypothetical protein	
2407195	A>*				
2407389	G>*				
2415870	G>A	SO_2304	ald	other	silent mutation
2453867	T>G				
2632050	C>T				
2632051	C>T				
2632076	A>C				
2632079	C>T				
2632106	C>G				
2632194	C>A				
2632262	A>C				
2632279	C>A				
2632295	A>T				
2632364	C>G				

Position SNP S.oneidensis MR-1	Change in nucleotide	Locus tag	Gene symbol	Gene description	Remarks
2632476	T>G				
2799389	A>G	SO_2671		hypothetical protein	silent mutation
2876561	A>*	SO_2754		MotY sodium type flagellar protein	Stop-Codon>TAT
2900888	G>C	SO_2778	fabH-1	3-oxoacyl-(acyl carrier protein) synthase III	
3001147	G>C	SO_2880		glutaredoxin domain-containing protein	
3001210	G>C	SO_2880		glutaredoxin domain-containing protein	
3242135	T>C	SO_3113	tgt	queuine tRNA-ribosyltransferase	
3259672	G>C	SO_t072	tRNA-Ala-3	tRNA	
3260658	A>C	SO_3128.2		glutamate tRNA synthetase	
3261767	C>G	SO_t073	tRNA-Val-5	tRNA	
3261770	T>C	SO_t073	tRNA-Val-5	tRNA	
3384877	C>T	SO_3245	flgF	flagellar basal body rod protein FlgF	
3417774	A>G				
3419919	T>A	SO_3279		AcrB/AcrD/AcrF family protein	
3427554	C>A	SO_3286	cydA	cytochrome d ubiquinol oxidase, subunit I	
3427582	T>A	SO_3286	cydA	cytochrome d ubiquinol oxidase, subunit I	
3489938	T>G				
3588500	Y>A	SO_3443		ISSod4, transposase	
3588512	Y>A	SO_3443		ISSod4, transposase	
3588719	Y>G	SO_3443		ISSod4, transposase	silent mutation
3588812	Y>G	SO_3443		ISSod4, transposase	silent mutation

Position SNP S.oneidensis MR-1	Change in nucleotide	Locus tag	Gene symbol	Gene description	Remarks
3653128	C>G	SO_3502		hypothetical protein	silent mutation
3655317	A>C	SO_3504		hypothetical protein	silent mutation
3750389	C>G	SO_3583	rsuA-1	other	
3783035	T>C	SO_3622		hypothetical protein	silent mutation
3843377	C>A	SO_3692		ABC transporter, ATP-binding protei	
4052809	T>A	SO_3904	tolC	outer membrane channel protein	silent mutation
4216207	A>G	SO_4062	psrA	polysulfide reductase, subunit A	
4505871	C>T	SO_4319		HlyD family secretion protein	
4512655	C>T	SO_4324		GGDEF domain-containing protein	silent mutation
4521417	G>*	SO_4327		HlyD family secretion protein	
4614019	G>*	SO_4423		hypothetical protein	
4687941	A>G				
4687972	C>T				
4687973	T>C				
4687987	A>G				
4721421	T>*	SO_4525		hypothetical protein	
4841973	A>G	SO_4645		hypothetical protein	
4842089	A>C	SO_4645		hypothetical protein	
4894203	Y>C	SO_4692		AcrB/AcrD/AcrF family protein	silent mutation

1

A microbial fuel cell biosensor based on *Shewanella oneidensis* outer membrane protein complexes

Frederik Golitsch[#], Clemens Bücking[#], and Johannes Gescher*

Institut für angewandte Biowissenschaften, Angewandte Biologie, Karlsruher Institut für Technologie, Fritz-Haber-Weg 2, D-76131 Karlsruhe, Germany.

[#]These authors contributed equally to this study.

*Corresponding author:

Phone:+49-721-608-41940. Fax:+49-721-608-41941.

E-mail: johannes.gescher@kit.edu

Running title: Microbial biosensor based on *Shewanella oneidensis*

Key words: specific microbial biosensor, *Shewanella oneidensis*, outer membrane cytochromes, MtrA, MtrB, MtrF,

Abstract

Shewanella oneidensis is known for its ability to respire on extracellular electron acceptors. The spectrum of these acceptors includes anode surfaces in a microbial fuel cell. Based on this activity, a versatile *S. oneidensis* based biosensor strain was constructed in which electricity production can be modulated. Construction started with the identification of a usable rate-limiting step of electron transfer to an anode. Thereafter, the sensor strain was developed by means of synthetic biology to contain a protein complex consisting of the three proteins MtrA, MtrB and MtrF. This complex is associated to the outer membrane and most probably enables membrane spanning electron transfer. MtrF is an outer membrane cytochrome that catalyzes electron transfer reactions on the cell surface. Under anoxic conditions, wild type cells do not express MtrF but rather MtrC as electron transferring outer membrane cytochrome. Still, our analysis revealed that MtrF compared to MtrC overexpression is less toxic which gives MtrF a superior position for biosensor based applications. Transcription of *mtrA, mtrB* and *mtrF* was linked up to an inducible promoter system, which positively reacts to rising L-arabinose concentrations. Current production mediated by this strain was linearly dependent on the arabinose content of the medium. This linear dependency was detectable over a wide range of arabinose concentrations. The L-arabinose biosensor presented in this study could be easily modified to different specificities by a simple change of the promoter region.

Introduction

Microbial biosensors use physiological capabilities of microbial cells. These capabilities have to be linked to an output signal that can be detected for instance via optical or electrical devices. The great potential of microbial biosensors lies in the development of inexpensive monitoring techniques that can be operated easily and without sophisticated technical equipment. Many highly specific microbial biosensors rely on the use of genetically modified microorganisms. The organisms have usually a specific promoter region that is responsive to a certain analyte. The promoter region triggers the expression of a reporter gene which produces a measurable signal. Measuring techniques for these rather specific systems are often based on the detection of optical stimuli (luminescence, color changes or fluorescence). The other major group of microbial biosensors is based on electrochemical measurements (Pasco et al. 2011; Su et al. 2011). Here, amperometry is the most common electrochemical-measuring technique used in biosensors. The strategy is to apply a certain potential to working and reference electrode and to detect and quantify a current signal that results from oxidation or reduction of an electroactive compound. This technique is widely used to measure the biological oxygen demand of solutions that contain a mixture of reduced organic carbon sources (Kumlanghan et al. 2008; Nakamura et al. 2007). These measurements rely on aerobic respiration, since microbes couple the oxidation of suitable reduced organic carbon sources to the reduction of oxygen to water.

Recently microbial fuel cell (MFC) based systems were introduced to the field of biosensors (Gil et al. 2003; Kim et al. 2003). MFCs are usually known as an approach to harvest electricity by means of microbial catalyzed oxidation of an organic carbon source to electricity production. So-called exoelectrogenic microorganisms transfer electrons directly or via a mediator to an anode. This can be easily measured and quantified since a current is

produced as a result of this form of anaerobic respiration. To date, it was shown in several studies that MFCs can be applied to measure the biological oxygen demand (Chang et al. 2004; Di Lorenzo et al. 2009; Gil et al. 2003; Kim et al. 2003; Kumlanghan et al. 2007). The same technique can also be used to quantify specific analytes if the solution that is measured contains only one compound that can be oxidized by the microbes or if the microbes have a rather restricted spectrum of usable carbon sources. A slight modification of the above-mentioned principles leads to techniques for detection and quantification of toxic compounds. These compounds interfere negatively with the respiratory capabilities of microorganisms. In other words, microbes will need more time to respire available oxygen in the presence of an oxidizable carbon source if toxic compounds like phenol or chromium inhibit them (Davila et al. 2011; Kim et al. 2007). To our knowledge, the only MFC based biosensors that claim to be specific for an analyte depend directly on the carbon metabolism of the microorganism used. Trond et al. for instance used *Geobacter sulfurreducens* and *Shewanella oneidensis* MR-1 cells to quantify acetate and lactate concentrations, respectively (Tront et al. 2008a, 2008b). Still, recent analysis showed that these organisms are not as limited in their spectrum of oxidizible carbon sources as formerly believed (Call and Logan 2011; Yang et al. 2006) which questions the specificity of the biosensor if operated in a mixture of organic carbon sources.

In this study, we propose a platform for a MFC based biosensor that is highly specific and can be adapted to many different analytes by the insertion of new promoter regions. It is based on *S. oneidensis*, one of the best-characterized model organisms for anode respiration besides *G. sulfurreducens*. This non-pathogenic facultative anaerobic γ-proteobacterium is known for its ability to respire insoluble metal oxides which also enables electron transfer to an anode without addition of an external mediator. Furthermore *S. oneidensis* is closely related to *E. coli* and shows a good genetic tractability (Hau and Gralnick 2007; Richter et al. 2012).

The organism’s ability to respire on insoluble electron acceptors is based on an extended

respiratory chain that transports electrons to the cell surface (Richter et al. 2012). The current model of the extended respiratory chain in *S. oneidensis* is depicted in Fig. 1. It consists mainly of multiheme *c*-type cytochromes. They are required for transport of respiratory electrons through periplasm and outer membrane and the final reduction of extracellular electron acceptors. This final reduction step seems to be rate limiting in most cases (Ross et al. 2009). It is catalyzed in *S. oneidensis* by outer membrane cytochromes (OMC). Evidence was provided that two decaheme OMCs are of outstanding importance for anode respiration (Bretschger et al. 2007; Meitl et al. 2009). These OMCs are called OmcA (**o**uter **m**embrane **c**ytochrome **A**) and MtrC (**m**e**t**al **r**educing protein **C**). The latter one was shown to be part of an electron transferring protein complex that spans the outer membrane (Hartshorne et al. 2009; Richter et al. 2012). Therefore, anode respiration necessitates the presence of MtrC. An additional gene for an outer membrane cytochrome, *mtrF*, was shown to encode for a functional protein that can rescue the phenotype of *mtrC* deletion mutants (Bücking et al. 2010; Clarke et al. 2011). Still, *mtrF* seems to be expressed only under microoxic conditions (McLean et al. 2008). As mentioned above, OMCs catalyze direct reduction of metal oxides and anodes but they are furthermore necessary for the reduction of endogenous or exogenous electron shuttles that facilitate extracellular electron transfer (Coursolle et al. 2010; Jiang et al. 2010; Marsili et al. 2008; Ross et al. 2009).

The here presented specific MFC biosensor is based on the construction of an operon composed of the genes *mtrF*, *mtrA* and *mtrB*. This operon was inserted in the genome of a recently published strain that is devoid of any gene encoding an outer membrane cytochrome (Bücking et al. 2010). The new operon was linked up to a P_{BAD} promoter. We show that modulation of the operon expression levels is a powerful tool to adjust ferric iron reduction capacity and consequently MFC performance.

Materials and methods

Chemicals and biochemicals were obtained from Sigma-Aldrich, Roth and Promega. Enzymes were purchased from New England Biolabs.

Growth conditions and media

All microorganisms used in this study are listed in table 1. *Escherichia coli* strains were grown in LB medium at 37°C, *S. oneidensis* strains were grown aerobically at 30°C in LB medium or under anoxic conditions in minimal medium, supplemented with lactate (50 mM) as electron donor and carbon source and 50 mM Fe(III) citrate or 100 mM fumarate as electron acceptor as described previously (Schuetz et al. 2009). If necessary, kanamycin (50 µg ml^{-1}) and arabinose (0.01 to 2 mM) was added to the medium. For experiments in the MFC, the growth medium was a modified PBS buffer with lactate (50 mM) as electron donor and carbon source (2.7 mM KCl, 1.76 mM KH_2PO_4, 137 mM NaCl, 10 mM Na_2HPO_4 , 9 mM $(NH_4)_2SO_4$, 1 mM Mg_2SO_4, 0.1 mM $CaCl_2$, 1 g l^{-1} casamino acids, and trace elements (5 µM $CoCl_2$, 0.2 µM $CuSO_4$, 57 µM H_3BO_3, 5.4 µM $FeCl_2$, 1.3 µM $MnSO_4$, 67.2 µM Na_2EDTA, 3.9 µM Na_2MoO_4, 1.5 µM Na_2SeO_4, 5 µM $NiCl_2$, and 1 µM $ZnSO_4$)).

Construction of *S. oneidensis* MTR-FAB mutant

All primers used are listed in table 2. The gene *mtrF* containing a C-terminal strep tag was introduced into the existing strain ΔOMC in front of the genes *mtrA* and *mtrB* (Bücking et al. 2010). Primers 1 and 2 were used to amplify a 500 bp region upstream of the insertion site in ΔOMC and *mtrF* using plasmid DNA from pBAD$mtrF_{strep}$ as a template (Bücking et al. 2010). Primers 3 and 4 were used to amplify a 500 bp region downstream of the insertion site. The resulting fragments were fused by a further PCR step utilizing Primers 1 and 4. The merged fragment was cloned into a linearized pMQ150 plasmid using an isothermal assembly method (Gibson et al. 2009). The resulting plasmid pMQ150-*mtrFAB* was transformed into

E. coli S17, which was then used as conjugal donor strain for mating with *S. oneidensis* ΔOMC. The introduced DNA and its adjacent regions of the resulting mutant, designated *S. oneidensis* MTR-FAB, were sequenced by GATC Biotech.

Membrane-preparation, SDS-PAGE, heme-staining, and western-blotting

Membrane fractions were prepared as described elsewhere (Schuetz et al. 2009). Protein concentrations were determined by the method of Bradford (Bradford 1976) with bovine serum albumin as standard. For quantification of protein concentrations in cell suspensions, 0.2 mM NaOH was added to the suspensions prior to a 10 min incubation at 95°C.

Proteins were separated on polyacrylamide gels according to Laemmli (Laemmli 1970). Heme proteins were visualized by peroxidase staining (Thomas et al. 1976). Proteins containing a C-terminal strep-tag were detected on a western blot using a primary strep-tag antibody (Qiagen) and a secondary alkaline phosphatase labeled antibody (Sigma-Aldrich). The blot was developed using the AP conjugate detection kit (Biorad).

Fe(III) citrate reduction experiments

Cells were pre-grown overnight in minimal medium under anoxic conditions with fumarate as electron acceptor and induced with 0-2 mM arabinose as indicated. Cells were then washed twice, resuspended to a final OD_{600} of 0.4 and 500 µl of this cell suspension were used to inoculate 100 ml anoxic Fe(III) citrate medium. Reduction of Fe(III) citrate was determined by measuring ferrous iron concentrations with ferrozine reagent (Stookey 1970). All experiments were conducted in independent triplicates. The maximal reduction rate was determined by a non-linear curve fit done with GraphPad Prism software.

Microbial fuel cell (MFC) experiments

The MFC setup used in this study features an anode and cathode chamber with a working

volume of 25 ml each, separated by a Fumion F950 membrane (Quintech). A saturated calomel reference electrode (SCE) (Sensortechnik Meinsberg) was separated from the anode compartment by another Fumion membrane. Potentials measured against SCE were converted to normal hydrogen electrode (NHE) potentials by addition of 237.9 mV. Working electrodes were made of graphite felt (SGL Carbon SE). Cells were pre-grown over night under anoxic conditions with fumarate as electron acceptor and the same arabinose induction as used later in the MFC experiments. Culture were thereafter spun down and washed twice with anoxic medium that did not contain an electron acceptor to remove residual fumarate. MFC experiments were initiated using a starting OD_{600nm} of 0.4. The medium in the MFC contained arabinose as indicated. The whole setup was connected to a potentiostat (Pine Instruments), which controlled the standard measurement protocol that contained two phases: First, a constant current was applied (conditioning period) for 10 h (278 nA cm^{-2}). Then, this current was continuously increased (current sweep phase) with a rate of 2.88 µA h^{-1} until 120 µA were reached. The limiting current density that is characterized by a steep rise in potential was defined to be +750 mV vs. NHE according to earlier work (Bücking et al. 2010).

A fast measurement protocol was developed for biosensor applications. Here, cells were also pregrown over night under anoxic conditions but were not induced with arabinose. Operation of the MFC was similar but consisted only of the first phase with a constant current of 444 nA cm^{-2}. The anode compartment was continuously flushed with nitrogen gas to maintain anoxic conditions. Additional terminal electron acceptors were not added. All MFC experiments were conducted in independent duplicates or triplicates at a constant temperature of 30°C.

Results

Finding the right outer membrane cytochrome

Most dissimilatory iron reducers are able to catalyze electron transfer to anode surfaces. This is certainly not due to an evolutionary adaptation but rather to an unspecificity of the terminal reductases. These enzymes bring respiratory electrons into contact with extracellular electron acceptors and it is not important whether this electron acceptor is a graphite electrode or hydrous ferric oxide or Fe(III) citrate. Hence, the components of the electron transport chain to an anode and to iron oxides are either highly similar or even identical. Therefore, most of the experiments described in this study were conducted first with ferric iron as electron acceptor and at certain stage were expanded in MFCs. The rate of extracellular respiration of insoluble electron acceptors is most probably limited by the availability of reactive surfaces. The final reduction is catalyzed by outer membrane cytochromes which is the rate-limiting step if a sufficient amount of reduced carbon sources is available. It was shown in a previous study, that the inability of a *S. oneidensis* mutant devoid of any outer membrane cytochrome (strain ΔOMC) could be rescued by expression of the outer membrane cytochromes MtrC or MtrF (Bücking et al. 2010). Therefore, it was tested first whether and to what extent MtrC and MtrF can be overexpressed in this ΔOMC strain. This information was necessary for the construction of the biosensor since the window in which electron transfer can be modulated by OMC expression defines the spectrum of concentrations that can be assessed by the biosensor itself. A first set of expression experiments revealed that controlled overexpression of outer membrane cytochromes from plasmid DNA regulates the rate Fe(III) citrate reduction only within a very narrow range of inductor concentrations (Fig. 2). This is probably due to the fact that the components of the outer membrane spanning complex are not produced in equal amounts being either encoded in the genome with one copy per cell (*mtrA* and *mtrB*) or

expressed from a low copy plasmid and probably have a 10 to 30-fold higher copy number (*mtrC* and *mtrF*).

This results consequently in a higher concentration of the OMCs compared to MtrA and MtrB. It seems as if OMCs that are produced in excess were unable to connect to the underlying electron transfer chain. The second conclusion that could be drawn from these experiments was that high amounts of outer membrane cytochromes seem to be toxic for the cell. This effect was much more pronounced for MtrC than for MtrF (Fig. 2). Another disadvantage of these strains is that their function in a MFC would rely on plasmids which need to be maintained in the cell through a continuous addition of an antibiotic.

Genomic insertion widens the usable induction window

A new *S. oneidensis* strain was constructed to overcome the limitations mentioned above and to integrate the information gained from the expression experiments. Therefore a ΔOMC strain backbone was used and the genes encoding *mtrF*, *mtrA* and *mtrB* were placed in a row behind a P_{BAD}-promoter in the genome resulting in strain MTR-FAB (JG410). The newly inserted operon should allow for the expression of similar amounts of each component of the outer membrane spanning MtrFAB-complex (Fig. 3). To verify this hypothesis MTR-FAB cells were grown under ferric iron reducing conditions in the presence of varying levels of arabinose. As Fig. 4 indicates the concentration of MtrF and MtrA increases proportionally with the induction level (Fig. 4). Although the expression of MtrB could not be shown directly due to the absence of a specific antibody, the protein is very likely to be present in similar amounts since it is part of the same operon (Fig. 3).

The Fe(III) citrate reduction rate of MTR-FAB responded to a much greater range of inductor concentrations as compared to the above described experiments with plasmid encoded copies of *mtrF*. Fastest ferric iron reduction rates were reached using 1 mM arabinose (Fig. 5).

Further increase in arabinose concentration did not increase the maximal reduction rate and the onset of reduction was delayed, probably due to a negative effect from protein overproduction. Interestingly, the maximal reduction rate of MTR-FAB with an induction of 1 mM arabinose was 1.8-fold higher than that of the wild type. As the final electron transfer to the terminal acceptor is most probably the rate limiting step of the extended respiratory chain, a higher number of complexes than in the wild type might be responsible for the higher rate.

Microbial fuel cell (MFC) performance of MTR-FAB

The ultimate goal of this study was to construct a biosensor strain that can be used in a MFC based system. The MTR-FAB strain was therefore tested in a MFC to test if a higher ferric iron reduction rate also results higher current production if an anode is used as terminal electron acceptor. The MFC was set under potentiostatic control to compare wild type and MTR-FAB strain under different induction levels. While at first a fixed low current was applied to allow for anode colonization, the current was then increased linearly and the potential was measured. The current density at which bacteria failed to provide sufficient quantities of electrons to sustain a given current abstraction is characterized by a steep increase in slope of the current density-potential plot (Fig. 6a). It is defined as the limiting current density (LCD) which is characteristic for each strain (Bücking et al. 2010).

The LCDs (means of triplicate measurements) of strain MTR-FAB increased with the induction level reaching a maximum at 2 mM arabinose. At this point, the LCD of MTR-FAB is 1.13-fold higher than the one of the wild type (Fig. 6b). The relation between induction level and LCD is linear over a wide range of inductor concentrations. The curve levels off when more than 1 mM arabinose was added to the MFC-medium. Still, the linear dependence between 0 and 1 mM arabinose allows for the use of this system for sensor applications (Fig. 6c). A measured current value could then be traced back to an unknown inductor concentration.

Decreasing the measurement period

A faster MFC measurement protocol was developed to show that the different inductions levels could be sensed without performing a time consuming current-sweep experiment. Therefore the potential generated by the bacteria was compared at a fixed current density. This proof-of-principle experiment was performed using inductor concentrations of 0, 0.5, and 1 mM. To be closer to a putative application, we performed the experiment with cells that were not precultured with arabinose as inductor. Consequently, these cells were expected to show a delay in MtrFAB expression which is consistent with the almost identical progression of the determined potentials of all three setups during the first 0.75 h (Fig. 7a). Beyond that period the potential of the induced setups started to drop whereas that of the non-induced setup was barely affected. After 2 h of chronopotentiometry a difference between all three induction levels was clearly visible. Compared to the non-induced setup those with induction levels of 0.5 and 1 mM arabinose reached a 1.13- and 1.75-fold lower potential, respectively (Fig 7b). Thereby, the described drops of the potentials seemed to be related to the increasing number of expressed MtrFAB-complexes in this phase. Due to these results this method could be a promising approach for a relatively quick and specific detection of so far not measurable compounds.

Discussion

In this article, we showed the development of a platform for a versatile microbial biosensor using a genetically modified *S. oneidensis* strain. It is based on MFC technology which has been successfully used before for instance for the determination of biological oxygen demands (Chang et al. 2004; Kim et al. 2003). Our approach is based on the controlled expression of proteins that are necessary for electron transfer through the outer membrane and onto solid phase extracellular electron acceptors.

It was interesting to observe that the developed strain reduced Fe(III) citrate with reduction rates that were dependent on the inductor concentration. At a certain concentration the rates did not increase further but rather reached a plateau. This plateau was propably reached because the capabilities of the promoter were maxed out by inductor concentrations of more than 1 mM arabinose in the medium. In other words, the expression level could not have been increased beyond that point. Another possibility is that maturation of the c-type cytochromes MtrF and MtrA or membrane insertion of MtrB was limiting. These latter points might especially contribute to the toxic effects that were observed when MtrC or MtrF were expressed form plasmid encoded copies of the corresponding genes. Still, the developed MTR-FAB strain reduced Fe(III) citrate faster than wild type cells. This means that the ecological niche of *S. oneidensis* might not select for the fastest ferric iron reducer but that other factors contribute most probably as well. It furthermore suggests that there are further possibilities to accelerate iron reduction in engineered strains, which will provide an interesting field for future research.

It was surprising to see, that most but not all results from ferric iron reduction experiments were transferrable to MFC experiments. Certainly, it was the most important point to show that current production could be modulated by the inductor concentration in the medium. This is the prerequisite for a quantitative biosensor. The here presented experiments clearly demonstrate that MTR-FAB can be operated as a microbial biosensor and future experiments will expand the spectrum of detectable substances. This spectrum depends only on available promoter systems and the capability of the target compounds to enter a *Shewanella* cell. Still, the effect of MtrFAB expression on current production was not as pronounced as what we could observe for the ferric iron reduction rate. MTR-FAB produced more current than the wild type but only 1.13-fold more while ferric iron reduction was 1.8-fold accelerated. So far, it is not possible to undoubtedly answer specifiy the reasons for this difference. What we

know is that Fe(III) citrate is a substance that is reduced extracellularly and that its reduction necessitates MtrF in the MTR-FAB strain. This is also true for anode reduction by MTR-FAB. We hypothesize that the availability of the two electron acceptors causes the observed difference. Fe(III) citrate is a soluble or colloidal electron acceptor that is unable to pass the outer membrane. Still, one would imagine that Fe(III) citrate is by far more available to outer membrane cytochromes at the cell surface than a graphite felt anode. Hence, only a subfraction of the produced MtrFAB complexes is able to interact with the anode surface. This fraction is most likely smaller than the fraction that can interact with Fe(III) citrate as diffusible electron acceptor. Therefore, we hypothesize that part of the protein complexes cannot interact with the anode and therefore do not contribute to current production. Therefore it is coherent that the effect of MtrFAB expression is not as pronounced in anode reduction compared to Fe(III) citrate reduction.

Conclusions

This study describes the development of an engineered microbial biosensor. An arabinose inducible promoter system was used here to conduct proof of principle experiments. The results display nicely that current production depends on the addition of arabinose in a linear fashion. The developed strain can be easily adapted to detect and quantify a number of other compounds. This would require only a simple exchange of the promoter system. The measurement period was reduced to less than two hours. This will be sufficient for a multitude of applications. To our knowledge, this is the first report about a MFC based microbial biosensor that is responsive to a specific analyte, which is not used as carbon or electron source. It can be adapted to various specifications by changing the promoter region using established protocols.

Tables

Table 1: Bacterial strains used in this study.

Number	Strain	relevant genotype	Source or reference
JG144	*E. coli* S17-1	*thi pro recA hsdR* [RP4-2Tc::Mu-Km::Tn7] *λpir Tpr Smr*	(Simon et al. 1983)
JG7	*S. oneidensis* MR-1	wild type	(Venkateswaran et al. 1999)
JG132	*S. oneidensis* MR-1 ΔOMC	Δ(mtrD-mtrC) ΔSO_2931, ΔSO_1659, 3100633 :: (araC, P_{BAD})	(Bücking et al. 2010)
JG138	*S. oneidensis* MR-1 ΔOMC pBAD*mtrC*$_{strep}$	JG132 / pBAD*mtrC*$_{strep}$	(Bücking et al. 2010)
JG139	*S. oneidensis* MR-1 ΔOMC pBAD*mtrF*$_{strep}$	JG132 / pBAD*mtrF*$_{strep}$	(Bücking et al. 2010)
JG410	*S. oneidensis* MR-1 MTR-FAB	Δ(*mtrD-mtrC*) ΔSO_2931 ΔSO_1659, 3100633 ::	this study

		(araC, P_{BAD}, *mtrF*$_{strep}$)	

1

2 **Table 2: Oligonucleotides used in this study**

Number	Name	Sequence
1	mtrFAB UP_for	*ATGATTACGAATTCGAGCTCGGTACCCGGG*CTGAC CGCGAATGGTGAG
2	mtrFAB Strep_rev	TCTTCATAATAGGCTTCCCAATTTGTCCCATTATT TTTCGAACTGCGGGTG
3	mtrFAB DOWN_for	TGGGACAAATTGGGAAGCC
4	mtrFAB DOWN_rev	CGGCCAGTGCCAAGCTTGCATGCCTGCAGGGCA ACATCGGCATTGTCATG

3

Table 3: Plasmids used in this study.

Name	relevant genotype	Source or reference
pMQ150	Kan^R, *sacB*	Provided by Rob Shanks, accession no.: EU546823
pBAD*mtrF*$_{strep}$	Kan^R , *araC*, P_{BAD}; *mtrF*$_{strep}$	(Bücking et al. 2010)

pBAD*mtrC*$_{strep}$	Kan^{R} , *araC*, P_{BAD}; *mtrC*$_{strep}$	(Bücking et al. 2010)

1

References

Bradford, M.M., 1976. A rapid and sensitive method for the quantitation of microgram quantities of protein utilizing the principle of protein-dye binding. Anal Biochem 72, 248-254.

Bretschger, O., Obraztsova, A., Sturm, C.A., Chang, I.S., Gorby, Y.A., Reed, S.B., Culley, D.E., Reardon, C.L., Barua, S., Romine, M.F., Zhou, J., Beliaev, A.S., Bouhenni, R., Saffarini, D., Mansfeld, F., Kim, B.H., Fredrickson, J.K., Nealson, K.H., 2007. Current production and metal oxide reduction by *Shewanella oneidensis* MR-1 wild type and mutants. Appl Environ Microbiol 73(21), 7003-7012.

Bücking, C., Popp, F., Kerzenmacher, S., Gescher, J., 2010. Involvement and specificity of *Shewanella oneidensis* outer membrane cytochromes in the reduction of soluble and solid-phase terminal electron acceptors. FEMS Microbiol Lett 306(2), 144-151.

Call, D.F., Logan, B.E., 2011. Lactate oxidation coupled to iron or electrode reduction by *Geobacter sulfurreducens* PCA. Appl Environ Microbiol.

Chang, I.S., Jang, J.K., Gil, G.C., Kim, M., Kim, H.J., Cho, B.W., Kim, B.H., 2004. Continuous determination of biochemical oxygen demand using microbial fuel cell type biosensor. Biosens Bioelectron 19(6), 607-613.

Clarke, T.A., Edwards, M.J., Gates, A.J., Hall, A., White, G.F., Bradley, J., Reardon, C.L., Shi, L., Beliaev, A.S., Marshall, M.J., Wang, Z., Watmough, N.J., Fredrickson, J.K., Zachara, J.M., Butt, J.N., Richardson, D.J., 2011. Structure of a bacterial cell surface decaheme electron conduit. Proc Natl Acad Sci U S A 108(23), 9384-9389.

Coursolle, D., Baron, D.B., Bond, D.R., Gralnick, J.A., 2010. The Mtr respiratory pathway is essential for reducing flavins and electrodes in *Shewanella oneidensis*. J Bacteriol 192(2), 467-474.

Davila, D., Esquivel, J.P., Sabate, N., Mas, J., 2011. Silicon-based microfabricated microbial fuel cell toxicity sensor. Biosens Bioelectron 26(5), 2426-2430.

Di Lorenzo, M., Curtis, T.P., Head, I.M., Scott, K., 2009. A single-chamber microbial fuel cell as a biosensor for wastewaters. Water Res 43(13), 3145-3154.

Gibson, D.G., Young, L., Chuang, R.Y., Venter, J.C., Hutchison, C.A., Smith, H.O., 2009. Enzymatic assembly of DNA molecules up to several hundred kilobases. Nature Methods 6(5), 343-U341.

Gil, G.C., Chang, I.S., Kim, B.H., Kim, M., Jang, J.K., Park, H.S., Kim, H.J., 2003. Operational parameters affecting the performance of a mediator-less microbial fuel cell. Biosens Bioelectron 18(4), 327-334.

Hartshorne, R.S., Reardon, C.L., Ross, D., Nuester, J., Clarke, T.A., Gates, A.J., Mills, P.C., Fredrickson, J.K., Zachara, J.M., Shi, L., Beliaev, A.S., Marshall, M.J., Tien, M., Brantley, S., Butt, J.N., Richardson, D.J., 2009. Characterization of an electron conduit between bacteria and the extracellular environment. Proc Natl Acad Sci U S A 106(52), 22169-22174.

Hau, H.H., Gralnick, J.A., 2007. Ecology and biotechnology of the genus *Shewanella*. Annu Rev Microbiol 61, 237-258.

Jiang, X., Hu, J., Fitzgerald, L.A., Biffinger, J.C., Xie, P., Ringeisen, B.R., Lieber, C.M., 2010. Probing electron transfer mechanisms in *Shewanella oneidensis* MR-1 using a nanoelectrode platform and single-cell imaging. Proc Natl Acad Sci U S A 107(39), 16806-16810.

Kim, B.H., Chang, I.S., Gil, G.C., Park, H.S., Kim, H.J., 2003. Novel BOD (biological oxygen demand) sensor using mediator-less microbial fuel cell. Biotechnol Lett 25(7), 541-545.

Kim, M., Hyun, M.S., Gadd, G.M., Kim, H.J., 2007. A novel biomonitoring system using microbial fuel cells. J Environ Monitor 9(12), 1323-1328.

Kumlanghan, A., Kanatharana, P., Asawatreratanakul, P., Mattiasson, B., Thavarungkul, P., 2008. Microbial BOD sensor for monitoring treatment of wastewater from a rubber latex industry. Enzyme and Microbial Technology 42(6), 483-491.
Kumlanghan, A., Liu, J., Thavarungkul, P., Kanatharana, P., Mattiasson, B., 2007. Microbial fuel cell-based biosensor for fast analysis of biodegradable organic matter. Biosens Bioelectron 22(12), 2939-2944.
Laemmli, U.K., 1970. Cleavage of structural proteins during the assembly of the head of bacteriophage T4. Nature 227(5259), 680-685.
Marsili, E., Baron, D.B., Shikhare, I.D., Coursolle, D., Gralnick, J.A., Bond, D.R., 2008. *Shewanella* secretes flavins that mediate extracellular electron transfer. Proc Natl Acad Sci U S A 105(10), 3968-3973.
McLean, J.S., Pinchuk, G.E., Geydebrekht, O.V., Bilskis, C.L., Zakrajsek, B.A., Hill, E.A., Saffarini, D.A., Romine, M.F., Gorby, Y.A., Fredrickson, J.K., Beliaev, A.S., 2008. Oxygen-dependent autoaggregation in *Shewanella oneidensis* MR-1. Environ Microbiol 10(7), 1861-1876.
Meitl, L.A., Eggleston, C.M., Colberg, P.J.S., Khare, N., Reardon, C.L., Shi, L., 2009. Electrochemical interaction of *Shewanella oneidensis* MR-1 and its outer membrane cytochromes OmcA and MtrC with hematite electrodes. Geochim Cosmochim Acta 73(18), 5292-5307.
Nakamura, H., Suzuki, K., Ishikuro, H., Kinoshita, S., Koizumi, R., Okuma, S., Gotoh, M., Karube, I., 2007. A new BOD estimation method employing a double-mediator system by ferricyanide and menadione using the eukaryote *Saccharomyces cerevisiae*. Talanta 72(1), 210-216.
Pasco, N.F., Weld, R.J., Hay, J.M., Gooneratne, R., 2011. Development and applications of whole cell biosensors for ecotoxicity testing. Anal. Bioanal. Chem. 400(4), 931-945.
Richter, K., Schicklberger, M., Gescher, J., 2012. Dissimilatory reduction of extracellular electron acceptors in anaerobic respiration. Appl Environ Microbiol 78(4), 913-921.
Ross, D.E., Brantley, S.L., Tien, M., 2009. Kinetic characterization of terminal reductases OmcA and MtrC involved in respiratory electron transfer for dissimilatory iron reduction in *Shewanella oneidensis* MR-1. Appl Environ Microbiol 75, 5218-5226.
Schuetz, B., Schicklberger, M., Kuermann, J., Spormann, A.M., Gescher, J., 2009. Periplasmic electron transfer via the *c*-type cytochromes MtrA and FccA of *Shewanella oneidensis* MR-1. Appl Environ Microbiol 75(24), 7789-7796.
Simon, R., Priefer, U., Pühler, A., 1983. A broad host range mobilization system for in vivo genetic engineering: Transposon mutagenesis in gram negative bacteria. Bio/Technology 1, 784 - 791.
Stookey, L.L., 1970. Ferrozine - a new spectrophotometric reagent for iron. Anal Chem 42(779-81).
Su, L.A., Jia, W.Z., Hou, C.J., Lei, Y., 2011. Microbial biosensors: A review. Biosens Bioelectron 26(5), 1788-1799.
Thomas, P.E., Ryan, D., Levin, W., 1976. An improved staining procedure for the detection of the peroxidase activity of cytochrome P-450 on sodium dodecyl sulfate polyacrylamide gels. Anal Biochem 75(1), 168-176.
Tront, J.M., Fortner, J.D., Ploetze, M., Hughes, J.B., Puzrin, A.M., 2008a. Microbial fuel cell biosensor for in situ assessment of microbial activity. Biosens Bioelectron 24(4), 586-590.
Tront, J.M., Fortner, J.D., Ploetze, M., Hughes, J.B., Puzrin, A.M., 2008b. Microbial fuel cell technology for measurement of microbial respiration of lactate as an example of bioremediation amendment. Biotechnol Lett 30(8), 1385-1390.
Venkateswaran, K., Moser, D.P., Dollhopf, M.E., Lies, D.P., Saffarini, D.A., MacGregor, B.J., Ringelberg, D.B., White, D.C., Nishijima, M., Sano, H., Burghardt, J., Stackebrandt, E.,

Nealson, K.H., 1999. Polyphasic taxonomy of the genus *Shewanella* and description of *Shewanella oneidensis* sp. nov. Int J Syst Bacteriol 49 Pt 2, 705-724.
Yang, C., Rodionov, D.A., Li, X., Laikova, O.N., Gelfand, M.S., Zagnitko, O.P., Romine, M.F., Obraztsova, A.Y., Nealson, K.H., Osterman, A.L., 2006. Comparative genomics and experimental characterization of N-acetylglucosamine utilization pathway of *Shewanella oneidensis*. J Biol Chem 281(40), 29872-29885.

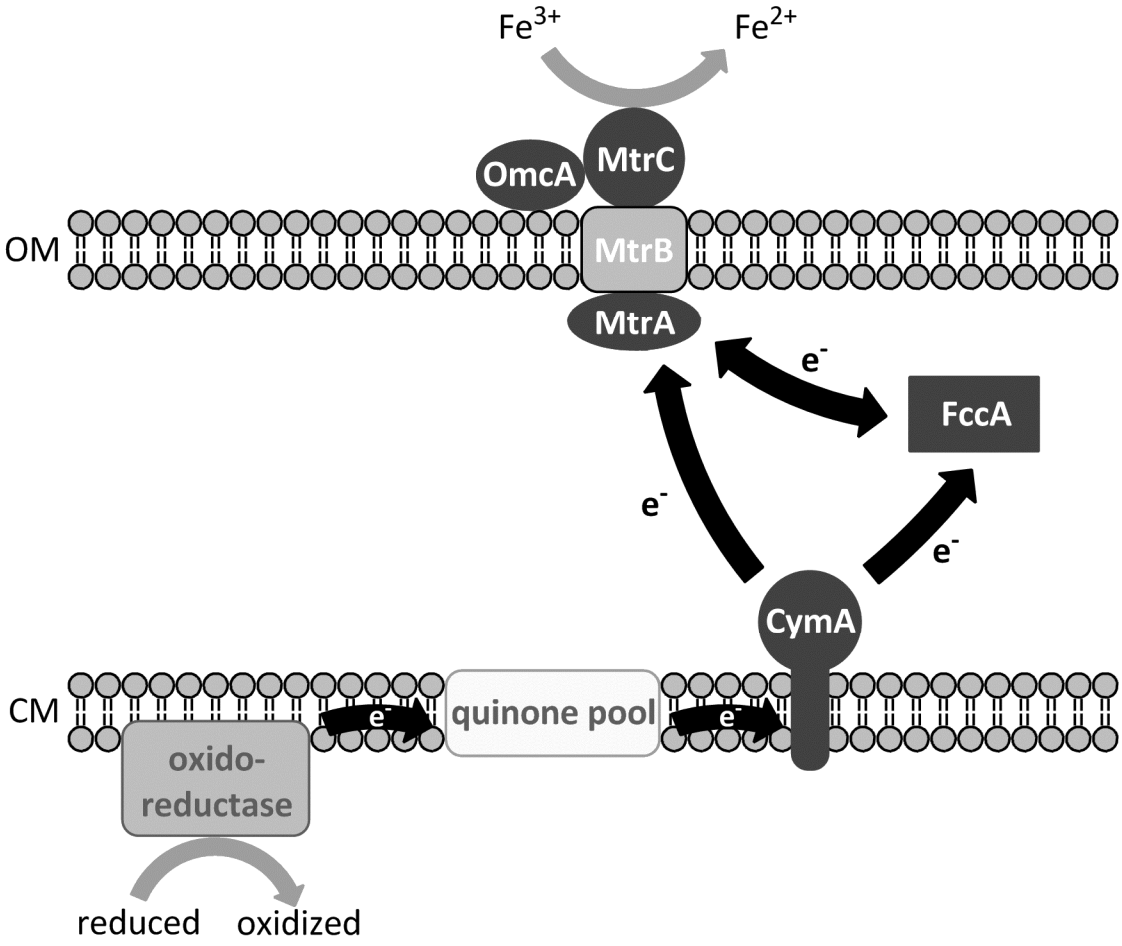

Figure 1: Current model of the extended respiratory chain of *S. oneidensis*. *c*-type cytochrome proteins are depicted in dark grey. OM= outer membrane, CM= cytoplasmic membrane.

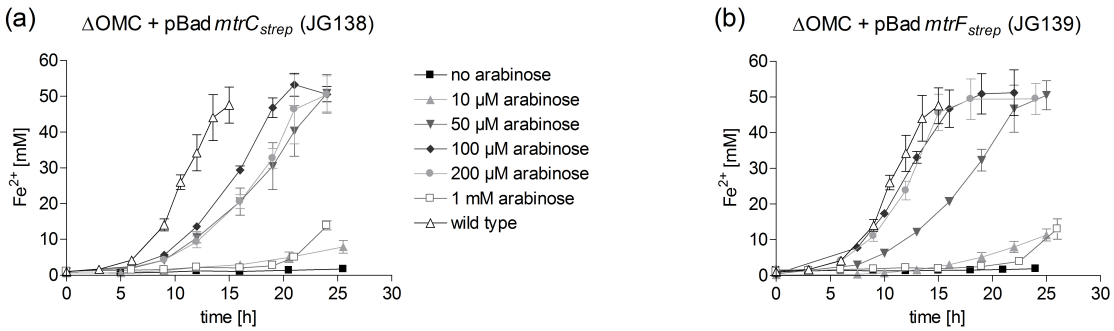

Figure 2: Iron reduction with ΔOMC cells complemented with pBad*mtrC*$_{strep}$ and pBad*mtrF*$_{strep}$ plasmids. Fe(II) production was monitored over time using the ferrozine assay. Mutant strains were induced with arabinose as indicated. Symbols refer to means of triplicate experiments, error bars indicate standard deviation.

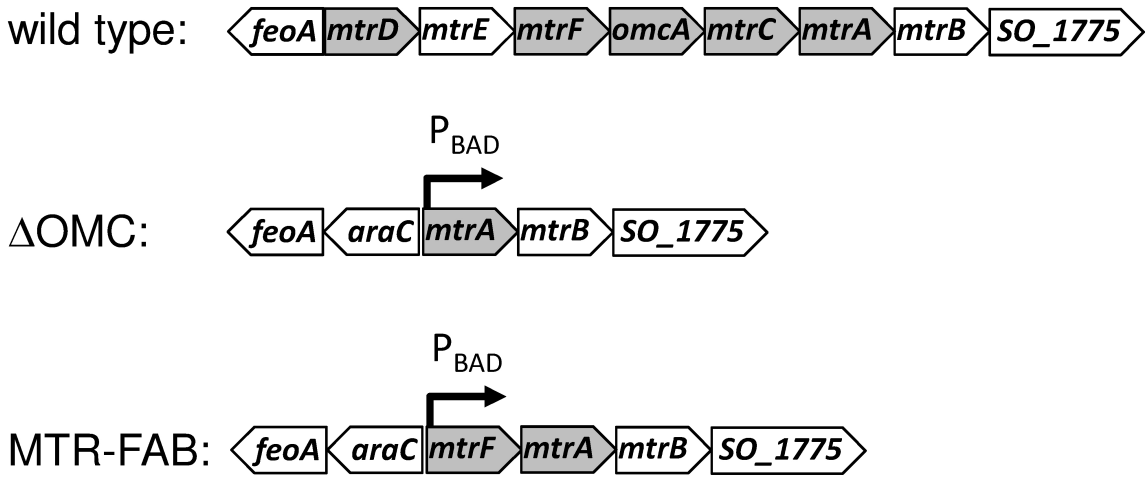

Figure 3: Schematic view of the *mtr*-gene clusters of *S. oneidensis* MR-1 and mutant strains. Genes coding for *c*-type cytochrome proteins are depicted in grey. The gene *araC* codes for the repressor/activator protein AraC that is interacting with the P_{BAD} promoter which is symbolized by a black arrow.

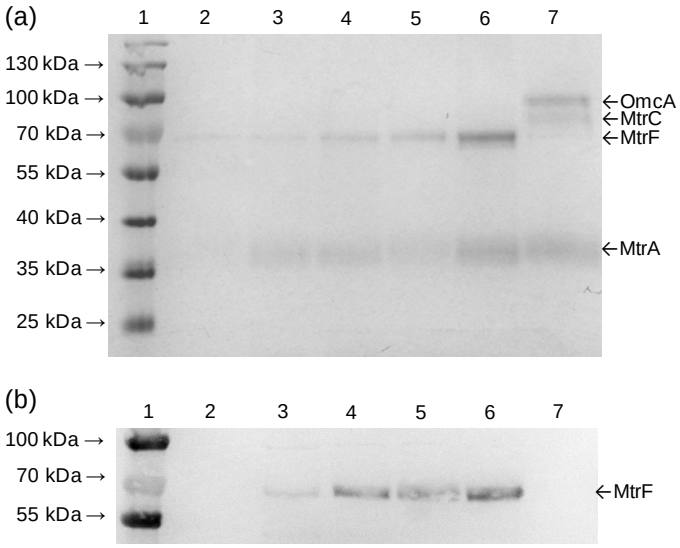

1

2 **Figure 4: SDS-PAGE of membrane fractions from strain *S. oneidensis* MTR-FAB and**
3 **wild type.** (a) Heme acitivity staining (b) Western Blot with anti-strep antibody to detect
4 $MtrF_{strep}$. Lanes 1: protein marker; lanes 2-6: *S. oneidensis* MTR-FAB with 100 µM, 200 µM,
5 500 µM, 1 mM, and 2 mM arabinose, respectively; lane 7: *S. oneidensis* wild type.

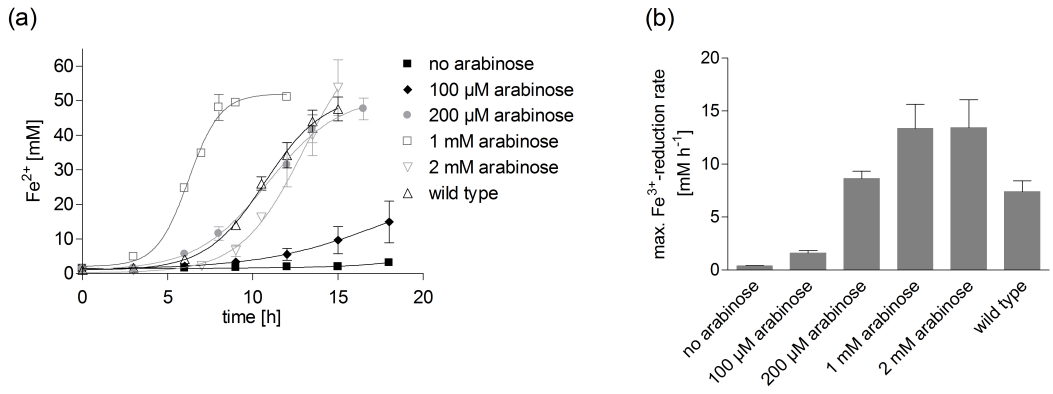

Figure 5: Fe(III)-citrate reduction and maximal reduction rates by strain MTR-FAB (JG410). (a) Fe(II) production was monitored over time using the ferrozine assay. MTR-FAB strain was induced with arabinose as indicated. Symbols refer to means of triplicate experiments, error bars indicate standard deviation. (b) Maximal reduction rates during the course of the experiment calculated for each biological replicate with GraphPad Prism 4. Error bars represent standard deviations.

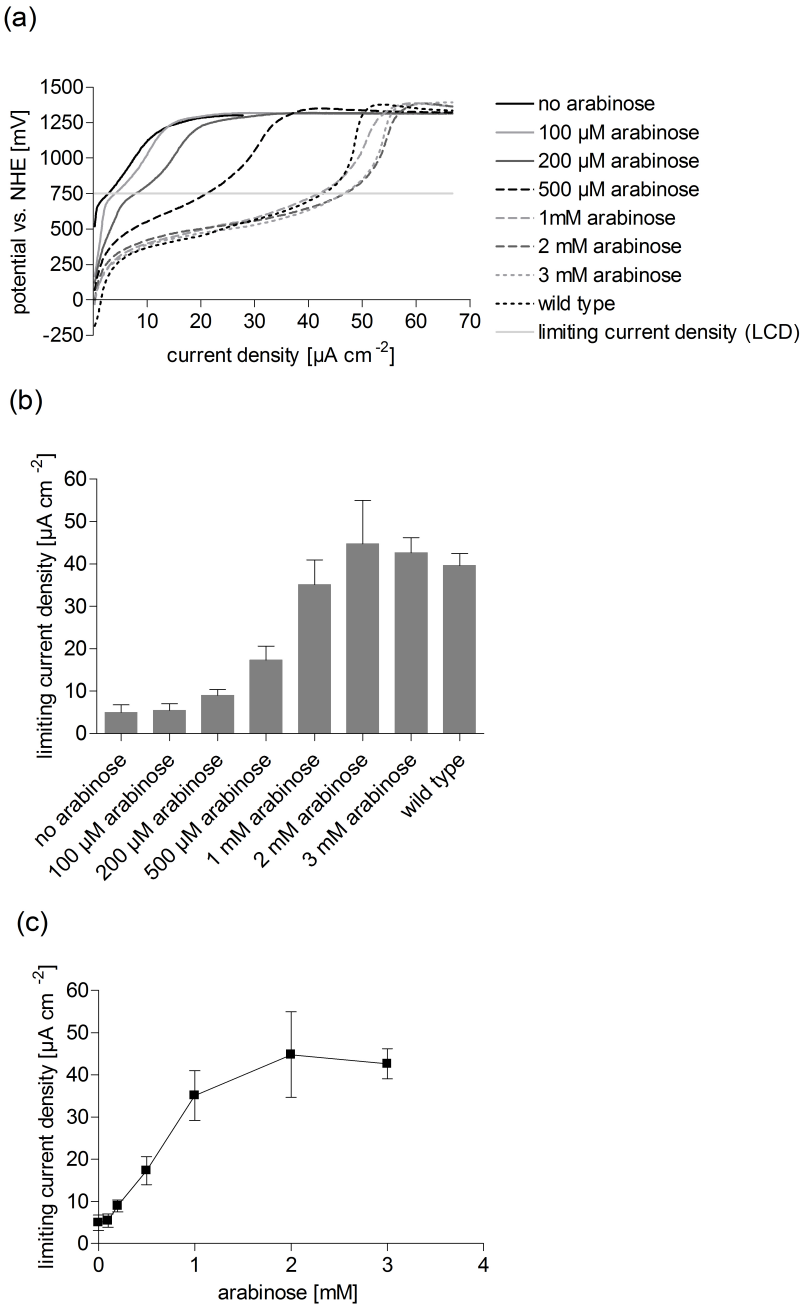

Figure 6: Microbial fuel cell experiments with MTR-FAB. (a) The current density in the microbial fuel cells was increased continuously and the reached potentials were recorded. Solid lines are representative plots. (b) Limiting current density was determined by measuring the current density when the potential reached 750 mV vs. NHE. Error bars indicate standard deviation from triplicate experiments. (c) Arabinose concentration plotted against limiting current density showing a linear dependence from 0-1 mM.

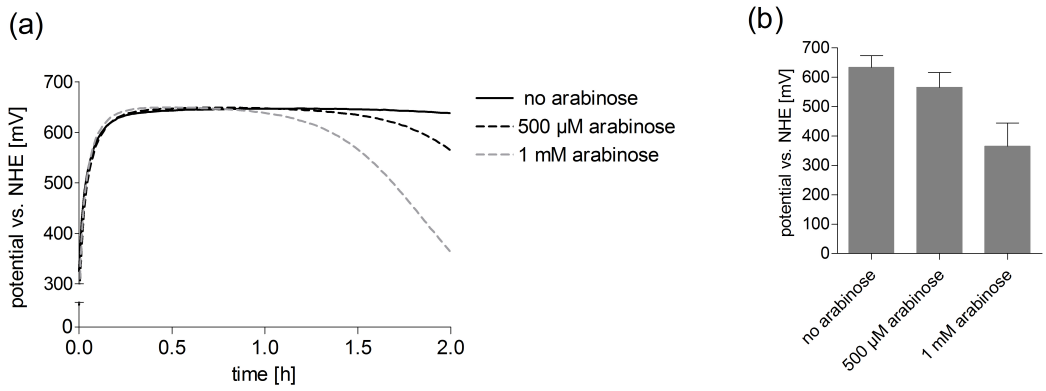

1

2 **Figure 7: Development of the potential during a fast conditioning period.** (a) The
3 development of the anode potentials for three different induction levels is shown. The lines
4 represent mean values of the experiments. (b) The columns represent the potential that was
5 reached two hours after starting the experiment. They were calculated from duplicate
6 experiments. Error bars represent the range of the values.